SKI Activates Hippo Signalling to Modulate Cardiac Fibroblast Function and Activation

by

Natalie M. Landry

A thesis submitted to the Faculty of Graduate Studies of
The University of Manitoba
in partial fulfillment of the requirements for the degree of

DOCTOR OF PHILOSOPHY

Department of Physiology & Pathophysiology
Rady Faculty of Health Sciences
University of Manitoba

Abstract

Even with ongoing improvements in cardiac patient treatment and outcomes, current therapies for cardiac fibrosis only alleviate the symptoms of heart failure, rather than treating the underlying cause of the disease. Furthermore, the ability to study cardiac fibroblast activation and pro-fibrotic signalling *in vitro* is complicated by the cells' phenotypic plasticity and sensitivity to mechanical input. Our lab has previously established that SKI, an endogenous TGF-β_1 signalling inhibitor, halts fibroblast activation and deactivates the myofibroblast phenotype. We have also determined that conventional cell culture does not lend itself to accurate physiological studies of primary cardiac fibroblasts, *in vitro*. The thesis presented herein establishes a method of maintaining primary cardiac fibroblasts in a resting state in two-dimensional cell culture. In addition, this improved technique is applied to test the hypothesis that SKI is a multi-functional protein that can act independently of TGF-β to specifically activate Hippo signalling, and in turn inhibit the cardiac myofibroblast phenotype.

In order to study cardiac fibroblast activation *in vitro*, we developed cell culture conditions which better maintain the native phenotype of primary cells by limiting mechanical, hormonal, and nutritional input. Both rat and mouse primary cardiac fibroblasts could be maintained in a quiescent state for up to ten days post-isolation, which is sufficient for most commonly-used cellular and molecular assays. Using this optimized method, we first sought to determine the role of the primary nuclear effectors of the Hippo pathway, Yes-Associated Protein (YAP) and Transcriptional co-Activator with PDZ-binding motif (TAZ, or WWTR1), in cardiac fibroblast activation. Constitutively-active forms of YAP and TAZ were overexpressed in primary rat cardiac fibroblasts, and demonstrated their ability to overcome external stimuli to promote fibroblast activation and pro-fibrotic gene expression. However,

TAZ demonstrated greater activation of the Collagen 1αI and 3α1 promoters. Subsequently, YAP and TAZ expression were examined in a rat post-myocardial infarction (post-MI) model of fibrosis. It was found that TAZ expression increases and translocates to the nucleus, while YAP expression was relatively unchanged in the infarcted left ventricle. Taken together, these data suggest that TAZ has a greater role in the pathogenesis of cardiac fibrosis.

Ensuing studies used first-passage (P1) primary cardiac myofibroblasts to examine the effects of SKI on YAP/TAZ signalling. Overexpression of SKI induced the degradation of endogenous TAZ, but not YAP. Moreover, loss-of-function studies suggested that the Large Tumor-Suppressor kinase 2 (LATS2) is required for SKI's specific effects on TAZ, but not its homolog, LATS1. To better understand the SKI-TAZ link, and whether it results from direct interaction with the Hippo pathway, the human cardiac fibroblast-specific SKI interactome was elucidated by using BioID2 and novel interactors were identified by tandem mass spectrometry. We identified the focal adhesion-associated protein, LIMD1, as a mediator between LATS2 and SKI. Additionally, knockdown of *Limd1* in myofibroblasts resulted in the proteasomal degradation of TAZ, but not YAP, recapitulating the TAZ-specific effects of SKI overexpression. Overall, our data suggest that LIMD1 is an important component of the regulatory effects between SKI and TAZ/LATS2, and presents a novel point of crosstalk among pro- and anti-fibrotic pathways.

This study is the first report of the role of TAZ-Hippo signalling in post-MI remodelling and fibrogenesis using optimized *in vitro* and *in* vivo models of fibrotic disease. The findings described herein postulate that the SKI-LIMD1-TAZ signalling axis as a novel and selective therapeutic target for consideration in future treatments for cardiac fibrosis.

Acknowledgements

First and foremost, I must thank my supervisor, Dr. Ian Dixon, for his support and encouragement during my graduate studies. I am so grateful to have had an advisor that allowed me to take risks and "follow the data" with respect to my project. I will miss our morning chats, armchair quarterback analyses of Blue Bombers games, and hearing about your latest adventures in astrophotography. I am proud to have been part of your lab, and even prouder to call you a friend and colleague.

Many thanks are extended to my advisory committee members, Drs. Barbara Triggs-Raine and Andrew Halayko, who have been invaluable sources of insight through every iteration of my project. Thank you for never letting me rest on my laurels and challenging me to better myself as a scientist. I am grateful to have had you both as mentors during the formative years of my academic career. I must also acknowledge Dr. Peter Cattini, whose unwavering support from day one has truly been invaluable in my success as a graduate student.

I would like to thank the members of the Dixon lab, past and present. A special thanks to Sunil Rattan, whose technical expertise and steadfast friendship I consider to be second to none. To my "work wife," Krista Filomeno, whose legendary sneezes and wicked sense of humour made long days in the lab feel much shorter. I am also indebted to the incomparable Dr. Mark Hnatowich, whose meticulousness and supernatural skills in everything DNA-related made all the difference in completing my project. I will especially miss your ability to conjure up the most interesting conversation topics and your devilish sense of humour. I consider you a dear friend, and will continue to hope that one day, your "Math and Cheese" dreams will come true. I must also thank Dixon lab members, Drs. Matthew Zeglinski, Morvarid Kavosh, Shivika Gupta, Jared Davies, and Rebeca de Oliveira Camargo for their friendship and support throughout my time at ICS. Finally, I am eternally grateful to all the summer students that helped me complete (too) many Western blots and qPCR assays for my project: Sarah Foran, Thomas Meier, Simon Meier, Nikita Sarangal, Ken Xing, Jooyeon Seung, and Claire Meier. As we say in French, "*mille mercis, mes amis*"!

I would be remiss to not recognize my extended ICS family for all their help during my graduate studies. To all the PI's who have mentored and encouraged me to better my skills as a scientist and communicator, I thank you for your dedication to student development and to the culture of success at ICS. To the members of Dr. Elissavet Kardami's lab: thank you for all your technical help and your comradery. A special thanks to Dr. Navid Koleini, whose friendship I will always hold dear, and whose infectious laugh was always a welcome sound in the hallways of the Albrechtsen Research Centre. I am also thankful to all the friendships I have made with the other graduate students of ICS. A special thanks to the members of the ICS "Cheese Club," Matthew Guberman and Cameron Eekhoudt—thank you for all the great conversations, laughs, and I wish you all the best in your future endeavours.

I must also thank my other work family, the team at the Youth BIOlab Jeunesse. To Steve Jones: thank you for taking a risk on a shy French-Canadian when you hired me nine

years ago and giving me the opportunity to better myself as a scientist, communicator, and teacher. To Meghan Kynoch, I am so thankful for your friendship and positive attitude, even when things get tough. I am so grateful to have met both of you, and wish you continued success in everything you do.

Many thanks are also extended to the administrative staff in the Department of Physiology & Pathophysiology. To the angels in the Department office, Gail McIndless, Judy Olfert, and Sharon McCartney, thank you for being endless wells of knowledge and wisdom, and for being so patient with all the lost paperwork, award deadlines, and committee meeting mix-ups. I would not have survived graduate studies without you!

Last, but definitely not least, I am so thankful for the support provided by my dear friends and family, who have been endlessly understanding and generous cheerleaders throughout my graduate studies. A giant *merci* to my parents, Lise & Normand, who have unconditionally supported me my entire life. To Marc, Sylvie, Janelle, and Kim: thank you for always knowing how to make me laugh—there is no better cure for the dejection from a failed experiment than a reminder of how weird our pets are. And to my SMA family, Ashley, Mai, Chelsea, Alison, Lauren and Sabrina: despite not seeing you all as often as I would like, our quarterly "Meetings of the Minds" are a great reminder of how lucky I am to have such strong, independent women in my life. I am also grateful for my chosen family, Ray & Ann, and Debbie & Gregg, with whom I have been so fortunate to share my triumphs and failures. Finally, I must thank my incredibly loving and patient husband, Cameron, who saw me through all the highs and lows with unwavering positivity and constant encouragement. I am so lucky to have had my best friend by my side through this incredible journey.

"Don't be afraid of hard work. Nothing worthwhile comes easily. Don't let others discourage you or tell you that you can't do it. In my day, I was told women didn't go into chemistry— I saw no reason why we couldn't."

-Gertrude B. Elion, Nobel Laureate (Physiology & Medicine, 1988)

To my husband and best friend, Cameron.

.

TABLE OF CONTENTS

List of Tables

List of Figures

List of Appendices

List of Abbreviations

AAV	Adeno-Associated Virus
ACE	Angiotensin Converting Enzyme
αSMA	alpha-Smooth Muscle Actin
AJUBA	LIM domain-containing protein Ajuba
AMOT	Angiomotin
AMOTL	Angiomotin-Like
AngII	Angiotensin-II
AP-1	Activator Protein-1
BMP	Bone Morphogenic Protein
β-TrCP1	beta-Transducin repeat Containing Protein 1
CARMIL2	Capping Protein Regulator And Myosin 1 Linker 2 (also called RLTPR)
CBP	CREB Binding Protein
CCN	Cellular Communication Network factor
CD44	Cluster of Differentiation 44 (also called Phagocytic Glyocoprotein-1, PGP-1)
CK1	Casein Kinase 1
CTGF	Connective Tissue Growth Factor (also called CCN2)
CVD	Cardiovascular Disease
Col1a1	Collagen Type I, alpha 1
Col1a2	Collagen Type I, alpha 2
Col3a1	Collagen Type III, alpha 1
CYR61	Cysteine-Rich angiogenic inducer 61 (also called CCN1)
DAC	Dachshund protein
DACH	Dachshund Homolog
DHD	Dachshund Homology Domain
DMEM	Dulbecco's Modified Essential Medium
DMSO	Dimethyl sulfoxide
E	Elastic (Young's) Modulus
ECM	Extracellular Matrix
ED-A	Extracellular Domain-A
EMT	Epithelial-Mesenchymal Transition
EndoMT	Endothelial-Mesenchymal Transition
F-actin	Filamentous actin
FAK	Focal Adhesion Kinase
FAT4	Protocadherin Fat 4 (also called Atypical Cadherin 4)
FGF	Fibroblast Growth Factor
FN	Fibronectin
G-actin	Globular actin
GAG	Glycosaminoglycan
GAPDH	Glyceraldehyde 3-Phosphate Dehydrogenase

HA	Hemagglutinin
HDAC	Histone Deacetylase
HEK	Human Embryonic Kidney
HFpEF	Heart Failure with Preserved Ejection Fraction
HFrEF	Heart Failure with Reduced Ejection Fraction
HPRT	Hypoxanthine Phosphoribosyltransferase
IPF	Idiopathic Pulmonary Fibrosis
ITS	Insulin-Transferrin-Selenium
KIBRA	Kidney and Brain expressed protein (also called WWC1)
LAD	Left Anterior Descending coronary artery
LAP	Latency-Associated Peptide
LATS	Large Tumor Suppressor
LB	Luria Broth (also called Lysogeny Broth)
LIM	Lin11, Isl-1, Mec-3
LIMD1	LIM Domain-containing protein 1
LLC	Large Latent Complex
LOX	Lysyl oxidase
LTBP	Latent TGF-β Binding Protein
LV	Left Ventricle
MACE	Major Adverse Cardiac Event
MI	Myocardial Infarction
MMP	Matrix Metalloproteinase
MOB	Mps-One Binder kinase
MOI	Multiplicity of Infection
MRTF	Myocardin Related Transcription Factor
MST	Macrophage-Stimulating factor
NASH	Non-Alcoholic Steatohepatitis
NCoR	Nuclear Co-Repressor
NDR	Nuclear Dbf2-Related
NF2	Neurofibromin 2
NFκB	Nuclear Factor Kappa B
$P2Y_{12}$	Purigenic G-protein coupled receptor 12
PDGF	Platelet-Derived Growth Factor
PDGFRα	Platelet-Derived Growth Factor Receptor Alpha
PDZ	Post-Synaptic Density protein 95, Drosophila disc Large tumor suppressor 1, Zonula Occludens-1
POSTN	Periostin
RelA	REL-Associated protein (also called NFκB p65 subunit, or p65)
RGD	Arginine-Glycine-Aspartic Acid

RLTPR	RGD, Leucine-Rich Repeat, Tropomodulin And Proline-Rich-Containing Protein (also called CARMIL2)
RV	Right Ventricle
SAND	Sp100, Autoimmune Regulator 1, NucP41/75, Deformed Epidermal Autoregulator Factor 1
SAV1	Salvador homolog 1
SCF	Skp, Cullin, F-box containing complex
SKI	Sloan-Kettering Institute protein (cellular homolog of viral v-SKI)
SKIP	SKI-Interacting Protein
SLRP	Small Leucine-Rich Proteoglycan
SMAD	Mothers Against Decapentaplegic homolog
S-MEM	Minimum Essential Media, Spinner's modification
SMemb	Embryonic non-muscle Myosin heavy chain (Non-muscle Myosin IIB)
SMURF	SMAD Ubiquitin Regulatory Factor
SNO	SKI-related Novel protein
SRF	Serum Response Factor
STK38	Serine-Threonine Kinase 38 (also called NDR1)
TAZ	Transcriptional co-Activator with PDZ-binding motif (also called WWTR1)
TβR	TGF-β Receptor
TCF21	Transcription Factor 21
TEAD	TEA Domain family member
TEF	Transcriptional Enhancer Factor
TGF-β	Transforming Growth Factor-beta
TGFβR	Transforming Growth Factor-beta Receptor
TIMP	Tissue Inhibitor of Metalloproteinases
TNC	Tenascin-C
TNFα	Tumor Necrosis Factor alpha
TRAF6	TNF Receptor Associated Factor 6
VCL	Vinculin
VSMC	Vascular Smooth Muscle Cell
WASHC5	WASH Complex Subunit 5
WISP2	WNT- Inducible-Signalling pathway Protein 2 (also called CCN5)
WNT	Wingless int-1
WT	Wild Type
WWC1	WW domain-containing protein 1 (also called KIBRA)
WWTR1	WW domain-containing Transcription Regulator protein 1 (also called TAZ)
YAP	Yes-Associated Protein
YWHAZ	Tyrosine 3-Monooxygenase/Tryptophan 5-Monooxygenase Activation protein Zeta
ZYX	Zyxin

List of Publications from this Thesis

Landry NM, Rattan SG, Dixon IMC. (2020) <u>Soft substrate culture to mechanically control cardiac myofibroblast activation</u>. In: Hinz B, Lagares, D. (eds) Myofibroblasts: Fundamentals, Laboratory Methods and Anti-fibrotic Drug Discovery. Springer Nature.

Landry NM*,* Hnatowich M, Rattan SG, Filomeno KL, Meier TW, Meier SC, Foran SJ, Koleini N, Fandrich RR, Duhamel TA, Kardami E, Dixon IMC. SKI Activates the Hippo Pathway via LIMD1 to Inhibit Cardiac Fibroblast Activation. 2020.
Submitted to: *Basic Res Cardiol*

Landry NM, Rattan SG, Dixon IMC. An Improved Method of Maintaining Primary Murine Cardiac Fibroblasts in Two-Dimensional Cell Culture. *Sci Rep*. 2019; 9(1): 12889. doi: 10.1038/s41598-019-49285-9.

Landry NM, Cohen S, Dixon IMC. Periostin in cardiovascular disease and development: a tale of two distinct roles. Review. *Basic Res Cardiol*. 2017; **113** (1):1. doi: 10.1007/s00395-017-0659-5.

Zeglinski MR*, **Landry NM***, Dixon IMC. (2015) <u>Non-Canonical Regulation of TGF-β1 Signalling: A Role for Ski/Sno and YAP/TAZ</u>. In: Dixon I., Wigle J. (eds) Cardiac Fibrosis and Heart Failure: Cause or Effect?. Advances in Biochemistry in Health and Disease, vol 13. Springer Nature. https://doi.org/10.1007/ 978-3-319-17437-2_9.

* Denotes shared first-authorship

CHAPTER 1: INTRODUCTION

1.1 The Cardiac Extracellular Matrix: Structure and Composition

The extracellular matrix (ECM) of the myocardium is a dynamic milieu comprised of structural, regulatory, and cell-associated proteins [3, 4]. Within this space, further stratification into basement membrane and interstitial environments allow for the specific function, maintenance, and injury response mechanisms of cardiac muscle and resident fibroblasts. Disruption of the ECM network, as observed post-myocardial infarction (post-MI), disturbs its structure, impairs ventricular function, and promotes the pathological expansion of the cardiac interstitium, a pathology known as cardiac fibrosis [5-7] (Fig. 1.1). The delicate balance among composition, organization, and tissue turnover within the myocardial interstitium dictates cardiovascular health, and ultimately determines the rate of progression into heart failure [8].

1.1.1 Structural Proteins

1.1.1.1 Fibrillar Collagens

The cardiac ECM has been typically regarded as predominantly composed of collagen, a large family of glycoproteins characterized by the presence of at least one proline-rich triple helix domain [9]. As one of the most abundant family of proteins, collagens comprise approximately 96% of the cardiac interstitium and play an important role in overall cardiac structure, as well as maintaining the electrical syncytium between cardiomyocytes [8, 10]. Of special importance are a subgroup called fibrillar collagens, which form long, striated fibrils which function to provide mechanical support and stability. While 30 types of collagen have been identified to date, the most abundant types in the cardiac ECM are fibrillar collagen types I, III, and to a lesser extent, V [11]. Other fibrillar collagens include types II and XI; however,
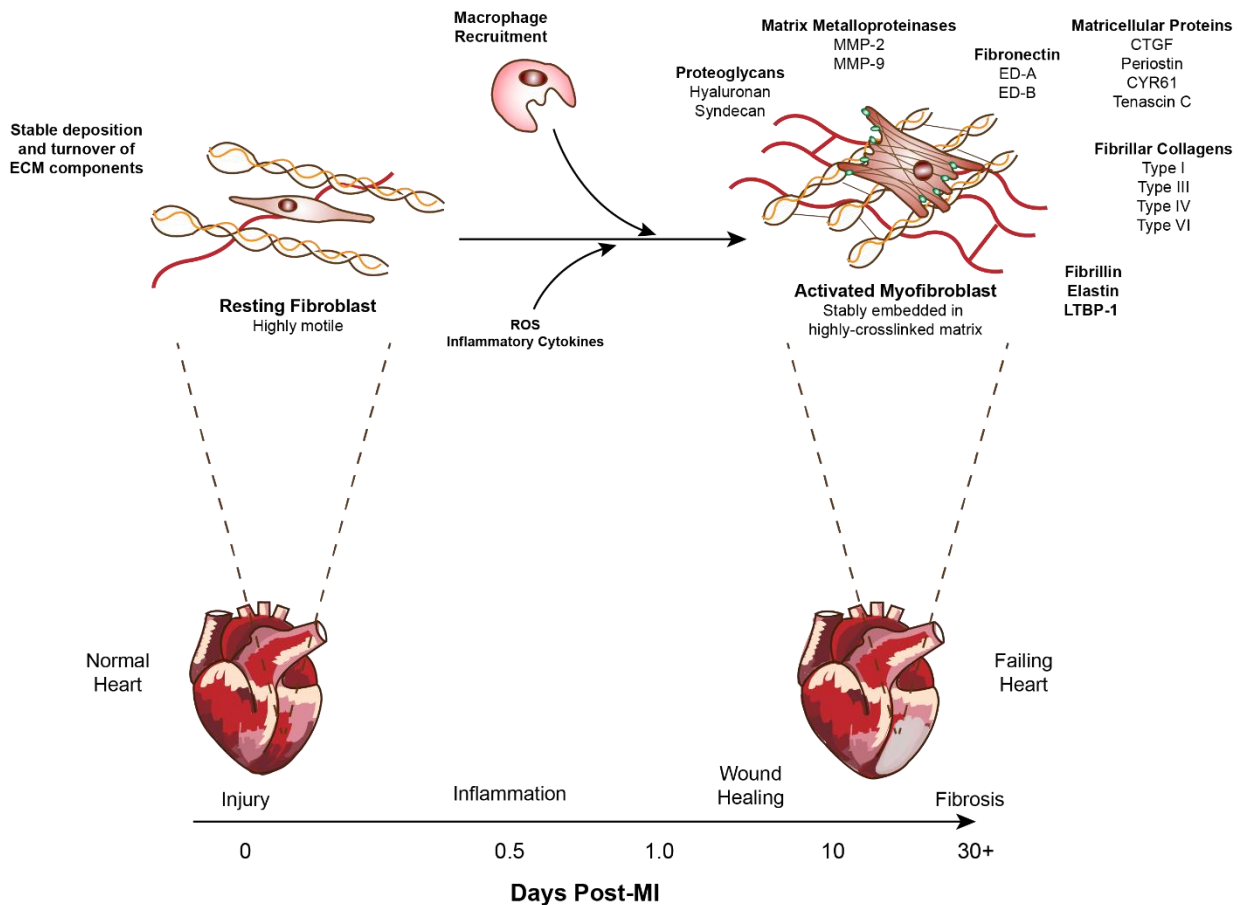
Figure 1.1 Changes in the cardiac extracellular matrix, post-myocardial infarction.
The cardiac myofibroblast phenotype (right) activates after MI, in response to the sudden, necrotic loss of myocardium and infiltration of immune cells into the infarcted area. Normal tissue homeostasis is disrupted, and resident fibroblasts stably attach themselves to the surrounding matrix and form mature focal adhesions (green ovals). Excessive production of ECM components by myofibroblasts (listed around cell on the right) allows the pro-fibrotic environment to persist, leading to heart failure.

these subtypes are predominantly produced in cartilaginous tissue in mammals [12].

Transcriptional regulation of collagens in the myocardium is primarily governed by cytokines, of which Transforming Growth Factor-beta (TGF-β) is the most significant contributor [13].

Transcription factors such as the AP-1 complex and p300/CBP are known to interact with SMAD proteins downstream of TGF-β and enhance the expression of collagen types I and III, although non-SMAD signalling such as p38 Mitogen-Activated Protein Kinase (MAPK) may also contribute to increased collagen transcription and synthesis [14].

Fibrillar collagens are synthesized and secreted by various cell types, mostly of mesenchymal origin, through a complex series of intra- and extracellular events. Present in almost all higher-order animals, fibrillar collagens are all composed of either a mono- or heterotrimeric protein chains, each containing multiple domains [15]. For example, in the human myocardium, the dominant collagen type I is a heterotrimeric protein composed of two α1 chains, and one α2 chain, while collagen type III is homotrimeric and contains three α3 chains [12]. The synthesis of collagen begins with the translation of pre-procollagen peptide chains in the rough endoplasmic reticulum. Signal peptides are cleaved from the N- and C-termini; this is followed by the hydroxylation of lysine and proline residues, and further glycosylation of the newly formed hydroxylysine residues. From here, three pro-alpha chains are combined to form the procollagen triple helix and is secreted to the extracellular space [15]. The procollagen molecule is cleaved by procollagen peptidase, forming tropocollagen fibril complexes. The complexes are then stabilized by lysyl oxidase (LOX), which joins individual helices together by crosslinking lysine and hydroxylysine residues. Mature collagen fibers result from the successive addition and crosslinking of multiple collagen fibrils, although excessive crosslinking is associated with a loss of myocardial compliance and can negatively affect cardiac output [15, 16]. While collagen synthesis is paramount to the cardiac wound healing response, the excessive deposition of fibrillar collagen is a hallmark of cardiac fibrosis; this occurs in tissue both proximal (i.e. replacement fibrosis) and distal (i.e. reactive fibrosis) to the initial injury [5, 7, 17].

The maintenance of the cardiac collagen matrix is largely regulated by the activity of matrix metalloproteinases (MMPs) and their tissue inhibitors (TIMPs) [18]. MMPs are a family of endopeptidases that function to breakdown ECM and regulate the homeostasis of collagen

synthesis and deposition. The most widely-studied cardiac metalloproteinases are MMP-2 and

-9, also called type IV collagenases or gelatinases, and possess a variety of substrates such as

collagen type I, fibronectin (FN), periostin (POSTN) [19]. About half of all known MMPs are

expressed at some point during cardiac development, homeostasis, and disease, and each is

distinguished by their respective ratios of MMP:TIMP activity in the interstitium [18-21]. For

example, during post-MI wound healing, increased secretion and activity of MMP2 and MMP9

results in the rapid turnover of collagen type I. However, chronic pro-inflammatory signalling

leads to increased expression of TIMPs, which results in the persistence of interstitial

remodelling, increased collagen deposition, and eventual heart failure [19]. Thus, the

physiological turnover of fibrillar collagen in the heart is of significant interest as any

disruption to its homeostasis results in pathological remodelling and cardiac dysfunction.

1.1.1.2 Basement Membrane Proteins

While fibrillar collagens comprise much of the cardiac ECM, non-fibrillar collagens

and other basement membrane proteins make up a small, yet important portion of the structural

underpinnings of the myocardium. The basement membrane provides further anchoring and

framework for the organization of cardiomyocytes and endothelial cells, and is mainly

comprised of proteoglycans, laminin, and collagens type IV and VI [8, 22, 23]. Laminin plays an

especially important role in cardiac structure as it is the primary substrate for cardiomyocyte

anchoring, and interacts with integrin receptors to mediate the migration of non-myocytes

throughout the myocardium [24]. Collagen type VI is highly expressed in the infarcted

myocardium, although transgenic *Col6a1*$^{-/-}$ mouse models showed improvement in cardiac

function post-MI, and the prevention of reactive fibrosis in viable tissue surrounding the infarct

[25, 26]. Finally, collagen type IV comprises nearly 50% of the basement membrane within the

cardiovascular system, and primarily functions to anchor endothelial cells to maintain their proper function [27, 28]. Collagen IV is also overexpressed in the infarcted myocardium, and alterations to its expression (e.g. glycosylation) is associated with impaired endothelial function and pro-fibrotic signalling [29-31]. The basement membrane may not be the largest element of the cardiac ECM, nevertheless it is a vital player in cell-ECM interaction and myocardial physiology.

1.1.1.3 Fibronectin

Fibronectin exists in two forms generated by a single gene: the first is soluble fibronectin, which is secreted into the circulation by hepatocytes, while the second is insoluble cellular fibronectin, a multifunctional component of the cardiac ECM synthesized by mesenchymal and endothelial cells [32-34]. Expressed as a high molecular weight protein, cell-associated fibronectin is initially secreted as a soluble ~450 kDa dimer which then polymerizes into a complex fibril network [35]. In its final, polymerized form, fibronectin regulates the deposition and stabilization of other structural proteins, including collagen type I, and modulates cell-matrix physiology and signalling via $\alpha 5\beta 1$ integrins [36-39].

In the healthy heart, cellular fibronectin is highly expressed during fetal development, accounting for approximately 26% of structural cardiac ECM [40]. In adult tissues, fibronectin is weakly expressed in cardiac ECM, comprising only 4% of total ECM, suggesting that it may have a role in the organization and proliferation of cardiomyocytes during early development [40]. In disease states such as heart failure, cellular fibronectin is highly expressed in the myocardial interstitium and promotes further infiltration of inflammatory cells; but it is also thought to increase the mechanical strength of damaged tissue and prevent rupture of the free wall of the ventricle [41]. Furthermore, cellular fibronectin splice variants are differentially

expressed during adverse cardiac remodelling. The type III segments in fibronectin comprise the extracellular domain, and produce variants type A (ED-A) and type B (ED-B) [42-44]. Both alternatively-spliced ED-A and ED-B fibronectin are present in fetal myocardium, as well as during adverse cardiac remodelling [42, 45]. The ED-A splice variant is of special interest, as its presence heralds the activation of pro-fibrotic signalling by resident cardiac fibroblasts and is apparently necessary for the maintenance of the hypersecretory myofibroblast phenotype [41, 43, 46]. Both genetic ablation and molecular inhibition of cardiac ED-A fibronectin demonstrate improved cardiac function post-MI, and results in impaired infiltration of inflammatory cells after infarction [34, 38, 41]. Furthermore, it has been shown that the ED-A domain acts as a TGF-β_1 reservoir, as it immobilizes Latent TGF-β-binding Protein-1 (LTBP-1) and its bound substrate, thus priming the ECM for continued TGF-β_1 signalling even in the absence of inflammatory cells [46]. While cellular fibronectin is integral to the development and overall structure of the myocardium, its role in modulating wound healing and inflammation is of crucial consideration when studying pathological ECM remodelling.

1.1.1.4 Elastin

Despite being subject to continuous and variable mechanical strain, the healthy heart expresses relatively low amounts of elastin, when compared to the rest of the vasculature. In the injured heart, elastin levels decrease as healthy tissue is replaced with infarct scar, and elastic recoil becomes impaired [47-49]. Knock-in studies in cardiac elastin have shown that introduction of ectopic elastin production in a rat model of post-MI fibrosis increased fractional shortening and reduced infarct expansion in the chronic phases of collagen deposition [50]. In addition, elastin can be crosslinked into fibrils by lysyl oxidase, and forms larger bundles when bound to fibrillin [51]. The result is a larger elastic fibre comprised of an

outer layer of fibrillin, and an unstructured core of crosslinked elastin, which offers more resistance and less distensibility when compared to elastin alone [51]. Fibrillin-rich elastin bundles such as these are found in most higher-order vertebrates, and are highly-conserved in the closed circulatory systems of mammals [52].

1.1.2 Non-Structural and Matricellular Proteins

Along with its structural role, the cardiac ECM also functions as a reservoir and cell-matrix signalling regulatory centre. Several proteins exist and function within the matrix in both physiological and pathological settings to regulate the turnover and deposition of other ECM components, as well as cell-matrix signalling. Matricellular proteins are cell-associated proteins that do not contain any transmembrane domains, nor do they serve any structural purpose; however, they do mediate cytokine, growth factor, and protease-related responses to ECM changes and are typically upregulated following injury [53, 54].

1.1.2.1 Periostin[†]

Periostin was first recognized as an essential player in osteoblast differentiation and response to Transforming Growth Factor-β (TGF-β) signalling [55, 56]. More recently, periostin has been identified as a transiently-expressed matricellular protein secreted by actively-remodelling stromal cells within the myocardium and vasculature [57-59]. Despite being relatively conserved across phyla, the 23 exons of human periostin can be alternatively spliced to form seven possible splice variants, most of which have not been well-studied [55, 60-63].

As a potent modulator of cell-matrix interaction, periostin has been implicated in crosstalk between multiple signalling pathways which regulate cell migration, adhesion, and proliferation. The most studied pathways associated with periostin expression are of the TGF-β superfamily in mesenchymal cells, which has established periostin as a focal contributor to

collagen fibrillogenesis in response to injury and inflammation [57, 64-67]. Early *in vitro* studies demonstrated that exogenous treatment of primary cardiac fibroblasts and vascular smooth muscle cells (VSMCs) with recombinant TGF-β_1 promoted the expression of periostin *via* canonical SMAD-dependent signalling [65, 68-70]. Besides being induced by TGF-β_1 signalling, periostin also promotes collagen fibrillogenesis by supporting Bone Morphogenic Protein-1 (BMP-1) in mediating the activation of matricellular LOX [71, 72]. Specifically, secreted periostin sequesters BMP-1 and increases its deposition on fibronectin-rich ECM; this promotes the proteolytic activation of pro-LOX and collagen cross-linking [71]. Although there exists much data to substantiate the TGF-β/BMP-periostin signalling axis, further studies are needed to identify the regulatory components that govern periostin transcription.

Apart from being expressed in response to SMAD-dependent TGF-β/BMP signalling, periostin activates a multitude of intracellular signalling pathways via its interaction with cell-surface receptors and in response to mechanical stress. Periostin-associated ECM components including fibronectin and tenascin-C (TNC) [73], and collagens type I, III and V [64, 74, 75], are responsible for governing the biomechanical properties of tissues, ergo periostin-associated regulation of these components may determine tissue biomechanics. It has been reported that periostin stimulates cell migration and invasion through biomechanically and biochemically-sensitive integrin communication [76-78]. Finally, it has been shown in various pathologies that latent TGF-β associated with αv integrin subunits is released upon stimulation by mechanical stress [79-82]. Cell contraction or a change in ECM composition leading to the release of latent TGF-β might leave integrins open to interaction with periostin, triggering a feed-forward loop of pro-fibrotic periostin signalling.

Given the growing evidence suggesting its importance in post-MI remodelling, the specific targeting of periostin as a point of intervention in post-MI cardiac fibrosis is of great interest. A study using periostin-neutralizing antibodies in an *in vivo* rat MI model showed promising evidence that not only does post-MI infusion of anti-periostin antibodies reduce infarct size, but also improved cardiac fractional shortening and ejection fraction eight weeks after MI [61]. It was specifically found that periostin exon 17 was the preferential target for reducing the effects of chronic post-MI fibrogenesis, confirming previous reports that periostin splice variants lacking exon 17 are beneficial in combatting cardiac remodelling [83]. The cumulative body of evidence supporting periostin's role in cardiac fibrosis and the ability to target it *in vivo* generates an auspicious vision for future animal models and potentially, clinical trials.

1.1.2.3 CCN Proteins

Named after its first three members, Cysteine-Rich protein 61 (CYR61/CCN1), Connective Tissue Growth Factor (CTGF/CCN2), and Nephroblastoma Overexpressed protein (NOV/CCN3), the CCN family of proteins modulate cellular function by bridging interactions between the matrix and cell-surface receptors [54, 84-86]. While CCN proteins share significant structural homology, their function within the matrix vary considerably. When considering the cardiac ECM, the most important CCN family members include CYR61, CTGF, and the recently-studied WNT-Inducible Signalling pathway Protein 2 (WISP2, or CCN5) [3, 54, 87]. Transcriptional regulation of CYR61 and CTGF is largely attributed to TGF-β, Hippo pathway, and Fibroblast Growth Factor 2 (FGF2) signalling, while WISP2 is synthesized and secreted in response to WNT1 signalling [84, 86, 88]. In any case, all of these proteins are

upregulated in the cardiac ECM following acute injury, and persist in chronic states of ECM expansion and fibrosis [54, 87, 89].

CYR61 plays important roles in cardiac development and disease, as it facilitates cell adhesion, migration, and proliferation [54]. As a cell-matrix mediator for several cell types, CYR61 was the first matricellular protein to be described as integrin-binding [90]. In the heart, CYR61 is most commonly-associated with integrin αvβ3 to facilitate endothelial cell adhesion, but it has also been found to associate with syndecan-4 to facilitate FGF2 signalling in fibroblasts [91]. When considering its overall physiological effects, homozygotic *Cyr61* deletion is embryonic lethal due to cardiovascular and placental defects, while 20% of heterozygotes exhibit atrial septal defects [92]. In cardiac fibrosis and remodelling, CYR61 is believed to promote angiogenesis and the formation of collateral circulation while inducing fibroblast senescence to limit wound healing [93, 94].

In contrast to CYR61, CTGF is the most well-studied CCN protein in the heart and is generally viewed as a pro-fibrotic factor [95-97]. It is secreted by fibroblasts, endothelial and smooth muscle cells, and its synthesis is stimulated in response to TGF-β and Angiotensin-II (AngII) [96, 98]. Also known as CCN Intercellular Signalling Protein, CTGF acts as an enhancer of SMAD/TGF-β and MAPK pathways, while it inhibits Vascular Endothelial Growth Factor (VEGF) signalling [3, 84, 99]. Counter to CYR61, CTGF is not required for cardiac development; however, its genetic ablation in mice led to chondrocyte hypoplasia and lethal respiratory failure soon after birth [100]. In replacement and reactive fibrosis—regardless of the organ of interest—CTGF is highly upregulated. Its expression is induced in myocardial ECM by pressure overload, diabetic hyperglycemia, as well as viral myocarditis [101-103]. Reports have also indicated that plasma CTGF in chronic heart failure patients is elevated, especially in heart

failure with reduced ejection fraction (HFrEF), suggesting that it may be used as a companion biomarker for post-MI treatment and prognosis [104]. Interestingly, several *Ccn2* overexpression studies in have shown that presence of CTGF alone is not sufficient for the initiation and persistence of fibrosis. Rather, CTGF potentiates the effects of matrix-bound cytokines like TGF-β, and further aggravates the deposition of aberrant ECM [105-107]. Thus, CTGF is an important target to consider when studying cardiac fibrosis, as its presence can be predictive of the severity and rate of progression of the disease.

Finally, the CCN protein WISP2 has recently garnered interest in cardiovascular research as its effects appear to counteract the TGF-β-potentiating function of CTGF in the heart. Although nearly identical in structure, and also secreted by mesenchymal cells, WISP2 lacks the C-terminal domain that is found in CTGF [105]. Moreover, its expression is inverse to that of CTGF in the myocardium: post-MI and chronically failing hearts show little or no expression of WISP2 [87]. In transgenic mice overexpressing WISP2, pressure overload-induced fibrosis was markedly reduced when compared to wild-type animals; these results were interpreted such that WISP2 may act like a dominant-negative version of CTGF [105]. Furthermore, adeno-associated virus (AAV) delivery of WISP2 in LV tissue with established fibrosis and cardiac dysfunction led to a reduction in TGF-β signalling and apoptosis of cardiac myofibroblasts [87]. However, the study did not report any improvements in functional parameters, such as ejection fraction. Even though WISP2 may not explicitly improve cardiac function and physiology, *Ccn5*^{-/-} knockout mice generated a mildly obese phenotype with a greater propensity for spontaneous interstitial and perivascular fibrosis [108].

While CCN proteins echo the complex and dynamic physiology of cardiac ECM, understanding their—and other matricellular proteins'—role in health and disease is of great

importance when considering cardiac fibrosis and heart failure.

1.1.3 Other Notable Cardiac Extracellular Matrix Components

1.1.3.1 Glycosaminoglycans

Glycosaminoglycans (GAGs) are a diverse group of negatively-charged, linear polysaccharides, consisting of repeating disaccharide units [109]. GAGs are categorized into several subgroups based on their disaccharide subunit and accompanying linkage between monomeric units: chondroitin sulfate, dermatan sulfate, keratan sulfate, heparin, heparan sulfate and hyaluronan [109-111]. In the heart, GAGs play an integral role in maintaining tissue homeostasis and form a lubricative network to mitigate shear forces during cardiac contraction. They are especially concentrated in the valve leaflets and cusps, as well as major arteries, but myocardial GAGs are integral to injury response and remodelling [112].

Functionally, GAGs are diverse and often context-specific; however, hyaluronan is the most widely-studied in the heart, and is the only GAG that has been observed without being attached to a core protein [110]. When considering healthy cardiac ECM, hyaluronan exists in an intact form composed of long polysaccharide chains, upwards of 4 000 kDa in size [110]. Its function, like in most tissues, is to form transient linkages with water to contribute to the overall strength and compressibility of the myocardium [113]. Hyaluronan is also the ligand of membrane receptors such as CD44, which regulates the migration, proliferation, and adhesion of mesenchymal, epithelial, and immune cells [113]. In the injured myocardium, hyaluronan synthesis and deposition is upregulated, but it is in a fragmented, low molecular weight form (100-500 kDa) [8, 109, 113]. This shift in expression is an important contributor to the cardiac fibroblast response to injury, as the low molecular weight fragments promote the infiltration of monocytes, macrophages, and dendritic cells, which in turn generate pro-inflammatory

cytokines and growth factors [8, 113]. In addition to these growth factor signals, the synergistic activation of fibroblast CD44 receptors causes a shift in actin cytoskeleton dynamics which inhibits Hippo signalling and activates a pro-fibrotic feed-forward loop of excessive ECM deposition [113].

1.1.3.2 Proteoglycans

Matrix proteoglycans encompass a broad group of proteins covalently bound to GAGs[111]. Proteoglycans exist as basement membrane and structural elements, as well as cell-surface and secreted ECM components [8, 111]. Many proteoglycans are involved in delimiting the deposition and organization of fibrillar collagen, but others are more involved in the cell-matrix crosstalk and cytokine sequestration within the collagen ECM [54, 110]. With respect to myocardial physiology and the cardiac ECM, several proteoglycans play an important role in cardiac function, homeostasis and disease. Of note are Decorin, Tenascin-C, Osteopontin, and Syndecan-1 and -4, all of which contribute to the regulation of collagen matrix turnover and cardiac fibroblast physiology [54, 110, 114-118].

1.1.3.3 Matrikines and Matricryptins

As part of their biological activity within the cardiac ECM, many proteins, proteoglycans, and GAGs undergo partial enzymatic cleavage which gives rise to small peptide fragments that possess different functions than their parent molecule [119]. These fragments, called matrikines, may modulate cell proliferation, migration, and apoptosis, and are an important marker of cardiac ECM health. In the myocardium, upregulation of matrikines arising from the enzymatic cleaving of elastin and collagen are a hallmark of interstitial pathologies [119-121].

Elastin-derived matrikines possess chemotactic and matrix remodelling properties, and target a broad range of cell types. For example, the insoluble elastin kappa molecule stimulates the secretion and activity of MMP-2, and has been found to increase fibroblast activation and proliferation [122, 123]. Kappa elastin has also been associated with impaired thrombosis during vascular remodelling and pathological angiogenesis [124]. Similar effects have been observed with another elastin matrikine, a short peptide bearing the sequence VGVAPG, which has been implicated with increased MMP-1 activity as well [119, 124].

Collagen-derived matrikines are more widely-studied and exert a broad variety of cellular responses. Collagen fragments generated by MMP proteolysis, such as the C-terminal DGGRYY cleavage product from the type I α1 chain, is a strong activator of neutrophils in injured tissue [119, 125]. Conversely, several non-fibrillar collagens, such as type basement membrane type IV, also generate matrikines which are associated with MMP-2 activation and inhibiting cell proliferation and migration [119, 126, 127].

Matricryptic sites, or matricryptins, on the other hand, are biologically-active amino acid sequences that are not exposed in the native form of a given ECM component [128]. Rather, matricryptic sites become active after alterations in the conformation or organization of the parent molecule reveal the active site to exert some sort of biological function. This activation can occur from a multitude of events, including mechanical stimulation, substrate binding, protein denaturation, and the formation of multimers [128]. The most well-known matricryptic site is the RGD (or Arg-Gly-Asp) motif found on several matrix components, including collagen type I and fibronectin [129-131]. RGD sites are known to interact with integrins and promote injury-inflammation responses in most tissues [132, 133]. In the heart, the RGD trimer is viewed as essential to proper cardiomyocyte organization and angiogenesis, but it is also

overexpressed in actively-remodelling fibronectin and collagen matrix in injury myocardium [134, 135]. Furthermore, non-specific RGD-containing peptides administered to murine hearts *ex vivo* have been shown to promote the same pro-inflammatory response as RGD sites found in ECM proteins [132]. Nevertheless, the RGD matricryptin remains as an important anchor point for cardiac cell-matrix interaction.

Because of their acute upregulation in post-MI hearts, and their unique quality of possessing "neo-epitopes", matrikines and matricryptins have been put forward as potential serological biomarkers for the diagnosis and prognosis of cardiovascular disease [4, 121]. Whether or not cardiac-specific matrikines and matricryptins can be isolated from patient samples has yet to be determined.

1.1.4 Cardiac Fibroblasts

The cardiac fibroblast is the resident stromal cell within the myocardium which shoulders the majority of ECM deposition and turnover. While early studies of the cardiac interstitium argued that cardiac fibroblasts are a heterogenous and undefinable cell type, more recent examinations have revealed that cardiac fibroblasts are distinct from other cells of mesenchymal origin, and possess a unique biology which sets them apart within the ECM [58, 136-138]. Rather than existing as a static phenotype, cardiac fibroblasts reside on a spectrum which vacillates between "resting" (i.e. physiological) and "activated" (i.e. pathological) states.

1.1.4.1 Origin and Role in Cardiac Development and Homeostasis

Resident ventricular fibroblasts arise primarily from epicardial progenitors during embryonic development, through epithelial-mesenchymal transition (EMT) [139, 140]. The fibroblast progenitors are further defined by the expression of Transcription Factor 21 (TCF21), which is typically associated with the resting fibroblast phenotype [137, 140]. A smaller

subset (<20%) of ventricular fibroblasts originate through endothelial-mesenchymal transition (EndoMT), as they invade the nascent myocardium from embryonic endothelium [17, 141]. In the adult heart, there is much debate as to whether there exists another source of fibroblast progenitors, particularly those observed after injury. Some speculate that non-fibroblast sources of mesenchymal cells such as smooth muscle cells, circulating fibrocytes, and bone marrow stem cells can give rise to new fibroblasts in post-MI hearts [142-144]. However, recent lineage-tracing studies in transgenic mice report that resident fibroblasts are the primary cells responsible for injury-induced wound healing and fibrosis [58, 145]. These studies have also concluded that in their resting state, these cells are positive for TCF21 and Platelet-Derived Growth Factor Receptor alpha (PDGFRα), and are distinct from other stromal cells which express collagen type I.

1.1.4.2 Resting Cardiac Fibroblast Phenotype

Despite recent breakthroughs in identifying endogenous sources of fibroblasts in the heart, defining the resting cardiac fibroblast phenotype remains a contentious task, largely due to the absence of a cell-specific marker [17, 136, 137]. Within intact tissue, cardiac fibroblasts are usually identified by their location between cardiomyocytes, where they perform critical structural maintenance of the cardiac ECM. When isolated from tissue, cardiac fibroblasts are spindle-shaped and possess little contractile ability, with a weakly-organized actin cytoskeleton [3, 146]. Resting fibroblasts within the myocardium are also highly-motile as they lack a basement membrane, and this enhances their capacity to respond rapidly to changes in their microenvironment [147]. They stain positive for fibrillar collagens and their respective precursor molecules, albeit at low expression levels [58, 138, 145]. Although all cardiac fibroblasts

express the mesenchymal marker vimentin, there is no absolute consensus as to the panel of molecular markers to specifically use when isolating primary cells or labelling them *in situ*.

Early studies in transgenic mice using once-believed fibroblast specific promoters quickly demonstrated that observing the baseline phenotype of cardiac fibroblasts is much more difficult than predicted. Markers such as Discoidin Domain Receptor 2 (DDR2), Fibroblast-Specific Protein-1 (FSP-1), and Thy-1 (or CD90) have all been implemented in conditional knockout studies that proved unfruitful in their pursuit of elucidating cardiac fibroblast physiology [148-150]. Unlike the mesenchymal specificity of vimentin, DDR2 is also highly expressed in endocardial tissue; FSP-1 is expressed in nearly all cardiac cells, and CD90 is a membrane glycoprotein expressed on smooth muscle cells, endothelial cells, immune cells, and cells of hematopoietic lineage. However, with the emergence of *in vivo* genetic lineage tracing, single-cell transcriptomics, and proteomics, contemporary studies have given rise to a more reliable gamut of markers that better represent the resident cardiac fibroblast (Summarized in Fig. 1.2) [8, 58, 151]. The most consistent panel of resting cardiac fibroblast markers used in recent literature is comprised of: TCF21, PDGFRα, Collagen type I and III, and vimentin [3, 8, 137, 145]. As the search for cardiac fibroblast-specific proteins continues, the ability to positively identify the cells with moderate confidence is much simpler with this newly adopted set of markers and the broad availability of more sophisticated, high-throughput screening techniques.

1.1.4.3 Fibroblast Activation and the Myofibroblast Phenotype

A key event in myocardial wound healing, cardiac fibroblast activation (formerly and incorrectly referred to as "transdifferentiation" or "phenoconversion") exemplifies the cells' sentinel-like behaviour and ability to shift to the myofibroblast phenotype in response to
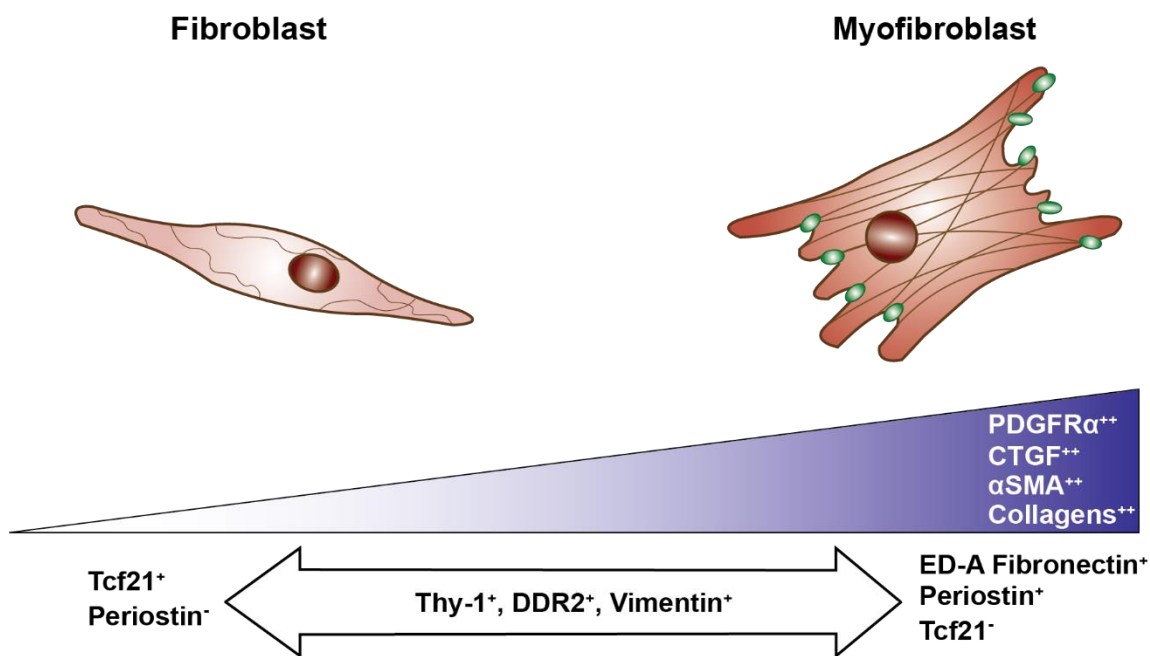
Figure 1.2: The Cardiac Fibroblast-Myofibroblast Phenotype Spectrum.
Resident cardiac fibroblasts undergo phenotypic changes (or "activation") in response to acute injury (e.g. MI) or chronic stressors (e.g. hypertension). Activation to the myofibroblast phenotype results in a cell that is no longer motile, and is hyper-proliferative and hyper-secretory for cardiac ECM components. Several markers span the two phenotypes with relatively stable expression (i.e. Thy-1, DDR2, Vimentin), while others have varying degrees of expression, depending on the cell's place on the spectrum (i.e. αSMA, PDGFRα, fibrillar collagens). Tcf21 is only expressed in resting fibroblasts, while Periostin is only expressed in the activated state. There is no known marker that is entirely specific for either phenotype.

various forms of injury. In most soft tissues, the gold standard marker associated with fibroblast activation is the distinct shift to a highly-organized actin cytoskeleton, denoted by αSMA-positive stress fibers [152-155]. However, in the heart, this marker is less specific, as vascular smooth muscle cells and stressed or injured cardiomyocytes are also known to overexpress αSMA[156, 157]. In addition to αSMA, the actin cytoskeleton of myofibroblasts is enriched with Non-Muscle Myosin IIB (SMemb) which, along with the activation of Rho-GTPase signalling, imparts a contractile phenotype to these cells[158]. Myofibroblast contractility

is believed to help with wound closure, and provides critical structural stability to prevent ventricular rupture, post-MI[7, 159]. Morphologically, cardiac myofibroblasts are described as having a wide, kite-like surface area[160]. They also lose a great deal of their motility due to the development of mature focal adhesion complexes, also called "fibronexus complexes"[161]. These focal adhesions play an integral role in allowing myofibroblasts to sense their surroundings, especially changes in ECM composition and stiffness (further discussed in Section 1.2.2)[162-164].

Along with the structural and morphological changes involved in fibroblast activation, cardiac myofibroblasts also become hypersecretory for structural ECM components, matricellular proteins, cytokines, and a multitude of mitotic factors which contribute to tissue remodelling. The most well-studied and reliable secreted markers of fibroblast activation include: POSTN, Collagen I and III, and CTGF (Fig 1.2) [3, 59, 97]. Finally, overexpression of the cell-surface marker PDGFRα has recently been associated with cardiac myofibroblast activation, both *in vitro* and *in vivo*[165, 166]. Again, while this broad panel of markers does enable relatively accurate identification of activated myofibroblasts, there still exists significant crossover with other cardiac cell types, especially VSMCs and endothelial cells.

1.2 Cardiac Fibrosis

Cardiac fibrosis is clinically defined as the excess deposition of cardiac ECM, which is often attended by impaired ejection fraction, ventricular wall compliance, and/or electrical conductance [167]. Fibrosis is a companion to most cardiac pathologies, and its severity often dictates adverse patient outcomes. It can be classified under two broad types: replacement fibrosis (i.e. post-MI) and reactive interstitial fibrosis (i.e. in chronic heart failure, or due to

pressure overload)[168]. Because adult cardiomyocytes possess inadequate regenerative capacity, the initial wound healing response after myocardial injury is required to partially restore structural integrity to the ventricular free wall after the sudden loss of heart muscle. While post-MI and pressure overload-induced fibrosis are most commonly studied, several other pathologies such as metabolic and aging-related stressors, genetic cardiomyopathies, and viral myocarditis can also induce the replacement of cardiomyocytes with collagenous scar tissue[3, 5, 7]. The initial insult notwithstanding, the pathogenesis of cardiac fibrosis is propagated by a concerted stimulus of pro-inflammatory growth factor signalling (Fig. 1.3), as well as mechanical input from the interstitial microenvironment (Fig. 1.4).

1.2.1 Cardiac Fibroblast Activation and Fibrosis: Growth Factor Signalling

1.2.1.1 Transforming Growth Factor-β

The archetypal growth factor signalling cascade associated with cardiac fibrosis is that of TGF-β_1. While most growth factors act in a paracrine or autocrine fashion, TGF- β_1 is unique in that it exists in a latent form within the cardiac ECM, and needs to be "activated" to stimulate myofibroblast gene expression and pro-fibrotic signalling [82, 169, 170].

The TGF-β Superfamily of growth factors consists of over 30 regulatory proteins which are classed into five functionally-related subfamilies, including TGF-β, Bone Morphogenic Protein (BMP), and activin/inhibin[13]. The TGF-β subfamily consists of 3 pleiotropic isoforms, TGF-β_1, -β_2, and -β_3, whose functions include modulating inflammatory responses, cell proliferation, apoptosis, and ECM synthesis and deposition[171, 172]. TGF-β_1 is particularly potent in its ability to stimulate the pro-fibrotic response, as its activation and intercellular signalling cascade stimulates the myofibroblast phenotype and the secretion of fibrillar collagens[7, 171, 173].
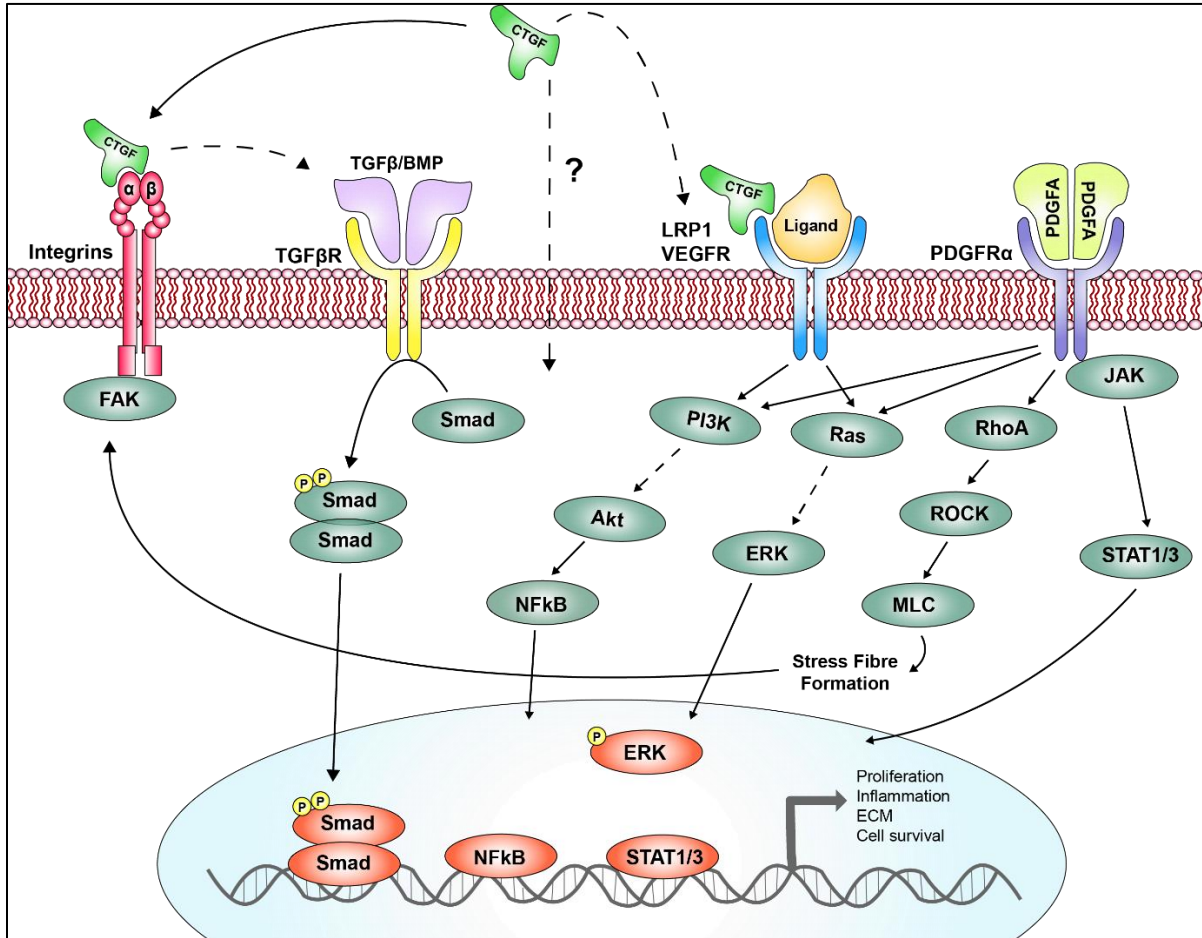
Figure 1.3: Summary of growth factor signalling in fibroblast activation and fibrosis.
The TGF-β, CTGF, and PDGF signalling pathways promote the activation of cardiac fibroblasts through several common intermediaries. The canonical TGF-β_1 signalling cascade is stimulated through SMAD signalling, but can also be transduced via p38/MAPK kinases (not shown). CTGF signalling is multifaceted as the protein does not have its own receptor; rather, CTGF binds other receptors to enhance signalling, and may be endocytosed into the cytosol where it can further enhance pro-fibrotic signalling. Finally, cardiac fibroblast activation is also mediated by PDGFRα, which activates a number of downstream signalling cascades, including PI3K/Akt, Ras/Raf/ERK, and RhoA/ROCK/MLC. Regardless of the growth factor indicated, all induce cardiac fibroblast activation and promote cell proliferation and survival, ECM synthesis and deposition, as well as inflammatory signalling.

It is secreted by several cell types, including stromal and immune cells, as a large latent

complex (LLC) [170]. The LLC is composed of TGF-β_1, its latency-associated protein (LAP), and

a covalently-bound, RGD-rich Latent TGF-β_1 Binding Protein (LTBP)[170, 174]. The LTBP

enables the LLC to interact with matrix proteins and sequester TGF-β_1 until it is released by

proteolytic cleavage, ROS and low pH, or tensile and contractile forces exerted by the ECM and myofibroblasts [170, 175, 176].

Once released from its latent form, the active TGF-β_1 ligand binds to heterotetrameric membrane-bound TGF-β receptors type I (TβRI) and II (TβRII) [13, 177]. From here, several intracellular signalling cascades are activated, but fibrosis is typically associated with canonical SMAD-dependent pathways [13]. SMADs consist of three groups of signaling proteins: Receptor-associated (R-SMAD1, 2, 3, 5, and 8), Co-SMAD (SMAD4), and Inhibitory (I-SMAD6 and 7) [13, 178, 179]. It should be noted that SMADs 1,5,6, and 8 and associated with BMP signalling, while SMAD 2,3 and 7 are downstream of TGF-β_1 [13]. After ligand binding, cytoplasmic R-SMADs are phosphorylated by TβRI, which then allows them to associate with co-SMAD4. The phospho-R-SMAD/co-SMAD complex translocates to the nucleus, and recruits other transcriptional co-activators such as CREB Binding Protein (CBP) and p300[13, 179]. These active SMAD transcriptional complexes preferentially localize to SMAD-Binding Elements (SBEs) in the promoters of >500 mammalian genes, to promote both physiological and pathological gene expression[13, 178]. Conversely, I-SMADs form a negative feedback loop which inhibits the formation of R-SMAD/Co-SMAD complexes, leading to the eventual downregulation of TGF-β-triggered events[13].

1.2.1.2 Connective Tissue Growth Factor

Unlike TGF-β_1, CTGF does not behave like a growth factor in traditional way because it does not have a distinct receptor through which it induces signal transduction. Rather, CTGF acts as an intermediary between cytokines (e.g. TGF-$\beta_{1, 2}$, VEGF, BMP4), matrix proteins (e.g. fibronectin, proteoglycans) and cell surface receptors (e.g. integrins, LRP1)[99, 180]. Although CTGF has very discrete, observable effects on the cellular environment and phenotype, the

mechanisms by which it modulates cell physiology remain at times contradictory. When considering cardiac fibrosis, CTGF may induce myofibroblast activation and enhance cell-matrix interactions, directly bind cell-surface receptors, or alter stromal cell adhesion and motility[85, 181]. It has also been suggested that CTGF could potentially be taken up by fibroblasts via endocytosis, where it can function as a modulator of intracellular signal transduction[180]. At a transcriptional level, CTGF expression is regulated by several regulatory factors[182]. Fibroblast-selective induction of *Ctgf* transcription has been reported as TGF-β-dependent, but does not always act via SMAD-dependent signalling[183]. In addition, recent investigations into Hippo signalling in post-MI fibrosis indicated that *Ctgf* transcription is markedly overexpressed in cardiac myofibroblasts from mice with conditional ablation of Hippo pathway kinases[184]. The Hippo pathway and its regulation of myofibroblast gene expression is discussed further in Section 1.3.5.

What is undeniable about CTGF, is its central role in tissue remodelling and cardiac fibrosis[159, 185, 186]. Upon myocardial injury, CTGF is released by both cardiomyocytes and fibroblasts; however, it only acts in an autocrine manner[97]. That is, fibroblast-specific deletion of *Ctgf* yields less myofibroblast activation, post-MI scarring, and fibrosis, while cardiomyocyte-specific deletion has no observable effects on tissue remodelling[97]. It was also found that it is required for the persistence of chronic TGF-β signalling and the formation of mature scar tissue[183]. Lastly, CTGF-neutralizing antibodies have shown promising results in reducing collagen deposition and cardiac dysfunction in murine models of dilated cardiomyopathy and pressure overload induced heart failure[187]. Furthermore, targeting upstream regulators of *Ctgf* transcription (e.g. serum response factor, SRF) and the *Ctgf* mRNA transcript, has yielded similar results in models of diabetic cardiomyopathy and AngII-induced

pressure overload[188, 189]. While the pre-clinical data is promising, there is limited information

regarding CTGF and its therapeutic potential in human heart failure patients. Thus far, it has

only been studied as a prognostic marker of diastolic heart failure in a very small cohort of

patients diagnosed with heart failure with preserved ejection fraction (HFpEF) [190].

1.2.1.3 Platelet-Derived Growth Factor

Another important mediator in cardiac fibrosis is the PDGF family of proteins. The five

known PDGF isoforms are potent angiogenic and mitotic factors, and induce signal

transduction via homo- or heterodimerization prior to binding their specific tyrosine kinase

receptors[3, 191]. Cardiac fibroblasts, as well as pericytes and VSMCs, express both α and β

PDGF receptors (PDGFR), and ligand binding events lead to fibroblast activation,

proliferation, and hypersecretion of ECM components[192]. The primary intracellular signalling

cascade associated with PDGFRs is through phosphoinositide 3-kinases (PI3Ks) and Ras

GTPase-associated mitogen-activated protein kinases (MAPKs)[180]. These pathways follow a

series phosphorylation events by MAPK kinases, which eventually result in the activation of

pro-fibrotic transcription factors. For example, PDGFR signalling in the heart is primarily

associated with gene transcription controlled by SRF and the Activator Protein 1 (AP-1)

complex, both of which modulate cell proliferation, apoptosis, and differentiation[180, 189]. PDGF

signalling is also associated with stress fibre formation, as it has been shown to activate

Rho/ROCK signalling and thus promote cell contractility[180,193].

Overexpression of PDGFRs and their ligands is associated with cardiac fibrosis in both

human and murine hearts[145, 192, 194]. This is especially true in the case of PDGF isoform A

(PDGF-A) and its receptor, PDGFRα, in post-MI remodelling and fibrosis. Injured

cardiomyocytes produce large amounts of PDGF-A, which then induces a significant pro-

fibrotic reaction in mesenchymal cells expressing PDGFRα[3]. Recent studies have shown that Collagen Iα1-expressing cardiac myofibroblasts overexpress PDGFRα in the infarct scar from 7 to 21 days post-MI, making it a good marker for identifying activated fibroblasts in tissue histology[145, 166]. Conversely, PDGFRα antagonism led to an apparent reduction in ventricular collagen deposition after ischemia-reperfusion injury[194]. Similar results were observed in a pressure-overload model, as an antibody-mediated PDGFRα blockade reduced atrial fibrosis and atrial fibrillation[195]. However, because PDGFRα is expressed in both the resting and activated fibroblast phenotypes, its validity and safety as a "druggable" target for cardiac fibrosis still requires further investigation.

1.2.2 Cardiac Fibroblast Activation and Fibrosis: Mechanical Stress

Cells within soft tissues exist in a physiological state that is governed by the structure and composition of their native environment. Mesenchymal cells are especially sensitive to the internal and external cues transmitted by the stiffness, or elastic modulus (E), of the ECM[196]. This change is readily observed in isolated cardiac fibroblasts, whose spontaneous phenotype on conventional polystyrene culture surfaces is pro-fibrotic, while modified soft-substrate cell culture yields a phenotype that is closer to the resting fibroblast[1, 165]. Healthy human myocardium has a stiffness of E = 5-10 kPa, while fibrotic ventricle loses much of its elasticity at $E > 100$ kPa[196, 197]. Thus, the mechanosensory behavior of cardiac fibroblasts and their related signalling cascades is an important factor to consider when studying the remodelling myocardium.

1.2.2.1 Mechanotransduction from the Cell Surface: Focal Adhesions

Focal adhesions are discrete protein complexes which form on the plasma membrane

and create an indirect signalling network between the ECM and the cell's actin cytoskeleton[198]. The complexes are highly sensitive to mechanical forces and dictate cellular response. changes in the matrix environment; this can include ECM adhesion and cell migration, triggering gene expression, or remodelling of the actin cytoskeleton[198, 199]. For cardiac fibroblasts, integrins play a central role in dictating their phenotype in homeostasis and disease[200].

The pivotal components of focal adhesion complexes are integrins, a class of heterodimeric transmembrane receptors which cluster to mediate matrix-dependent signal transduction[200, 201]. Integrins do not possess any innate enzymatic activity, and so their signaling capacity is entirely dependent on protein-protein interactions and mechanical input from the extra- and intra-cellular environment[202]. Integrin complexes consist of one α and one β subunit, creating a possible 24 heterodimers, and the combinatorial effects of αβ groupings yields different extra- and intracellular responses[203]. In cardiac fibroblasts, integrins are upregulated in the fetal gene program and in myofibroblast activation[199]. Stretch-induced activation of integrin signalling is mediated in an ECM-dependent way. For example, collagen-binding integrins (e.g. α1β1 and α3β1) will yield different intracellular signals and gene expression than fibronectin-binding integrins (e.g. α5β1 and α8β1), and both types are highly responsive to the stiffness of their tissue microenvironment [204-207]. A very important feature of integrin signalling is their role in the activation of latent TGF-β_1, especially by dimers containing the α5 subunit[207]. Cell traction forces (i.e. ECM strains induced by cell contraction via focal adhesions) are transmitted to RGD binding sites on the LAP, which induces a conformational change in the LLC, releasing TGF-β_1 into the extracellular space[201].
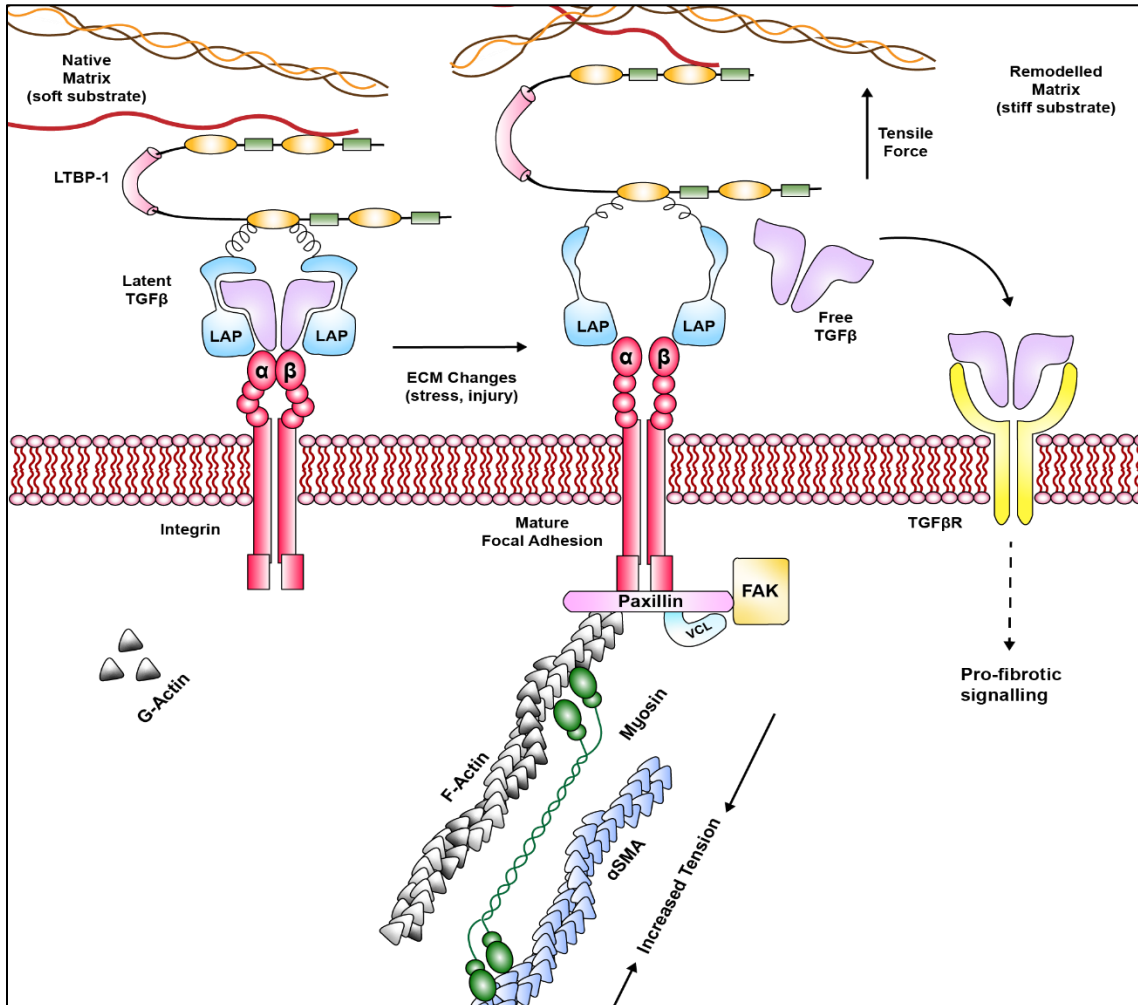
Figure 1.4: Summary of mechanotransduction in fibroblast activation and fibrosis.
Integrin binding to the RGD-rich latent TGF-β_1 complex transmits intracellular force to the extracellular matrix. Native (soft) matrix does not promote F-actin polymerization, and results in a closed LAP conformation. Conversely, remodelled (stiff) matrix increases tensile force on the latency complex, forcing it open, releasing latent TGF-β_1, and making it available to its receptor. The result is a feedforward loop of pro-fibrotic signalling.

Along with integrins, focal adhesions contain several adaptor proteins which associate with the cytoplasmic domains of the protein heterodimers. These other components possess enzymatic, catalytic, or scaffolding properties which drive signal transduction from the ECM into the cell, or from the actin cytoskeleton into the extracellular space. One important protein involved in integrin-mediated fibrotic signalling is Focal Adhesion Kinase (FAK), which is

activated by tensile forces in the ECM as well as growth factor signalling. Co-localized with FAK are Paxillin and Vinculin (VCL), which act as important anchoring points with the actin cytoskeleton and transmit forces to and from the ECM[208]. Other proteins, including those of the LIM Domain family (see Section 1.5.1), also concentrate at focal adhesion complexes and act as messengers in mechanosensitive and adhesion-stimulated signal transduction[209]. Most importantly, these messenger proteins dictate actin cytoskeleton dynamics in response to changes in the cardiac ECM, and the degree to which filamentous actin (F-actin) stress fibers form and depolymerize to globular (G-actin)[208, 209].

1.2.2.3 Mechanotransduction by the Cytoskeleton: Actin Dynamics

The actin cytoskeleton is an ever-changing structural network that controls cell motility and shape, and serves as a framework for signalling and organelle connectivity. Cardiac fibroblasts, and nearly all cell types, adjust their cytoskeleton's composition in response to the ECM stiffness, and these changes affect their gene expression, function, and physiology[196, 210]. Cytoskeletal stiffness and contractility are delimited by the ratio of F-actin stress fibers and soluble G-actin monomers, and the flux between these states occurs concurrently to the shifts between the fibroblast and myofibroblast phenotypes[196].

The signalling pathways involved in cardiac fibroblast actin dynamics originate at focal adhesions and transmit to the intracellular environment, primarily via RhoA GTPase[199]. Downstream activation of Rho Kinase (ROCK) then leads to the phosphorylation of Myosin Light Chain (MLC), which in turn promotes αSMA-positive stress fibre formation and actin contractility. This signalling cascade is complemented by a number of actin-associated proteins which finely modulate fibroblast physiology. For example, F-actin polymerization also modulates the Hippo signalling pathway by competitively interacting with regulatory elements

upstream of its nuclear effectors[199]. With upregulation of cytoskeletal stress, Angiomotin (AMOT) and Angiomotin-Like (AMOTL) proteins inhibit Hippo signalling by upregulating the nuclear translocation of the Yes-Associated Protein (YAP) and Transcriptional co-Activator with PDZ binding motif (TAZ, or WWTR1)[211, 212]. YAP/TAZ are potent co-activators of *Ctgf* transcription, and have been associated with enhanced TGF-β_1 signalling[213]. Until now, this phenomenon has not been studied in cardiac fibroblasts, though nuclear localization of YAP/TAZ has been observed in lung, liver, and kidney fibrosis[213-215]. Mechanical regulation of YAP/TAZ signalling is elaborated upon in Section 1.3.2.

Although they are often overlooked in traditional molecular experiments, mechanical cues are crucial to our understanding of cardiac fibroblast physiology. Manipulation of ECM stiffness both *in vivo* and *in vitro* is becoming an important factor when evaluating new data, and should inform future research into the prevention and treatment of cardiac fibrosis.

1.2.3 Human vs. Murine Cardiac Fibroblasts and Fibrosis

Most of the current knowledge regarding cardiac fibroblast physiology has been acquired using mouse and rat models of disease, and this presents the concern that we know very little about human cardiac fibroblast biology[137, 216]. Studies using primary human cardiac fibroblasts typically involve the use of cells isolated from discarded tissue from sick patients undergoing elective surgery[216]. As such, the cells are not only observed in physiologically extraneous conditions, but are also acquired from sources that pre-condition them to a pro-fibrotic phenotype. Conversely, when observing murine cardiac fibroblasts *in vitro*, the spontaneous phenotype of mouse and rat cardiac fibroblasts expresses large amounts of αSMA, the gold-standard marker for fibrosis in human myofibroblasts[1, 165]. Furthermore, recent studies have suggested that human and murine cardiac physiology and pathophysiology are much

more divergent than once thought[217]. When comparing circulating markers and miRNAs from human heart failure patients to slowly-hypertensive Ren2 rats and AngII-treated mice, it is not possible to validate established animal models with respect to actual human heart failure[217]. These results could indeed represent an ongoing inability to generate truly translatable data in cardiac fibrosis research, or it could simply reflect the problem that chronic fibrosis and heart failure models are difficult to generate in animals with such a short lifespan[218]. It would be easy to dismiss the validity of murine models of heart disease and fibrosis; however more high-throughput, cell-specific studies (i.e. proteomics, transcriptomics, interactomics) will likely lead to emerging targets and companion biomarkers to better predict the pathogenesis of fibrosis and heart failure in the future.

1.2.4 Current and Future Treatments for Cardiac Fibrosis

Regardless of its prevalence in the Western world, cardiac fibrosis is a condition that remains relatively enigmatic in its pathogenesis and treatment. Conventional clinical intervention for post-MI fibrosis involves the use of pharmacological tools to stave off the onset of heart failure with reduced ejection fraction (HFrEF), improve hemodynamics, and to alleviate the overall symptoms of cardiac insufficiency[219]. The first-line treatment algorithm recommended by the National Institute for Health Care Excellence for post-MI heart failure patients consists of what is colloquially referred to as "triple therapy": ACE inhibitors, beta-blockers, and a mineralocorticoid receptor antagonist, often in conjunction with dual anticoagulant therapy (i.e. aspirin and a $P2Y_{12}$ receptor inhibitor, such as Clopidogrel or Ticagrelor)[219]. The combination of these therapies reduces blood pressure, cardiac contractility and heart rate, regulates serum sodium levels, and prevents the reoccurrence of a MACE, respectively. Because this line of attack is intended only to alleviate symptoms, there is much

interest in therapeutic interventions that can reduce the rate of fibrogenesis and preventing heart failure.

There are currently several clinical trials which are attempting to prevent the expansion of the cardiac interstitium after the initial wound healing response, targeting fibrosis at its source. The PIROUETTE trial is testing the efficacy of the drug Pirfenidone in patients with heart failure, especially those with reactive fibrosis and HFpEF[220]. The mechanism of action of Pirfenidone is poorly understood, but it has been shown to inhibit TGF-β and pro-collagen synthesis, as well as pro-inflammatory Tumor Necrosis Factor-alpha (TNFα) signalling[221, 222]. It is believed that this synergistic action prevents further proliferation of myofibroblasts, extending the time between the tissue injury, and the onset of fibrosis. Currently approved for the treatment of idiopathic pulmonary fibrosis, Pirfenidone is showing promise as a true anti-fibrotic agent as the PIROUETTE trial has entered Phase II.

Another promising treatment for cardiac fibrosis is the use of Sodium-Glucose Transporter 2 (SGLT2) inhibitors, or the "gliflozin" class of drugs[223]. Originally developed as a replacement for metformin for the treatment of type II diabetes mellitus, the drugs Canagliflozin (CANVAS trial), Empagliflozin (EMPA-REG trial), and Dapagliflozin (DECLARE-TIMI trial) have all shown promise in their ability to reduce the occurrence of heart failure in post-MI patients, regardless of whether the individual is diabetic[224]. Subsequent *in vitro* investigations of Empagliflozin determined that one unexpected benefit of the drug is its ability to reverse myofibroblast activation, and promote a resident fibroblast phenotype[225]. Isolated cardiac myofibroblasts treated with Empagliflozin presented fewer F-actin stress fibers, less pro-fibrotic gene expression, and lessened the cells' ability to respond to TGF-β treatment[225]. Ongoing trials (DEFINE-HF, and EMBRACE-HF) to test the efficacy of these

drugs in a larger cohort of patients with HFrEF and/or with worsening heart failure are expected to confirm whether gliflozins should be indicated for first-line treatment of cardiac fibrosis and heart failure[224].

Finally, another method of intervention for post-MI fibrosis involves the use of hydrogel-based injectable biomaterials, and using native cardiac ECM as a vehicle for treatment delivery. This moderately-invasive method is currently in Phase I of clinical trials, where Ventrigel™ (Ventrix Inc., San Diego, CA, USA), a proprietary flowable material composed of decellularized porcine cardiac ECM, is administered by repeated transendocardial injections into the damaged ventricle after the maturation of the infarct scar (i.e. >60 days post-MI)[226]. The technique is based on the hypothesis that introducing healthy ECM into the damaged would stabilize the interstitium, provide extra structural support, and promote physiological fibroblast signalling, rather than a pro-fibrotic phenotype[226]. Early results in a small cohort of patients (n = 15) with mild heart failure demonstrated that there was marked improvement in in LV remodelling and fibrosis, viable myocardial mass, and a decrease in circulating Brain Natriuretic Peptide (BNP), a companion biomarker used to estimate the severity of heart failure[226]. The beneficial effects were especially noticeable in patients whose MI occurred >12 months prior to receiving the Ventrigel. While these results are promising, it should be noted that the cohort was overwhelmingly (80%) male, and that some patients were unable to receive all 18 injections of the material due to an increase in ventricular wall thickness[226]. As such, Phase I trials are ongoing and are expected to further demonstrate the safety and efficacy of using the ECM itself as a tool for healing failing hearts.

1.3 Hippo Signalling Pathway

The Hippo signalling pathway was first observed in genetic knockout studies in *Drosophila melanogaster* [227-229]. When upstream components of the signalling cascade were genetically ablated, the resulting *Drosophila* acquired a tumorigenic phenotype which gave a hippopotamus-like appearance, hence the pathway's clever moniker [227, 228]. Subsequently, the Hippo pathway was found to be an essential developmental pathway that regulates cell fate and organogenesis across phyla (Fig. 1.5) [230]. The Hippo pathway has also been referred to as a tumor-suppressor pathway, and its dysfunction has been associated with hyperplastic pathologies including cancer metastasis, neurodegenerative disease, and fibrosis [231-233].

Bearing significant resemblance to the mitotic exit network in *Saccharomyces cerevisiae*, the Hippo pathway serves as a point of cell cycle exit in eukaryotes[234]. In mammals, the canonical sequence of intracellular signaling transduction is initiated when Macrophage Stimulating factors (MST1/2) and Salvador homolog 1 (SAV1) form a complex which phosphorylates and activates Large Tumor Suppressor kinases 1 or 2 (LATS1/2)[235]. From here, LATS1/2 binds Mps One Binder kinases (MOB1/2) which catalyzes their activity. In its activated state, the LATS/MOB complex can then proceed to phosphorylate YAP and/or TAZ, the primary nuclear targets of the pathway[235]. When phosphorylated, YAP and TAZ are sequestered to the cytoplasm, where they are degraded via the ubiquitin-proteasome system[236]. When not phosphorylated (i.e. Hippo pathway is inactive), YAP/TAZ exert their regulatory activity by associating with SRF, SMAD, and TEA Domain (TEAD) transcription factors to promote pro-mitotic gene expression[236]. As a result, the Hippo pathway and YAP/TAZ signalling has garnered significant interest as potential points of intervention for metastatic and fibrotic disease.
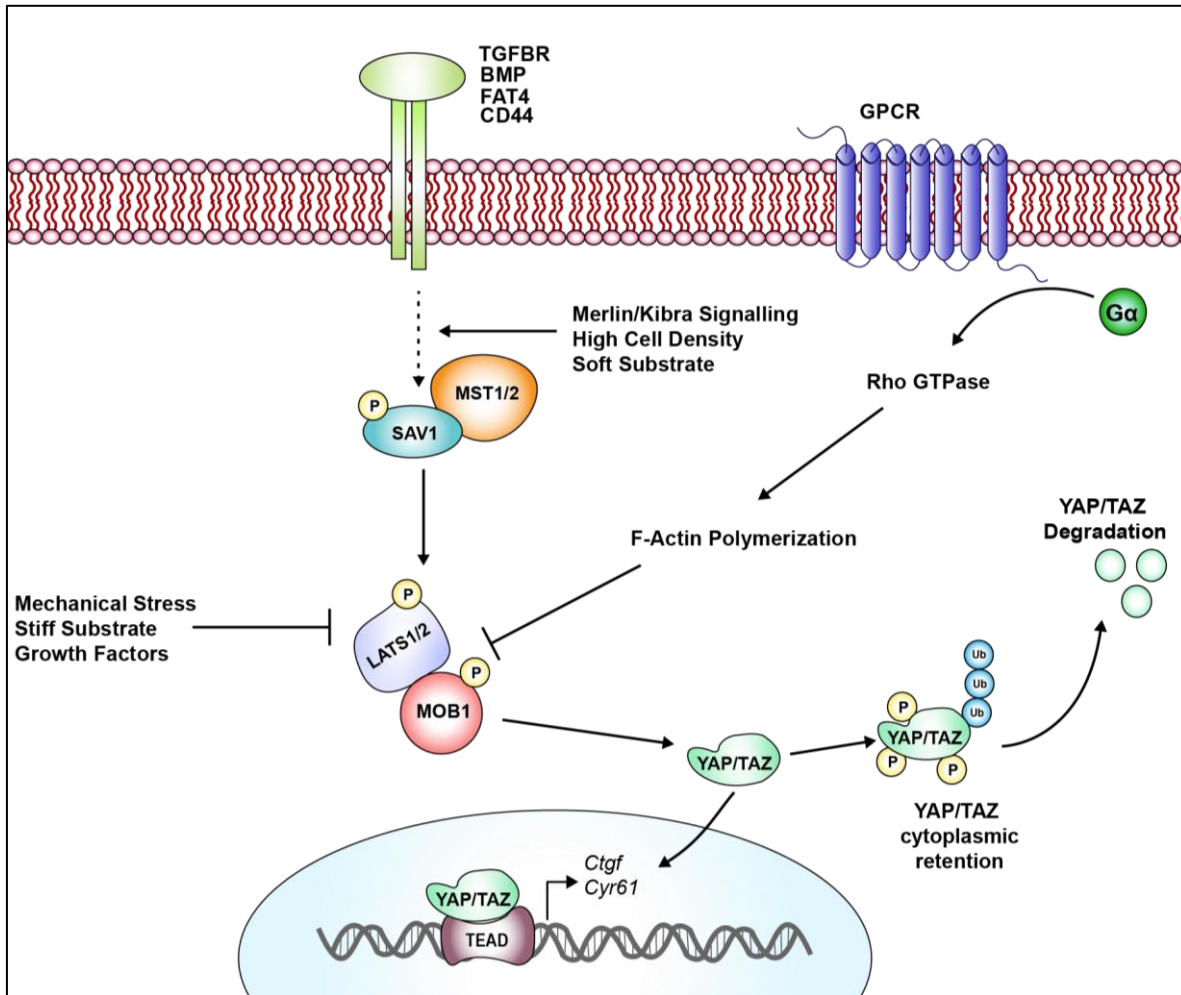
Figure 1.5: The core Hippo signalling pathway.
Mst1/2 kinase (Hippo in *Drosophila*) forms a complex with SAV1, which in turn phosphorylates and activates LATS1/2. Active LATS1/2 associates with MOB1, which potentiates its kinase activity on YAP and TAZ. If phosphorylated, YAP and/or TAZ are sequestered to the cytoplasm, where they are subject to polyubiquitination and proteasomal degradation. If LATS1/2 complex is inhibited (i.e. Hippo signalling is "off"), YAP/TAZ can translocate to the nucleus to associated with TEAD transcription factors and influence gene transcription.

1.3.1 Large Tumor Suppressor kinases (LATS)

The LATS kinases belong to the AGC family of proteins, and are ubiquitously expressed in mammalian tissues, except for the spleen[237, 238]. While the literature often describes LATS1 and LATS2 as having similar functions within the cell as they likely exist

due to gene duplication, there is ample evidence they are differentially regulated and do not necessarily possess the same binding partners[239, 240]. In fact, several pathway analyses have shown that LATS2 has up to 25 times more binding partners than LATS1, depending on the context, and may play a more significant role in regulating intracellular signal transduction[239].

Human LATS1 and LATS2 share significant sequence homology at their C-termini (~85%), but diverge in the regions near their N-termini[239]. The C-terminal region in LATS1/2 contain the activation loops which form the kinase catalytic domain, and a hydrophobic motif which resembles the functional domain of AKT kinase[241]. Just upstream of the kinase domain lies the protein binding domain, which is crucial for interactions with MOB1 and LIM domain proteins[209, 239]. Within the N-terminus of LATS1, there is a proline-rich region, while in LATS2 the same region contains a PAPA repeat; each of these is thought to possess unique protein interaction abilities[239]. Finally, the relatively-conserved area of the N-termini is the PPxY motif, of which LATS1 has two and LATS2 has one[242]. The PPxY motif is critically important for LATS1/2 interaction with YAP/TAZ, and other proteins which contain a hydrophobic tryptophan repeat (WW) domain[239].

In developmental pathways, individual *Lats* genes have been observed to have disparate functions. Genetic ablation of *Lats2* is embryonic lethal, and it is believed that the lethality arises from excessive cell proliferation accompanied by genetic instability. Conversely, transgenic mice with global knockout of *Lats1* were viable, albeit with pituitary gland dysfunction and infertility, and a propensity for the spontaneous formation of soft tissue sarcomas[243]. In humans, somatic mutations in the kinase domain of *LATS1* and *LATS2* have been found in primary stomach, endometrial, and lung adenocarcinomas[244]. There are no known congenital diseases associated with *LATS* gene mutations, but if the murine knockout

models reflect the human response, any non-silent mutation might negatively affect fetal development and viability.

Like many other proteins, LATS kinase function is governed by its subcellular localization and binding partners. LATS1/2 function is regulated by a series of post-translation modifications, as well as upstream signals of contact inhibition, tethering to focal adhesions, and cytoskeletal alterations (discussed in Section 1.3.2). Both LATS1 and LATS2 possess autophosphorylation and protein kinase abilities which modulate their inhibitory function. Interaction with MOB1 at their hydrophobic domain leads to the autophosphorylation of a series of serine and threonine residues which augment the LATS1/2 kinase activity towards YAP/TAZ. The MOB1-LATS interaction is precipitated by a number of different kinases, including MST1/2, MAP4Ks, KIBRA (Kidney and Brain expressed protein), and Merlin (also called Neurofibromin 2)[239, 241]. The phosphorylation status of LATS kinases also affects their stability, and can signal for their polyubiquitination and proteasomal degradation. E3 ubiquitin ligases target both LATS1 and LATS2 equally, while WW domain-containing ligases preferentially target LATS1[239]. LATS2 has also been observed in an inactive, polyubiquitinated state without loss of protein stability, suggesting that it is subject to more nuance post-translational regulation. Furthermore, LATS2 is likely to possess some function beyond YAP/TAZ inhibition, as recent investigations have reported that it can act upstream of LATS1 to enhance its activity towards other proteins[245].

Due to their central role in the activation of Hippo signalling, and their key function in the regulation of YAP/TAZ, LATS1/2 are targets of high interest for hyperplastic pathologies. Despite this notion, LATS1 is highly expressed in most tissues, while LATS2 expression is

much more variable[246]. Thus, the tissue- and pathology-specific impact of each kinase remains to be fully revealed.

1.3.2 YAP and TAZ (WWTR1) Transcriptional o-Regulators

The paralogs YAP and TAZ are canonical nuclear targets of Hippo signalling in mammals, and function to activate and enhance proliferative and pro-survival gene expression[247]. Originally described by the laboratory of Marius Sudol, YAP was identified for its ability to bind proteins containing Src Homology domain 3 (SH3), such as FAK, Ras GTPase, and myosins[248]. It was not until several years later when the gene product of WW domain-containing Transcriptional Regulator 1 (*WWTR1*), TAZ, was identified as having significant sequence and structural similarity to YAP (Fig 1.6)[249]. Both proteins were soon found to be homologous to the *Drosophila* protein Yorkie, a component of the then-nascent Hippo tumor suppressor pathway[230]. Since then, much research has been conducted to demonstrate the function and regulation of YAP and TAZ, and whether they can be of therapeutic value in the treatment of proliferative disease, such as cancer and fibrosis (as reviewed by Noguchi *et al.*)[250].

1.3.2.1 YAP/TAZ Structure and Function

The most prominent structural feature common to both YAP and TAZ is the conserved central WW domain. Possessing mostly protein-binding function, the WW domain consists of two tryptophan residues separated by 20-23 amino acids which form a hydrophobic pocket[251]. Human TAZ contains one WW domain, while YAP contains two as tandem repeats, although truncated YAP isoforms with only one WW motif have been identified[236, 252]. The WW domains in YAP/TAZ specifically recognize other WW-containing proteins, as well as the PPxY motifs in upstream regulatory elements, including LATS1/2[239, 240]. At the C-terminus,

both YAP and TAZ contain yet another protein-interacting domain, the PDZ-binding motif.

Composed of 80-90 amino acids, the PDZ-binding motif is found in signaling peptides across

phyla, and they often associate with the actin cytoskeleton and transmembrane anchoring

complexes[253]. For YAP/TAZ signalling, the post-translational modification of the PDZ-binding

motif can also dictate its subcellular localization. Just upstream of the PDZ sequence lies what
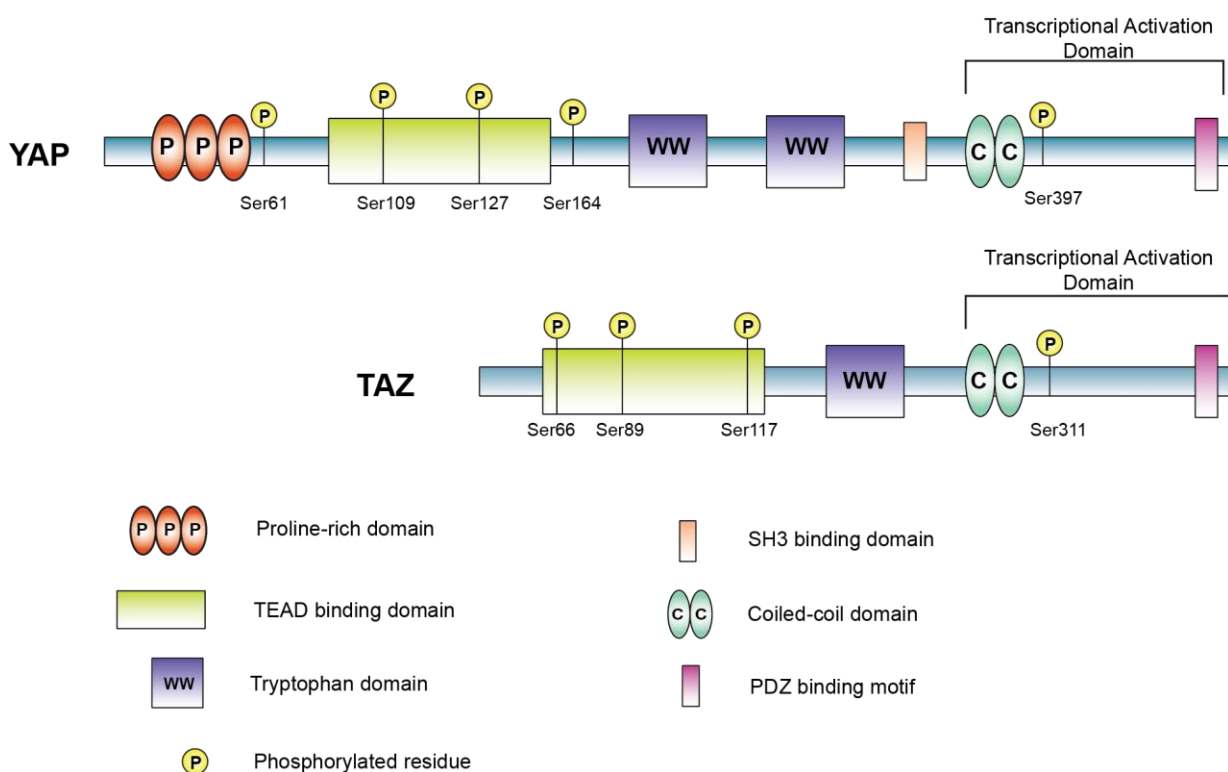
Figure 1.6: A comparison of YAP and TAZ protein structure.
The primary functional domains of YAP and TAZ include the TEAD-interacting and Transcriptional
Activation domains. Both proteins contain tryptophan (WW) domains, which promote interaction with
other WW-containing proteins. Important post-translational phosphorylation sites which regulate
subcellular localization and protein stability are indicated. Figure was adapted from information
reviewed in *Development*. 2014 Apr;141(8):1614-26, and *J Cell Sci*. 2020 Jan 29;133(2). pii:
jcs230425.

is commonly-referred to as the "transcriptional activation domain"; however, this term is solely based on limited information regarding the phosphorylation of a specific tyrosine residue (Y321 in TAZ; Y407 in YAP) and its resulting transcriptional effects[236, 254]. Apart from the tyrosine residue, the transcriptional activation domain bears little structural resemblance between the two paralogs. Finally, the N-terminal region of YAP/TAZ structure is composed of two highly-conserved elements: a TEAD transcription factor binding domain, and a 14-3-3 binding motif[236]. The YAP/TAZ TEAD binding domains contain two α-helices separated by a loop; however, the YAP loop structure contains a PXXΦP motif (where Φ denotes any hydrophobic residue)[255]. As such, YAP and TAZ have differential affinity towards TEAD transcription factors, but the physiological ramifications of this distinction have yet to be determined[256]. What is known, is that studies involving site-directed mutagenesis of the TEAD binding domain have demonstrated that it is required for the hyperplastic and tumorigenic phenotypes associated with YAP/TAZ activation[257, 258]. Immediately following the TEAD binding domain is a nearly-conserved phosphor-serine motif RSXpSXP (S89 in TAZ, S127 in YAP) which binds 14-3-3 proteins[249]. When phosphorylated, 14-3-3 proteins sequester YAP/TAZ to the cytosol where they are subsequently ubiquitinated and degraded. Substitution of alanine at these serine residues has been shown to be sufficient to promote nuclear retention of both YAP and TAZ, and mutations at these sites has been identified in several aggressive cancer genotypes[236, 237, 250].

Due to their enhanced activity in cancer and cell survival, it is unsurprising that YAP and TAZ enhance the transcription of genes that are also highly-expressed in fibrotic disease[250, 259, 260]. While the two proteins do not directly bind DNA, YAP and TAZ have been found to occupy regulatory elements in the promoters of *CTGF*, *BIRC5*, *CYR61*, *AREG*, and

ANKRD1 in human cells and tissues[250, 260]. These genes are targets of the TEAD family of transcription factors, all of which are associated with pro-survival and -proliferation gene activation. Still, YAP/TAZ-associated gene transcription is not entirely dependent on TEAD proteins. Several studies have immunoprecipitated either paralog in conjunction with SRF, RUNX2, as well as SMAD transcription factors. As such, YAP/TAZ and Hippo signalling are often studied in contexts which bear significant crosstalk with other pathways that govern cell cycle re-entry (e.g. TGF-β, MAPK).

1.3.2.2 Regulation of YAP/TAZ Protein Stability

Very little is known regarding the regulation of *YAP/TAZ* gene transcription, and so much of the available information pertaining to their expression and activity relates to post-translational modification and Hippo-mediated activation of the ubiquitin-proteasome system[259]. YAP/TAZ protein turnover is regulated much like LATS1/2, via phosphorylation of a several serine residues in a phosphodegron motif, as well as modifications leading to nuclear-cytoplasmic shuttling. Several kinases other than LATS1/2 have been shown to regulate YAP/TAZ stability in a fairly conserved manner, such as Casein Kinase 1 (CK1) family members. However, some preferentially target one paralog over the other; for example, Glycogen Synthase Kinase 3β (GSK3β) has only been shown to regulate TAZ expression[259]. Regardless of the kinase involved, the phosphorylation of the phosphodegron motif then primes YAP/TAZ for polyubiquitination by a number of potential ubiquitin ligases. The most commonly recruited is β-TrCP/SCF E3 ubiquitin ligase, which equally labels YAP and TAZ for proteasomal degradation, albeit from different phosphodegron signals[259, 261, 262].

1.3.2.3 Mechanoregulation of YAP/TAZ Activity

Along with post-translational modifications, YAP/TAZ activity is intimately linked to mechanical cues at the cell and tissue level. The formation of mature focal adhesions, attended by ECM tensile forces and induction of cytoskeletal contractility, is a nearly universal requirement for the maintenance of active nuclear YAP and TAZ in stromal cells[213, 259, 261]. Both F-actin and Rho GTPase play essential roles in the cytoskeleton dynamics and stress fiber formation, and thus their activity is closely linked with YAP/TAZ subcellular localization. Work published simultaneously by two independent groups demonstrated the link between F-actin stabilization and the downregulation of Hippo activity in *Drosophila* [263, 264]. These studies demonstrated that inhibition of F-actin in isolated cells prevented nuclear localization of Yorkie (YAP/TAZ), and that genetic deletion of actin-capping protein (*Capz*) yields the same results[264]. These effects were specific to F-actin polymerization, as inhibition of myotubule formation by nocodazole did not produce any change in Yorkie activity[263].

In mammalian cells, YAP/TAZ activity is regulated by cell morphology and attachment, as well as ECM elasticity[211]. Cell spreading requires the activation of Rho GTPase to form F-actin stress fibers and contractile actomyosin systems; this process can be accelerated *in vitro* by culturing cells on stiff plastic matrices[265, 266]. With this in mind, Hippo signalling was examined in various epithelial cell lines as well as mesenchymal stem cells cultured on hydrogels with increasing elastic moduli (0.2-40 kPa)[211, 267]. It was found that culturing on stiffer hydrogels drastically increased YAP/TAZ nuclear retention and target gene transcription, while softer hydrogels yielded the opposite result. Similarly, YAP/TAZ nuclear translocation could be controlled by limiting or extending the available area for cell adhesion: a larger surface area (i.e. more cell spreading) yielded more nuclear YAP/TAZ, while a smaller

surface area promoting cytosolic retention of the proteins[211]. YAP could also be artificially driven to nuclear or cytoplasmic translocation by treating cultured cells with F-actin stabilizing agents like Jasplakinolide, or disrupting agents such as Latrunculin A[211, 268, 269]. As a result of these findings, the gold-standard demarcation for the measurement of YAP/TAZ activity is now the nuclear localization of either paralog.

In addition to actin dynamics, cell-matrix and other adhesion-associated signals have been shown to modulate YAP/TAZ activity[270, 271]. Also heavily influenced by ECM stiffness, focal adhesion maturation—that is, the formation large integrin-based complexes which promote stable attachment of cells to the matrix—promotes nuclear localization of YAP/TAZ[272]. While it is not a direct result of the flux between F- and G-actin levels in the cell, but the organization of the cytoskeleton, actomyosin tension, and the mechanosensory mediators downstream of focal adhesions which finely regulate YAP/TAZ activity. Several intermediaries, such as Angiomotin (AMOT) and their homologs (AMOT-like, AMOTL), stabilize the interaction of LATS1/2 with F-actin and prevent them from phosphorylating YAP/TAZ, allowing their nuclear translocation[273, 274]. These subcellular events can be dictated by perturbations in ECM composition. For example, cells cultured on collagen- or fibronectin-coated surfaces have a much higher attachment rate, lower motility, and marked induction of YAP/TAZ transcriptional activity when compared to uncoated surfaces[275, 276].

Transduction of tensile forces and attachment signals from the cellular microenvironment modulate YAP/TAZ localization, and thus determine the cell's response to its surroundings. As such, the mechanosensory regulation of Hippo signalling is of paramount importance in regulating cell phenotype and function; this axis of signal transduction is of particular consequence for fibroblasts, as discussed below.

1.3.3 YAP/TAZ in Development and Disease

Due to their mechanosensory role in orchestrating cell behavior, YAP and TAZ localization are essential for the determination of cell fate and tissue organization during embryogenesis. The nuclear-cytoplasmic shuttling of both paralogs enable the renewal and expansion of stem cell populations, and contribute to the determination of cell fate[236]. In transgenic mouse models mimicking upstream Hippo pathway defects (e.g. *Lats1/2 $^{-/-}$ Mst1/2$^{-/-}$*) result in embryonic lethality due to the failure of tissue patterning, especially in the heart field and neuroectoderm[277, 278]. *Yap* null mice share a similar fate, as they lose their viability at embryonic day 8.5 due to placental and vascular defects[279]. Interestingly, *Taz* knockout mice are generally viable, but spontaneously develop emphysema-like pulmonary disease, as well as chronic renal cysts[280]. Global double knockout studies (*Yap$^{-/-}$*, *Taz$^{-/-}$*) result in embryonic death prior to implantation. Several organ-specific models (i.e. liver, kidney, lung, skin, intestine, pancreas, and heart) of *Yap, Taz*, and *Yap/Taz* deletion demonstrate decreased organ size, and/or lethal loss of organ function, as well as impaired epithelial/endothelial barrier capacity (as reviewed by Varelas X., 2014; Zhao B., 2010) [236, 278, 281]. Unsurprisingly, overexpression or introduction of mutations generating constitutively-active *Yap* and *Taz* generate phenotypes which demonstrate hyperplastic growth, as well as impaired organ function[233, 250, 281].

Because YAP/TAZ activation strongly influences cell cycle re-entry, it is not surprising that their activity is upregulated in proliferative diseases. In cancer, several mechanisms which upregulated YAP/TAZ nuclear retention have been identified. For example, many cancers possess altered copy numbers of the chromosome 11q22 locus, which contains the *YAP* gene[282]. There have also been observations in rare hemangiosarcomas of aberrant N-terminal gene fusions (i.e. *TAZ-CAMTA1* and *YAP-TFE3*) which prevent the phosphorylation of YAP

and TAZ by the LATS kinases[283, 284]. It is surprising, however, that genetic mutations of any

Hippo component are exceedingly rare, and that there are currently no known cancers

associated with a specific activating mutation in *YAP/TAZ*[250]. Rather, increased YAP/TAZ

activity is often attributed to perturbations in upstream regulatory factors, as well as multiple

extrinsic factors that are concentrated in cancerous tissues. In a similar vein, fibrosis is also

associated with increased YAP and TAZ activation, albeit often in an etiology-specific manner.

For instance, in liver fibrosis specimens acquired from Hepatitis C Virus-positive patients,

YAP expression was upregulated and predominantly nuclear[214]. However, in non-alcoholic

steatohepatitis (NASH) induced fibrosis, TAZ was found to be the paralog which drove the

pro-fibrotic gene expression in hepatic stellate cells[285]. Apart from the liver, an increasing

number of investigations have associated upregulation of YAP and/or TAZ activity with

fibrosis in several other organs, including the skin, kidney, lung, and most recently, the

heart[184, 250].

 Overall, the current literature suggests that YAP and TAZ have interchangeable, or

even redundant, functions. While it is apparent that the global effects of overexpression or

knockdown of one can be recapitulated by the other, more recent investigations have brought

to light the possibility that their function diverges in a context-specific manner. Continued

investigation of the function of YAP and TAZ individually will render a better understanding

of specific disease states and whether the perceived YAP/TAZ redundancy is actually

emblematic of the diverse functions of two proteins.

1.3.4 YAP/TAZ in the Heart

 Mammalian hearts undergo two general phases of development: the hyperplastic

growth during embryogenesis, followed by the hypertrophic growth in postnatal heart

maturation. Numerous gain- and loss-of-function studies involving cardiac-specific *Yap* and/or *Taz* manipulation have associated the genes with both phases of cardiac development. At present, most transgenic analyses have only investigated the effects of *Yap* overexpression or knockout, as one study in mice with cardiomyocyte-specific knockout of *Taz* did not show any apparent differences from wild-type littermates[286]. Cardiomyocyte-specific *Yap* deletion generates a number of hypoplastic defects of the chambers of the heart, and the mice die anywhere from embryonic day 10.5 and 11 weeks postpartum, depending on the promoter used to induce the knockout[287]. However, because adult cardiomyocytes possess negligible proliferative capacity after injury, YAP and TAZ have garnered significant interest for its potential in regenerative medicine, especially in the post-MI heart. Embryonic induction of constitutively-active *Yap* (*S127A or S112A*) in cardiomyocytes produces a thickened myocardium and cardiomegaly[286]. When induced postnatally, constitutive *Yap* activation increases heart weight by upregulating cardiomyocyte proliferation, but not hypertrophy[288]. There are at present no cardiac-specific mouse models of *Taz* activation in the literature, yet it would be of value to investigate whether its produces similar or diverging effects to *Yap* in a cell-specific manner.

In addition to cardiomyocyte-specific manipulation of *Yap/Taz*, a very recent investigation by Xiao *et al*. has demonstrated the importance of YAP signalling in cardiac fibroblasts[184]. Using a *Tcf21*-inducible Cre mouse model, the group studied the effects of *Lats1/2* deletion, with and without *Yap* deletion, in adult cardiac fibroblasts. Upon deletion of *Lats1/2* alone, the mice developed spontaneous interstitial fibrosis of the ventricles, enlarged and fibrotic atria, and HFpEF[184]. Still, it was determined that *Lats1/2* are required for proper infarct scar maturation, as mice subject to coronary artery ligation only survived 3 weeks post-

MI due to extensive reactive fibrosis and ventricular rupture. When combined with genetic ablation of *Yap*, the *Lats1/2$^{-/-}$* mouse hearts showed a marked reduction of reactive fibrosis, but did not indicate any amelioration in infarct size or overall survival[184]. Once again, due to this study's explicit focus on *Yap* and not *Taz*, it is unknown whether the latter is implicated in the pathogenesis of cardiac fibrosis, and whether its manipulation in the post-MI heart could improve heart function and survival outcomes.

1.4 SKI

Originally identified by the laboratory of Edward Stavnezer as the cellular homolog of the avian Sloan-Kettering retrovirus (*v-ski*), SKI was characterized as a necessary nuclear factor in muscle cell differentiation that could also contribute to tissue-specific cell transformation [289, 290]. Several years later, the group then established SKI as a pleiotropic transcriptional co-repressor that exerts widespread inhibitory activity, but seemed to preferentially target SMAD-dependent TGF-β signalling [291, 292]. Investigations by other groups then identified SKI novel protein (SNO), as well as the *Drosophila* Dachshund protein (Dac) and its human homologs (DACH1/2) as closely-related proteins that exhibit paradoxical function which can both mimic and oppose SKI [293-295]. Since then, several proteins bearing similar functional domains have populated the SKI/SNO/DAC family, and their cell- and disease-specific functions remain to be fully defined.

1.4.1.1. Phylogeny, Structure, and Function

SKI is one of 13 members of the SKI protein Superfamily of TGF-β transcriptional co-regulators (Table 1.1). The *Ski* gene is highly-conserved among higher-order vertebrates, and consists of seven exons, with two unique isoforms[179]. The predominant SKI isoform observed

in humans is the full-length 90 kDa protein, while a 60 kDa isoform lacking exon 2 has also

been isolated[296]. Although originally speculated to result from alternative splicing, it has been

suggested that the two *SKI* transcripts arise from differences in the length of the 3' untranslated

region[297]. Both versions of human SKI tend to localize in the nucleus, however the low

molecular weight isoform possesses a much shorter half-life and has not been characterized to

have any function resembling its full-length counterpart[296].

Table 1.1: SKI Superfamily of proteins

Gene Name	Gene Product	Expression*
SKI	SKI	Ubiquitous, except in thymus
SKIDA1	SKIDA1	Ubiquitous, especially thyroid gland
SKIL	SNON	Ubiquitous
	SNON2	Ubiquitous, less abundant than SnoN
	SNOA	Ubiquitous
	SNOI	Skeletal muscle only
DACH1	DACH1	Ubiquitous
DACH2	DACH2	Ubiquitous, except in immune cells
SKOR1	SKOR1	Predominantly neuronal
SKOR2	SKOR2	Spinal cord, cerebellum, testis

*Based on entries from Genotype-Tissue Expression (GTEx) project, https://www.gtexportal.org/home/

SKI protein structure is described as having three primary domains (Fig. 1.7). The N-

terminus consists of a Dachshund Homology Domain (DHD) which is comprised of 100 amino

acids that alter between α-helical and β-sheet secondary structure. The DHD does not possess

any DNA-binding ability like its namesake (DAC protein), however it appears to be

responsible for the majority of SKI's protein-interacting functionality[179]. Transcriptional co-

regulators such as NCoR, Methyl CpG binding protein 2 (MeCP2), and histone deacetylases

(HDACs), have been shown to bind SKI via the DHD[298]. Several transcription factors also

associate with this domain, including GATA-binding factors and retinoblastoma protein

(Rb)[179]. Downstream of the DHD lies a SAND-like domain (named after $\underline{S}$p100, $\underline{A}$IRE-1,

$\underline{N}$ucP41/75, $\underline{D}$EAF-1), which facilitates SKI binding to SMAD4[299]. Genuine SAND domains

typically bind DNA in a Zn^{2+} dependent manner; however, the SKI SAND-like domain has not

demonstrated any DNA-binding properties[299]. The interaction between SKI and SMAD4 leads

to the downregulation of TGF-β_1 target gene transcription by recruiting NCoR and HDACs to

promoter SMAD-binding elements[300]. Finally, the C-terminus of human SKI has a coiled-coil
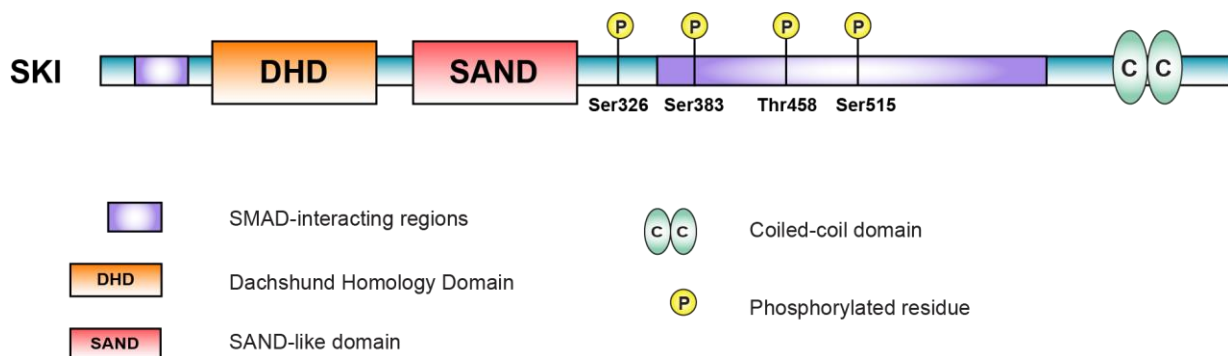
Figure 1.7: Human SKI protein structure.
The functional regions of human SKI include the Dachshund Homology Domain and SAND-like
domains. The central portion of the protein, while lacking any distinct secondary structure, is crucial for
SMAD interaction. Known post-translational phosphorylation sites which regulate protein stability are
indicated.

domain which is believed to facilitate the formation of SKI homodimers and SKI/SNO

heterodimers, although this observation was made in cell-free system, *in vitro*[301].

The middle segment of SKI does not bear any defined secondary structure, yet it

possesses much of its SMAD-binding capacity. The region spanning amino acid residues 312-

480 is especially important for the negative regulation of SMAD2/3-dependent signalling [302]. It

is believed that SKI wedges itself between SMAD2/3 and co-SMAD4, disrupting the active

transcription complex, which in turn enables the recruitment of HDACs to the gene promoter (Fig. 1.8) [302]. However, this mechanism of action has only been observed *in vitro*, and in the presence of exogenous TGF-β_1 treatment. Thus, the physiological and pathophysiological interaction of SKI with SMADs remains to be elucidated *in vivo* and/or in a TGF-β independent manner.

1.4.1.3 Regulation of SKI Expression

Until recently, little was known about the transcriptional regulation of SKI. Investigations by Xie and colleagues have demonstrated that the human *SKI* gene and promoter were hypermethylated (i.e. silenced) in lung cancer specimens, which supports the notion that is may act as a tumor suppressor[303]. While the specific transcription factors and co-regulators involved are unknown, *SKI* transcription can be upregulated in response to retinoic acid signalling, as well as SRF in differentiating cardiomyocytes[304, 305]. Conversely, the only confirmed negative regulators of *SKI* mRNA expression are miRNA-21, 29a, 127-3p, and 155, all of which are associated with promoting fibro-proliferative and metastatic disease[306-309].

Although the transcriptional modulation of SKI is still poorly defined, its post-translational regulation is much better studied. SKI expression is predominantly controlled by ubiquitin-mediated proteasomal degradation. Two serine residues (S326 and S383) are subject to phosphorylation by Aurora A kinase (AURKA), which in turn decreases SKI protein stability[179, 310]. Similarly, AKT kinase has been shown to phosphorylate the Thr458 residue in response to hepatocyte and insulin-like growth factors to label SKI for degradation[296, 311]. The residue at Ser515 has also been identified as a point of phosphorylation; however, the kinase responsible for the modification has yet to be identified[312]. Once phosphorylated, SKI becomes polyubiquitinated by the E3 ubiquitin ligase Arkadia, although the exact lysine or arginine

residues responsible for the formation of the SKI phosphodegron remain undefined[313].

Arkadia-dependent ubiquitination of SKI is apparently dependent on the induction of TGF-β₁

signalling, and is catalyzed by the interaction of SKI with SMAD2/3 (Fig. 1.8). While this

TGF-β-triggered action is mimicked by SMAD-Ubiquitination-Related Factor 2 (SMURF2), it

has only been confirmed in SNO, and not SKI[314]. SNON has also been shown to possess two

SUMOylation sites at lysine residues (K50 and K383) which facilitate its interaction with

SMURF2, whereas SKI has not been shown to have homologous regulatory motifs[315, 316].
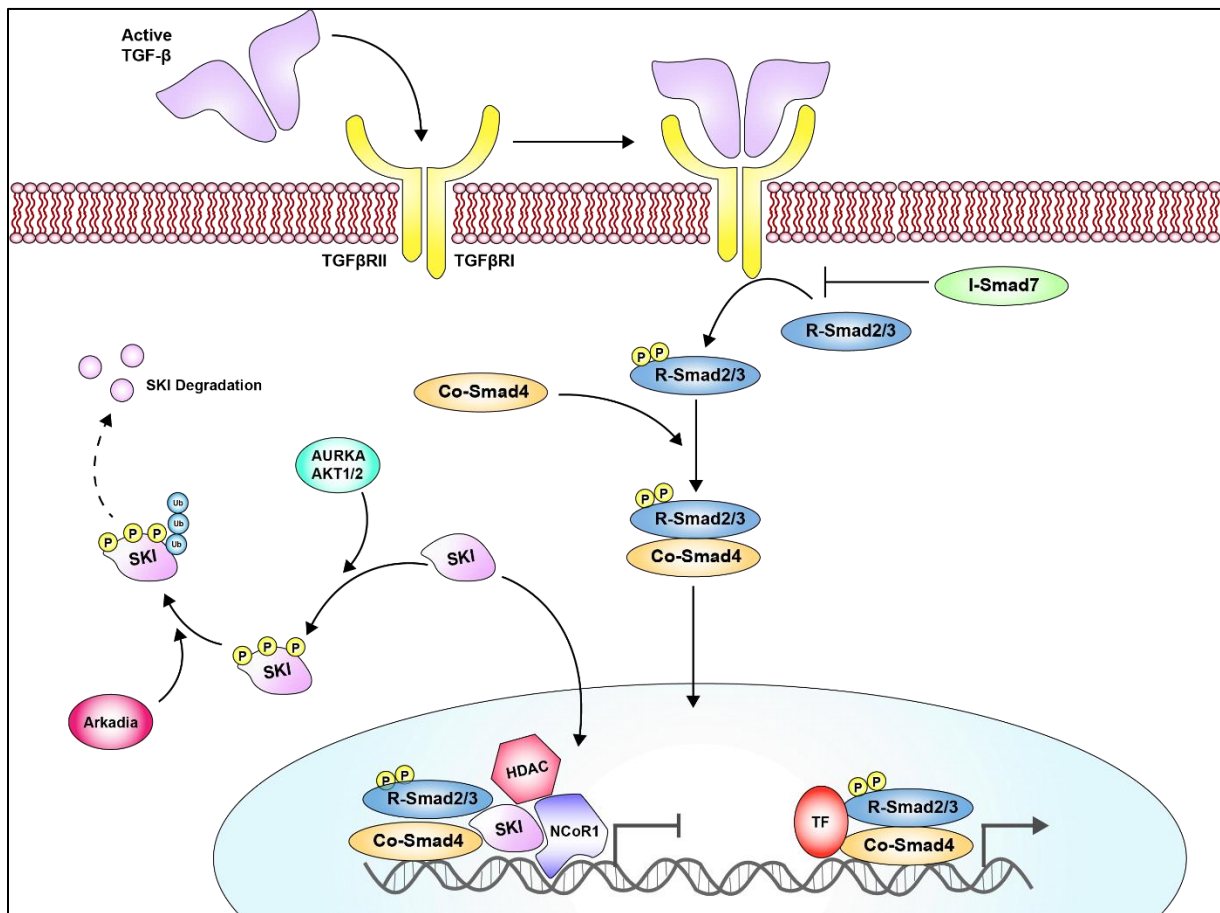
Figure 1.8: Summary of TGF-β/SMAD-dependent SKI signalling and regulation.
TGF-β₁ signalling induces the nuclear translocation of active SMAD2/3 complexes. SKI inhibits the formation of active SMAD complexes at promoter SMAD-binding elements by recruiting co-repressors (e.g. NCoR1) and HDACs to promote gene silencing. SKI stability is regulated by TGF-β₁-induced activation of AURKA and AKT kinases, which then signal Arkadia to polyubiquitinate SKI and promote proteasomal degradation.

1.4.2 SKI in Development and Disease

As TGF-β signalling plays a critical role in cell determination and embryogenesis, SKI is intimately involved in regulating the strength and spatio-temporal effects of SMAD-dependent signals. SKI is specifically important in regulating the formation of the central nervous system during embryonic development, and is required for the proper development of skeletal muscle and limb morphology [179, 300]. Global *Ski* knockout mice result in embryo lethality due to impaired neural tube and eye formation, truncated limb formation, craniofacial abnormalities, and the failure of muscle mass formation[317]. It was also found that partial knockdown of *Ski* in mice generates significant defects in eye and neural tube formation[317]. Conversely, ectopic expression of *ski* in zebrafish resulted in impaired BMP4 signalling, and generated zebrafish with altered brain patterning and the malformation of the neural plate's dorsal-ventral boundaries[318]. The study concluded that *ski* is required for proper gastrulation, and increased expression promotes abnormal expansion of the mesoderm[318].

In contrast to the zebrafish studies, transgenic mouse models of *Ski* overexpression under the control of a viral promoter generated animals without any obvious embryonic defects[319]. However, the mice presented with significant muscle hypertrophy which was paradoxically devoid of a corresponding increase in strength or mitochondrial capacity. Corroborating studies demonstrated that overexpression of *Ski* results in increased expression of genes encoding myogenic factors such as muscle creatine kinase, myosin light chain, and myogenin, and alters the muscle's capacity for glycolytic metabolism[320-322].

In humans, the only known disease associated with genetic defects in *SKI* is Shprintzen-Goldberg Syndrome (SGS), an autosomal-dominant disorder that arises from a spontaneous in-frame deletion within the SMAD-binding domain of exon 1 [323-325]. Patients

born with SGS present with craniosynostosis, which then causes facial dysmorphisms such as hypertelorism, exophthalmos, and a narrowing of the palate and jaw[325]. Those afflicted with SGS are often described as having Marfan-like bodies, with common features such as scoliosis, arachnodactyly, as well as severe skeletal muscle hypotonia and abdominal hernias[326]. Unsurprisingly, SGS-afflicted individuals often have intellectual disabilities and a propensity for epileptic seizures, among other neural defects[323]. There is also a small subset of SGS patients who develop aortic aneurysms, although the reason behind this selective abnormality is poorly understood[327]. Regardless of the patient presentation, the pathophysiology of the disease lies within the uncontrolled TGF-β signalling that manifests from the inability of defective SKI to bind SMADs[324]. As a result, unmitigated regulation of myogenic and mesenchymal cell signalling results in abnormal connective and muscle tissue development. Typically, SGS patients live to about 40 years of age, and their death is often related to the neural and/or cardiovascular defects that accompany their diagnosis. Fortunately, the prevalence of SGS is very rare, as fewer than 50 patients have been reported in the current worldwide population[326].

1.4.3 SKI in Cardiovascular Health and Disease

SKI participates in the homeostasis of myocardial and vascular tissues, as they are considerably affected by the regulation of TGF-β signalling. In studies using human coronary artery endothelial cells, SKI was found to inhibit EndoMT and prevent the expression of fibrogenic factors such as Snail and Twist in response to TGF-$β_1$ treatment[328]. In addition, SKI expression is negatively-regulated by miR-155 in vascular endothelial cells, as its overexpression was found to be causal to SKI downregulation in perivascular fibrosis[328]. Similarly, work done by Li and colleagues demonstrated that SKI inhibits VSMC proliferation

in a rat model of vascular remodelling[329]. *In vivo* delivery of SKI after vascular balloon injury suppressed neointima formation by reducing VSMC hyperplasia. In addition, *in vitro* studies in A10 (rat VSMC) cells showed reduced p38/MAPK signalling upon ectopic SKI expression[329].

In addition to vascular health, our group has previously reported several mechanisms by which SKI contributes to the promotion of resting cardiac fibroblast physiology. First, *in vivo* analyses of SKI expression in a rat model of post-MI wound healing revealed that while SKI expression increases in cardiac fibrosis, its expression is predominantly cytosolic, rather than nuclear[330]. Furthermore, *in vitro* overexpression of SKI in primary cardiac myofibroblasts showed a marked reduction in ED-A fibronectin expression, cell contractility, and collagen I synthesis. Subsequent studies demonstrated that SKI overexpression also results in the de-repression of *Meox2* gene expression, as well as inhibition of *Scxa*, which in turn prohibits activated cardiac myofibroblasts from cell cycle re-entry[331, 332]. We have also established that SKI regulates intracellular MMP-9 expression, as well as its secretion *in vitro*[333]. Ectopic expression of SKI under pro-fibrotic cell culture conditions showed a marked increase in MMP-9 secretion and gelatinase activity in a dose-dependent manner. Moreover, SKI reduced FAK phosphorylation, as well as paxillin expression, which then resulted in increased cell motility[333]. Finally, induction of SKI expression promotes the fibroblast phenotype by inhibiting autophagy, a known contributor to myofibroblast survival and proliferation[334, 335]. With chronic SKI expression (i.e. >72 hours of induction), primary cardiac fibroblasts underwent intrinsic apoptotic cell death[335]. This mechanism of cell death was hastened by the addition of autophagic inhibitors such as Bafilomycin, and could not be rescued by the addition of recombinant TGF-β_1.

Because SKI's effects on cardiac fibroblast function are robust and cause multiple changes in cell physiology and phenotype, it is likely that its mechanism of action encompasses multiple avenues of signal transduction. While SKI has been well-established as an inhibitor of SMAD-dependent signalling across multiple pathologies, this thesis explores SKI's anti-fibrotic properties which stem from a multitude of functions beyond SMAD inhibition.

1.4.4 SKI and the Hippo Signalling Pathway

To date, there is limited evidence of SKI interacting with Hippo signalling in primary cells a direct way—that is, by implicating the core components of the pathway. The only evidence of a causal link between SKI and Hippo signalling activation was demonstrated in two oncological studies, both of which utilized breast (i.e. MCF10A, MDA-MB-231), kidney (i.e. ACHN), and lung (i.e. NCI-H358, A549, NCI-H1299, HCC827, NCI-H1838, NCI-H1975, NCI-H292, and SK-MES-1) cancer cell lines [303, 336]. Both studies demonstrate a decrease in TAZ protein expression with ectopic SKI expression, as well as a marked reduction in cell proliferation, migration, and tumorigenicity. The work done by Rashidian *et al.* suggests that SKI directly interacts with several components of the Hippo pathway (e.g. LATS2, MOB1, MOB2)[336]. However, these conclusions are questionable in the context of genuine pathology, as the experiments done to provide this data were conducted in HEK 293T cells overexpressing both the bait and prey proteins, and no data was provided to support any interaction with endogenous Hippo effectors. Several other groups have remarked that physiological SKI functionality is not observable in most cell lines, and that such experiments should be cautiously interpreted, or used solely for proof-of-concept studies[179, 300, 330, 337, 338].

1.5 LIMD1

LIM Domain-containing protein 1 (LIMD1) belongs to a class of proteins which appear to primarily function as mediators of protein-protein interactions[339]. LIM domains are phylogenetically conserved among eukaryotes, and consist of two zinc fingers joined by a short hydrophobic linker [340, 341]. Proteins containing LIM domains do not appear to have conserved amino acid sequences, despite any similarities in their secondary structure. They have various subcellular functions, including cytoskeletal organization, regulation of gene transcription, and oncogenic transformation [340-342]. Predictably, several of these proteins possess paradoxical functions that are often contested in the literature[343-346]. It is quite evident that the function of LIM-containing proteins are cell, tissue, and/or pathology-specific[347]. Nevertheless, the LIM Superclass of proteins is a diverse group of molecular adapters which function to link seemingly unrelated or incompatible proteins to one another.

1.5.1.1 LIM-Containing Protein Structure, Classification and Function

Named after the first three proteins in which LIM domains were discovered (Linl-1, Isl-1, and Mec-3), this diverse family of peptides was initially characterized as protein scaffolds [347]. LIM domains are uniquely characterized by an extended cysteine-rich motif with two conserved histidine residues, C-X_2-C-X_{17-19}-H-X_2-C-X2-C-X2-C-X_{15-19}-C, which bears resemblance to DNA-binding zinc fingers[342, 348]. Although LIM domains do not necessarily bind DNA, the motif serves as an interface for interactions with other LIM-containing proteins[349, 350].

Apart from the conserved zinc finger domain, LIM protein functions and sequences are highly variable, and so they are subdivided into three broad groups based on those properties. Thus far, LIM-containing proteins have been found to contain two lone LIM domains (nuclear

"LIM-Only" proteins), a pair of LIM domains in conjunction with a homeodomain, or more complex protein structure with up to five LIM domains[347, 351]. Group 1 LIM-containing proteins consist of nuclear LIM-Only and small LIM-homeodomain proteins, while Group 2 is categorized as Cysteine-Rich Proteins (CRP1-CRP3) which are crucial for cell differentiation, especially in myogenesis[346, 347]. Proteins in Group 3 are the most structurally-diverse, and are exemplified by integrin- and cytoskeleton-associated proteins such as PINCH (5 LIM domains), Paxillin (4 LIM domains) and the AJUBA (3 LIM domains) class of proteins [347, 352].

The most recently discovered member of the AJUBA LIM protein family, a subset of the ZYXIN family of actin-associated LIM proteins, is LIMD1 (Fig. 1.9)[339]. First characterized in tumor gene mapping by elimination tests in a joint study of mouse and human cancers, *LIMD1* was viewed as a potential oncogene[339]. The central part of LIMD1 (the "pre-LIM" domain) contains a proline-rich region, which is believed to behave as a transcriptional (co-)activation domain[339]. There is currently little evidence that LIMD1 directly binds DNA, despite its ability to shuttle between the nucleus and cytoplasm[353]. However, the proline motif in LIMD1 does bear some resemblance to a SH3 domain found in many proliferative signal transduction pathways, which may exert further protein-binding activity[339]. The pre-LIM domain is also subject to phosphorylation, which dictates the protein's stability and signals for interaction with various binding partners, including actin[354, 355]. One important LIMD1 interactor is VCL, an actin-binding cytoplasmic protein that is recruited to cell-cell junctions and focal adhesions in a tension-dependent manner[344, 356, 357]. It is often co-localized with Paxillin and integrins, and is believed to be a significant contributor to fibroblast motility and cell-matrix adhesion[358]. The consequences of the LIMD1-Vinculin interaction remain unclear in solid tissues, but in the context of discrete cell physiology, it has been associated with the

mechanosensory apparatus which governs the activation of the Hippo pathway (discussed

below, Section 1.5.3)[352, 359].
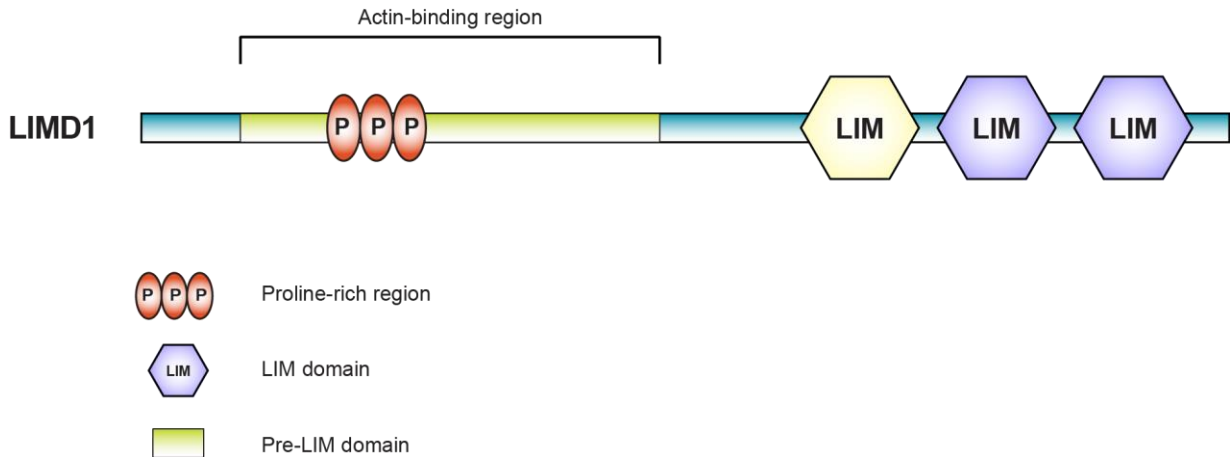
Figure 1.9: General structure of AJUBA Family proteins.
The functional regions of human LIMD1 are shown, but are representative of all members of the AJUBA LIM family of proteins: AJUBA, LIMD1, and WTIP1. The actin binding region is subject to phosphorylation, although the exact residues responsible for this regulatory mechanism are unknown. The proline-rich region is common to all AJUBA Family members, and also interacts with other proteins in an SH3-like manner. The three tandem LIM domains at the C-terminus vary in their sequences, but the last two (purple) bear more semblance to each other than to the first LIM domain (yellow). *WTIP1, Wilms Tumor Interacting Protein 1.*

Finally, at the C-terminus lies a 3-LIM domain-containing section, which exerts its own set of

protein binding abilities, and imparts its capacity for both nuclear and cytoplasmic

signalling[354]. Studies in AJUBA protein determined that the 3-LIM domain is required for

interaction with other proteins at adherens junctions, centrosomes, and focal adhesion

complexes[354, 360]. Overall, LIMD1 appears to primarily function in signal transduction buy

shuttling between subcellular compartments to relay information from the cell membrane to the

nucleus, and vice versa.

1.5.2 Role of LIMD1 in Development and Disease

As Hippo signalling is paramount to organogenesis, LIMD1 and the AJUBA family of proteins are integral to providing mechanosensory input for proper tissue structure and composition[344, 359, 361]. Due to the functional heterogeneity of AJUBA proteins, there is a dearth of information in the literature regarding the physiological function of *LIMD1*. Studies in the homologous *Drosophila* gene *dJub* have demonstrated that it is essential for embryonic development[352, 354]. Tissue-specific deletion of *dJub* resulted in marked reduction in organ size, and demonstrated that the protein product dJub colocalizes with centrosomes in neuroblasts[352]. Conversely, in transgenic *Limd1*^{-/-} mice, global ablation of *Limd1* did not affect embryo viability[357]. The pups presented normal bone density, but isolated *Limd1*^{-/-} osteoblasts failed to respond to any osteoclastic stimuli. The study also concluded that Limd1 was upregulated during osteogenesis and bone resorption, but was not essential for proper bone development[357]. Concurrent studies by another group demonstrated that Limd1 is necessary for the recruitment of TNF Receptor Associated Factor 6 (TRAF6) to the AP-1 complex in osteoblasts, a canonical event in osteoclast activation[361]. These findings are of potential value when considering fibrotic disease, as osteoclast and fibroblast activation share significant overlap in their signaling pathways, including TGF-β and the induction of AP-1-dependent gene transcription[361-363].

In human pathology, LIMD1 has been implicated in both tumor development and tumor suppression. Studies in A549 cells demonstrated that nuclear LIMD1 can interact with Rb in the nucleus to induce cell cycle arrest, and that this process can be reversed with RNA interference (RNAi)[364]. Several other studies in cancers arising from deletions at chromosome 3p21.3 containing the *LIMD1* locus postulated that loss of LIMD1 is associated with

adenocarcinomas and squamous cell carcinomas of the head and neck, kidney, as well as the

lung[365, 366]. Furthermore, a rare variant of LIMD1 containing the Ser255Arg amino acid

substitution has been identified in sporadic breast cancer, although this was the only gene that

was probed in the study and the physiological relevance of Ser255 has yet to be investigated[367].

It should also be noted that the 3p21.3 genetic locus contains 17 genes, and genetic mappings

of this region showed several potential tumor suppressor genes that did not include *LIMD1*[368].

Thus, inference between deletion or mutation of the 3p21.3 locus should be examined as

perhaps a synergistic effect of the loss of multiple cell cycle regulators, rather than solely due

to the loss of LIMD1.

1.5.3 LIMD1 and the Hippo Signalling Pathway

When examining its enigmatic tumor-promoting properties, LIMD1 is primarily

characterized as being cytosolic and often associated with adhesion complexes. When in the

cytosol, LIMD1 is a negative regulator of the Hippo pathway, enabling the nuclear shuttling of

YAP/TAZ and resulting in proliferative gene activation[344, 352, 369, 370]. Studies in *Drosophila*

were the first to identify AJUBA family proteins as central regulators of Hippo signalling, as

knockdown of homologous *dJub* resulted in impaired organogenesis[352]. Subsequent

investigations determined that dJub protein associates with α-catenin at adherens junctions

where it recruits Warts (the *Drosophila* equivalent of LATS1/2) to the complex in a JNK- and

tension-dependent manner[360, 370]. In immortalized mammalian cells, cyclic stretching promotes

JNK-dependent LIMD1 binding to LATS1, which in turn promotes the nuclear localization of

YAP[369]. This phenomenon was recapitulated simply by culturing the cells on stiff plastic

surfaces, and inhibited by culturing on soft surfaces (0.2 kPa) or pharmacological inhibition of

JNK signalling.

Most recently, it was found that junctional localization of LIMD1 with both LATS1 and LATS2 is dependent on cell density, as well as Rho GTPase activity (i.e. increased myosin-dependent mechanotension)[344]. Using MCF10A and MDCKIIG cell lines, LIMD1 was co-localized to the cell membrane with LATS1, LATS2, and VCL at low cell density, and this was attended by nuclear localization of YAP. After the formation of confluent monolayers, or with treatment with blebbistatin, cytoplasmic shuttling of YAP was observed in concert with a loss of LIMD1 and LATS1 co-localization[344]. While both studies were conducted in immortalized cells, it is important to consider the applicability of the findings to primary cells and the function and phenotype of stromal cells *in vivo*. When examining fibroblasts and myofibroblasts, cells which are highly sensitive to mechanical signals in pathological settings, LIMD1 may be a significant factor to examine when identifying points of intervention in fibroproliferative disease.

CHAPTER 2: RATIONALE, HYPOTHESIS, AND AIMS

2.1 Study Rationale and Disease Context

The World Health Organization has recognized heart disease as the leading cause of death in the world, accounting for 33% of all-cause mortality[371, 372]. However, due to recent advancements in the treatment of heart disease and major adverse cardiac events (MACE) such as MI, it is estimated that 35% fewer patients die from the initial MACE[371, 372]. Rather, most patients die 5 years post-MACE due to the onset of cardiac fibrosis and eventual heart failure[371, 373]. In Canada, approximately 50 000 patients are diagnosed with heart failure every year, adding to a rising total of over 600 000 Canadians currently living with the disease[373]. To further complicate approximations, it is likely that upwards of 1 million Canadians have some degree of undiagnosed cardiac fibrosis[373]. Moreover, it is estimated that heart failure alone accounts for nearly $3 billion in direct healthcare costs, while the indirect costs are valued at over $20 billion annually[373]. Apart from the socio-economic costs of cardiac fibrosis, heart failure patients and their caregivers face significant psychological and physical burdens. Depression, anxiety and other mental health disorders are diagnosed in over 30% of heart failure patients; this is also the case for caregivers who are tasked with dealing with the stresses of frequent appointments, medication requirements, and limited physical capabilities of heart failure patients[373]. Despite the rising healthcare and societal costs associated with heart failure, there exists no effective therapeutic intervention to prevent or treat the underlying cause, cardiac fibrosis.

Our lab previously established that SKI is a driver of the resting fibroblast phenotype, and that its overexpression in primary cardiac myofibroblasts reverts their phenotype to a more physiological state[330-332, 335]. While SKI has been shown to inhibit TGF-β signalling in

hyperplastic pathologies such as cancer metastasis, this singular pathway of cell cycle arrest cannot account for the overt phenotype shift that is observed upon overexpression. Thus, the question arises as to whether SKI possesses further inhibitory function, such as crosstalk with other signalling pathways or unique mechanisms of gene suppression. Novel data presented in this thesis indicate that SKI is indeed a multi-functional inhibitor of fibro-proliferative disease, and that a key component of its action includes the activation of the Hippo pathway. This concept merits investigation as Hippo signalling may be implicated in the initiation and progression of cardiac fibrosis, which makes the SKI-Hippo relationship a clinically-relevant therapeutic target.

2.2 Hypothesis

Central hypothesis: SKI regulates myofibroblast function and activation state both *in vitro* and *in vivo* in the post-MI heart. We have established a causal link between increased Ski expression and an attenuation of the myofibroblast phenotype, which is denoted by decreased collagen synthesis and contractility, and a reduction in the expression of several pro-fibrotic and ECM markers.

Specific hypothesis: TAZ (WWTR1) expression is negatively regulated by SKI, and the induction of this signalling axis promotes the fibroblast phenotype.

2.3 Study Objectives and Specific Aims

Objective 1: *In vitro studies.* To develop cell culture conditions which promote and/or maintain a quiescent phenotype in primary cardiac fibroblasts.

If we are to study cardiac fibroblast activation at a molecular level, conventional cell culture techniques must be modified as they do not lend themselves to promoting resting

fibroblast physiology. Optimization of two-dimensional cell culture conditions ought to be performed in order to limit external factors which produce the spontaneous activation of cardiac fibroblasts *in vitro.*

Specific Aim 1.1: *To regulate mechanical, nutritional, and hormonal input in order to produce more physiologically-relevant conditions to study cardiac fibroblast activation in isolated primary cells.*

Objective 2: *In vivo and in vitro studies.* To establish the role, if any, of Hippo signalling in cardiac fibroblast activation.

The nuclear effectors of the Hippo pathways, YAP and TAZ, are known to promote the pathogenesis of fibrotic disease in soft tissues. With respect to cardiac fibrosis, only YAP has been explored as a contributor to fibroblast activation; however, TAZ has been shown to be the primary contributor to fibrogenesis in the lung, another mechanically-active organ. Identifying the roles of YAP and/or TAZ in cardiac fibroblast activation would ultimately support the concept that Hippo signalling is an important regulator of fibrosis in the heart.

Specific Aim 2.1: To fully characterize the role YAP/TAZ signalling in the activation of cardiac myofibroblasts, in vitro.

Specific Aim 2.2: To fully elucidate the expression of YAP/TAZ in and in vivo model of post-MI fibrosis.

Objective 3: *In vitro studies*. To decipher the mechanism by which SKI activates Hippo signalling to specifically target TAZ in cardiac myofibroblasts.

Our preliminary studies suggested that SKI overexpression in primary cardiac fibroblasts leads to a marked decreased in both nuclear and cytoplasmic TAZ expression,

leaving YAP expression unchanged. Because this phenomenon is very specific for only one homolog, it is of interest to know whether this interaction is direct (i.e. protein-protein) or indirect (i.e. negative transcriptional regulation, or upstream Hippo targeting), so as to provide insight into potential targets for future anti-fibrotic therapies.

Specific Aim 3.1: To fully characterize the regulatory effects of SKI on TAZ, and determine whether it occurs at the level of transcription, translation, or post-translational modification.

Specific Aim 3.2: To describe the SKI and TAZ protein interactomes in primary human cardiac fibroblasts and demonstrate whether there is a direct link between the two proteins.

CHAPTER 3: MAINTAINING PRIMARY MURINE CARDIAC FIBROBLASTS IN TWO-DIMENSIONAL CELL CULTURE

Natalie M. Landry, Sunil G. Rattan, Ian M.C. Dixon

Institute of Cardiovascular Sciences, St. Boniface Hospital Albrechtsen Research Centre, Department of Physiology and Pathophysiology, Rady Faculty of Health Sciences, Max Rady College of Medicine, University of Manitoba, Winnipeg, Manitoba, Canada.

The methodology described in this chapter outline necessary optimizations to two-dimensional primary cardiac fibroblast cell culture which then facilitated the physiologically-relevant *in vitro* studies of cardiac fibroblast activation in Chapter 4. Prior to this, primary cardiac fibroblasts were typically maintained under conditions which favour the activated myofibroblast phenotype, preventing the execution of more nuanced molecular assays, *in vitro*. The results presented here address the objectives of Aim 1 of this thesis, and suggest that mechanical, hormonal, and nutritional input should be considered in primary cell culture of cardiac fibroblasts. I, Natalie Landry, was responsible for the study design and optimizations, execution of experiments, data collection, statistical analyses, and writing of the manuscript. Sunil Rattan assisted in primary rat cardiac fibroblast isolation for this study and assisted with data analysis. Finally, Ian Dixon supervised this study, and contributed to the initial study design, final data interpretation, and editing of the published manuscript.

3.1 Abstract

Primary cardiac fibroblasts are notoriously difficult to maintain for extended periods of time in cell culture due to plasticity of their phenotype and sensitivity to mechanical input. In order to study cardiac fibroblast activation *in vitro*, we have developed cell culture conditions which promote the quiescent fibroblast phenotype in primary cells. Using elastic silicone substrata, both rat and mouse primary cardiac fibroblasts could be maintained in a quiescent state for more than 3 days after isolation and these cells showed low expression of myofibroblast markers, including fibronectin extracellular domain A, non-muscle myosin IIB, platelet-derived growth factor receptor-alpha and alpha-smooth muscle actin. Gene expression was also more fibroblast-like *vs.* that of myofibroblast, as *Tcf21* was significantly upregulated, while *Fn1-EDA*, *Col1A1* and *Col1A2* were markedly downregulated. Cell culture conditions (e.g. serum, nutrient concentration) are critical for the control of temporal fibroblast proliferation. We propose that eliminating mechanical stimulus and limiting the nutrient content of cell culture media can extend the quiescent nature of primary cardiac fibroblasts for physiological analyses *in vitro*.

3.2 Introduction

The term "fibroblast" is assigned to a heterogeneous group of highly-motile stromal cells found in the interstitium, whose function and phenotype is tissue-dependent[151, 160, 374]. In the heart, cardiac fibroblasts serve to maintain tissue homeostasis and regulate extracellular matrix turnover. While there are no molecular markers that are entirely specific to cardiac fibroblasts, they are typically positive for transcription factor 21 (TCF21) [58, 375, 376], vimentin [377-379], and CD90 (or Thy-1) [380-382]. When subject to stress or injury, fibroblasts lose their normal phenotype and activate into myofibroblasts. Unlike quiescent fibroblasts, myofibroblasts are highly contractile and are characterized by a radically organized cytoskeleton featuring alpha-smooth muscle actin (αSMA) -positive stress fibers [153, 154, 383, 384], mature focal adhesions [164, 385, 386], and increased production of periostin [387, 388] and fibrillar collagens [389, 390]. In addition, the activation of cardiac myofibroblasts is also associated with alternative splicing of fibronectin, specifically denoted by the inclusion of the cell-associated extracellular domain A (ED-A) [391, 392].

Myofibroblast activation is a hallmark of cardiovascular disease, as these cells are responsible for the excessive deposition of extracellular matrix (ECM) proteins and are the primary drivers of fibrosis and its related pathologies [393, 394]. Induction of the myofibroblast phenotype has been associated with a multitude of stimuli and the most common effector in this process is transforming growth factor-beta (TGF-β) [172, 395], which is associated with the initial inflammatory response after vascular or myocardial injury. Moreover, cardiac myofibroblasts are further driven to promote fibrogenesis in response to the autocrine and paracrine effects of other pro-inflammatory cytokines, such as platelet-derived growth factor (PDGF) [146]. Along with this response, cardiac myofibroblasts also exhibit a pronounced

increase in PDGF receptor-alpha (PDGFRα) expression in disease states[194, 396, 397].

Hypertrophic agents such as growth factors and AngII [398, 399], hyperglycemia [400, 401], and the

presence of reactive oxygen species (ROS) [402, 403] have also been shown to contribute to this

transition in phenotype. Finally, biomechanical input has also been implicated in myofibroblast

activation. Isometric tension promotes the release of latent TGF-β present in the ECM [404, 405],

and the formation of stress fibers with the incorporation of αSMA [162] and this could be likened

in vitro to seeding cells on stiff plastic surfaces. Similarly, mechanical loading and stretching

modulates fibroblast function and phenotype, promoting the deposition of ED-A fibronectin [392]

and enhancing TGF-β signalling [169]. While it has traditionally been viewed as a permanent

event, the activation of myofibroblasts has recently been observed as a reversible process in

resident fibroblasts *in vivo* [375, 406].

Despite these findings, the mechanisms which govern the cardiac fibroblast and

myofibroblast phenotypes are largely uncharacterized, as common cell culture techniques are

not commensurate to physiologically-relevant conditions, and *in vivo* transgenic models are

difficult to generate without affecting other stromal cells. Even when isolated from healthy

myocardium, the spontaneous phenotype of primary cardiac fibroblasts in conventional cell

culture is of pro-fibrotic, activated myofibroblasts within hours of plating [1]. However, it has

been shown that culturing primary fibroblasts on elastic surfaces which are biomimetic to their

native tissues can help to alleviate myofibroblast activation [265]. In the case of myocardium,

culture surfaces with a compressibility, or elastic modulus (E), of ~7 kPa are representative of

healthy tissue, while surfaces with $E > 10$ kPa are considered fibrotic [407, 408]. This presents a

considerable hurdle in that conventional polystyrene tissue culture plates are significantly

stiffer, often upwards of $E = 3$ GPa [409, 410]. In addition, while it is common practice to passage

primary cells to promote homogeneity in the culture population, passaging further drives

myofibroblast activation and prevents physiologically- pertinent studies [1]. This phenotypic

plasticity presents a unique problem in that fibroblast physiology that is representative of

healthy myocardium cannot be readily observed and manipulated *in vitro*.

In spite of the unstable nature of the cardiac fibroblast phenotype, the capacity to

maintain these cells in a quiescent state in two-dimensional cell culture would enable much

more accurate and reproducible means by which to study their physiology, and their response

to genetic manipulation and pharmacological treatment. In this study, we present conditions in

which unpassaged (P0) primary cardiac fibroblasts can be maintained for more than 72 hours

in vitro without significant activation of the myofibroblast phenotype. These data support an

alternative means by which to investigate the molecular and cellular physiology of primary

cardiac fibroblasts *in vivo* studies.

3.3 Materials and Methods

3.3.1 Animal Ethics

All experimental protocols involving live animals were reviewed and approved by the

University of Manitoba Animal Care Committee, and were generated in accordance with the

standards of the Canadian Council of Animal Care.

3.3.2 Preparation of Elastic Tissue Culture Surfaces

PrimeCoat silicone elastic tissue culture plates (10 cm) and coverslips (ExCellness

Biotech SA, Lausanne, Switzerland) were coated with 10 μg/mL porcine gelatin type A (0.2

mL/cm2) in sterile water overnight at 37°C, 5% CO_2. Prior to plating cells, the supernatant was

removed and replaced with complete culture medium. Polystyrene (non-elastic plastic) tissue

culture dishes and glass coverslips were also treated in a similar manner and used as comparative controls when evaluating various elastic moduli.

3.3.3 Isolation of Rat Primary Cardiac Fibroblasts

Rat primary cardiac fibroblasts were isolated, as previously described[56,57,63] with some modifications. Male Sprague-Dawley rats weighing 101-125 g were anaesthetized with a ketamine-xylazine cocktail (100 mg/kg ketamine; 10 mg/kg xylazine) via intraperitoneal injection. Upon loss of limb reflexes, heparin (6 mg/kg) was administered intravenously via the femoral artery. Hearts were excised and briefly placed in Dulbecco's Modified Eagle's medium/Ham's F12 nutrient mixture (DMEM/F12) prior to cannulating via the aorta on a Langendorff apparatus. The hearts were then subject to retrograde perfusion with DMEM/F12, followed by Minimum Essential Medium, Spinner's Modification (S-MEM) to cease cardiac contraction and promote cell dissociation. Finally, the hearts were perfused with S-MEM supplemented with 640 U/mL collagenase type II (Worthington Biochemical Corporation, Lakewood, NJ) with recirculation for 25 minutes. Once digested, the tissue was incubated at 37°C, 5% CO_2 for 10 minutes before neutralizing the collagenase with 10 mL of DMEM/F12 supplemented with 2% fetal bovine serum (FBS) and further dissociated by trituration with a serological pipette. The resulting cell suspension was then passed through a 40 μm sterile cell strainer (Thermo Fisher Scientific, Waltham, MA) to remove any undigested tissue and debris. The cells were pelleted by centrifugation at 200 x g for 7 minutes, and re-suspended in 45 mL of complete cell culture medium. Three different types of media were used for comparison: F10 with 2% FBS, F10 with 10% FBS, and DMEM/F12 with 1 μM ascorbic acid and 10% FBS. All media was supplemented with 100 U/mL penicillin-streptomycin. For each 10 dish, 3 mL of cell suspension was added to a total of 10 mL of medium at plating. For coverslips in 35

mm or 6-well dishes, 0.5 mL of cell suspension was added to a total of 2 mL medium per dish or well. Fibroblasts were allowed to adhere for 2.5 hours at 37°C, 5% CO_2; cultures were then briefly washed twice with phosphate buffered saline (PBS; pH 7.4) supplemented with penicillin-streptomycin and then fresh complete culture medium was added. The following day, the cultures were once again washed twice with PBS, and the growth medium was replaced. The culture medium was subsequently replaced once per day until harvesting.

3.3.4 Isolation of Mouse Primary Cardiac Fibroblasts

Primary mouse cardiac fibroblasts were isolated using a modified version of a previously-published protocol[411]. In short, 8- to 12-week old male C57BL/6 mice were anaesthetized with 3% isofluorane until loss of limb reflexes. The chest was opened to excise the heart with a portion of the ascending aorta remaining attached. The heart was promptly flushed with 10 mL of EDTA buffer (5 mM EDTA, 130 mM NaCl, 5 mM KCl, 500 nM NaH2PO4, 10 mM HEPES, 10 mM Glucose, 10 mM 2,3-Butanedione 2-monoxime, and 10 mM Taurine, pH 7.8), followed by 3 mL of perfusion buffer (1 mM MgCl2, 130 mM NaCl, 5 mM KCl, 500 nM NaH2PO4, 10 mM HEPES, 10 mM Glucose, 10 mM 2,3-Butanedione 2-monoxime, and 10 mM Taurine, pH 7.8) using a 27-gauge needle inserted into the ventricles via the apex. While still injecting through the apex, the heart was perfused twice with 25 mL S-MEM supplemented with collagenase type II (330 U/mL), while collecting the solution in a 10 cm tissue culture dish. Once the heart was sufficiently digested, it was gently pulled apart with forceps and allowed to digest in 20 mL of the collagenase solution at 37°C, 5% CO_2 for another 10 minutes. After triturating the tissue, the resulting suspension was neutralized with 10 mL of complete culture medium and passed through a 40 μm cell strainer and pelleted by centrifugation, as mentioned above. The resulting pellet was resuspended in 40 mL of

DMEM/F12 supplemented with 10% FBS, 1 μM ascorbic acid, and 100 U/mL penicillin-streptomycin and the cells were then evenly distributed among 4 – 10 cm dishes and allowed to adhere for 3 hours. Adherent cells were then gently washed once with pre-warmed PBS (pH 7.4) supplemented with antibiotics, and the DMEM/F12 growth medium was replaced. The culture medium was replaced in a similar fashion every 24 hours until they adopted a spindle-shaped morphology (~3-4 days), after which the medium was switched to F10 supplemented with 2% FBS and Insulin-Transferrin-Selenium-Sodium Pyruvate (ITS-A; Thermo Fisher). The cells were harvested once they reached 40-50% confluency, at approximately 10 days post-isolation.

3.3.5 Cell Proliferation Imaging and Counting

Approximately 18 hours after plating, unpassaged (P0) fibroblast cultures were washed twice with PBS. Pre-warmed, serum-free and antibiotic-free medium was then supplemented with Cytopainter Green Cell Proliferation Agent (Abcam, Cambridge, UK). Cells were treated with the dye solution at 37°C, 5% CO_2 for 30 minutes, protected from light. The dye solution was removed, and the cells were briefly washed twice with PBS before replacing with complete culture medium. The cells were imaged every 24 hours post-plating with a Zeiss LSM 5 Pascal microscope using 4X and 10X objectives and an excitation wavelength of 488 nm. Images were processed using AxioVision Microscopy software (Zeiss, rel. 4.8). Initial cell counts at 18 hours post-plating were performed by using phase contrast microscopy images and ImageJ software[65], using three randomly-selected fields for each biological replicate, totaling 9 technical replicates for each cell culture condition. Manual cell counting was accomplished using a Moxi Z automated cell counter (Orflo Technologies, Ketchum, ID). Cells were trypsinized and re-suspended in an excess volume of complete culture medium, and

a 1:10 dilution of the cell suspension was used for each count. Two counts were taken for each biological replicate to ensure accuracy for each measurement. Manual cell counting was performed in triplicate for each time point and cell proliferation imaging was accomplished by selecting three randomly-chosen fields for each cell culture condition.

3.3.6 Protein Isolation

Approximately 80 hours after plating, cells were trypsinized and pelleted by centrifugation at 200 x g for 5 minutes. Cell pellets were then washed with PBS and re-pelleted by centrifugation for 3 minutes. The supernatant was removed and the pellets were lysed with RIPA lysis buffer supplemented with protease inhibitor cocktail (P8340; Sigma-Aldrich Canada Co., Oakville, ON) and phosphatase inhibitors (10 mM NaF, 1 mM Na3VO4, and 10 mM EGTA). The resulting lysates were then vortexed and incubated on ice for 30 minutes. Following incubation, the lysates were briefly sonicated for 5 seconds, and then centrifuged at 16 000 x g for 15 minutes at 4°C. Supernatants were transferred to new microcentrifuge tubes and protein concentrations were determined using a bicinchoninic acid (BCA) assay.

3.3.7 Immunoblotting

SDS-PAGE of 25 µg of protein was performed on 8% reducing gels. Proteins were transferred at 4°C onto PVDF membranes in tris-glycine buffer containing 20% methanol. Total protein loading was measured prior to blotting using Ponceau S staining and densitometric analysis. Non-specific binding sites were blocked with 5% skim milk in tris-buffered saline supplemented with 0.1% Tween-20 (TBS-T) at room temperature. The blots were thoroughly washed in TBS-T before applying primary antibodies overnight at 4°C with shaking. Primary antibodies were used at the following dilutions: ED-A (cellular) fibronectin (1:1000; MAB1940; MilliporeSigma, Burlington, MA; or NBP1-91258; Novus), SMemb

(1:1000; ab684; Abcam), αSMA (1:5000; A2547; Sigma). Because the primary fibroblasts originated from a heterogenous population of cells, vimentin (1:2000; ab8069; Abcam) and platelet-derived growth factor receptor alpha (PDGFRα; 1:1000; ab134123; Abcam) were used as a phenotype controls on each blot. Appropriate HRP-conjugated secondary antibodies (Jackson ImmunoResearch, West Grove, PA) were applied at a 1:5000 dilution for 1 hour at room temperature. Protein detection was done using ECL substrate, and protein bands were visualized on blue X-ray film. Protein expression was measured by relative densitometry using Quantity One® analysis software (version 4.6.9; Bio-Rad).

3.3.8 RNA Isolation and Quantitative PCR

Primary cardiac fibroblasts were isolated by trypsinization and centrifugation at 200 x g for 5 minutes. Column-based RNA isolation was performed using the PureLink® RNA Mini kit (Invitrogen, Carlsbad, CA) according to the manufacturer's instructions. Approximate RNA concentration and purity was assessed by measuring the absorbance at 260 and 280 nm using a NanoDrop™ Lite Spectrophotometer (Thermo Scientific).

Two-step qPCR was performed first by synthesizing cDNA from 100 ng of RNA, using the Maxima™ First Strand cDNA synthesis for RT-qPCR (Thermo Scientific), and included initial treatment with dsDNase. Amplification reactions were prepared according to the Luna® Universal qPCR Master Mix (New England Biolabs, Ipswich, MA) protocol, using 1 µL of cDNA template and 200 nM of forward and reverse primers in a final volume of 10 µL. PCR amplification was performed in triplicate for each reaction on a QuantStudio 3 Real-Time PCR System (Applied Biosystems, Foster City, CA) using the fast cycling mode. The following cycling program was used: initial denaturation at 95°C (60 seconds), followed by 40 cycles of denaturation at 95°C (15 seconds) and extension at 60°C (30 seconds). After amplification, a

continuous melt curve was generated from 60°C to 95°C. Relative gene expression was
calculated using the $2^{-\Delta\Delta Ct}$ method[412], using the samples from cells plated on plastic as controls
for each sample set, and normalized to HPRT. Primer pairs and their corresponding targets are
listed in Table 3.1.

Table 3.1: List of primer pairs used in quantitative PCR

Gene	Accession	Forward Primer (5' - 3')	Reverse Primer (5' - 3')
Acta2	NM_031004.2	AGATCGTCCGTGACATCAAGG	TCATTCCCGATGGTGATCAC
Col1a1	NM_053304.1	TGCTCCTCTTAGGGGCCA	CGTCTCACCATTAGGGACCCT
Col1a2	NM_053356.1	TGACCAGCCTCGCTCACAG	CAATCCAGTAGTAATCGCTCTTCCA
Fn1	NM_019143.2	ACTGCAGTGACCAACATTGACC	CACCCTGTACCTGGAAACTTGC
Hprt1	NM_012583.2	CTCATGGACTGATTATGGACAGGAC	GCAGGTCAGCAAAGAACTTATAGCC
Postn	NM_001108550.1	GCTTCAGAAGCCACTTTGTC	CGCCAACTACATCGACAAGG
Tcf21	NM_001032397.1	CATTCACCCAGTCAACCTGA	CCACTTCCTTTAGGTCACTCTC

3.3.9 Fluorescence Immunocytochemistry (ICC-F)

Primary cardiac fibroblasts were seeded at a low confluency onto either glass coverslips
in 6-well dishes, or elastic (E = 5 kPa) silicone coverslips (ExCellness) in 35 mm dishes,
coated with porcine gelatin type A, and maintained in culture with F10 medium with 2% FBS
for 72 hours. The cells were briefly washed in PBS and fixed in 4% paraformaldehyde for 15
minutes at room temperature. After another brief wash in PBS, the cells were permeabilized
with 0.1% Triton X-100 in PBS for 15 minutes, and non-specific binding sites were blocked
for 1 hour in 5% normal goat serum (Invitrogen) in PBS. The blocking agent was removed by
another set of washes before applying primary antibodies diluted in 1% bovine serum albumin
(BSA) in PBS. αSMA was probed using a 1:50 dilution (A2547; Sigma) and incubated
overnight at 4°C in a humidified chamber. The following day, the cells were thoroughly

washed three times in PBS and incubated with Alexa Fluor 488-conjugated secondary antibody (1:500; A27023; Invitrogen) for 1 hour at room temperature. After a brief wash in PBS, F-actin was stained using a 1:500 dilution of rhodamine-phalloidin (R415; Invitrogen) in PBS. After several washes over a period of 30 minutes, the coverslips were thoroughly dried using gentle suction and mounted on glass slides using Fluoroshield™ mounting medium with DAPI (Abcam) and allowed to cure at room temperature for 24 hours. Cells were imaged using a Zeiss LSM 5 Pascal microscope as described above, using DAPI, FITC and Texas Red detection channels.

3.3.10 Cell Viability Assay

The viability of cells in each culture condition was assessed after 96 hours in culture. Cells were washed twice with pre-warmed PBS, then treated with 2 µM Calcein-AM (C3100, Thermo Fisher) and 2.5 µM ethidium homodimer (E1169, Thermo Fisher) in PBS for 30 minutes at 37°C, 5% CO_2. The stains were then gently removed by aspiration and replaced with fresh PBS. Cells were imaged immediately, using FITC and Texas Red detection channels.

3.3.11 Data Analysis and Statistics

Statistical analyses and graphs were generated using Graph Pad Prism 7. All data are presented as the mean ± standard deviation, unless otherwise indicated in figure legends. Individual biological replicates are counted as one experiment involving cells from only one animal. Grouped data analyses were performed using one-way or two-way ANOVA followed by Tukey's post-hoc test, with significance recorded if $P > 0.05$.

3.4 Results

3.4.1 Myofibroblast markers are downregulated in low nutrient conditions with restricted biomechanical input

Mechanobiological properties of the ECM govern myofibroblast activation and function, and do so in the absence of input from TGFβ1/Smad signalling[410]. Moreover, myofibroblasts are contractile and sense and modulate stiffness within the ECM through focal adhesions via integrin binding [390]. In order to determine the physiological effects of two-dimensional cell culture on primary cardiac fibroblasts, we not only examined the influence of cell culture medium and serum, but also whether the compressibility of the culture surface was a greater factor in the spontaneous phenotype of the cells *in vitro*. After three days in culture, variable expression of myofibroblast markers ED-A fibronectin, non-muscle myosin heavy chain (SMemb or myosin IIB), and αSMA was observed in conditions of either low nutrient media (F10 with 2% FBS) or high nutrient media (DMEM/F12 with 10% FBS), plated on substrates that mimic the compressibility of healthy myocardium (5kPa), or fibrosis-stiff substrate (100 kPa) (Fig. 3.1).

On stiff substrate in combination with high serum, the preponderance of expression of myofibroblast markers is evident and significantly greater the other conditions tested. This increase was markedly evident with the expression of PDGRFα, which had a strong response to both substrate stiffness and medium composition. In mouse primary cardiac fibroblasts, we observed a significant increase in ED-A fibronectin, and PDGFRα, which was exhibited in concert with an increase in substrate stiffness (Supplemental Fig. A.1). While conditions which favored the fibroblast phenotype were of F10 medium with low serum, it was evident that lower plate compressibility also imparted greater control of cell phenotype. The data supports
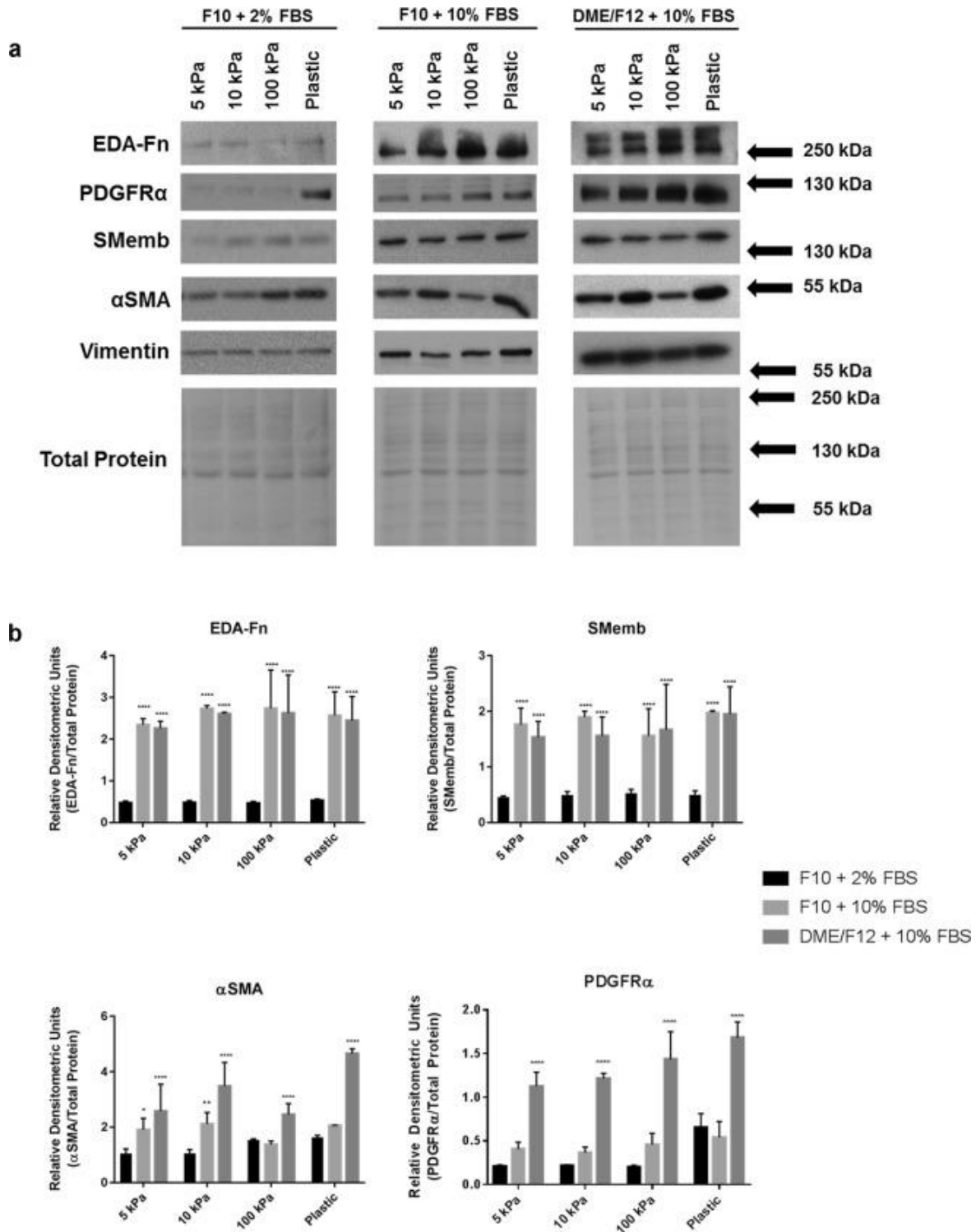
Figure 3.1. Myofibroblast marker expression in rat primary cardiac fibroblasts after >72 hours in culture. A. Rat cardiac fibroblasts were plated on elastic plates with characteristic elastic moduli of 5kPa, 10kPa, and 100 kPa, with the indicated culture medium. Cells plated on conventional polystyrene tissue culture plates (rigid substrate – ranging from 30 to 100 MPa) were used as a comparative control. Protein from unpassaged primary cardiac fibroblasts was harvested ~3 days after plating. Vimentin expression was used as a pan-phenotypic control, and protein expression was normalized to total protein loading. **B.** Graphical representation of data in (A). Data shown as the mean ± SD and is representative of n = 3-6 biological replicates. *$P < 0.05$, **$P < 0.01$, ***$P < 0.005$, ****$P < 0.001$ when compared to cells cultured in F10 medium with 2% FBS on the same substrate.

the hypothesis that tuning the fibroblast substrate for reduced biomechanical input (i.e. cells plated on elastic substrate versus stiff plastic) in combination with low nutrient conditions reduces the activation of fibroblasts cultured for extended periods.

3.4.2 αSMA is excluded from the cytoskeleton in quiescent cardiac fibroblasts.

As αSMA is often viewed as the gold-standard marker for tissue fibrosis, and was evidently present in all samples we studied, we sought to compare its subcellular localization in our proposed *in* vitro model. Unpassaged primary rat cardiac fibroblasts were maintained *in vitro* for >72 hours; Figure 3.2 provides comparative fields of cardiac fibroblasts plated on glass (rigid substrate) and fibroblasts plated on "cardiac soft" 5 kPa plates. F-actin and αSMA are double-stained in these fields, and the relative size of the cells in each set is remarkably different. αSMA is not incorporated into the cytoskeleton of the inactivated fibroblasts plated on the elastic substrata, indicating that these cells have not formed stress fibers, and are not actively contractile [163]. The merged fields of cells plated on glass show complete incorporation of αSMA into stress fibers, which reflects their phenotype of activated myofibroblasts.
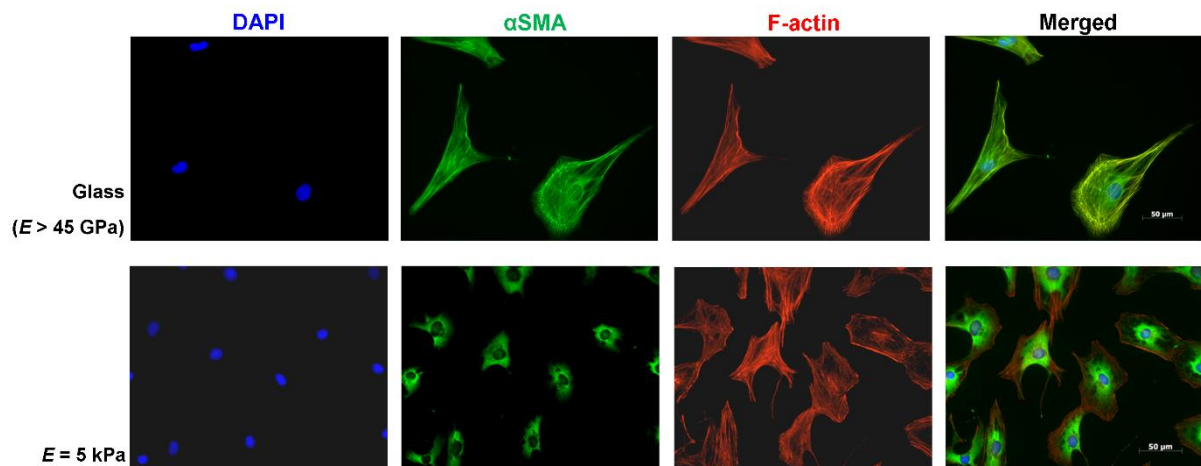
Figure 3.2. αSMA is excluded from F-actin stress fibers when cultured on 5 kPa culture surfaces. P0 rat cardiac fibroblasts were seeded at low confluency (<10%) on either glass (rigid substrate) or elastic coverslips and probed for αSMA (green) and F-actin (red) 3 days after plating. Images are representative of n = 3 independent biological replicates. Scale bar = 50 μm.

3.4.3 Cardiac fibroblast gene expression is further affected by biomechanical input

In addition to protein expression, we sought to determine the effects of culture medium and/or substrate stiffness on gene expression in cultured primary cardiac fibroblasts. After three days *in vitro*, relative mRNA abundance of fibroblast- and myofibroblast-expressed genes including collagen type I monomers, αSMA, ED-A fibronectin, periostin (a secreted, matricellular protein), and Tcf21 were examined. Tcf21 is required for fibroblast formation, and is a nucleus-localized protein expressed in adult fibroblasts[413], whereas periostin is a marker for activated fibroblasts[156, 414]. We found *Tcf21* expression to be significantly elevated in the fibroblasts harvested from 5kPa substrate with F10 medium and 2% FBS, versus expression on plastic plates, whereas *Postn* was elevated in the 100 kPa plates relative to its expression on plastic plates in similar conditions (Fig. 3.3). ED-A fibronectin (*Fn1-EDA*) gene expression was significantly lower on 5 kPa plates versus the non-elastic plastic controls, whereas αSMA was elevated in 10 and 100 kPa plates versus plastic in low nutrient and low serum conditions. Collagen monomer (*Col1a1* and *Col1a2)* expression also shows similar responsiveness to plate stiffness, with expression increasing as substrate stiffness increases.

While our results show some heterogeneity in the variable expression of marker mRNAs, which appears to be gene-dependent, the myofibroblast markers are generally upregulated in response to plating of fibroblasts on stiff substrates. When considering the effects of the cell culture medium, the conditions which resulted in the most inhibition of myofibroblast gene expression were those in F10 medium with 2% serum, although this effect can apparently be overridden by the compressibility of the tissue culture plate.
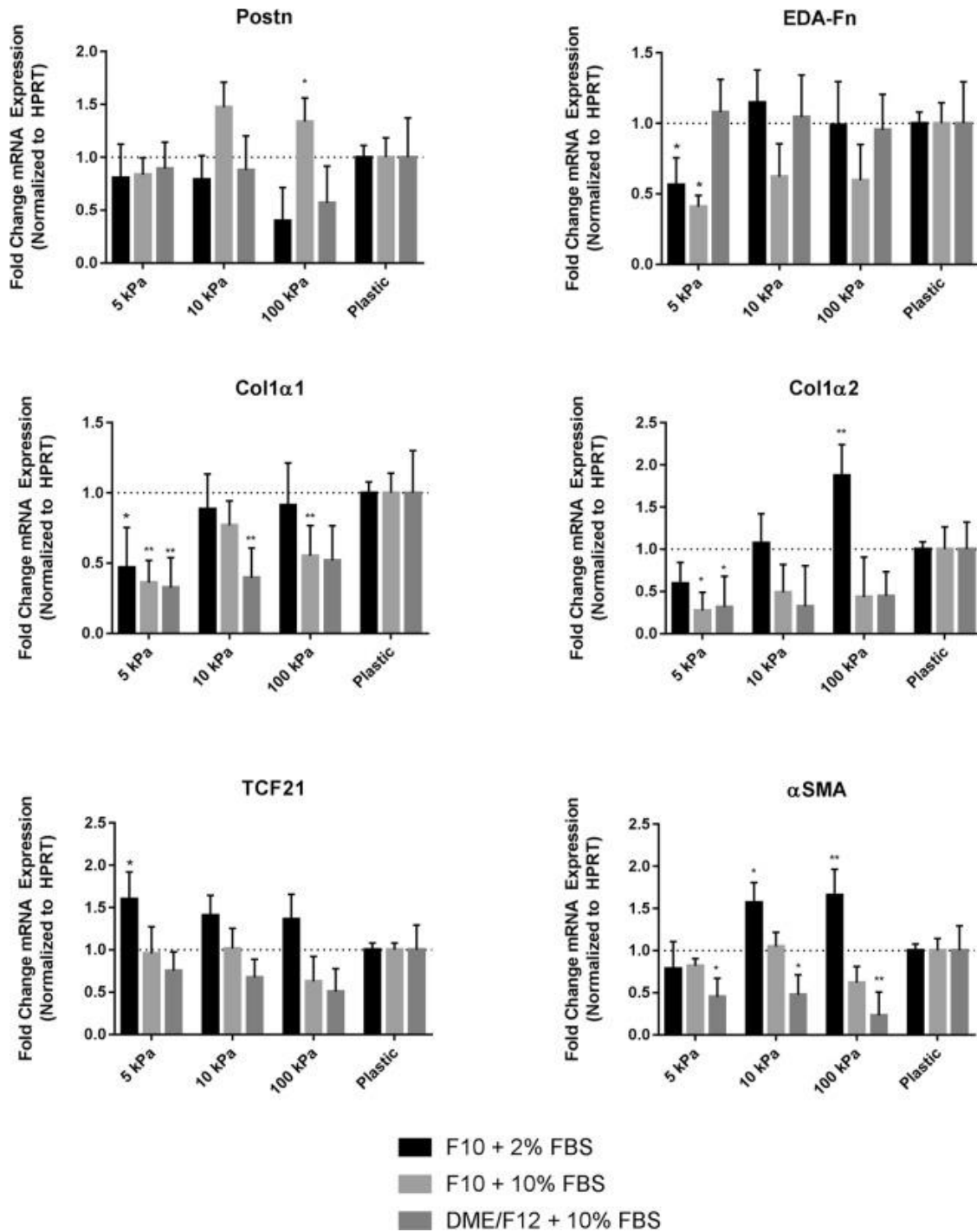
Figure 3.3. Fibroblast and myofibroblast gene expression in primary cardiac fibroblasts after >72 hours in culture. RNA was harvested from P0 rat cardiac fibroblasts 3 days after plating and used for qPCR. Samples from cells cultured on conventional plastic tissue (rigid substrate) culture surfaces were used as comparative controls. All reactions were performed in technical triplicates and were normalized to *Hprt*. Data shown as the mean ± SD and is representative of n = 3 biological replicates. *****$P < 0.05$, ******$P < 0.01$, when compared to cells cultured on plastic in the same culture medium (i.e. comparison of 5 kPa, 10 kPa, or 100 kPa *vs.* plastic).

3.4.4 Cardiac fibroblast proliferation can be limited in extended cell culture.

To further characterize isolated rat primary cardiac fibroblasts *in vitro*, we examined their proliferative behavior under various conditions. Specifically, we sought to investigate the responsiveness of fibroblast and myofibroblast proliferation in low and high serum conditions using media with low nutrient (F10) and high nutrient (DMEM/F12) content. In low serum conditions, cardiac fibroblast proliferation is suppressed by plating on 5 kPa, 10 kPa and 100 kPa plates with F10 medium, versus plastic controls (Fig. 3.4). A similar trend was observed using high serum conditions with the same medium, as well as with DMEM/F12 however the expansion of the cell population in conditions with DMEM/F12 was much more pronounced, especially on stiff plastic. To determine whether this observation was due to a difference in initial cell attachment between culture conditions, we counted the number of attached cells at 18 hours post-plating, after washing off any debris. We did not observe a significant difference in cell attachment when cells were cultured in low nutrient conditions however there was preferential attachment on stiffer culture surfaces when the cells were maintained in DMEM/F12 + 10% FBS.

Additionally, to confirm that the observe lack of proliferation in F10 culture medium was not due to excessive cell death, at 96 hours post-plating the cells were stained with Calcein-AM (stains viable cells) and ethidium homodimer (stains nucleic acid/dead cells). We observed no significant difference in cell death between the various elastic moduli of the cell culture plates, suggesting that the compressibility of the culture substrata does indeed affect primary cardiac fibroblast activation and proliferation in vitro (Fig. 3.5). These results support the suggestion that proliferation of activated myofibroblasts is higher than inactive fibroblasts in culture, and that the state of activation can be controlled by both substrate stiffness and the
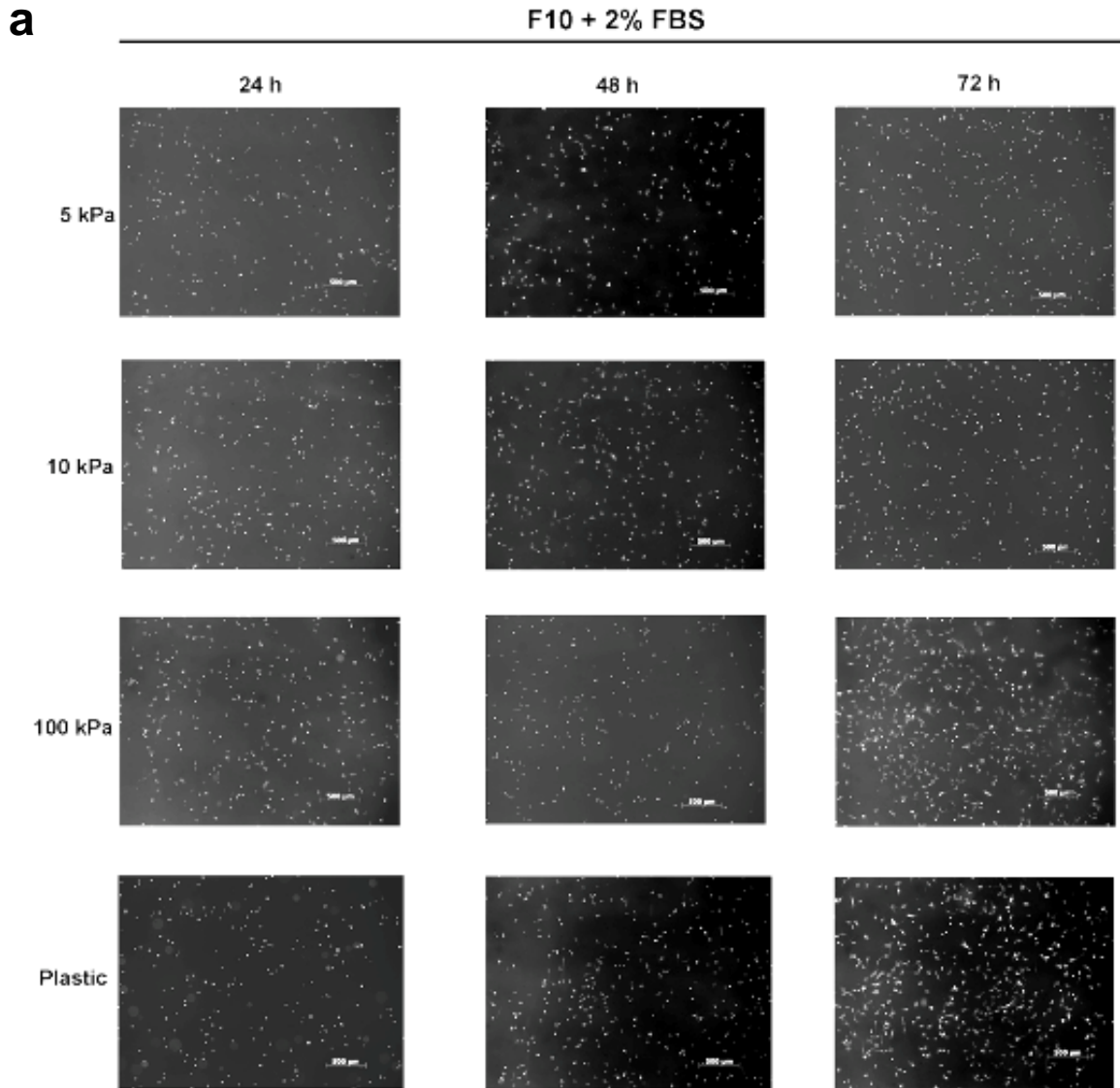
Figure 3.4. Nutrient restriction and decreased biomechanical input inhibit proliferation in primary cardiac fibroblasts. A. P0 rat cardiac fibroblasts were plated on elastic plates with various elastic moduli, with F10 culture medium supplemented with 2% FBS, and stained with proliferation staining agent 24 hours after seeding. Images were captured immediately after staining and every 24 hours subsequently. Cells plated on conventional plastic tissue culture plates (rigid substrate) were used as a comparative control. Images are representative of n = 3 biological replicates, with 3 technical replicates per condition.

b
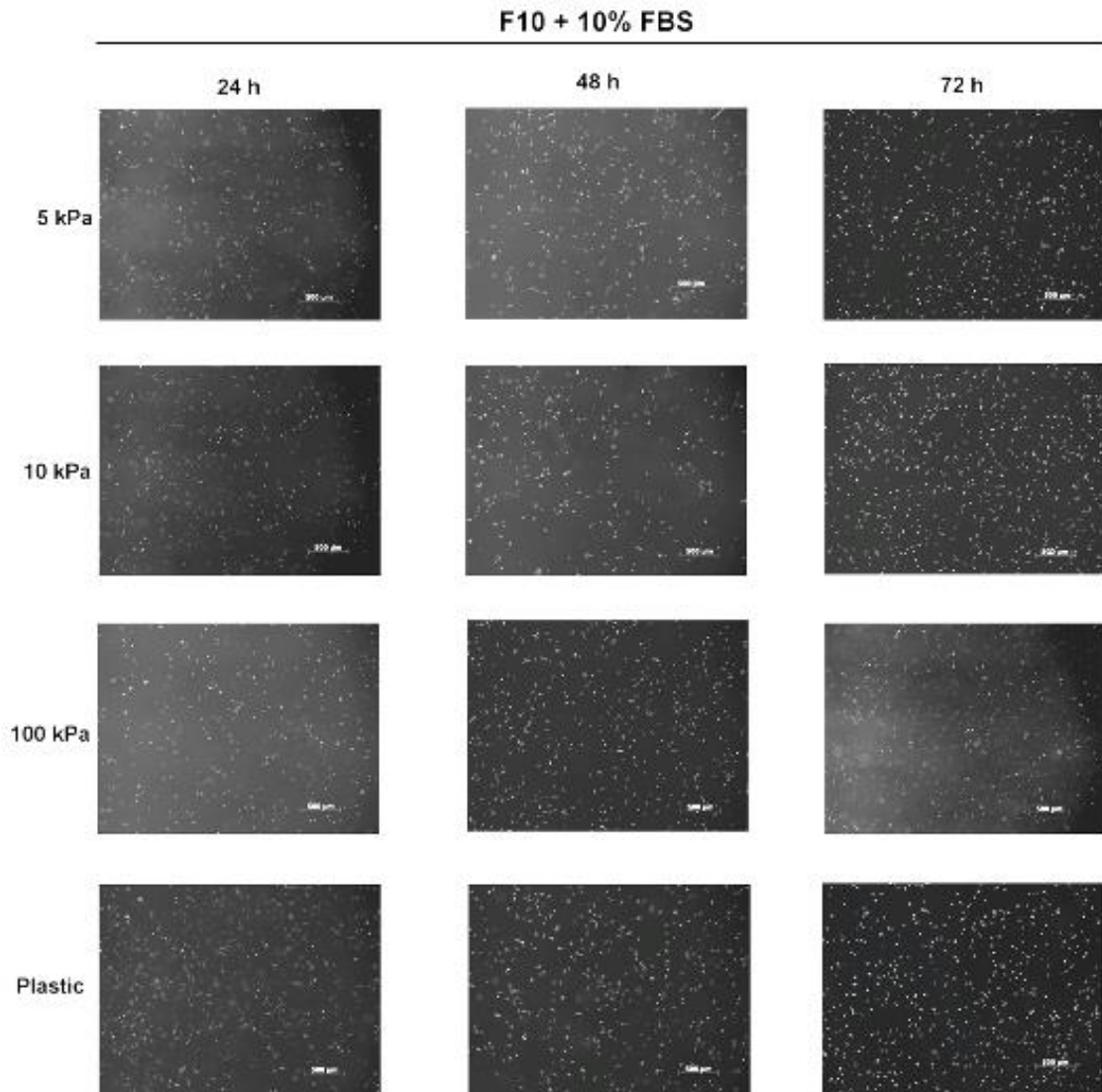
Figure 3.4. Nutrient restriction and decreased biomechanical input inhibit proliferation in primary cardiac fibroblasts. B. P0 rat cardiac fibroblasts were plated on elastic plates with various elastic moduli, with F10 culture medium supplemented with 10% FBS, and stained with proliferation staining agent 24 hours after seeding. Images were captured immediately after staining and every 24 hours subsequently. Cells plated on conventional plastic tissue culture plates (rigid substrate) were used as a comparative control. Images are representative of n = 3 biological replicates, with 3 technical replicates per condition.

Figure 3.4. Nutrient restriction and decreased biomechanical input inhibit proliferation in primary cardiac fibroblasts. C. P0 rat cardiac fibroblasts were plated on elastic plates with various elastic moduli, with DME/F12 (1:1) culture medium supplemented with 10% FBS, and stained with proliferation staining agent 24 hours after seeding. Images were captured immediately after staining and every 24 hours subsequently. Cells plated on conventional plastic tissue culture plates (rigid substrate) were used as a comparative control. Images are representative of n = 3 biological replicates, with 3 technical replicates per condition.

d
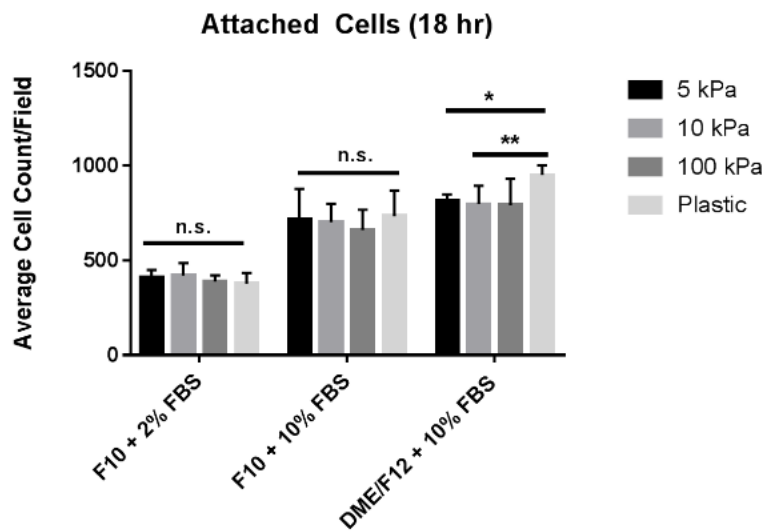
e
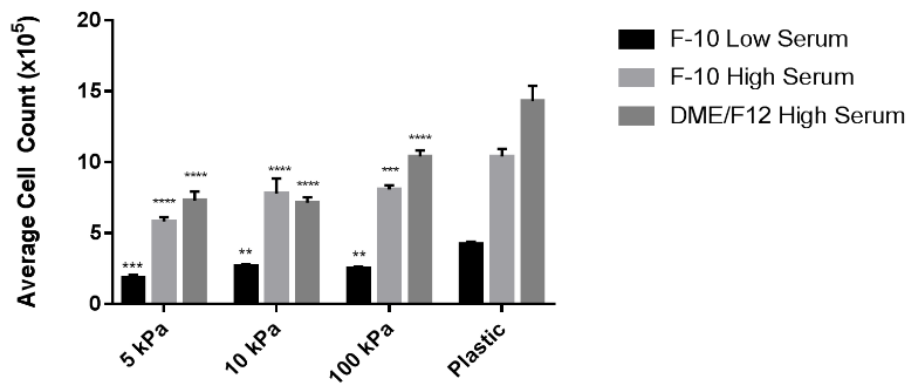
Figure 3.4. Nutrient restriction and decreased biomechanical input inhibit proliferation in primary cardiac fibroblasts. D. Histrographical representation of cell counts 18 hours after plating and attachment. **E.** Graphical representation of cell counts obtained after 3 days in culture (t > 72 hours). Data displayed as mean ± SD and is representative of n = 3-6 biological replicates. ****P<0.01, ***P<0.005, ****P<0.001** when compared to cells cultured on plastic in the same medium.
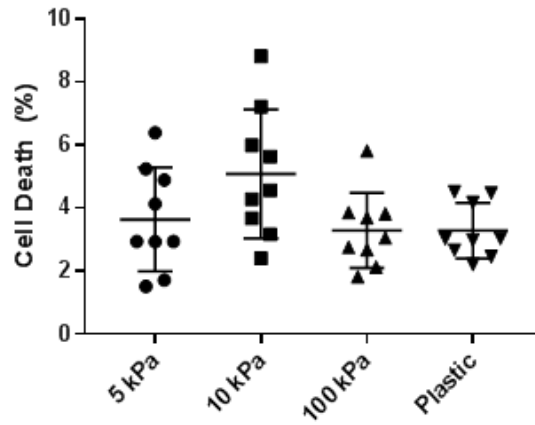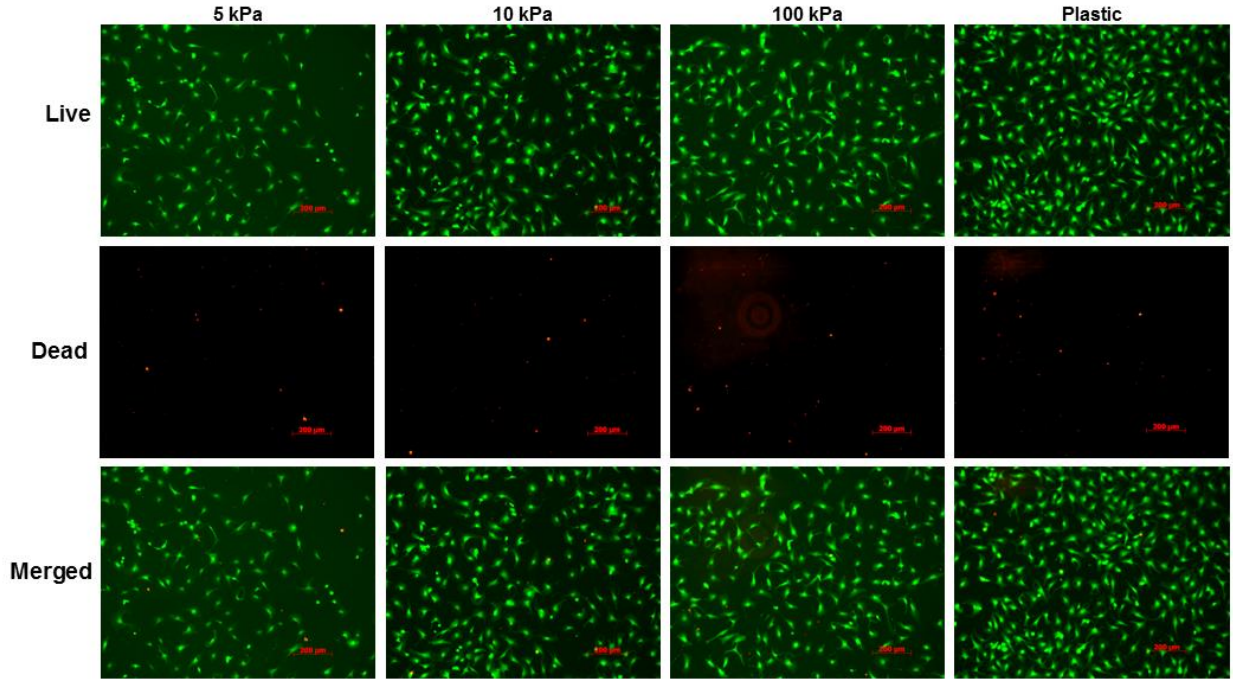
Figure 3.5. Assessment of cell viability in restricted nutrient conditions after >72 hours in culture. P0 rat cardiac fibroblasts were seeded onto substrata of various elastic moduli and cultured in F10 medium supplemented with 2% FBS for 4 days. Cell viability was assessed with Calcein-AM (green) staining, and cell death by ethidium homodimer (red). Each biological replicate was assessed by capturing 3 random fields at 10X magnification. Images are representative of n=3 biological replicates, with 9 technical replicates each.

nutrient content of the culture medium. Thus, we reveal an interaction between substrate stiffness, activation state of cardiac fibroblasts, and the proliferative capacity of primary cardiac fibroblasts *in vitro*.

3.5 Discussion and Conclusions

Cardiac fibroblasts and activated myofibroblasts are component cells of the myocardium that contribute to the maintenance of the ECM in homeostatic hearts and to cardiac fibrosis after injury, respectively[160]. A novel interpretation of cardiac fibrosis (and other tissue fibrosis) is that rather than simply described as "over-active" wound healing, the organism may be attempting to utilize developmental programs that are typically active when generating functional muscle [390]. In the heart, fibroblasts are derived from different embryonic sources, with the majority from the epicardium (EMT contributing 80% of cells), and most of the remaining fibroblasts from the endocardium (EndoMT contributing 18%)[157]. Thus, defining these cells in a molecular context is difficult due to the lack of identification of a specific marker common to all fibroblasts. The mixed origin of cardiac fibroblasts notwithstanding, the common role of the activated myofibroblast is to generate and remodel the ECM [390]. Furthermore, the recent focus on cardiac fibrosis and the involvement of myofibroblasts and specific markers for them, including periostin, ED-A fibronectin, SMemb, and αSMA provides new impetus to direct fibrosis research to focus on activated myofibroblasts, which require refinements in approaches for their practical study [1, 58, 164].

Accordingly, the estimation of the impact of fibroblast activation to myofibroblasts in the damaged and failing heart have become a much sought-after topic. Nonetheless, while the burgeoning number of scientific reports published during the past ten years reflects the overall

acceptance of cardiac fibrosis as a player in the evolution of heart failure, methods to distinguish the activated from non-activated form of cardiac fibroblasts have not kept pace, with few exceptions. We, and other groups, have previously published studies including both unpassaged and passaged primary cardiac fibroblasts plated on stiff plastic substrata in an attempt to procure a baseline phenotype *in vitro*[334, 415, 416]. Despite these efforts, observing primary cardiac fibroblasts conventional cell culture is limited to the first 12 to 16 hours before seeing overt activation of the myofibroblast phenotype[1]. As a result, the maintenance of the quiescent phenotype in culture has become a pressing issue, and is regularly overlooked in experimental design.

Herein we have provided detailed results to contextualize the importance of nutrients in culture media, culturing cells to eliminate biomechanical input, and minimize the impact of serum on fibroblast activation to allow for reliable culture of inactive cardiac fibroblasts. Upon examination of protein expression in rat primary cardiac fibroblasts maintained in culture for three days, it was evident that ED-A fibronectin, αSMA, and SMemb are differentially expressed among all conditions tested. The most differentially-expressed pro-fibrotic marker was PDGFRα, which had increased expression on stiff plastic substrata, and was even more highly-expressed in conditions of high nutrient and serum concentrations. A similar expression pattern for myofibroblast markers was observed in mouse cardiac fibroblasts, which were maintained in culture for a total of 10 days post-isolation (Supplemental Fig. A.2). Recent evidence indicates that these markers may also serve to drive fibroblast activation as myosin II may mediate myofibroblast activation in stiffened fibrotic lungs [155], and that in the setting of a stiff matrix, αSMA incorporation into contractile stress fibers facilitates mesenchymal stromal cell fate by controlling YAP release[417]. In addition, PDGFRα has recently garnered interest as

a marker of fibroblast activation and ECM remodelling, as its expression is upregulated in models of fibrosis and heart failure[146, 194]. Along with the data presented here, the addition of PDGFRα to the gamut of markers often used to describe cardiac fibroblasts and myofibroblasts will provide a clearer understanding of a cell's position on the spectrum spanning the two phenotypes. Very recently, the fibronectin ED-A domain has been shown to promote binding to latent TGF-β-binding protein-1 (LTBP-1), and thus enhances fibronectin-associated storage of TGF-β, which may then increase its availability for extracellular activation and stimulation of fibrosis[392]. The appearance of fibronectin ED-A domain remains a useful marker heralding the activation of fibroblasts to myofibroblasts, and their subsequent production and local accumulation of disordered ECM. In addition, we also observed more severe upregulation of all three markers, along with Hippo and EMT markers, when the elastic substrata were coated with soluble fibronectin (Fig. A.1). These findings corroborate current work which postulates that fibronectin is an ECM component that drives fibrogenesis and heart failure[376]. Taken together, these results underscore the utility of ED-A fibronectin as a marker of phenotype plasticity in response to biomechanical and nutritive inputs in culture, and strengthen the case to use it as such in concert with αSMA incorporation into myofibroblasts' stress fibers.

Beyond the expression of αSMA, its subcellular localization is paramount to its effects on cell phenotype. We observed not only that αSMA is indeed present in unpassaged fibroblasts on elastic substrates, but also that its incorporation into stress fibers is a greater indicator of the myofibroblast phenotype. Similar findings have been demonstrated in other stromal cell types, including subcutaneous [418], dermal [155], and hepatic portal fibroblasts [417]. Furthermore, αSMA can itself be a driving force in myofibroblast activation, as ectopic overexpression in stromal cells has been shown to activate the myofibroblast phenotype, and

generate a feed-forward loop in fibrogenesis[419]. It should also be noted that in the myocardium, αSMA is not only expressed by cells of mesenchymal origin, but can also be expressed by stressed or injured cardiomyocytes expressing fetal gene programs during active remodelling and dedifferentiation [156, 157, 414]. Collectively, these results suggest that αSMA cannot be entirely relied upon for accurate characterization of cardiac fibroblasts, and that its subcellular localization should also be considered when conducting *in vitro* cardiovascular studies.

Based on the findings of this study, we propose that relatively inactive primary cardiac fibroblasts can indeed be maintained *in vitro* for a period of time that is adequate for most molecular assays, provided that certain parameters (i.e. passage number, culture medium, plate compressibility) are addressed (Fig. 3.6). The majority of published literature which implements primary cardiac cell culture, including those previously published by our lab, do not consider the biomechanical, nutritional, and hormonal input to which the cells are subject in two-dimensional culture. Likewise, primary cardiac fibroblasts which are subject to passaging are also often used in order to maximize cell numbers and decrease the number of animals or tissue specimens for a given experiment. This is often seen as reasonable as it is simple, convenient, and offers some flexibility to the type of molecular assays employed in fibroblast-centric research. Using the methods described here, fewer cells are required to seed plates and passaging is not used; this can significantly decrease the material requirements for a given experiment.

While diverging from traditional cell culture methods is not easily accomplished from a technical perspective, it is essential to consider all factors when designing experiments and interpreting data, especially as current *in vitro* studies are still using what would be considered as activated myofibroblasts. It is known that cardiac fibroblasts exist on a delicate phenotypic

spectrum that is highly reactive to the extracellular environment and methods should be adapted to generate accurate and reproducible results. This will not only facilitate the generation of data which is relevant to physiological conditions, but will also promote rigor and consistency in the literature. The ability to control myofibroblast activation greatly improves the sensitivity of genetic and pharmacological assays. Future exploration into medium composition (e.g. serum-free media) would certainly enable further refinements on this method. Thus, to better understand the pathogenesis of cardiac fibrosis and the effects of potential therapeutic interventions, the consequences of *in vitro* conditions on cell physiology should be carefully considered.
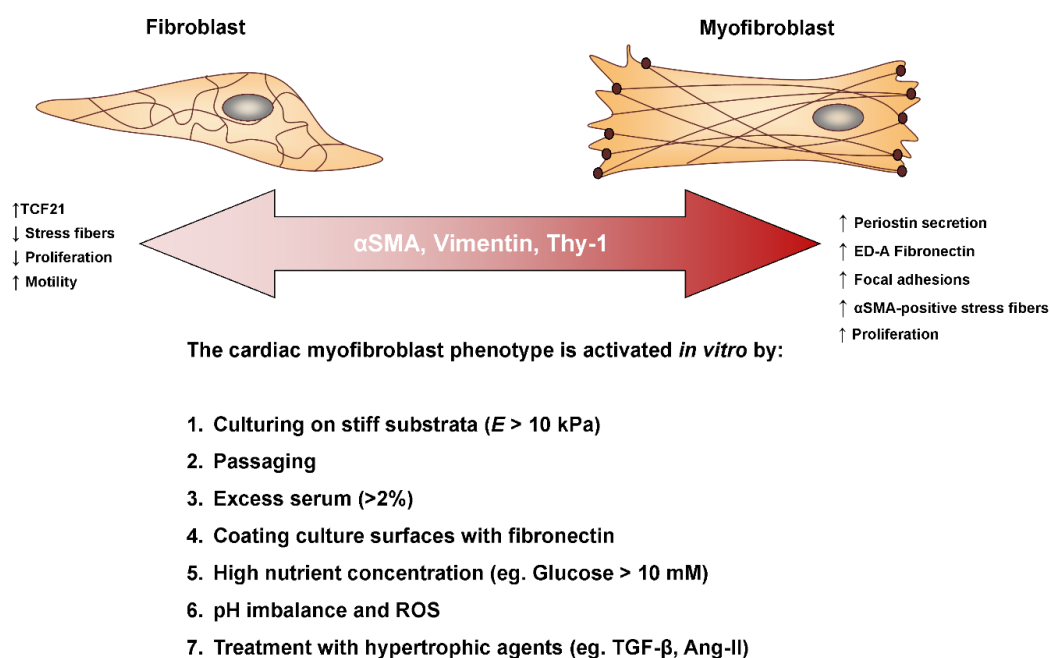
Figure 3.6. A schematic depicting the various factors affecting the fibroblast phenotype *in vitro*. Herein we summarize our main findings along with other known elements which influence primary cardiac fibroblast activation *in vitro*. We suggest that α-SMA is an ever-present marker on the cardiac fibroblast-myofibroblast spectrum, and that its incorporation in myofibroblast stress fibers is a key component of defining the activated phenotype. Previous studies on conventional plastic tissue culture plates have confirmed that passaging[1], hyperglycemic-like conditions[2], and treatment with ROS and hypertrophic agents indeed activate the myofibroblast phenotype and we conclude that excess serum also contributes to this activation.

CHAPTER 4: SKI PROMOTES LATS2-HIPPO SIGNALLING VIA LIMD1 TO INHIBIT CARDIAC FIBROBLAST ACTIVATION

The contents of this chapter have been submitted for publication in:

"SKI Activates the Hippo Pathway via LIMD1 to Inhibit Cardiac Fibroblast Activation"

Submitted to: *Basic Res Cardiol*

Natalie M. Landry[1,2,4], Sunil G. Rattan[1,2,4], Krista L. Filomeno[1,2,4], Thomas W. Meier[1,4], Simon C. Meier[1], Sarah J. Foran[1], Navid Koleini[1,2,4], Robert R. Fandrich[1], Elissavet Kardami[1,3,4], Todd A. Duhamel[1,5], Ian M.C. Dixon[1,2,4]

[1]Institute of Cardiovascular Sciences, St. Boniface Hospital Albrechtsen Research Centre, Winnipeg, Manitoba, Canada
[2]Department of Physiology and Pathophysiology, University of Manitoba
[3]Department of Human Anatomy and Cell Science, University of Manitoba
[4]Rady Faculty of Health Sciences, Max Rady College of Medicine, University of Manitoba
[5]Faculty of Kinesiology and Recreation Management, University of Manitoba
Winnipeg, Manitoba, Canada

Using the *in vitro* methods described in Chapter 3, along with the addition of an *in vivo* rat model of post-MI fibrosis, Chapter 4 comprises the bulk of the aims and objectives for this thesis. Several questions are addressed, primarily focusing on how the Hippo pathway influences cardiac fibroblast activation and how SKI functions to regulate Hippo signalling under pro-fibrotic conditions. The main objectives were first, to determine the effects of YAP and TAZ activation on the cardiac fibroblast phenotype, and whether the two paralogs function in a similar manner in the context of cardiac fibrosis (i.e. determine if TAZ is indeed redundant to YAP, as suggested by much of the literature). Second, the specific targeting of TAZ by SKI was to be explored initially by conventional molecular assays; however, a better, more profound understanding of SKI's physiological role in cardiac fibroblasts was obtained by capturing the SKI and TAZ interactome using biotin proximity-labelling and mass

spectrometry. Finally, using the data from the unique and blended interactomes, the potential avenues of crosstalk between SKI and the Hippo pathway were examined in a fibroblast-specific manner, giving rise to novel points of interest for phenotype regulation.

I, Natalie Landry, designed the study and performed all experiments, data collection (except the mass spectrometry), statistical analyses, and writing of the submitted manuscript. Sunil Rattan oversaw ethics approvals and animal protocols, and assisted in the isolation of primary cells. Krista Filomeno harvested tissue for the *in vivo* components, and isolated protein from frozen tissue specimens. Assistance with immunoblotting and qPCR were provided by Thomas Meier, Simon Meier, and Sarah Foran. Primary human cardiac fibroblast isolation and culture were performed by Navid Koleini and Robert Fandrich. Elissavet Kardami and Todd Duhamel contributed by overseeing the human tissue collection ethics approval, assisted with data analysis and interpretation, as well as editing of the final manuscript. Finally, Ian Dixon supervised the entire study, and assisted with experimental design, data interpretation, and editing of the manuscript.

4.1 Abstract

Despite the prevalence of cardiac fibrosis, there are no effective clinical interventions which target its pathogenesis and progression. We have previously shown that overexpression of the endogenous TGF-β_1 repressor, SKI, functions to deactivate the pro-fibrotic myofibroblast phenotype. Our current investigations indicate that SKI also functions in a SMAD/TGF-β-independent manner by activating the Hippo tumor-suppressor pathway and inhibiting Transcriptional co-Activator with PDZ-binding motif (TAZ or WWTR1). The molecular mechanisms by which SKI specifically targets TAZ to inhibit fibrosis remain undefined. Thus, we examined the Hippo signaling pathway in the context of cardiac fibroblast activation, and how its interaction with SKI mediates anti-fibrotic effects in the heart. Molecular and cell-based assays in primary rat and human cardiac fibroblasts demonstrated that SKI causes specific proteasomal degradation of TAZ and causes a shift in actin cytoskeleton dynamics to inhibit the activation of myofibroblasts. These findings were corroborated by examining the expression of TAZ in a rat model of post-MI remodeling and fibrosis. Employing BioID2-based interactomics and mass spectrometry, we demonstrate that SKI interacts with actin-modifying proteins and also with LIM Domain-containing protein 1 (LIMD1), a negative regulator of Hippo signalling, suggesting that SKI relays between the cytoskeleton and Hippo components to regulate the cardiac fibroblast phenotype. We postulate that the interaction between SKI and TAZ is arbitrated by LIMD1, an important mediator of focal adhesion-associated signaling pathways. As a novel point of convergence among pro-fibrotic pathways, we suggest that the SKI-LIMD1-TAZ axis may be considered for future therapeutic targeting of cardiac fibrosis.

4.2 Introduction

A result of both chronic and acute injury to soft tissues is the remodelling of the ECM, a normal aspect of the wound healing response. In the case of fibrosis, however, the persistence of activated, contractile fibroblasts (myofibroblasts) promotes the secretion matricellular proteins (e.g. CTGF, POSTN) and structural components like fibrillar collagens type I and III[83, 420-422]. Another hallmark of the pro-fibrotic, myofibroblast phenotype is the expression of the ED-A fibronectin splice variant, a cell-associated ECM component which further promotes the deposition and remodelling of matrix components[43, 46]. In addition, the incorporation of αSMA into actin stress fibers within the cytoskeleton is considered the gold-standard indication of the smooth muscle-like quality of the myofibroblast phenotype[419]. In the case of cardiac fibrosis, the chronic wound healing response presented in most patients results from the unmitigated expansion of the scar, post-MI. The initial formation of the infarct scar is required to impart tensile strength to the damaged tissue and to prevent myocardial rupture; however, the chronic expansion of the collagenous interstitium leads to heart failure as adult cardiomyocytes have no regenerative capacity. Thus, the five-year prognosis for patients having suffered a MI are poor as the rapid loss of functional myocardium and subsequent impairment of viable tissue are the root cause of the decline into heart failure[5]. Although cardiac patient outcomes immediately after MI have greatly improved in the last decade, there still is no effective therapeutic intervention for the treatment of cardiac fibrosis.

SKI, the cellular homolog of the Sloan-Kettering virus, is often viewed as an inhibitor of SMAD-associated TGF-β signalling[291, 423]. As a transcriptional co-regulator, SKI does not directly bind DNA, but is responsible for recruiting other regulatory factors such as NCoR1, CREB Binding Protein (CBP), and HDACs to deactivate gene promoters[179, 424]. SKI also

functions by "wedging" itself between SMAD2/3 and SMAD4, preventing the formation of active SMAD complexes in the nucleus[324, 332, 425]. This inhibitory action has been observed to negatively regulate factors such as the AP-1 complex, which normally bind pro-fibrotic promoters of genes such as *COL1A1* and *COL1A2*[332, 425]. When examining its function in the heart, our group has established that SKI is dysregulated during post-MI remodelling, as it is sequestered to the cytosol[330]. We found that reintroduction of a functional, nuclear SKI into cardiac myofibroblasts reduced the expression of fibrotic markers such as αSMA and procollagen I, which was attended by a decrease in cell contractility[331, 426]. Furthermore, SKI greatly increases MMP-9 expression, secretion, and activity by primary cardiac fibroblasts, suggesting that it may play a role in the regulation of ECM homeostasis[333]. Due to the overt phenotypic changes caused by ectopic SKI activation, we hypothesize that its actions in cardiac fibroblasts stem from multiple functions, rather than TGF-β inhibition alone.

Recently described as a regulatory pathway in the pathogenesis of several fibrotic pathologies, the Hippo pathway is another potential means by which SKI regulates the activation of cardiac fibroblasts. A key regulator of organ size and cell proliferation, the Hippo signalling cascade comprises of a series of kinases which activate the LATS1/2 tumor suppressors which exert their own kinase activity on the nuclear effectors YAP and TAZ[248, 249]. Like SKI, YAP and TAZ do not directly bind DNA, but co-regulate gene transcription by recruiting TEAD and TEF transcription factors to gene promoters associated with cell cycle re-entry, such as the pro-fibrotic factor *Ctgf* [183, 258, 427]. Activation of the Hippo pathway results in the phosphorylation and cytosolic retention of both YAP and TAZ, which subsequently results in their ubiquitination and proteasomal degradation[259]. During embryogenesis, Hippo signalling plays a central role in regulating heart size and the cellular organization of the

myocardium[236]. There has been keen interest in exploiting Hippo-mediated cell cycle re-entry for the purpose of cardiac regeneration post-MI, but inhibition of the pathway results in hyperplastic cardiomyocytes and a loss of the electrical syncytium within the myocardium[286, 288]. Although there are several reports linking YAP and/or TAZ to the pathogenesis of various fibrotic diseases, there is appreciably limited evidence regarding the role of Hippo signalling in regulating the cardiac fibroblast phenotype[213, 215, 428-430].

Here, we propose that SKI activates the Hippo pathway in cardiac fibroblasts to target TAZ for proteasomal degradation. We not only demonstrate the specificity of SKI's actions towards TAZ, and not YAP, but also that TAZ expression in increased during the chronic post-MI fibrotic response. To better understand the mechanism by which SKI regulates TAZ, we employed proximity labelling and affinity-purification to isolate the interactomes of SKI and TAZ in human cardiac fibroblasts. Our results suggest that SKI regulates TAZ by activating Hippo signalling and de-repressing LATS2 in activated myofibroblasts. We identified the actin-scaffold protein LIMD1 as the point of interaction between SKI and Hippo signalling, which proposes a mechanosensory component to SKI function in cardiac fibroblasts.

4.3 Materials and Methods

4.3.1 Ethics Statement

The studies involving primary tissues and cells of human and animal origin presented herein were conducted in accordance with the guidelines and principles of the Canadian Council on Animal Care (CCAC), and the Canadian Tri-Council Policy Statement for Ethical Conduct on Research Involving Humans (TCPS 2, 2018). Ethics approval for both animal and human tissue collection was provided by the University of Manitoba's Office of Research

Ethics and Compliance, and Protocol Management and Review Committee. Human atrial

tissue specimens were collected from patients receiving elective coronary artery bypass graft

(CABG) surgery. All cardiac surgery patients at St. Boniface General Hospital signed a

consent form allowing tissue materials removed and discarded as a normal part of surgery to be

used for research purposes, according to the University of Manitoba and St. Boniface General

Hospital institutional polices. As such, the Research Ethics Board of the University of

Manitoba waived the need for individual informed consent by donors and granted permission

for use of human tissue from patients receiving elective cardiac surgery (#H2016:274).

4.3.2 Rat Model of Myocardial Infarction

Young male Sprague-Dawley ranging from 125-150 g in mass underwent left anterior

descending (LAD) coronary artery ligation or sham surgery as previously described[431]. In brief,

after proper anesthesia, the ligation was performed at approximately 2 mm from the LAD

artery origin with a 6-0 silk suture, and securely tied prior to reposition of the heart into the

chest. Sham-operated animals received similar treatment; however, the suture was not secured.

Animals then recovered, received food and water *ad libidum*, and were monitored until their

respective endpoints post-surgery. Animals were randomly sorted into the following timepoints

for echocardiography and subsequent tissue harvest: 48 hours, 4 days, 1 week, 2 weeks, 4

weeks, and 8 weeks. Of n=84 animals designated for this study, a total of n= 30 sham-operated

and n= 49 LAD-ligated animals were used to acquire the samples for analysis. Of all the

animals in the study, 4.76% (n=4) did not survive to their designated timepoint and one LAD-

ligated animal did not form a visible infarct scar.

Tissues were collected from animals anaesthetized with 3% isoflurane for a minimum

of 10 minutes, after which limb reflexes were tested. Hearts were excised and immediately

washed in 1X PBS, after which they were dissected into discrete sections for future analyses. The sham-operated hearts were separated into right (RV) and left (LV) ventricles, while the LAD ligated hearts were separated into RV, viable LV, and infarcted LV (scar). Sections were then placed into cryogenic vials and flash-frozen in liquid nitrogen, then stored at -80°C until used for immunoblotting. Tissues intended for histology were frozen fresh, first by placing enough optimal cutting temperature (OCT) compound (VWR International, Radnor, PA; #95057-838) to cover the bottom of a cryomold and then flash-freezing it in a dry ice-ethanol bath. The tissue was then coated in OCT, and placed into the cryomold, making sure to orient it in such a way that sectioning would provide the largest surface area. The rest of the cryomold was filled with OCT, and flash-frozen once again in the ethanol bath. Freshly frozen blocks were immediately stored at -80°C until use.

4.3.3 Protein Isolation from Frozen Tissue Specimens

Frozen tissue samples were weighed on an analytical balance, ensuring that sections did not thaw prior to lysis. Samples were then crushed using a pre-chilled mortar and pestle while submerged in an excess volume of liquid nitrogen. The crushed tissue (and liquid nitrogen) was then decanted into a sterile 15 mL conical tube containing 1 mL tissue lysis buffer (125 mM Tris, pH 7.4; 1% SDS; 5% glycerol; 1X protease inhibitor cocktail (Sigma-Aldrich, #P8340), 10 mM NaF, 1.0 mM Na3VO4, and 1.0 mM EGTA) per 100 mg of tissue. The samples were then incubated on ice for 1 hour, with periodic vortexing to ensure complete lysis. Following 10 seconds of sonication, the lysate was transferred to QIAshredder columns (QIAgen, Hilden, Germany) and centrifuged according to the manufacturer's recommended conditions. The flow-through was collected into 1.5 mL microcentrifuge tubes and total protein concentration was determined by BCA assay; samples were stored at -80°C until use.

4.3.4 Preparation of Elastic Tissue Culture Surfaces

Silicone elastic tissue culture plates and coverslips bearing an elastic modulus of 5 kPa were prepared using the methods described in section 3.3.2 of this thesis.

4.3.5 Primary Rat Cardiac Fibroblast Cell Isolation and Culture Conditions

Primary cardiac fibroblasts were isolated from male Sprague-Dawley rats, as previously described, using similar methods to those described in section 3.3.3 of this thesis[165]. Upon confirmation of anesthesia, hearts were cannulated via the aorta on a Langendorff apparatus and then subject to retrograde perfusion with DMEM/F12 for 5 minutes, followed by Minimum Essential Medium, Spinner's Modification (S-MEM, Gibco # 11380-037) for another 5 minutes to flush out calcium and promote cell dissociation. To digest the tissue, the hearts were then perfused with S-MEM supplemented with 600 U/mL collagenase type II (Worthington Biochemical Corporation, Lakewood, NJ; #CLS-2) with recirculation for 25 minutes at 37°C.

For quiescent fibroblast culture, the digested tissue was incubated at 37°C, 5% CO_2 for 10 minutes, and then neutralized with 10 mL of Ham's F-10 medium (F-10, Gibco, # 11550-043) supplemented with 2% fetal bovine serum (FBS) and 100 U/mL penicillin-streptomycin. The tissue was further dissociated by trituration with a 10 mL serological pipette, and the final cell suspension was then gravimetrically passed through a 40 μm sterile cell strainer (Thermo Fisher Scientific, Waltham, MA) to remove any debris. The cells were pelleted by centrifugation at 200 x *g* for 5 minutes, and re-suspended in 40 mL of complete cell culture medium. For each 5 kPa 10 cm dish, 3 mL of cell suspension was added to a total of 10 mL of medium at plating. For 5 kPa coverslips in 35 mm or 6-well dishes, 0.5 mL of cell suspension was added to a total of 2 mL medium per dish or well. Fibroblasts were allowed to adhere for 3

hours at 37°C, 5% CO_2. Adherent cells were then briefly washed twice with pre-warmed 1X PBS supplemented with penicillin-streptomycin, and fresh complete F-10 culture medium was added. For the following 3 days, the cultures were once again washed twice with PBS, and the growth medium was replaced. Cells were used for experimentation 4 days post-plating.

For activated myofibroblast culture, digested tissue was incubated as described above, but was neutralized with DMEM/F12 supplemented with 10% FBS and penicillin-streptomycin. The tissue was dissociated and pelleted in a similar fashion as for quiescent cell culture, but the resulting 40 mL cell suspension was then plated on conventional polystyrene plastic surfaces, or glass coverslips coated in gelatin, as described above. Cells were allowed the adhere for 2 hours at 37°C, 5% CO_2, prior to brief washing in 1X PBS and replacing the complete DMEM/F12 culture medium. Cells were allowed to proliferate until ~75-80% confluence prior to passaging. Experiments using activated rat myofibroblasts were passaged once (P1).

4.3.6 Adenoviral Constructs and in vitro Infection Protocol

All adenoviral constructs were designed to overexpress the human gene product under control of the CMV promoter. The viruses overexpressing LacZ, HA-tagged SKI, and the MYC-BioID2 fusion proteins, were generated by our lab using Adeno-X Expression System (Takara Bio Inc., Kusatsu, Japan), as per the manufacturer's instructions. Details regarding the BioID2 vectors and assay are described in their own section below. The FLAG-tagged YAP[5SA] and MYC-tagged TAZ[4SA] viruses were designed by our lab and generated by VectorBuilder Inc. (Chicago, IL). Viral DNA vectors were sequenced for the presence of the transgene insert at The Centre for Applied Genomics (Hospital for Sick Children, Toronto, ON) prior to amplification. Viral titres were determined by using indirect cell-based ELISA

detection of adenovirus hexon protein in infected HEK 293A monolayers. The antibodies used were mouse anti-Adenovirus Type 1 Hexon (Invitrogen, #MA1-82982) and peroxidase goat anti-mouse (Jackson ImmunoResearch, #115-035-003); chromogenic detection was performed using DAB substrate (Thermo Scientific, #34002). All constructs and their sources are listed in Table 4.1.

Table 4.1. Adenoviral Constructs

Construct	Gene Product	Mutations	Source
Ad-LacZ	*E. coli* LacZ (NP_414878.1)	n/a	Dixon Lab
Ad-HA-SKI	Human SKI (NP_003027.1)	n/a	Dixon Lab
Ad-FLAG-YAP[5SA]	Human YAP1 (NP_001123617.1)	S61A, S109A, S127A, S164A, S397A	Vector Builder Inc.
Ad-MYC-TAZ[4SA]	Human TAZ (NP_001335291.1)	S66A, S89A, S117A, S311A	Vector Builder Inc.
Ad-MYC-BioID2	*A. Aeolicus* BirA* (NP_213397.1)	n/a	Dixon Lab
Ad-MYC-BioID2-SKI	Human SKI (NP_003027.1)	n/a	Dixon Lab
Ad-MYC-BioID2-TAZ	Human TAZ (NP_001335291.1)	n/a	Dixon Lab

To overexpress a given protein of interest, cells were serum-starved overnight (~16 hours) in F-10 medium supplemented with penicillin-streptomycin. The following day, the cells were transduced with a vector-dependent multiplicity of infection (MOI) of 20-50 in serum-free F-10 medium. Viral infection was allowed to proceed for approximately 36 hours prior to harvesting for analysis. This methodology was applied for both rat and human cardiac (myo)fibroblasts.

4.3.7 In vitro Drug Treatments

P1 primary rat cardiac fibroblasts were seeded onto stiff plastic culture plates at about 20% confluency (~7.0 x 105 cells/10 cm dish). Once the cells reached 40-50% confluency,

they were serum-starved overnight in DMEM/F12. The culture medium was then replenished (still serum-free), and supplemented with one of the following small-molecule inhibitors: MG132 (1 µM; Sigma-Aldrich; #M7449), GS143 (1 µM; Tocris Bioscience, Bristol, UK; #5636), D4476 (500 nM; Selleckchem, Houston, TX; #S7642). Control plates were treated with DMSO alone. Cells were pre-treated with the compounds for 3 hours, after which they were infected with either Ad-LacZ or Ad-HA-SKI (as described above; MOI of 50) and cells were harvested 24 hours post-infection.

4.3.8 siRNA-Mediated Gene Knockdown

First-passage (P1) cardiac myofibroblasts were seeded at 1.0×10^4 cells in each well of a 6-well dish. Cells were left to adhere overnight in DMEM/F12 supplemented with 10% FBS and 100 U/mL of penicillin-streptomycin. The cells were then gently washed twice with 1X PBS, then starved overnight in serum-free, antibiotic-free DMEM (Gibco, # 10564-011). The following day, the myofibroblasts were transfected for 24 hours with 50 nM of either a non-targeting siRNA pool (Dharmacon, Lafayette, CO) or a 4-oligo pool targeting the gene of interest using Lipofectamine RNAiMax (ThermoFisher) as per the manufacturer's protocol. If the assay was performed in conjunction with protein overexpression, the following day, the medium was changed (DMEM) and the cells were infected with the appropriate viral construct. Whole cell lysates were collected for analysis after approximately 36 hours of viral overexpression, and a total of 60 hours of gene knockdown. All oligo pools used are listed in Table 4.2.

Table 4.2. siRNA Oligo Pools

Target	Species	Accession	Pool (Dharmacon Cat#)
Lats1	*R. norvegicus*	NM_001134543.2	M-080189-01-0005
Lats2	*R. norvegicus*	NM_001107267.1	M-087043-01-0005
Limd1	*R. norvegicus*	NM_001112737.2	L-081750-02-0005
Wwtr1 (Taz)	*R. norvegicus*	NM_001024869.1	M-088521-01-0005
Non-targeting pool	*H. sapiens, M. musculus, R. norvegicus*	n/a	D-001810-10-05

4.3.9 Protein Isolation from Monolayer Cell Culture

Resting fibroblasts cultured on elastic surfaces were trypsinized and pelleted prior to lysis using the methods described in section 3.3.6 of this thesis. Protein isolated from first-passage myofibroblasts cultured on conventional polystyrene surfaces was harvested in a similar fashion, except that the cells were lysed by mechanical means. Using 100 µL RIPA lysis buffer and using a sterile cell scraper to lift the cells into solution directly in the culture dish, all contents were then transferred to a pre-chilled 1.5 mL microcentrifuge tube to continue processing for protein quantitation by BCA assay, as done in section 3.3.6.

Cytoplasmic and nuclear cell fractionation was achieved by using the Pierce NE-PER™ Extraction reagents (Thermo Scientific, #78833). All samples were kept at -20°C for short term use, or -80°C for long term storage.

4.3.10 Immunoblotting

SDS-PAGE of 20-30 µg of protein was performed on 4-15% gradient reducing gels, using the protocol described in section 3.3.7 of this thesis. Total protein loading was measured prior to blotting using Ponceau S (Alfa Aesar, Haverhill, MA; #J63139) staining, or after blotting using Pelikan 17 black India ink (Thomas Scientific, Swedesboro, NJ; #C861L76) and densitometric analysis. Blots were incubated with primary antibodies overnight at 4°C with

gentle shaking. Primary antibodies were used at the following dilutions: ED-A (cellular) fibronectin (1:1000; MilliporeSigma, Burlington, MA; #MAB1940), αSMA (1:5000; Sigma; #A2547), Periostin (1:1000; Abcam, Cambridge, UK; #14041), Vimentin (1:2000; Abcam; #ab8069), YAP(1:1000; Cell Signaling, Danvers, MA; # 14074), TAZ/WWTR1 (1:1000; Cell Signaling; #83669), GAPDH (1:5000; Cell Signaling; #97166), LIMD1 (1:1000; Abcepta Inc, San Diego, CA; # AP13132b), LATS1 (1:1000; Cell Signaling; #3477), LATS2 (1:1000; Cell Signaling; #5888), HA-tag (1:1000; Rockland Immunochemicals Inc., Limerick, PA; #600-401-384), MYC-tag (1:1000; Cell Signaling; #2278), NCoR1 (1:800; Cell Signaling; #5948), TEAD3 (1:1000; Cell Signaling; #13224). Corresponding HRP-conjugated secondary antibodies (Jackson ImmunoResearch, West Grove, PA) were applied at a 1:5000-1:10 000 dilution for 1 hour at room temperature. Antibody detection was done using ECL substrate, and protein bands were visualized on blue X-ray film (Mandel Scientific, Guelph, ON). Protein expression was measured by relative densitometry using Quantity One analysis software (version 4.6.9; Bio-Rad).

4.3.11 Total RNA Isolation and Quantitative PCR

Cardiac fibroblasts were harvested by trypsinization and centrifugation at 200 x g for 5 minutes. Column-based total RNA isolation and subsequent cDNA synthesis were performed as described in section 3.3.8 of this thesis. The final cDNA product was diluted to 200 μL sterile TE buffer (10 mM Tris-HCl, 1 mM EDTA, pH 8.0) and was stored at -80°C until use.

Gene expression was assayed using Luna® Universal qPCR Master Mix (New England Biolabs, Ipswich, MA; #M3003), and 1 μL template cDNA. Primers were used at a final concentration of 200 nM, and all reactions were performed in technical triplicates on a QuantStudio 3 Real-Time PCR System (Applied Biosystems, Foster City, CA), using the fast

cycling mode. Relative gene expression was calculated using the $2^{-\Delta\Delta Ct}$ method[412] All samples

from resting (P0, 5 kPa plates) fibroblasts were normalized to endogenous Tyrosine 3-

monooxygenase/ Tryptophan 5-monooxygenase Activation protein Zeta (*Ywhaz*) expression,

while samples from activated myofibroblasts (P1, plastic plates) were normalized to

Hypoxanthine-Guanine Phosphoribosyltransferase (*Hprt1*). All qPCR primer pairs and their

targets' respective Accession numbers are listed in Table 4.3.

Table 4.3. qPCR Primers

Gene	Accession	Forward Primer (5'- 3')	Reverse Primer (5'-3')
Acta2	NM_031004.2	AGATCGTCCGTGACATCAAGG	TCATTCCCGATGGTGATCAC
Ccn2 (Ctgf)	NM_022266.2	CAAGCTGCCCGGGAAAT	CGGTCCTTGGGCTCATCA
Col1a1	NM_053304.1	TGCTCCTCTTAGGGGCCA	CGTCTCACCATTAGGGACCCT
Col1a2	NM_053356.1	TGACCAGCCTCGCTCACAG	CAATCCAGTAGTAATCGCTCTTCCA
Col3a1	NM_032085.1	GGTTTCTTCTCACCCTGCTTC	GGTTCTGGCTTCCAGACATC
Fn1	NM_019143.2	ACTGCAGTGACCAACATTGACC	CACCCTGTACCTGGAAACTTGC
Limd1	NM_001112737.2	AACAGGCCTTTGGTCCACTG	GCCTCATATCCCAGACTCGAA
Hprt1	NM_012583.2	CTCATGGACTGATTATGGACAGGAC	GCAGGTCAGCAAAGAACTTATAGCC
Postn	NM_001108550.1	GCTTCAGAAGCCACTTTGTC	CGCCAACTACATCGACAAGG
RelA	NM_199267.2	TTCCCTGAAGTGGAGCTAGGA	CATGTCGAGGAAGACACTGGA
Tcf21	NM_001032397.1	CATTCACCCAGTCAACCTGA	CCACTTCCTTTAGGTCACTCTC
Wwtr1	NM_001024869.1	ACCTGGCTGTAGTGTGATGC	CCAGGCAATGATTAAGCGGC
Yap1	NM_001034002.2	CAGACAACAACATGGCAGGAC	CTTGCTCCCATCCATCAGGAAG
Ywhaz	NM_013011.3	TTGAGCAGAAGACGGAAGGT	GAAGCATTGGGGATCAAGAA

4.3.12 Plasmid Expression Vectors and Site-Directed Mutagenesis

Mutation of human YAP and TAZ to promote nuclear translocation was performed

using the QuickChange II Site-Directed Mutagenesis Kit (Agilent Technologies, Santa Clara,

CA; # 200523), with some modifications to the manufacturer's protocol, as described by

Zheng *et al[432]*. Both wild-type genes were cloned into pcDNA3 prior to mutagenesis. The YAP

S127A mutation was achieved by using the following primer pair: 5'- CATGTTCGA

GCTCATGCATCTCCAG CTTCTCTGCAGTTGGGAGCTG-3' and 5'- CAGAGAAGCTGG

AGATGCATGAGCTCGAA CATGCTGTGGAGTCAG3'. The TAZ S89A mutation was

achieved with the following primer pair: 5' – CAGCATGTCCGCTCGCACGCGTCGCCCG

CG TCCCTGCAGCTGGGCAC-3' and 5'- CGCGGGCGACGCGTGCGAGCGGACATGC

TGGG CACCCCCAGCCAGTCG-3'. All plasmid constructs were sequenced for confirmation

of the mutation and complete coverage of the insert.

4.3.13 Luciferase Reporter Vectors for Collagen 1a1 and 3a1 Promoters

Proximal promoters for the human *COL1A1* (1.4 kb) and *COL3A1* (1.5 kb) genes were

generated from genomic DNA isolated from HEK 293A cells, and subcloned into the

pGL4.1[*Luc2*] vector via the KpnI and NheI restriction sites. The following primer pairs were

used for PCR amplification of the promoters: *COL1A1,* forward 5'- CAGTGGTACCGAAGC

TGCTGATGGAGTTAACTTCTGC- 3' and reverse 5'- GACTGCTAGCGTCCGCGTATCC

ACAAAGCTGA- 3'; *COL3A1,* forward 5'- CAGTGGTACCGCCACTGTCCATGCTTAC-3',

and reverse 5'- GACTGCTAGCGATGAAGCAGAGCGAGAAG- 3'. Both promoters were

isolated from 100 ng genomic DNA, using Q5™ High-Fidelity DNA Polymerase (New

England Biolabs) according to the manufacturer's recommendations. After ligation into the

pGL4.1 vector, all plasmid constructs were sequenced for complete coverage of the insert prior

to performing any *in vitro* assays.

4.3.14 Luciferase Reporter Assay

NIH-3T3 fibroblasts were seeded in 6-well dishes 24 hours prior to transfection at a

density that would yield ~70% confluency. Wells were co-transfected using jetPRIME DNA

transfection reagent (Polyplus Transfection, Illkirch, France; #114-15) with 500 ng

pGL4.1[*Luc2*] promoter-reporter plasmid and 500 ng expression vector for 48 hours. Cells

transfected with empty expression vector with the corresponding promoter construct served as background control samples. Promoter activity was assayed using the Luciferase Reporter Assay Kit I (PromoCell GmbH, Heidelberg, Germany; # PK-CA707-30003-1) and luciferase activity was quantified on a GloMax Multi+ Multimode Plate Reader (Promega, Madison, WI). All samples were assayed in triplicate, and relative promoter activity was normalized to the total protein concentration of the corresponding sample.

4.3.15 Collagen Gel Contraction Assay

Three-dimensional collagen gels were prepared by mixing 16 mL of chilled collagen solution (PureCol® Type I bovine collagen; Advanced BioMatrix, Sand Diego, CA), with 2 mL of sterile 10X PBS. While keeping the solution on ice, the pH was adjusted to 7.4 using sterile 0.1 M NaOH, and the volume was brought up to 20 mL with sterile water. Gels were cast in a 24-well plate by adding 600 µL solution to each well and allowing them to solidify at 37°C, 5% CO_2 overnight. The following day, P0 fibroblasts cultured on 5 kPa elastic surfaces (in F-10 medium, 2% FBS) were passaged and seeded on the collagen matrices at a density of 1.5 x 10^4 cells per well and allowed to adhere for 24 hours. The gels were then released from the wells using a circular cutting tool and immediately infected with their corresponding adenoviral vector, or treated with 4 ng/mL recombinant human TGF-β_1 (Cell Signaling, #8915) as a positive control. Images were taken immediately following treatment, and subsequently every 24 hours for a total of 72 hours post-treatment. Gel contraction was estimated by measuring the surface area of the top of the gel using ImageJ image processing software[433].

4.3.16 In vitro Wound Healing Assay

Three silicone inserts (Ibidi, Martinsried, Germany; #81176) were placed into the wells of a porcine gelatin-coated 24-well 5 kPa elastic tissue culture dish (Excellness, as described

above). 70 uL of freshly-isolated primary rat cardiac fibroblast cell suspension (~5.0×10^4

cells/mL) was added to each chamber of the insert, and 0.5 mL of F-10 medium supplemented

with 2% FBS was added to the area surrounding the insert to prevent moisture loss. The culture

medium was changed every day for the following 3 days, after which the cells were allowed to

reach 80% confluency within the insert chambers. The inserts were then removed and the cells

were infected with a MOI of 50 of their corresponding adenoviral constructs in serum-free F-

10 medium. Light microscopy images were captured at 6, 12, and 18 hours post-infection, after

which percent surface area coverage was calculated using ImageJ software.

4.3.17 Isolation of Human Atrial Cardiac Fibroblasts

Discarded atrial tissue was obtained from (male) patients undergoing elective CABG

surgery, with no previous history of myocardial infarction. Cells were isolated as previously

described[434]. In brief, freshly-isolated atrial tissue was finely minced and placed in culture

dishes containing basal medium supplemented with 10% fetal bovine serum (FBS), 100

units/mL penicillin and 100 μg/mL streptomycin. Cells were allowed to migrate from the

explants for approximately 10 days prior to passaging, at which point they were maintained in

complete cardiac fibroblast growth medium (FGM™, Lonza Group AG, Basel, Switzerland).

Cells were passaged at least two times (P2) prior to using in experiments, and P3 cells were

frozen for future use and used for BioID2 experiments. These cells were considered activated

myofibroblasts, as they had been passaged multiple times.

4.3.18 BioID2 Assay and Mass Spectrometry Analysis

BioID2 fusion proteins were generated from the myc-BioID2-MCS plasmid and

Adeno-X Adenoviral Expression System 1 (Takara Bio, formerly Clontech, Mountain View,

CA). The myc-BioID2-MCS vector was a gift from Kyle Roux (Addgene plasmid # 74223;

http://n2t.net/addgene:74223 ; RRID:Addgene_74223). In brief, the human Ski and Taz

(Wwtr1) genes were cloned into multiple cloning sites of the myc-BioID2 vector using 5'

BamHI and 3' HindIII restriction sites. From here, both genes were sub-cloned into the

pShuttle2 vector via the 5' NheI and 3' AflII sites; this was repeated with the empty BioID2

vector as well. Following the methods described by the Adeno-X System 1, all three inserts

were then subcloned into the adenoviral backbone by using PI-SceI and I-CeuI homing sites.

From here, the adenoviral DNA was digested with PacI, and 3 μg of each was transfected into

a 60 mm dish of subconfluent HEK 293A cells using jetPRIME® transfection reagent

(Polyplus-transfection SA, New York, NY). Packaged virus was then amplified four times,

then titred by *in situ* hexon staining of serial dilutions of the viral stock.

In vitro biotinylation assays were performed on primary human cardiac fibroblasts isolated

from discarded atrial tissue from patients undergoing coronary bypass surgery, as described

above. Cells passaged three times (P3) were used in BioID2 assays, and were considered as

activated myofibroblasts.

Once at approximately 40% confluency, the cells were switched to serum-free F10

medium, and infected with a MOI of 20 of either: Ad-myc-BioID2-Empty, Ad-myc-BioID2-

hSKI, or Ad-myc-BioID2-hTAZ. After 24 hours, the medium was supplemented with 20 μM

biotin from a freshly prepared 100X stock diluted in warm culture medium. Finally, after

further incubation for 18 hours, the medium was removed and the cells were briefly washed

twice with room-temperature 1X phosphate buffered saline (PBS). Cells were lysed with 500

μL lysis buffer (1% NP-40; 0.5% deoxycholate; 0.2% SDS, 50 mM Tris HCl, pH 7.4; 150 mM

NaCl; 1 mM EDTA; 10% glycerol; supplemented with 1X Sigma protease inhibitor cocktail

P8340) and scraped into 2 mL microcentrifuge tubes. Samples were briefly sonicated, and then

Triton X-100 was added to a final concentration of 2%. After further sonication, the samples were then diluted with an equal volume of 50 mM Tris HCl, pH 7.4 and incubated overnight on a rotator at 4°C with 400 µL of magnetic streptavidin beads (#S1420S, New England Biolabs, Ipswich, MA) that had been pre-washed for 10 minutes in lysis buffer. The following day, the beads were washed once in 2% SDS for 10 minutes, followed by four times for 10 minutes each in 50 mM Tris HCl, pH 7.4. The beads were resuspended in 1 mL wash buffer, and 20% was saved for analysis by Western blot. The beads destined for immunoblotting were resuspended in 75 µL of 2X SDS-PAGE Laemmli loading buffer supplemented with 10% 2-β-mercaptoethanol and 1 mM biotin and heated at 95°C for 5 minutes. Supernatants were then stored at -80°C until needed. The remaining beads were resuspended in 250 µL of 50 mM NH_4HCO_3 and sent for mass spectrometry analysis at the Manitoba Centre for Proteomics and Systems Biology (Winnipeg, MB, Canada).

Samples isolated by BioID2 pulldown were subject to tryptic digestion in 50 mM NH_4HCO_3 on the magnetic beads for 16 hours. After separation by 1D liquid chromatography (LC) with a 90-minute nonlinear gradient, digested peptide solutions for each biological replicate was subject to two technical replicate analyses on a Q Exactive™ HF-X Orbitrap mass spectrometer (Thermo Scientific, Waltham, MA) in standard tandem MS/MS with data-dependent acquisition. The protein identification parameters were as follows: minimum fragment M/Z of 100; precursor mass tolerance of ± 10 ppm; fragment mass error of 0.02 Da, and a maximum E-value of 0.01. Fixed modifications for oxidation of methionine and tryptophan, deamination of asparagine and glutamine, and carboxyamidomethylation of cysteine were also included in the analytical parameters. Peptides were compared against the SwissProt human protein database and were identified and quantified using X!tandem

(Alanine, 2017.02.01). Proteins with fewer than 3 spectral counts, common background and contaminating proteins (e.g. keratins, histones, trypsin) were excluded from the resulting data. Technical replicates were then combined for interactome analysis.

Significance of interaction between bait (SKI or TAZ) and prey was determined using probabilistic scoring via the Significance of Analysis of Interactome express (SAINTexpress) algorithm[435]. Using the Contaminant Repository for Affinity Purification (CRAPome.org)[436], SAINTexpress was applied to the datasets using user-uploaded (untreated and empty BioID2 vector) controls, incorporation of iRefIndex data, and using all replicates per bait. SAINT scores and fold-change values for both SKI and TAZ are displayed in Tables E.1 and E.2, respectively. Proteins included in the final interactomes had a fold change of ≥3 compared to empty-BioID2 and untreated controls, and obtained a SAINT score ≥ 0.5. Our rationale for lowering the SAINT score was due to the fact that there exists no repository for primary human cardiac fibroblast protein interactions, and the vast majority of proximity-labelling data that is publicly available has been gathered in cell lines. Thus, we could not rely entirely on the iRefIndex data that is used in the scoring algorithm.

The resulting data were then formatted for use in Cytoscape (version 3.7.1) to generate interaction network graphics, and Gene Ontology (GO) and pathway analyses were performed using and the STRING database (version 11.0) and WikiPathways (wikipathways.org)[437]. Finally, novel interactions were confirmed by repeated affinity capture after culturing transduced cells in 50 μM biotin, and probing for targets by immunoblotting. Data was generated using cells isolated from n = 4 biological samples. Original mass spectrometry data for BioID2 in human cardiac fibroblasts can be accessed using the file numbers in Table 4.4 the following hyperlink to access the Global Proteome Machine (GPM):

Table 4.4. Global Proteome Machine (GPM) Numbers for Mass Spectrometry Data

Dataset Name	GPM number
Human Cardiac Fibroblast BioID2 - Control - Set 1	GPM10000002938
Human Cardiac Fibroblast BioID2 - Control - Set 2	GPM10000002939
Human Cardiac Fibroblast BioID2 - Empty - Set 1	GPM10000002941
Human Cardiac Fibroblast BioID2 - Empty - Set 2	GPM10000002940
Human Cardiac Fibroblast BioID2 - SKI - Set 1	GPM10000002942
Human Cardiac Fibroblast BioID2 - SKI - Set 2	GPM10000002943
Human Cardiac Fibroblast BioID2 - TAZ - Set 1	GPM10000002944
Human Cardiac Fibroblast BioID2 - TAZ - Set 2	GPM10000002945

4.3.19 F/G Actin Isolation and Fractionation

Cardiac myofibroblasts were cultured and treated in 10 cm dishes, and harvested at ~50-60% confluency. Cells were washed twice in pre-warmed 1X PBS to remove any excess medium and serum. After removing as much PBS as possible, F and G actin were isolated using a G-actin/F-actin *in vivo* Assay Kit (Cytoskeleton Inc., Denver, CO; #BK037), as per the manufacturer's directions. F/G actin ratios were determined by equal volume loading of each fraction for a given sample onto 4-15% gradient SDS-PAGE gels, followed by blotting on PVDF membranes. Immunoblotting was performed with pan-actin antibody (1:1000; Cell Signaling; #4968), and peroxidase-conjugated goat anti-rabbit secondary antibodies (1:10 000; Jackson ImmunoResearch).

4.3.20 Fluorescence Immunohistochemistry (IHC-F)

Frozen tissue blocks were warmed from -80°C to -20°C for a least 1 hour prior to sectioning. Tissues were cut into 6 µm sections using a cryostat microtome and mounted on glass slides which were kept in a Coplin jar on ice. Sections were allowed to air dry and adhere

to the slides for 30 minutes while remaining on ice. The slides were then washed twice for 5 minutes with warm PBS to remove as much OCT compound as possible.

Tissue sections were fixed in 4% paraformaldehyde in 1X PBS (pH 7.4) for 10 minutes, after which they were washed in neutralizing buffer (0.4 M Glycine in 1X PBS, pH 7.4) twice for 5 minutes each. Sections were then permeabilized for 15 minutes at room temperature in 0.1 % Triton X-100 in PBS. Non-specific binding sites were then blocked for 30 minutes in 5% Normal Goat Serum (Invitrogen, # 50-197Z) in PBS. Slides were then washed 3 times for 5 minutes each in PBS. Prior to removing the last wash, primary antibodies were diluted in 1% Bovine Serum Albumin (Alfa Aesar, #J64655) in PBS with 0.05% Triton X-100 to their appropriate concentration: rabbit anti-YAP (1:100), rabbit anti-TAZ (1:100), mouse anti-Vimentin (1:100). Sections were incubated in primary antibody solutions overnight at 4°C in a sealed, humidified chamber. Primary antibodies were suctioned off, and the slides were washed 5 times for 5 minutes each in PBS. Alexa Fluor-conjugated secondary antibodies were applied at a 1:500 dilution in the same dilution buffer at the primary antibodies: 488, 594. Secondary antibodies were removed, and sections were washed every 5 minutes for 45 minutes in PBS. Sections were thoroughly dried with gentle suctioning, and a glass coverslip was applied with 15 µL mounting medium with DAPI (Invitrogen, #P36971) per section. After allowing the slides to cure overnight at room temperature, sections were imaged with a Zeiss LSM 5 Pascal microscope using DAPI, FITC and Texas Red detection channels. Images were acquired and processed using AxioVision Microscopy software (Zeiss, rel. 4.8).

4.3.21 Fluorescence Immunocytochemistry (ICC-F)

Cells were seeded at a low (~10-15%) confluency onto either glass coverslips in 6-well dishes, or elastic (5 kPa) silicone coverslips (ExCellness) in 35 mm dishes, coated with porcine

gelatin type A. After appropriate treatments, the cells were briefly washed in PBS, followed by

fixing in 4% paraformaldehyde in PBS and permeabilization with 0.1% Triton X-100 in PBS,

as described in section 3.3.9 of this thesis.

The following primary antibodies were used to probe for targets of interest: αSMA

(1:200; Sigma; #A2547), YAP (1:100; Cell Signaling; #14074), TAZ/WWTR1 (1:100; Cell

Signaling; #83669), ED-A fibronectin (1:100; Millipore Sigma; #MAB1940), LIMD1 (1:100;

R&D Systems, Minneapolis, MN; #MAB8494) and incubated overnight at 4°C. The following

day, the cells were thoroughly washed three times in PBS and incubated with Alexa Fluor

fluorophore-conjugated secondary antibodies at 1:100 dilution for 1 hour at room temperature:

488 rabbit anti-mouse (Invitrogen, #A27023), 647 rabbit anti-mouse (Invitrogen, #A27029),

488 goat anti-rabbit (Invitrogen, #A27034). For the samples stained for αSMA, after the initial

incubation with secondary antibodies, F-actin was stained using a 1:500 dilution of rhodamine-

phalloidin (R415; Invitrogen) in PBS for 30 minutes. After several washes over a period of 30

minutes, the coverslips were thoroughly dried using gentle suction and mounted on glass slides

using mounting medium with DAPI (Invitrogen, #P36971) and allowed to cure at room

temperature for 24 hours. Coverslips were then sealed and cells were imaged using a Zeiss

LSM 5 Pascal microscope as described above.

4.3.22 Data Analysis and Statistics

Statistical analyses and graphic data representations were primarily generated using

GraphPad Prism 8 (version 8.1.2; May 2019). All data are represented by the mean ± standard

deviation, unless otherwise indicated in the figure legends. Individual biological replicates (n

values) are defined as originating from experiments involving cells or tissue from one single

animal or human donor. Biological replicates from assays involving cell lines were defined as

having originated from cells from different passages. Data distribution was assessed by the Shapiro-Wilk test. Non-parametric grouped data analyses were performed using Kruskal-Wallis tests. Grouped data with normal distribution ($P > 0.05$ Shapiro-Wilk test) were analyzed by one- or two-way ANOVA with Tukey's *post hoc* test for multiple comparisons or Dunnett's *post hoc* test when performing multiple comparisons to the controls only. *In vivo* data was analyzed with right (RV) and left ventricles (LV) as separate groups. Sham RV and MI RV were compared using two-way ANOVA with Sidak correction, while sham LV, viable MI viable LV and MI Scar LV were analyzed by two-way ANOVA with Dunnett's correction. Experiments involving only control and one test condition were analyzed by t-tests (e.g. F/G actin ratios were analyzed by paired t-tests). Significance was recorded if $P < 0.05$. BioID data were analyzed using the SAINTexpress algorithm for probability scoring of individual protein-protein interactions, and graphical representation of interactomes and their SAINT scores was generated using Cytoscape, as described above in section 4.3.18.

4.4 Results

4.4.1 TAZ Is a Stronger Activator of the Synthetic Activated Cardiac Myofibroblast Phenotype than YAP

To examine whether YAP and TAZ activation exert differential effects on the cardiac fibroblast phenotype, we employed soft substrate cell culture (described in Chapter 3) in conjunction with overexpression of constitutively-active forms of each paralog. This method was also used to determine whether either protein can overcome the lack of mechanical and growth factor input to promote fibroblast activation under such conditions. Unpassaged (P0) primary rat cardiac fibroblasts were isolated and treated with adenoviruses that overexpress constitutively-active, nuclear forms of YAP or TAZ. To generate these constructs, five serine

residues were modified to alanine for YAP (S61A, S109A, S127A, S164A, S397A) and four

for TAZ (S66A, S89A, S117A, S311A) as previously reported[213, 438-440]. These will henceforth

be referred to at YAP[5SA] and TAZ[4SA], respectively. Overexpression of both YAP[5SA]

and TAZ[4SA] increased expression of ED-A fibronectin, with a moderately more pronounced

effect with TAZ (Fig. 4.1A, B, C). There was no apparent change in global αSMA protein

expression with either paralog, when compared to Ad-LacZ infected controls (Fig. 4.1A, B).

When probing for both αSMA and F-actin by immunofluorescence, there was a marked

increase in αSMA inclusion in cytoskeletal stress fibers with both YAP[5SSA] and TAZ[4SA],

despite the cells being maintained on compressible ($E = 5$ kPa) surfaces (Fig. 4.1D). In

addition to this finding, two-dimensional collagen gel contraction assays confirmed that both

YAP[5SA] and TAZ[4SA] were able to increase cell contractility, which was comparable to

TGF-β_1 treated positive controls (Fig 4.2A). This contractile quality was nearly completely

abrogated by the co-expression of nuclear SKI with TAZ[4SA], suggesting that SKI's activity

exerted on TAZ is likely dependent on its phosphorylation and destabilization. In addition,

wound healing assays on soft substrates demonstrated a two-fold increase in closure rate with

either YAP[5SA] or TAZ[4SA] when compared to Ad-LacZ infected controls (Fig. 4.2B).

a

| | Control | Ad-LacZ | Ad-FLAG-YAP[5SA] | Ad-MYC-TAZ[4SA] |

EDA-Fn

αSMA

TAZ

YAP

Vimentin

Total Protein

b

EDA-Fn

Relative Densitometric Units (EDA-Fn/Total Protein)

3

2

1

*

***

**

Control   Ad-LacZ   Ad-YAP[5SA]   Ad-TAZ[4SA]

αSMA

Relative Densitometric Units (αSMA/Total Protein)

4

3

2

1

Control   Ad-LacZ   Ad-YAP[5SA]   Ad-TAZ[4SA]

c

DAPI   ED-A Fibronectin   Merged

Ad-LacZ

Ad-YAP[5SA]

Ad-TAZ[4SA]

200 µm

d

| DAPI | αSMA | F-Actin | Merged |
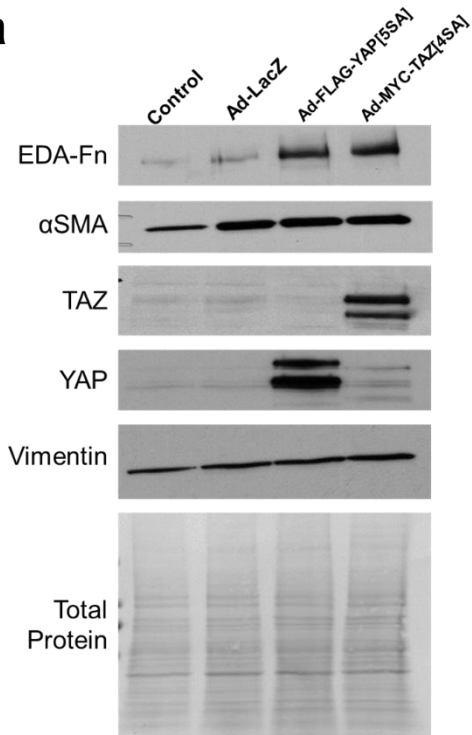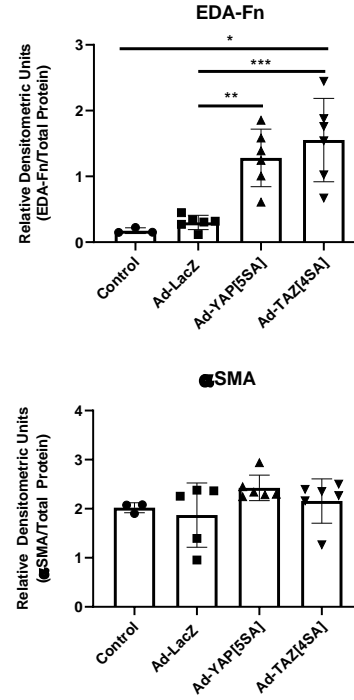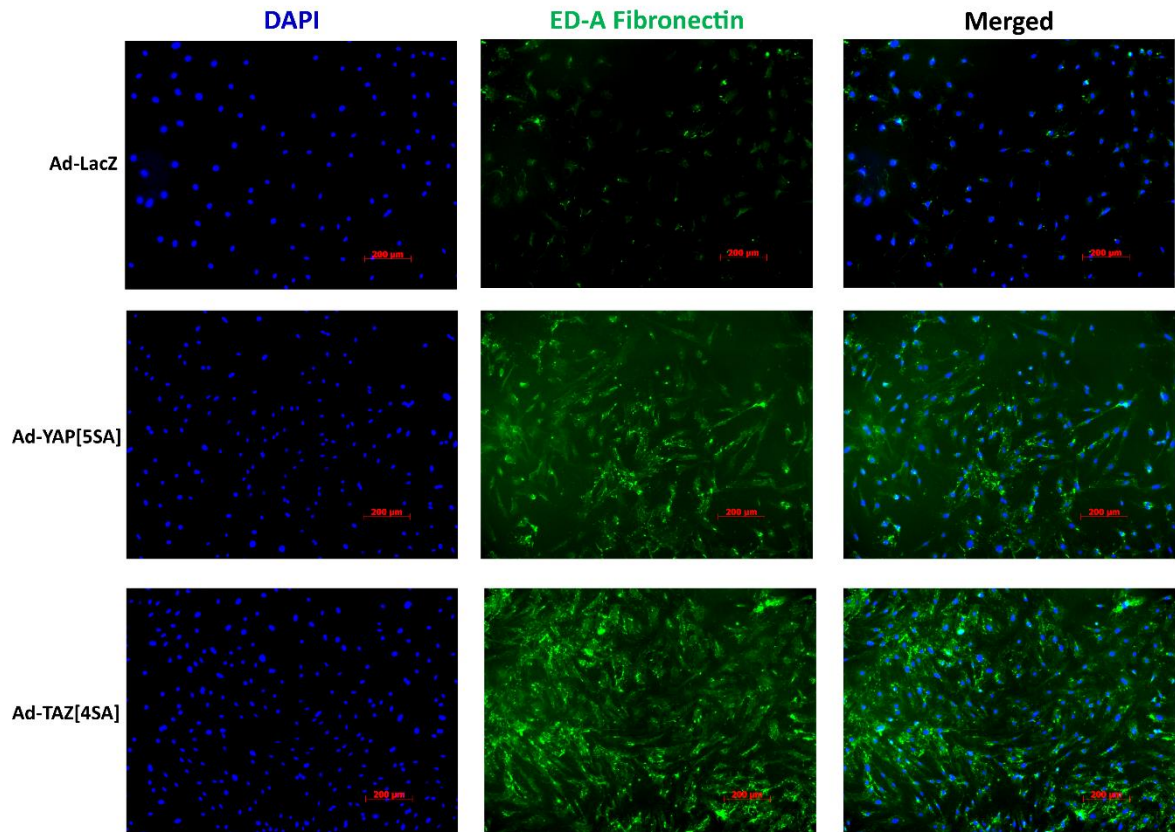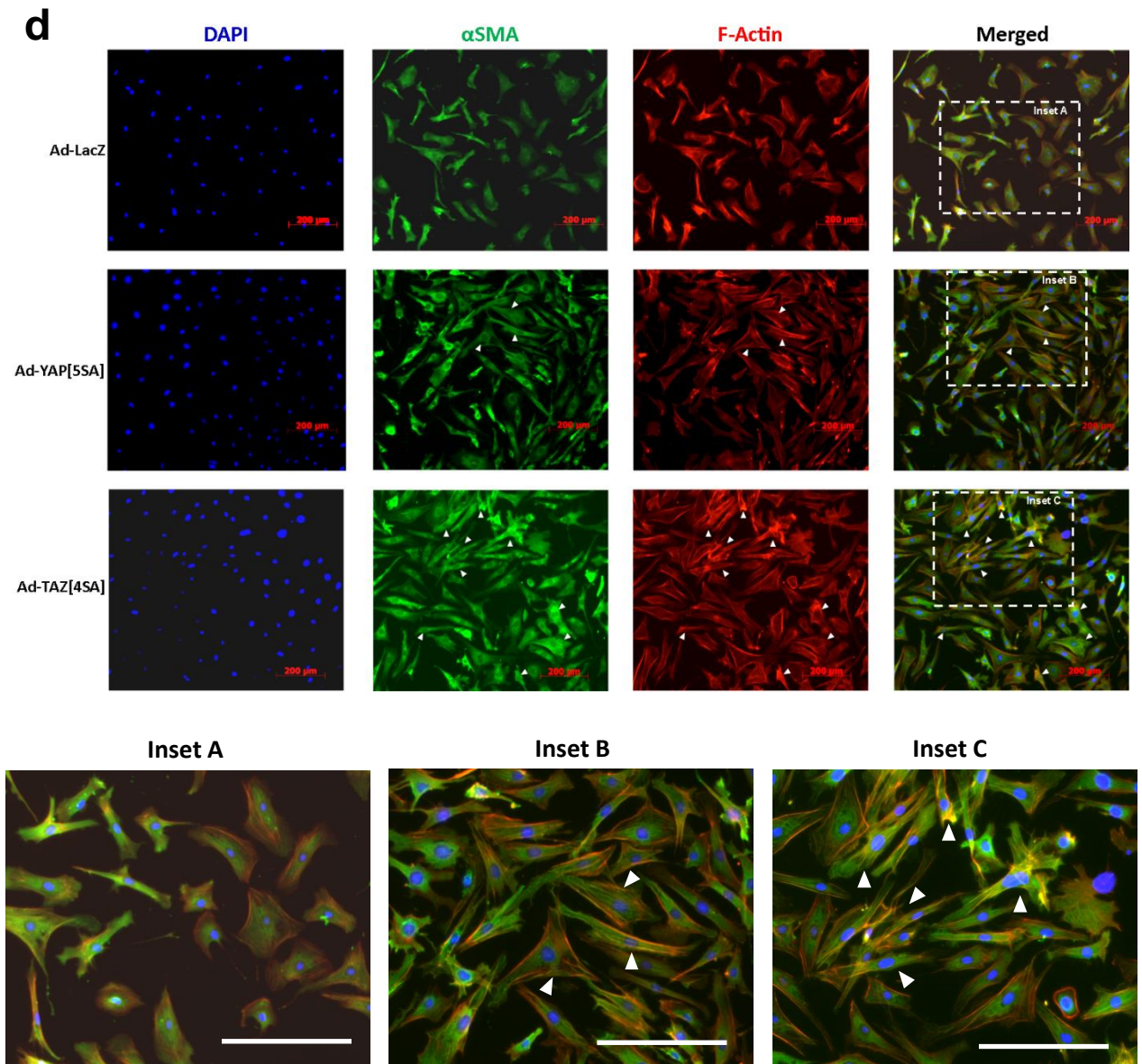
Figure 4.1. YAP and TAZ induce cardiac myofibroblast marker expression. A. Immunoblotting of whole cell lysates from unpassaged (P0) primary rat cardiac fibroblasts cultured on 5 kPa elastic silicone tissue culture surfaces coated with gelatin. Cells were treated with adenoviral constructs overexpressing constitutively-active forms of YAP (Ad-FLAG-YAP[5SA]), TAZ (Ad-MYC-TAZ[4SA]), or Ad-LacZ controls for approximately 36 hours. **B**. Quantification of densitometric measurements represented in panel A (n = 3 untreated controls; n= 6 biological replicates per test condition). Data are presented at mean ± SD. *P< 0.05 versus untreated and Ad-LacZ infected controls. **C**. P0 primary rat cardiac fibroblasts cultured on 5 kPa elastic silicone coverslips were infected with constitutively-active Ad-YAP[5SA], Ad-TAZ[4SA], or Ad-LacZ for 36 hours prior to fixation and for indirect immunofluorescence detection of fibronectin extracellular domain splice variant A (ED-A FN; green); nuclei were counterstained with DAPI (blue). Scale bar = 200 µm. **D**. P0 primary rat cardiac fibroblasts treated as described for panel C, with indirect immunofluorescence detection of alpha-Smooth Muscle Actin (αSMA; green) and F-actin (phalloidin staining; red). White arrows indicate cells with greater inclusion of αSMA into F-actin stress fibers. Scale bar = 200 µm. Data shown for C and D are representative of n=3 biological replicates.

a

+TGF-β | Ad-LacZ | Ad-YAP[5SA] | Ad-TAZ[4SA] | Ad-SKI | Ad-SKI + Ad-TAZ[4SA]

Collagen Gel Contraction

- TGF-β
- Ad-LacZ
- Ad-YAP[5SA]
- Ad-TAZ[4SA]
- Ad-SKI
- Ad-SKI + Ad-TAZ[4SA]

b

t = 0 h | t = 18 h

Ad-LacZ

Ad-MYC-TAZ[4SA]

Ad-FLAG-YAP[5SA]

Wound Healing (18 h)

c

Ctgf | *Col1a1* | *Col1a2* | *Acta2*

Col3a1 | *Fn1 (ED-A)* | *Tcf21* | *RelA*

d

Col1a1 Promoter

Col3a1 Promoter

pGL4.1[*luc2*]-Col1a1prom	+	+	+	+	–	–	–	–
pGL4.1[*luc2*]-Col3a1prom	–	–	–	–	+	+	+	+
pcDNA3 (no insert)	–	+	–	–	–	+	–	–
pcDNA3-FLAG-YAP[S127A]	–	–	+	–	–	–	+	–
pcDNA3-MYC-TAZ[S89A]	–	–	–	+	–	–	–	+
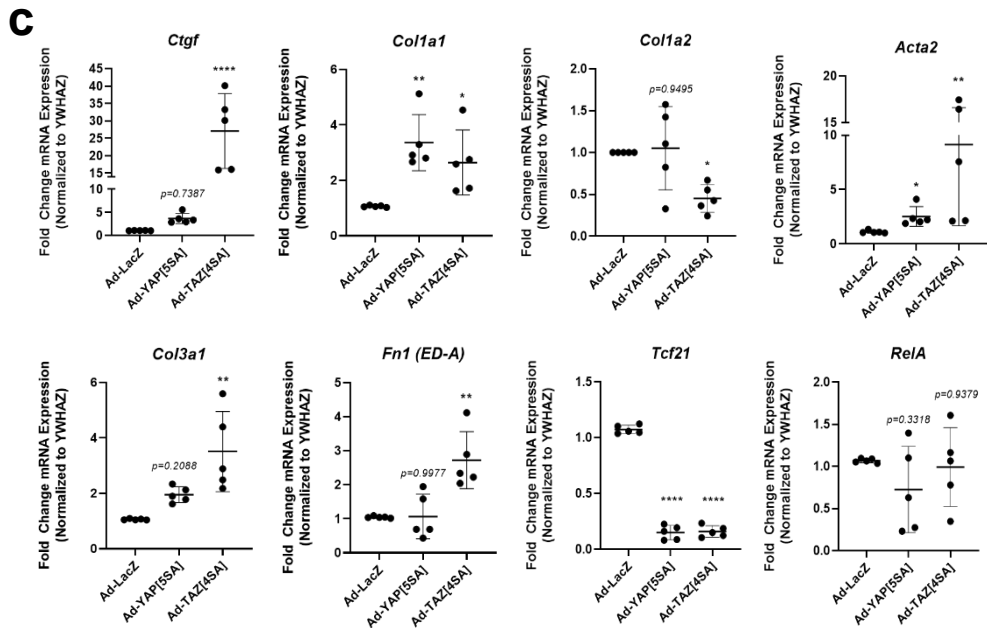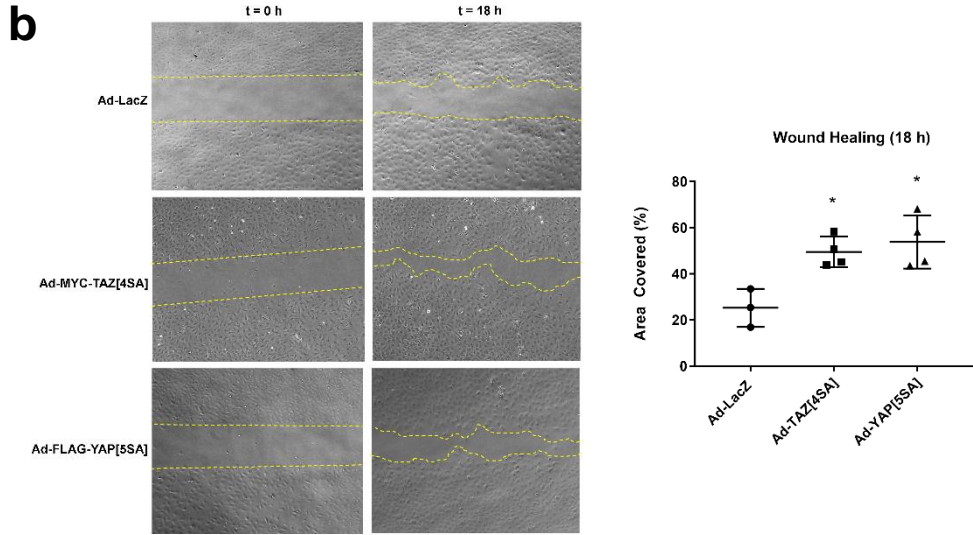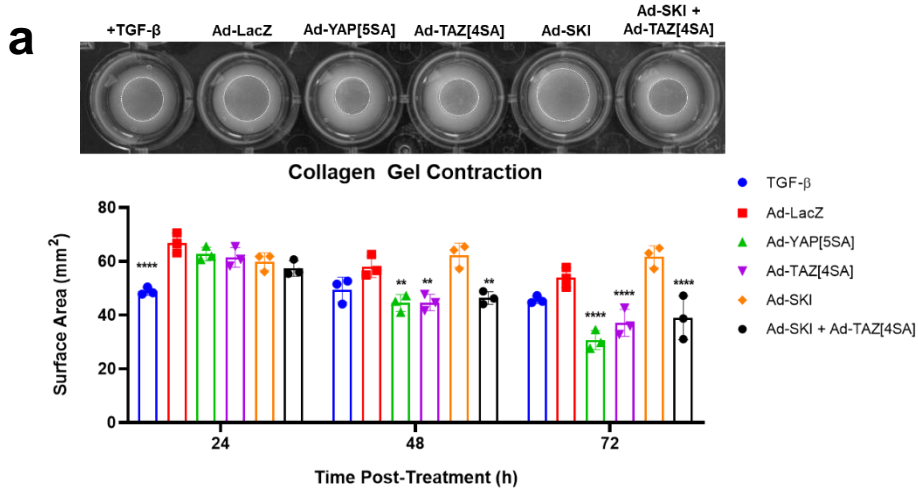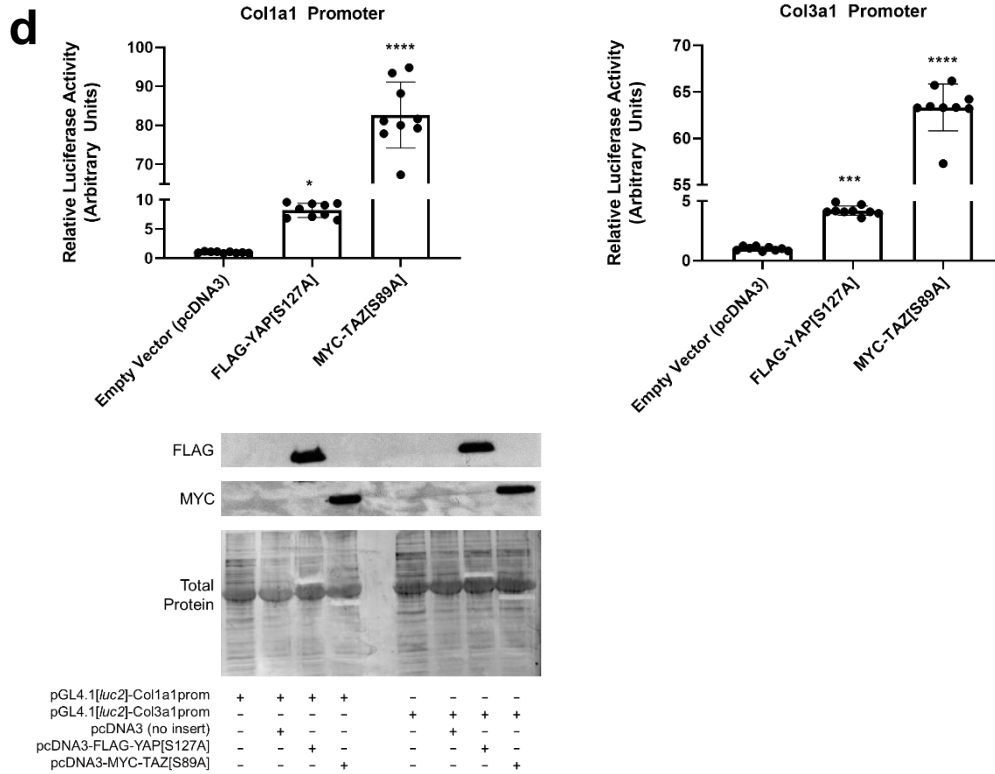
Figure 4.2. Cardiac myofibroblast gene expression, function, and physiology are enhanced by YAP and TAZ expression. A. P0 rat cardiac fibroblasts seeded on two-dimensional collagen matrices were assayed for gel contraction following infection with Ad-YAP[5SA], Ad-TAZ[4SA], Ad-SKI, a combination thereof, or with Ad-LacZ control. Treatment with recombinant human TGF-β_1 served as a positive control. The lower panel displays the quantification of the surface area of the top of the collagen matrices, measured in mm^2. Data shown is representative of n = 4 biological replicates, where **$P< 0.01$, ****$P<0.0001$ when compared to Ad-LacZ infected controls. **B.** Rat cardiac fibroblasts seeded into inserts with a defined cell-free gap on 5 kPa elastic silicone surfaces were infected with either YAP[5SA], TAZ[4SA], or LacZ-expressing adenoviral constructs at a MOI of 50. Wound healing rate was assessed as percent surface area covered by cells at 18 hours post-infection. Data is representative of n = 4 biological replicates, with *$P< 0.05$ when compared to Ad-LacZ infected controls. **C.** P0 primary rat cardiac fibroblasts cultured on 5 kPa elastic silicone tissue culture surfaces coated with gelatin were transduced with adenoviral constructs overexpressing Hippo effectors, Ad-YAP[5SA] or Ad-TAZ[4SA], or Ad-LacZ control. mRNA was isolated 48 hours post-infection, and analyzed by qRT-PCR, with n = 5 biological replicates per condition. *$P< 0.05$, **$P< 0.01$, ***$P< 0.001$, ****$P< 0.0001$ when compared to Ad-LacZ infected controls. **D.** NIH-3T3 fibroblasts were transfected with either an empty pcDNA3-NI (NI, no insert), -YAP[S127A], or -TAZ[S89A] expressing vectors in conjunction with a luciferase reporter-promoter plasmid (pGL4.1[*luc2*]) containing either the human Collagen 1α1 (*COL1A1*) or 3α1 (*COL3A1*) promoter. Luciferase activity was assayed 48 hours post-transfection, and normalized to pcDNA3 transfected controls. Data is representative of n = 3 biological replicates (3 technical replicates each), with ***$P< 0.001$, ****$P<0.00001$ when compared to pcDNA3-transfected controls. All data (A-D) is reported as mean ± SD.

Analysis of gene transcription by qPCR provided a clearer understanding of the activation state of primary fibroblasts with YAP[5SA] and TAZ[4SA] overexpression (Fig. 4.2C). The first gene of interest was *Ctgf*, as it is a known genetic target for both proteins. TAZ activation resulted in an acute increase in *Ctgf* transcription (~30-fold change) compared to YAP activation (~3.5-fold change). Similarly, expression of the ED-A splice variant of *Fn1* was upregulated in both conditions, but was markedly greater with TAZ[4SA] expression. Transcription of *Acta2* (encodes αSMA) was positively regulated by both YAP and TAZ activation, but with much greater variance with the latter. We then probed for *Tcf21*, a marker of resident (non-activated) cardiac fibroblasts, and found that both YAP[5SA] and TAZ[4SA] significantly reduced its transcription, compared to Ad-LacZ infected controls. Finally, we examined the transcription of genes encoding fibrillar collagen monomers, *Col1a1*, *Col1a2*, and *Col3a1*. With induction of both YAP and TAZ activity, *Col1a1* transcription was upregulated; however, only TAZ increased *Col3a1* transcription. Conversely, *Col1a2* expression was slightly downregulated with TAZ activation, but was unaffected by YAP. To further elucidate the effects of YAP and TAZ on collagen promoter activation, we performed luciferase assays on the human *COL1A1* and *COL3A1* promoters in NIH-3T3 fibroblasts. We used variants of YAP and TAZ with single serine mutations (S127A and S89A, respectively) for these experiments as they were sufficient to induce nuclear translocation with relatively equal expression of both paralogs (we could not achieve this in primary cells). With YAP activation, we observed an 8-fold and 4-fold increase in *COL1A1* and *COL3A1* promoter activity, respectively. In contrast, with active TAZ overexpression there was almost a 10-fold induction beyond that observed with YAP for both promoters. In addition, when *Taz* expression was knocked down by RNAi, it was found that the only myofibroblast marker

which was affected was ED-A FN, which was nearly absent in myofibroblasts devoid of TAZ expression (Fig. B.1). Taken together, these findings suggest that while both YAP and TAZ activation induce a myofibroblast-like phenotype in isolated primary cardiac fibroblasts, TAZ produces a more synthetic phenotype which could be indicative of its role in the pathogenesis of cardiac fibrosis.

4.4.2 TAZ and YAP Exhibit Contrasting Expression During Post-MI Fibrosis

To determine the role, if any, of TAZ in the pathogenesis of cardiac fibrosis, we temporally examined its expression in a rat model of post-MI cardiac remodelling. Animals were subject to left anterior descending (LAD) coronary artery ligation or sham operation, and cardiac tissue was isolated during a time course spanning 48 hours to 8 weeks post-MI. Using periostin as a marker of cardiac fibroblast activation, along with vimentin as a mesenchymal cell marker, we probed for both YAP and TAZ expression at each time point. Immunoblotting showed biphasic expression of TAZ which peaks at 2 weeks post-MI within the infarct scar, post-MI. Interestingly, we observed an increase in YAP expression in the RV tissue of sham-operated animals. When probing infarcted LV tissue by immunofluorescence, we found that there was differential expression between YAP and TAZ along the border of the advancing infarct scar (Fig 4.3C). The most striking feature was the nuclear localization of TAZ in tissue harvested 2 weeks post-MI in cells co-stained with vimentin. This activation/translocation was absent from tissues probed with anti-YAP antibodies, as the sham-operated and ligated LV tissue had no apparent difference in YAP localization. The increase in nuclear TAZ along the infarct border suggests that its activation is involved in the deposition of ECM and the spreading of the infarct scar.

a

48 hours post-MI 4 days post-MI 1 week post-MI

POSTN

YAP

TAZ

Vimentin

Total
Protein

Acute wound healing

2 weeks post-MI 4 weeks post-MI 8 weeks post-MI

POSTN

YAP

TAZ

Vimentin

Total
Protein

Chronic reactive fibrosis
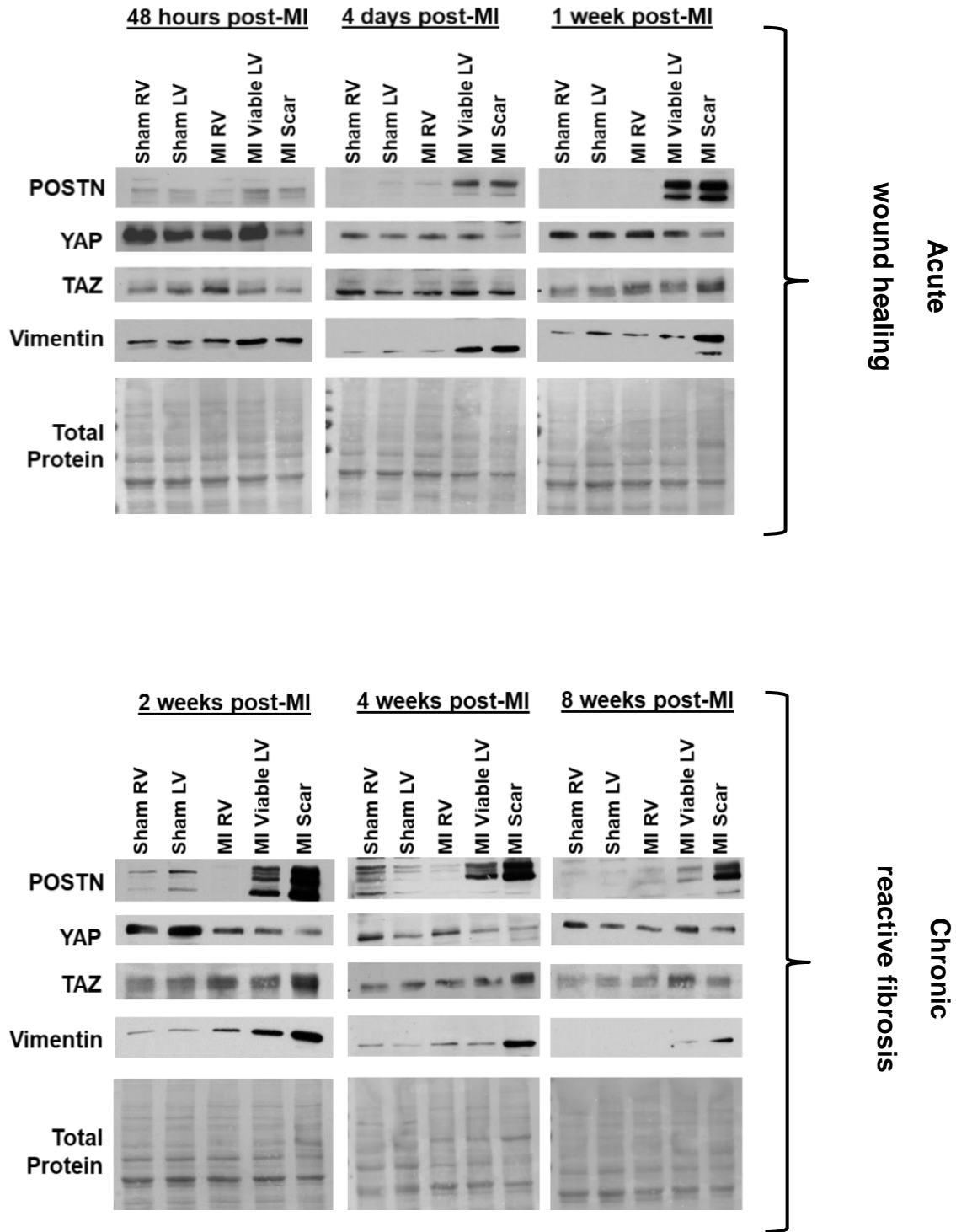
b
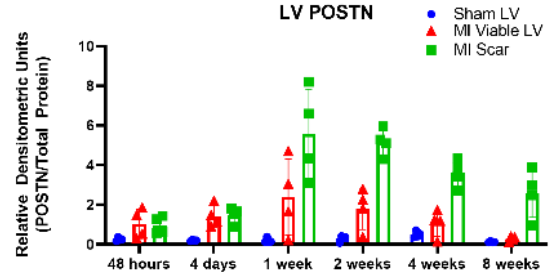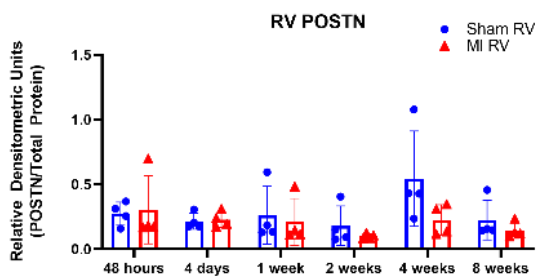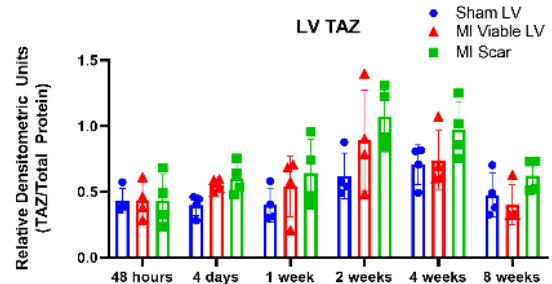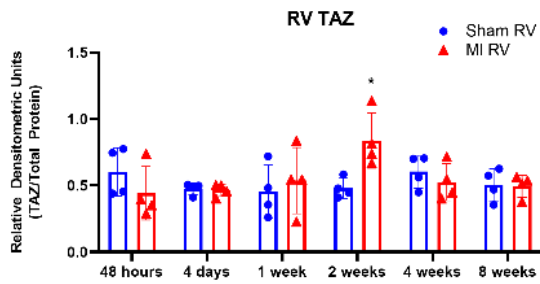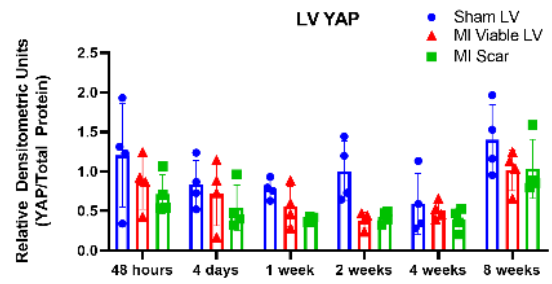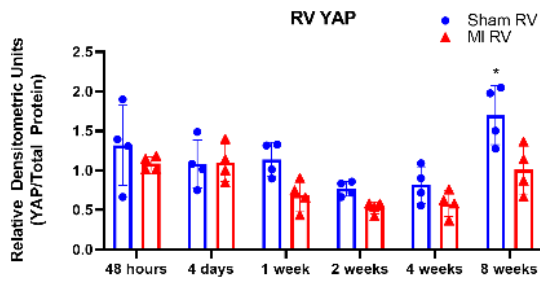
C
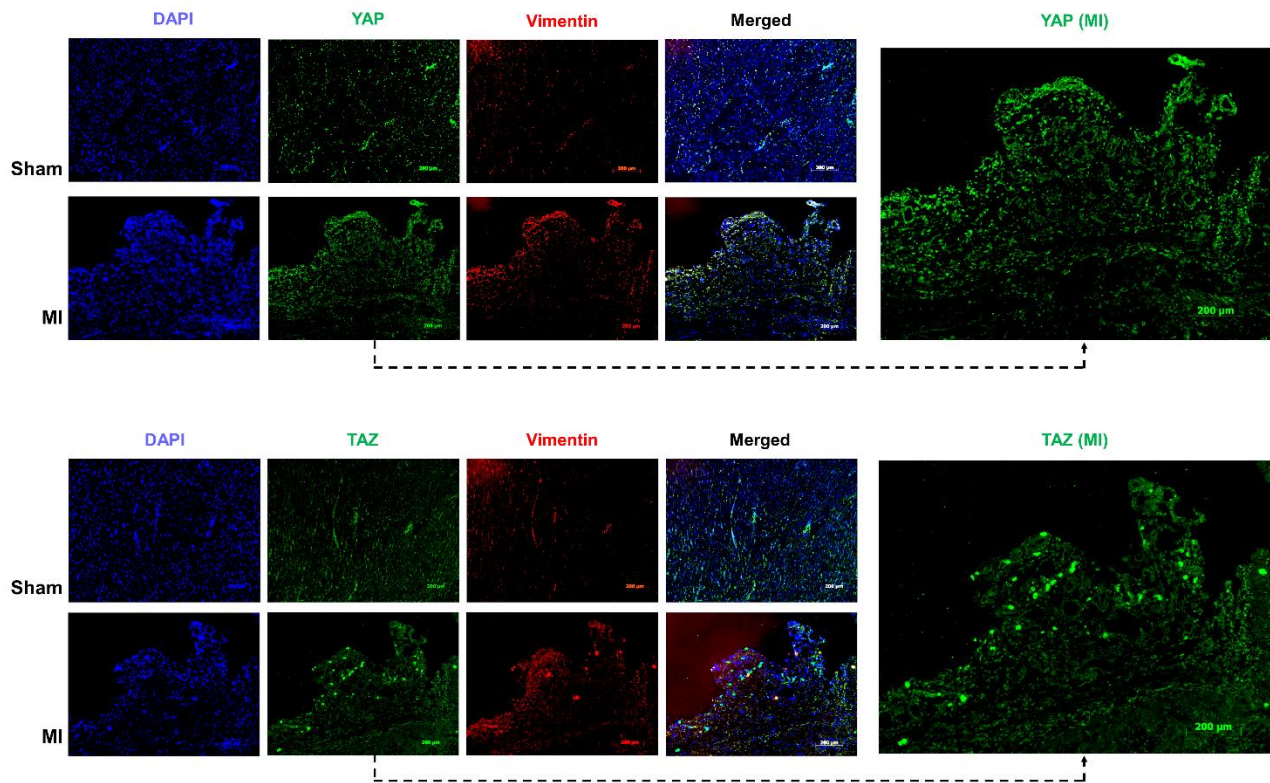
Figure 4.3. TAZ exhibits biphasic expression during post-MI fibrogenesis *in vivo*. **A.** Immunoblotting of whole tissue lysate from male Sprague-Dawley rats subject to left anterior descending (LAD) coronary artery ligation or sham operation. Hearts were excised at various time points, spanning 48 hours to 8 weeks post-ligation, and tissue from left (LV) and right (RV) ventricles were isolated for analysis. **B.** Quantification of densitometric measurements of data shown in A, as well as Online Figure I. Data is representative of experiments originating from n =4 to 6 animals per time point, and is reported as the mean ± SD. *$P<0.05$, **$P<0.01$, ***$P<0.001$, when compared to that tissue's (RV or LV) corresponding sham animals. **C.** Indirect immunofluorescence of LV scar at 2 weeks post-MI or sham operation. Sections were probed for YAP (top panel, green), or TAZ (lower panel, green) and Vimentin (red) for identification of cells of mesenchymal origin. Nuclei were counterstained with DAPI (blue). Scale bar = 200 µm. Images are representative of n = 3 biological replicates.

and remains elevated at until 4 weeks after injury (Fig. 4.3A, B). A similar pattern was found

in the RV of infarcted hearts, but resolved back to baseline before 4 weeks. In contrast, YAP

expression was markedly reduced in the LV infarct scar, and returned to baseline at 8 weeks

4.4.3 SKI Activates LATS2-Hippo Signalling to Specifically Target TAZ

Following the examination of YAP and TAZ in post-MI fibroblast activation, we

sought to elucidate the effects of SKI expression on the Hippo pathway. Using primary rat

cardiac fibroblasts cultured in pro-fibrotic conditions (i.e. on conventional plastic, DMEM/F12

medium with ascorbic acid and 10% FBS), we overexpressed nuclear human SKI using an

adenoviral vector. Probing whole cell lysates by immunoblotting revealed that even mild

overexpression of SKI leads to a stark reduction in TAZ protein expression (Fig. 4.4A, B).

What is peculiar about this observation is that YAP expression is apparently unaffected by

ectopic SKI. As SKI is known to recruit factors to gene promoters which inhibit transcription,

we sought to determine whether this regulation was occurring at the transcriptional level. *Taz*

and *Yap* expression in cells overexpressing SKI was analyzed by qPCR, and showed no

difference from Ad-LacZ infected controls (Fig. 4.4C). In contrast, *Ctgf*, a known genetic

target of YAP and TAZ, presented a three-fold reduction in its expression, suggesting that

indeed, SKI is affecting TAZ protein expression, and not its transcription.

Using a series of small molecule inhibitors which target various regulatory elements in

the Hippo pathway, we sought to better elucidate the mechanism by which SKI specifically

targets TAZ in cardiac myofibroblasts. We first used the pan-acting proteasome inhibitor,

MG132, which yielded moderate rescue of TAZ expression with SKI overexpression (Fig

4.4D).
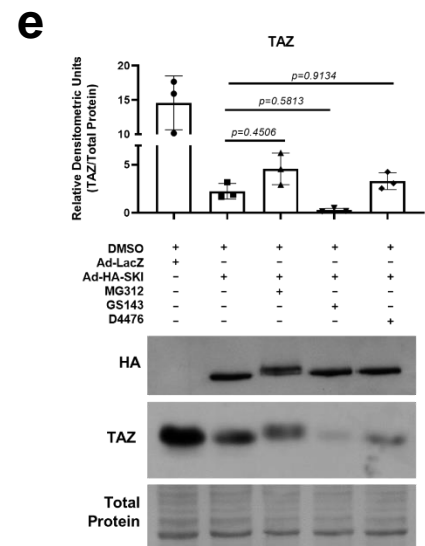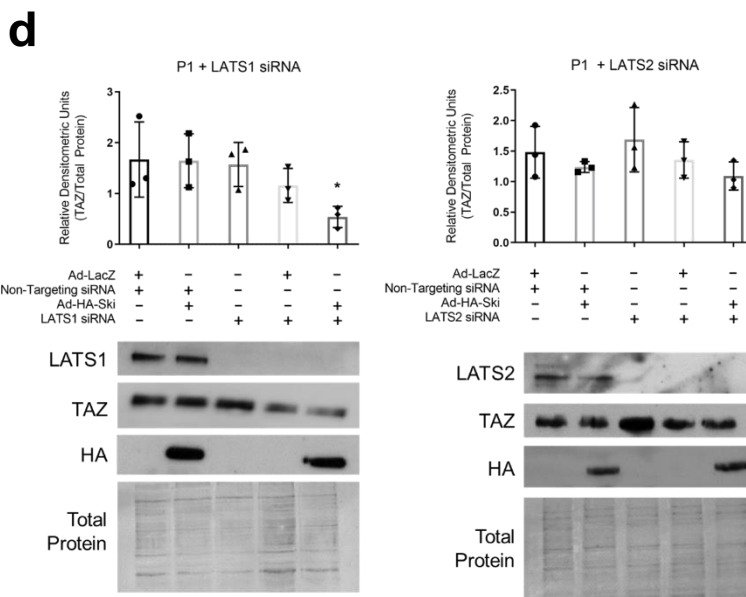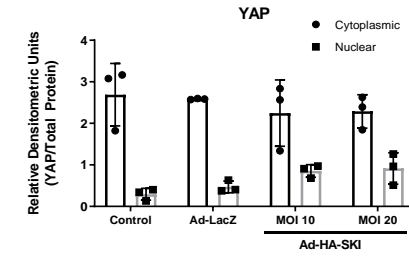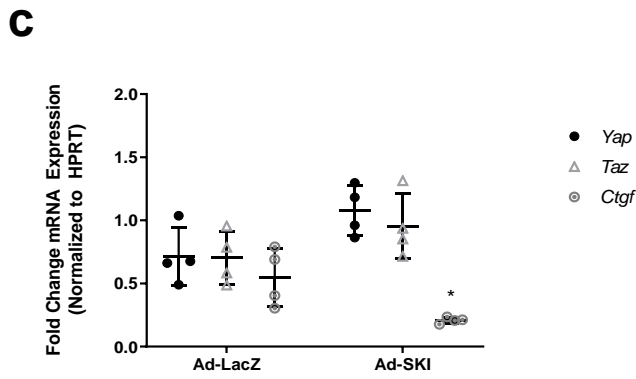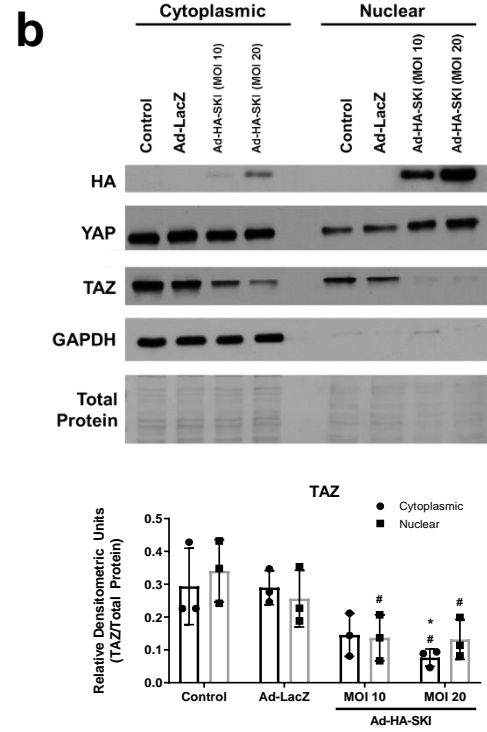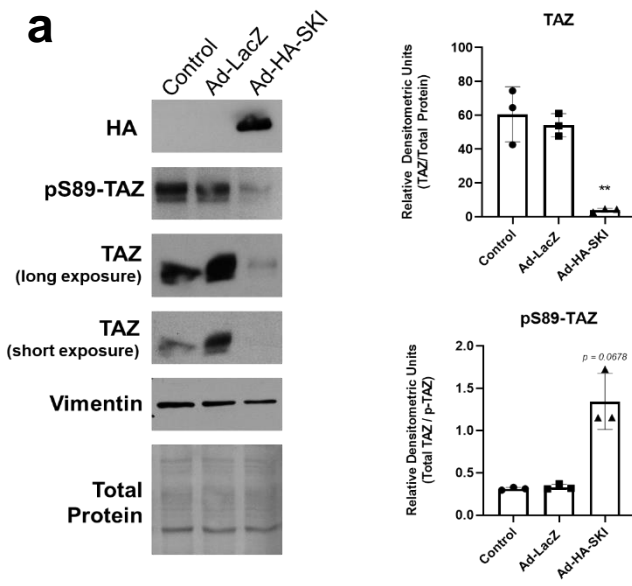
Figure 4.4. SKI induces proteasomal degradation of TAZ, but not YAP. First-passage (P1) primary rat cardiac myofibroblast were cultured on stiff plastic surfaces and infected with SKI overexpressing adenovirus (Ad-HA-SKI) at a low and high MOI (10 and 20, respectively) for 36 hours prior to harvesting. **A.** Whole cell lysates were probed by immunoblotting. Data is representative of n= 3 biological replicates, where **$P < 0.01$ when compared to non-treated and Ad-LacZ infected controls. **B.** Immunoblotting of nuclear and cytoplasmic subcellular fractions, showing an enrichment of nuclear-localized SKI. Data is representative of n = 3 biological replicates, where *$P<0.05$ when compared to Ad-LacZ infected controls and [#]$P<0.05$ when compared to untreated controls. **C.** Gene expression was assayed by qRT-PCR, specifically targeting *Yap* and *Taz*, as well as their genetic target, *Ctgf*. Data is representative of n = 4 biological replicates, where *$P< 0.05$ when compared to Ad-LacZ infected controls for the given genetic target. **D.** Prior to infection with SKI-expressing adenovirus, P1 rat cardiac myofibroblasts where transfected with siRNA targeting *Lats1* and *Lats2* kinases for 24 hours. Cells were subsequently harvested after 36 hours of viral infection. Data is representative of n = 3 biological replicates for each condition, where *$P< 0.05$ compared to cells treated with non-targeting siRNA and Ad-LacZ. **E.** P1 rat cardiac fibroblasts were pre-treated with either MG132 (1 µM), GS143 (1 µM), or D4476 (500 nM) for 3 hours prior to infection with either Ad-HA-SKI or Ad-LacZ control for 24 hours. Data is representative of n = 3 biological replicates. All data is displayed (A-E) as the mean ± SD.

We concomitantly treated cells in similar conditions with GS143, a β-TrCP1 E3 ubiquitin ligase inhibitor which has been shown to exert activity on YAP and TAZ. In contrast to MG132 treatment, the use of GS143 appeared to exacerbate the effects of SKI overexpression. Finally, we used D4476 to inhibit casein kinase 1 (CK1), which normally functions to activate LATS1/2 kinases and phosphorylate the TAZ phosphodegron motif. Much like with MG132, we observed a mild recovery of TAZ expression after D4476 treatment. Although these results were not as robust as those obtained with MG132 treatment, the moderate response of TAZ to CK1 inhibition still indicated that SKI may modify LATS1/2 function in cardiac myofibroblasts.

To determine whether LATS1/2 activity is required for SKI effects on TAZ, knockdown studies using RNAi were used. Using separate siRNA pools targeting *Lats1* and

Lats2 individually, expression of each kinase was knocked down in conjunction with SKI overexpression in primary cardiac fibroblasts (Fig. 4.4E). While *Lats1* knockdown did not prevent the proteasomal degradation of TAZ with ectopic induction of SKI, ablation of *Lats2* led to the retention of TAZ expression. These results suggest that LATS1 is not required for SKI's effects on the Hippo pathway, but LATS2 is necessary for the proteasomal degradation of TAZ. We conclude that SKI exerts some activity which promotes LATS2-mediated phosphorylation and subsequent degradation of TAZ.

Because LATS kinases are inhibited by F-actin polymerization and activated when the cytoskeleton shifts to a more motile organization, we were interested in the effects of SKI expression on actin dynamics. Using primary rat cardiac fibroblasts cultured on conventional polystyrene substrates, we overexpressed SKI and isolated F-actin and solubilized G-actin fractions from the cells. The F- to G-actin ration was markedly reduced in SKI-overexpressing cell lysates, compared to Ad-LacZ infected controls (Fig. 4.5A). These results were subsequently confirmed by immunofluorescent staining of F-actin with fluorophore-conjugated phalloidin (Fig. 4.5B). A distinct reduction in stress fiber staining was observed in myofibroblasts overexpressing SKI, even in the presence of high mechanotension (i.e. on stiff substrate) indicating that indeed, SKI can negate the mechanical cues that would otherwise inhibit Hippo signalling, shifting the cytoskeleton toward actin depolymerization. Taken together, the LATS2-dependent activation of Hippo in concert with cytoskeletal reorganization suggests that SKI exerts multifaceted antagonism on TAZ.
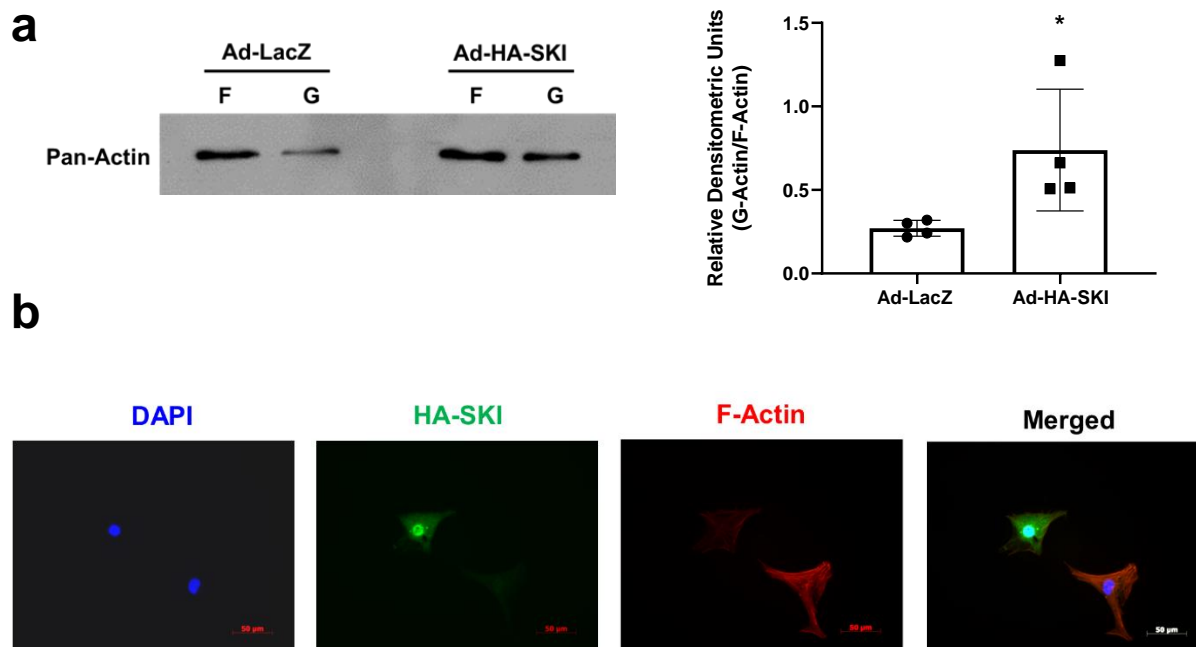
Figure 4.5. F-Actin polymerization is inhibited by ectopic SKI expression. First-passage (P1) primary rat cardiac myofibroblasts were infected with SKI-expressing adenovirus (Ad-HA-SKI) or LacZ-expressing control (Ad-LacZ) for 36 hours prior to harvesting and isolation of F-actin and soluble G-actin. **A.** Equal volumes of each F- or G-actin isolate from one culture dish was separated by SDS-PAGE and immunoblotted with pan-actin antibody. Data is reported as the ratio of G-actin to F-actin in a given sample. *$P<0.05$ when compared to Ad-LacZ infected control. **B.** HA-SKI overexpressing P1 rat cardiac myofibroblasts were cultured on glass coverslips for 48 hours prior to fixation. Cells were probed by indirect immunofluorescence for HA-SKI (green) and F-actin (red), with nuclei counterstained with DAPI (blue). Scale bar = 50 µm. Data shown are representative of n =3 biological replicates, with 2 technical replicates each.

4.4.4 SKI and TAZ Interactomes Intersect in Human Cardiac Myofibroblasts

Since SKI and TAZ have not been reported to directly bind each other, and we were

unable to co-immunoprecipitate core Hippo components in conjunction with SKI, we

performed bi-directional BioID2 assays between SKI and TAZ in primary human cardiac

myofibroblasts. The assay enabled us to not only determine whether SKI and TAZ interact in a

direct or indirect manner, but also to describe the unique interactomes of each protein in

primary cells. We used lysates from n=4 biological replicates for each bait protein, and used two different control conditions: untreated cells to rule out endogenously biotinylated proteins, and cells overexpressing BirA* ligase to gauge the background affinity of proteins to the biotin ligase domain in the BioID2 fusion proteins. Links to the original mass spectrometry data are provided in Table 4.4 (Section 4.3.18).

The interactome isolated for SKI was composed of 32 potential interactors, while the TAZ interactome contained 53 (Fig. 4.6A). Previously-published interactors were used as sentinel prey targets to validate mass spectrometry data (e.g. NCoR1 for SKI; TEAD3 for TAZ), and were further confirmed by repeated affinity purification and Western blot (Fig. 4.6B). We also confirmed the results of the LATS1/2 knockdown assays (Fig. 4.4E), as only LATS2 appeared in the TAZ interactome. Of interesting note, no SMAD isoforms were identified in the SKI interactome. After interrogating the SKI and TAZ interactomes against each other, it was found that the interactions which overlap between the two are predominantly involved in actin cytoskeleton remodelling. Palladin (PALLD), WASH Complex Subunit 5 (WASHC5, or KIAA0196), and Capping Protein Regulator and Myosin 1 Linker 2 (CARMIL2, formerly RLTPR) were found in both interactomes, and are all involved in F-actin polymerization and stabilization[441-444]. Pathway enrichment analysis revealed that the SKI interactome showed moderate enhancement of Notch signalling, adipogenesis, and autophagy (Fig 4.6C). Unsurprisingly, the TAZ interactome was enriched for Hippo signalling, gene transcription, and cellular responses to external stimuli. Although there were no explicit links between SKI and TAZ, the SKI interactome contained two candidates which have been linked to Hippo pathway regulation.

b

c

Enriched Pathways - BioID2-SKI

Androgen receptor signaling pathway
Notch Signaling Pathway
Pathways Affected in Adenoid Cystic Carcinoma
Ovarian Infertility Genes
Mecp2 and Associated Rett Syndrome
Senescence and Autophagy in Cancer
mRNA Processing
Adipogenesis

-log(FDR p-value)

Enriched Pathways - BioID2-TAZ

Infectious disease
Neuronal System
HIV Infection
HIV Life Cycle
Host Interactions of HIV factors
Gene Silencing by RNA
Transcriptional regulation by small RNAs
Interactions of Vpr with host cellular proteins
Vpr-mediated nuclear import of PICs
Signaling by Hippo
Processing of Capped Intron-Containing Pre-mRNA
Metabolism of RNA
Cellular responses to external stimuli
Cellular responses to stress
Disease
Gene expression (Transcription)

-log(FDR p-value)

d

BioID2-SKI

BioID2-TAZ

Figure 4.6. The SKI and TAZ interactomes overlap in primary human cardiac fibroblasts. Primary human cardiac fibroblasts were infected with adenovirus constructs overexpressing MYC-BioID2 fusion proteins (TAZ or SKI) or empty MYC-BioID2 for 24 hours. Cell cultures were then supplemented with 20 μM biotin, and incubated for another 24 hours prior to harvesting. Untreated controls were also included to exclude endogenously-biotinylated proteins. **A.** Graphical representation of the TAZ (WWTR1) and SKI interactomes in human cardiac fibroblasts. Edge thickness and color is representative of the fold-change enrichment of the prey obtained by affinity capture. Hippo pathway components are highlighted in violet, while known SKI interactors are highlighted in red. **B.** Pathway enrichment analysis for both SKI and TAZ interactomes. **C.** Plotting of SAINT scores vs log2 fold-change enrichment of potential interactors. A SAINT score closer to 1 indicates greater likelihood of interaction. Select known interactors are indicated in blue, while novel interactors are indicated in red. **D.** Immunoblotting was used to confirm novel interaction between SKI and LIMD1. Data shown is representative of n = 4 biological replicates.

The first was PJA2, a ubiquitin ligase that was found to negatively regulate MOB1, which in turn inhibits LATS1 activity, in glioblastoma[445]. The second candidate was LIMD1, a LIM domain containing protein which has been shown to inhibit LATS2 in development, EMT, and osteoclast activation[344, 370, 446]. Because the literature regarding LIMD1 and Hippo regulation was much more robust, and involved LATS2, we chose to pursue it as a putative link between SKI and TAZ.

4.4.5 LIMD1 Mediates SKI-Dependent TAZ Degradation in Cardiac Fibroblasts

Prior to this study, LIMD1 had not been examined in the context of cardiac fibroblast activation. Because we identified LIMD1 as a component of the SKI interactome, we sought to examine it in the context of SKI overexpression. Global expression of endogenous LIMD1 in primary rat cardiac myofibroblasts was apparently unaffected by infection with Ad-HA-SKI or Ad-LacZ control virus (Fig. 4.7A). However, when examining TAZ expression in the same cells co-transfected with siRNA pools targeting *Limd1*, it was found that once again it was markedly reduced, leaving YAP expression unaltered. Essentially, knockdown of *Limd1* recapitulated the effects of SKI overexpression. When visualizing SKI and LIMD1 using immunofluorescence, there was more diffuse, cytosolic LIMD1 expression in Ad-LacZ infected controls, with a distinct shift to nuclear LIMD1 expression with SKI overexpression (Fig. 4.7B). Finally, when looking at gene transcription with SKI overexpression, we did not detect any changes in *Limd1* when compared to LacZ expressing controls (Fig. 4.8C). Taken together in concert with the BioID2 assays, these results strongly suggest that indeed, SKI interacts with LIMD1 protein to de-repress LATS2 activity in cardiac fibroblasts, resulting in the deactivation of the pro-fibrotic phenotype.
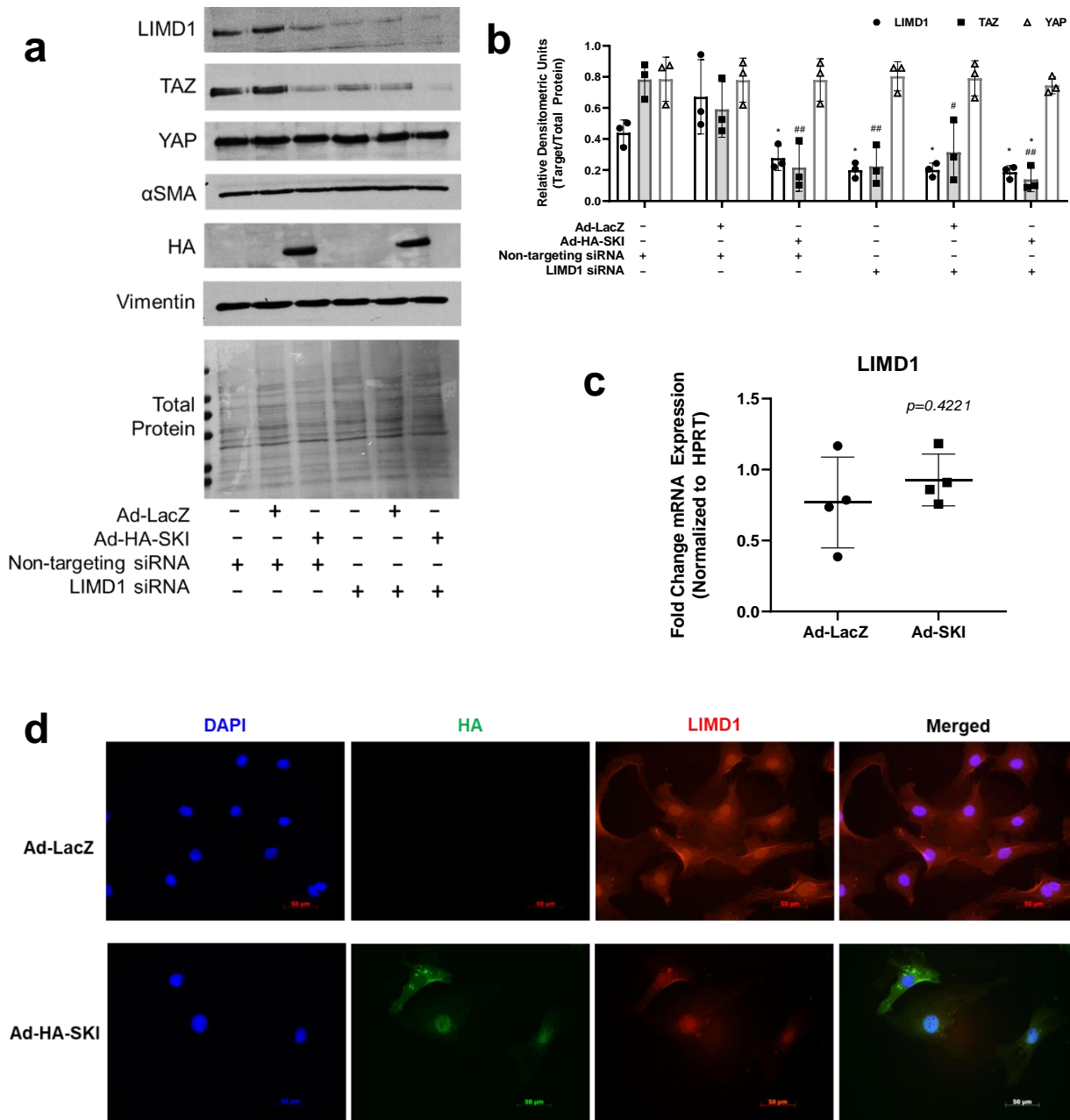
Figure 4.7. TAZ expression is regulated by LIMD1 in cardiac myofibroblasts. A.
Immunoblotting of whole cell lysates from activated (P1) primary rat cardiac myofibroblasts
transfected with siRNA targeting *Limd1* 24 hours prior to infection with Ad-HA-SKI or Ad-LacZ
control. A non-targeting siRNA pool functioned as a control. **B.** Quantification of data shown in A,
with n = 3 biological replicates. *$P<0.05$ when compared to Ad-LacZ infected controls; #$P<0.05$
and ##$P<0.01$ when compared to cells only treated with non-targeting siRNA pool. **C, D.** P1 primary
rat cardiac myofibroblasts were cultured on stiff plastic (C) or glass (D) surfaces and infected with
SKI-expressing adenovirus (Ad-HA-SKI) for 36 hours. mRNA was isolated and (C) qRT-PCR of
Limd1 was performed on n= 4 biological replicates. Fixed cells (D) were probed for LIMD1 (red)
and HA-SKI (green) by indirect immunofluorescence, with nuclei counterstained with DAPI (blue).
Scale bar = 50 µm. Images are representative of n = 3 biological replicates, with 2 technical
replicates each. Data shown in B and C are reported as the mean ± SD.

4.5 Discussion and Conclusions

       Cardiac fibroblast activation is a crucial event necessary for the physiological wound healing response in the myocardium. At the outset of ischemic insult, release of inflammatory cytokines promotes the shift to the hypersecretory, hyperproliferative myofibroblast phenotype. However, the chronic activation of this synthetic, contractile phenotype leads to the development of reactive fibrosis and eventually, heart failure. Here, we have shown that the Hippo pathway plays a role in modulating the cardiac fibroblast phenotype, and that it is positively-regulated by SKI. Our results suggest that SKI interacts with LIMD1 in an inhibitory fashion, which in turn activates Hippo signalling by de-repressing LATS2 kinase. Thus, LATS2 can exert its activity on TAZ which ultimately results in its proteasomal degradation (Summarized in Fig. 4.8). The ensuing signalling cascade results in a downregulation of myofibroblast markers which shifts the cells' phenotype closer to the resting cardiac fibroblast phenotype.

       Previous studies conducted by our group showed that SKI expression is pleiotropic, but dysregulated in reactive cardiac fibrosis, post-MI. Rather than being expressed in its nuclear, active form, SKI become sequestered to the cytosol where its function, if any, is unknown[331, 426]. In conjunction with these findings, SKI was found to increase MMP-9 expression and activity, and represses autophagy-mediated survival responses that assist the persistence of the myofibroblast phenotype[333, 447]. Most recently, SKI was found to inhibit the c-JUN/c-FOS AP-1 complex, an important transcription factor in collagen biosynthesis, via SMAD-independent signalling[332]. Our current study is the first to demonstrate that SKI activates the Hippo pathway in cardiac myofibroblasts, and does so to expressly target TAZ, and not YAP. We have also observed that myofibroblasts in the advancing infarct scar express nuclear, active TAZ during
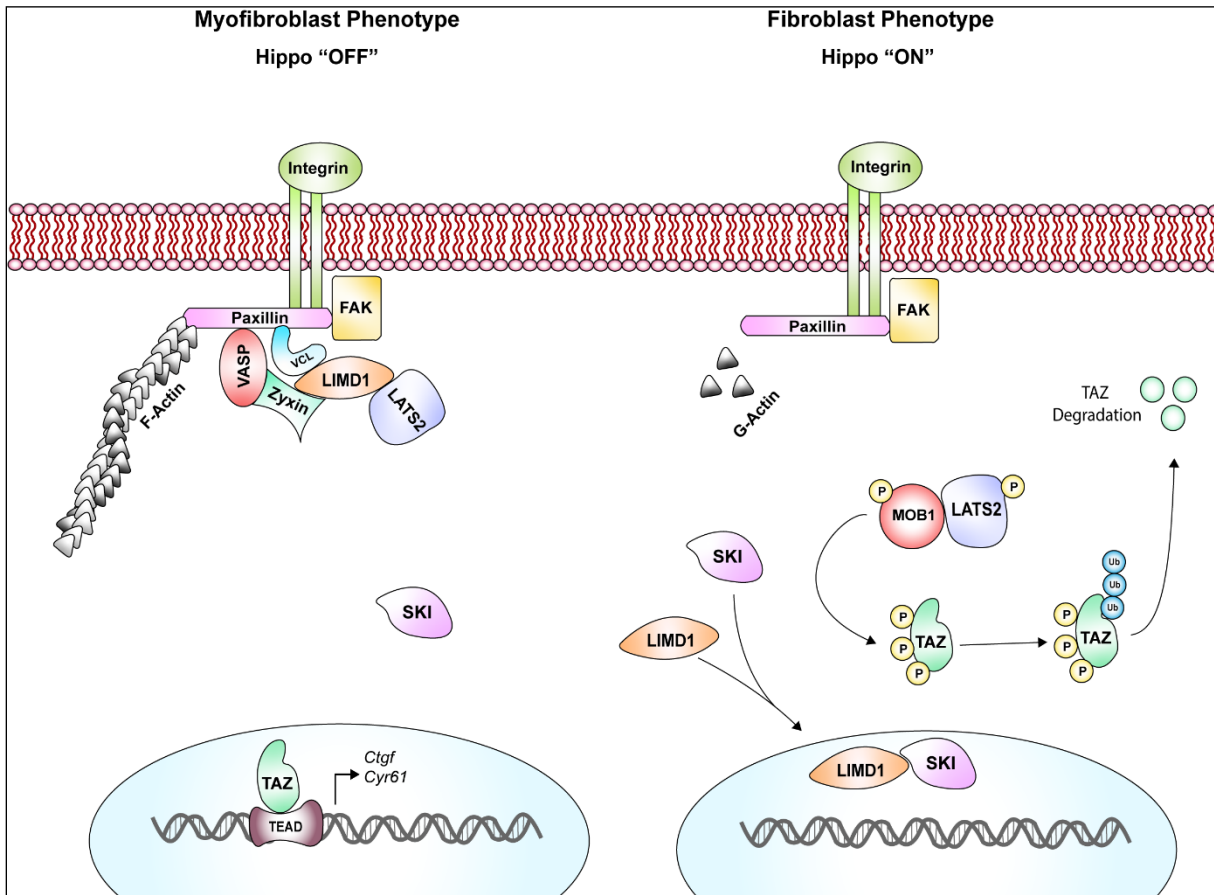
Figure 4.8. A model of SKI-mediated regulation of Hippo signaling and cardiac fibroblast activation. When SKI is localized in the cytoplasm, LIMD1 can freely associate and inhibit the function of LATS2 kinase, thus allowing TAZ-dependent, pro-fibrotic signaling to occur. Conversely, when SKI is functioning in the nucleus, it inhibits LIMD1 which, in turn, de-represses LATS2 kinase. The result is the phosphorylation and proteasomal degradation of TAZ, and the inhibition of the activated myofibroblast phenotype.

post-MI fibrogenesis; this is noteworthy as TAZ activity is often described as being redundant to YAP. We contend that while YAP does induce myofibroblast marker expression and function when activated *in vitro*, TAZ is possibly more intimately linked to the persistence of fibrosis and the expansion of the cardiac ECM as it produces a more synthetic myofibroblast phenotype.

Very recent work by Xiao *et al*. examined the role of Hippo signalling in a mouse model of post-MI fibrosis[184]. Using the *Tcf21* promoter to generate the conditional deletion of *Lats1* and *Lats2* in resting cardiac fibroblasts (*Tcf21iCre-Lats1/2$^{fl/fl}$*), the authors observed that the mice spontaneously developed subepicardial and subendocardial fibrosis. Animals subject to LAD ligation developed extreme interstitial fibrosis and did not survive past three weeks post-MI. While the study did include another set of *Lats1/2$^{fl/fl}$* animals which also had a genetic reduction of *Yap* (*Yap$^{fl/+}$*), it appears that the authors conflated *Yap* and *Taz* as the same gene and reported the mouse as *Yap/Taz$^{fl/+}$* without giving any evidence of reduction of *Taz* expression. Nevertheless, the partial reduction of *Yap* in conjunction with *Lats1/2* knockout in resting cardiac fibroblasts generated a less severe etiology of post-MI fibrosis than in the *Lats1/2$^{fl/fl}$* animals. It is unclear as to whether the combined *Lats1/2*+*Yap* deletion ameliorated cardiac function and chronic ECM expansion, as there was no apparent difference infarct scar size and cardiac function from the controls. Furthermore, all transgenic animals exhibited severe atrial fibrosis, regardless of their genotype. The group also provided single-cell RNAseq and ATACseq data acquired from NIH-3T3 fibroblasts devoid of LATS1/2 kinases and found that YAP activation promotes its localization to promoters of ECM-related genes, resulting in upregulation of their transcription. These results imply that *Yap* may be involved in the proper scar formation, but with only a partial genetic ablation of the gene, and it is unclear as to the degree. Despite this data, there was no examination of *Taz*, nor was there any knockout of *Lats1* or *Lats2* in isolation. It would be interesting to determine whether these transgenic models could be modified such that the conditional knockout would occur after myofibroblast activation (e.g. using the *Postn* promoter), since *Tcf21*expression is reduced in the post-MI heart. It would also be of interest to know if one LATS kinase is more important than the other

in the context of fibroblast activation. Moreover, a study of conditional *Taz* deletion would provide further insight as to whether its role is at the forefront of fibrosis-related Hippo signalling in the post-MI myocardium.

While many groups contend that TAZ plays a redundant role to YAP with respect to cell cycle re-entry, we postulate that TAZ induces a cell-specific, pro-fibrotic gene program during chronic post-MI wound healing. Studies of fibrotic disease in other tissues have revealed differential expression of the paralogs, indicating that perhaps YAP and TAZ should be evaluated both separately and in conjunction with each other. For instance, work by Liu *et al.* in idiopathic pulmonary fibrosis (IPF) revealed that TAZ activity is considerably more upregulated that YAP in some etiologies of the disease, and that probing IPF tissue sections showed nuclear localization of TAZ was predominantly observed in activated pulmonary fibroblasts[213]. Other groups have reported similar results, and differential YAP/TAZ expression has also been reported in chronic kidney disease and renal fibrosis[429, 448, 449]. The data presented here not only corroborates these findings, but also associate SKI in the specific regulation of TAZ during fibrogenesis. As the current literature is heavily focused on YAP as the primary nuclear effector of the Hippo pathway, and sometimes YAP and TAZ are referred to interchangeably, it would be beneficial to further examine YAP and TAZ as separate factors with unique, disease- and cell-specific functions.

We used BioID2 proximity labelling assays to identify novel mechanisms by which SKI regulates Hippo signalling in primary cardiac fibroblasts. Previously-published data by Rashidian *et al.* suggest that SKI activates the pathway by directly interacting with several key Hippo components, including LATS2[336]. It should be noted, however, that the co-immunoprecipitations involved the overexpression of both the bait and prey proteins in breast

cancer cell lines. Moreover, several reports have indicated that SKI's function varies significantly among immortalized cell lines, and is dependent on the type of cell and pathology being studied (this was thoroughly reviewed by Tecalo-Cruz and colleagues[179]). To first demonstrate the validity of the adenoviral BioID2 vectors, we first captured the SKI interactome in HEK 293A cells, and found that the resulting interactors largely corroborated with what was already found in the literature (Fig. C.1). However, when comparing this network to the one isolated from primary human cardiac fibroblasts, only three hits overlapped between the two interactomes (Fig. C.2). The SKI interactome described in human cardiac fibroblasts was much more limited, due to the lack of existing protein-protein interaction data from this cell type, but did reveal LIMD1 as a potential point of intersection between SKI and the Hippo pathway. It is also of importance that other LIM domain proteins appeared in the TAZ interactome (e.g. PDLIM5 and PDLIM7), which have been shown to regulate YAP/TAZ transport in and out of the nucleus in a mechanosensory manner[450]. Thus, LIM domain proteins present yet another potential avenue by which TAZ could be regulated in cardiac fibroblasts, although this mechanism has yet to be described.

The role of LIM domain proteins in cell physiology and pathophysiology remains largely unknown. With respect to LIMD1, there is some evidence that it functions as a protein scaffold, and may be involved in cytoskeletal organization[343, 451]. LIMD1 has also been shown to influence LATS kinase function by sequestering them to the cytosol at junctional complexes and focal adhesions. Recent work by Jagannathan *et al.* demonstrated that LIMD1 can modulate YAP activity in proliferating cells *in vitro*, via a mechanism that works independent from ECM stiffness[359]. As these studies were conducted in the cell lines, they may not be entirely reflective of LIMD1 function in a physiological setting. Even with the current lack of

studies supporting a link between TAZ and LIMD1, our findings were performed in primary cells and indicate that LIMD1 is a key inhibitor of the Hippo pathway in cardiac fibroblasts. The notion that LIMD1 may promote TAZ-dependent activation of the myofibroblast phenotype still requires further investigation.

When expressed in the nucleus, SKI is a potent anti-fibrotic factor whose function is not entirely dependent on TGF-β inhibition. The evidence presented here describes a novel mechanism which governs a shift in the cardiac fibroblast phenotype by the inactivation of LIMD1 and thus, TAZ. Further examination of Hippo signalling in the context of cardiac fibrosis are warranted, especially if its pharmaceutical targeting proves to be a viable means to stave off the onset of heart failure. Together with future investigations into LIMD1 and its function in cardiac fibroblasts, understanding SKI's role in fibroblast physiology could be used for the development of selective therapeutic interventions in cardiac fibrosis.

CHAPTER 5: DISCUSSION

5.1 Overall Discussion

Under physiological conditions, cardiac fibroblasts maintain myocardial matrix homeostasis through balanced synthesis and degradation of ECM components. In contrast, chronic stress or acute injury results in the activation of fibroblasts after the loss of cardiomyocytes, infiltration of immune cells, and the release of latent TGF-β_1 from the ECM[3-5]. The persistence of myofibroblasts within the infarct border and throughout the myocardium results from a feedforward loop. Myofibroblasts with αSMA-positive stress fibers are subject to greater intracellular tension, which then enables them to transmit tensile forces to the ECM via mature focal adhesions[152, 169]. On the cytoplasmic side of focal adhesion complexes, adapter proteins like LIMD1 mediate signals between the extra- and intracellular spaces, upregulating pro-fibrotic pathways[344, 352, 361]. The resulting stiffening of the ECM thus promotes continued activation of fibroblasts and mechanosensory signal transduction (i.e. nuclear YAP and/or TAZ), propagating further expansion of the interstitium. As a consequence of biomechanical changes, cardiac myofibroblasts increase expression of fibrillar collagens, PDGFRα, and ED-A fibronectin, and lose nearly all expression of TCF21[3, 137]. This process is apparently reversible in murine models of post-MI cardiac fibrosis but has yet to be observed in humans[58, 137, 138]. Nevertheless, the sensitivity of cardiac fibroblasts to changes in their microenvironment, coupled to the characteristic continuous shear and tensile forces of the contracting myocardium, present a complex suite of factors that contribute to cardiac fibrosis and heart failure.

This thesis highlights the importance of controlled *in vitro* conditions to better study cardiac fibroblast physiology and the unique role that TAZ plays in post-MI cardiac fibrosis.

Furthermore, it describes novel functions for SKI in mediating the mechanosensory properties of TAZ by modulating the actin cytoskeleton and acting as an intermediary in the LATS2-TAZ signalling axis.

5.1.1 The Hippo Pathway an as Anti-Fibrotic Target

Several contemporary studies in fibrosis across various tissues have recognized the Hippo pathway as an interesting point of intervention, especially due to its direct role in regulating cell cycle and its mechanosensory role in development[184, 213, 215, 250]. While not all fibroproliferative diseases are regulated in a YAP-, TAZ-, or YAP/TAZ-dependent manner, the consensus among researchers is that direct targeting of YAP/TAZ is not a viable means to regulate aberrant Hippo signalling. Rather, up- or downstream regulatory elements which are attuned to specific cell or tissue pathologies are a more practical and safer avenue to inhibit YAP/TAZ signalling.

As YAP was the first Hippo nuclear effector to be identified in humans, it has been far better studied than TAZ. The structural similarities notwithstanding, YAP and TAZ certainly do share significant functional qualities in most cell types. However, to equate one paralog to the other, or to categorize TAZ as a redundant or less-important form of YAP, is speculative at best and perhaps incorrect. There is undeniably a shortage of TAZ-specific studies in the literature, let alone full examinations of the functions of either or both paralogs in a given biological setting. Very recent work by Jorgenson and colleagues in NIH-3T3 fibroblasts demonstrated that constitutively-active TAZ [4SA] cannot drive increased *Col1a1, Col1a2,* and *Col3a1* expression without mechanical strain *in vitro* (i.e. stiff culture substrates)[452]. In contrast, cells cultured in spheroid suspension were only able to increase production of *Ctgf, Edn1* (encodes Endothelin-1), and *Serpine1*. While these studies were conducted in cell lines,

the group had previously established in primary lung fibroblasts that TAZ was both necessary and sufficient for cell contraction on both soft and stiff matrices[213, 430]. These findings further support the case for more cell-specific studies of Hippo signalling and the unique roles of YAP and TAZ. The capacity for TAZ to promote matrix tension may be contingent upon the initial injury to the tissue, followed by inflammatory signalling. Upstream factors that activate TAZ nuclear translocation may be the necessary impetus to generate contractile forces to remodel the ECM, and thus changing the stiffness of the local environment. Sustained fibroblast activation would then result from further induction of paracrine signals and pro-fibrotic mechano-responsive pathways.

The main question regarding Hippo signalling is whether it is a viable therapeutic target for fibrotic disease. To date, there are many small molecule inhibitors that target YAP/TAZ by acting on upstream regulatory pathways, but they are not specific for either paralog. For example, statins and dobutamine are widely used for the treatment of cardiovascular disease and heart failure, but also have the added benefit of activating Hippo signalling. Several other small molecules which are not primarily indicated for YAP/TAZ inhibition also have similar, Hippo-related side effects[259]. Other classes of small molecules have recently been identified as having direct inhibitory action on the active YAP/TAZ-TEAD complex. The most commonly employed in molecular studies is Verteporfin, a drug which was originally developed for the treatment of macular degeneration[453-455]. Unfortunately, one disadvantage of Verteporfin is that it is unstable when exposed to light or when in the presence of ascorbic acid[456, 457]. This causes it to produce high amounts of ROS within the cell, and this is not ideal when considering the ischemic nature of infarcted myocardium and fibrotic tissue in general[457, 458]. Other compounds which target TEAD activation are also being explored as possible cancer treatments; however

their patent filings demonstrate that they were only validated for YAP-TEAD inhibition, and

not TAZ-TEAD[459, 460]. Finally, there is also some interest in regulating factors which are

downstream from YAP/TAZ signalling, such as bromodomain-containing HDACs [461, 462].

Once again, concerns arise from inhibiting chromatin-modifying proteins, as their off-target,

generally toxic effects may counteract any anti-fibrotic benefits[463].

As YAP and/or TAZ activation is associated with many fibro-proliferative pathologies,

more research is required in determining the tissue- and cell-specific nature of Hippo

dysregulation. In the context of cardiovascular disease, it is helpful to remain cognizant of the

constant flux of biomechanically-charged input in the environment in which cardiac fibroblasts

reside, and that paracrine signalling may be just as important for TAZ activation as changes in

cardiac matrix structure and composition. In due course, the context-specific targeting of TAZ

in cardiac fibroblasts could be a selective target for the treatment of cardiac fibrosis, but further

investigations on its unique subcellular functions are needed.

5.1.2 SKI as a Multifunctional Protein: Looking Beyond TGF-β Inhibition

Given that SKI is a phylogenetically ancient protein, it would be an unusual expectation

for it to have a singular function within the cell. As SKI is a negative regulator of fibrillar

collagen expression, it is entirely possible that its function may be generally impaired in pro-

inflammatory, pro-fibrotic settings, allowing for the unmitigated deposition of scar tissue.

Because of the overt, deactivating effects that SKI exerts on primary cardiac fibroblasts,

postulating that it is multifunctional protein is not an unreasonable inference[330-333, 335].

With the advancement of the field of interactomics, significantly larger, more nuanced

data regarding protein-protein interactions can be acquired in very specific biological settings.

The results discussed in Chapter 4 present a unique human cardiac fibroblast SKI interactome

which bears little semblance to the interactions discovered in cell lines and oncological studies. Of important note is the absence of SMAD proteins altogether; but this could be attributed to the absence of exogenous TGF-β_1 stimulation, or the upregulation of PDGFRα signalling which downregulates SMAD/TGF-β signalling, *in vitro*[165, 330].

Because of its integral role in ECM organization and maturation during development, SKI is likely important for mechanosensory signal transduction and general fibroblast physiology. Our isolation of the cardiac fibroblast SKI interactome postulates that SKI can act as an intermediary between nuclear signalling molecules, the actin cytoskeleton, and focal adhesion components. While these interactions have not been explicitly explored in the literature, the SKI-actin relationship has been previously explored in the context of hepatocyte activation in liver regeneration[464]. SKI was found to be associated with the actin cytoskeleton in the cytosol normal hepatocytes, but was quickly dissociated with induction of TGF-β and Rho/ROCK signalling, and was consequently degraded upon F-actin polymerization[464]. The results presented herein suggest that there may be a bi-directional aspect to the SKI-actin relationship, as the ectopic induction of nuclear SKI decreases F-actin stress fibre formation, and promote the isolation of G-actin monomers. Furthermore, the SKI interactome in human cardiac fibroblasts suggests that SKI may modify actin organization by interacting with PALLD, ARP2/3, and CARMIL2 (RLTPR), all of which are integral to the dynamism of F- and G-actin, and regulate cell contractility, motility, and vesicle transport[441, 465, 466]. While this mode of regulating cell physiology has not been explored in fibroblasts, it has been reported that SKI inhibits F-actin polymerization in breast cancer cell lines[336]. The SKI-cytoskeleton relationship is still very much a nascent concept, and presents a distinct mechanism of action in cardiac fibroblasts.

In addition to interacting with the cytoskeleton, the data described herein suggests that SKI also interacts with LIMD1, an adapter protein known to inhibit Hippo signalling. While this interaction is novel, the idea of SKI family proteins interacting with AJUBA-associated proteins is not. Studies involving AURKA, a kinase which targets SKI, demonstrated that AJUBA is required for AURKA activation[467]. AURKA, SKI and AJUBA have been observed as co-localizing at centrosomes and focal adhesions in various parings (i.e. not all three proteins simultaneously), suggesting that there may be extra regulatory mechanisms involved when considering the potential role(s) of LIMD1[310, 467, 468]. This would be unsurprising for two reasons: 1) LIM-containing proteins have a diverse range of functions within the cell, and many are cell- or pathology-specific; 2) AJUBA family proteins appear to have cell-specific expression patterns. The AJUBA member Lipoma Preferred Partner (LPP) is highly expressed in vascular smooth muscle cells, while LIMD1 is highly expressed in stromal cells of the heart, lungs and reproductive organs, as well as peripheral blood mononuclear cells[469]. Because the literature regarding LIMD1 is still emergent, there is ample opportunity to better understand its function in various cell types. To this end, the SKI-LIMD1 relationship and whether it carries any significance in regulating cell function and phenotype will undoubtedly require further exploration, but may also be a springboard to better understand the importance of scaffold/adapter proteins in fibrotic disease.

5.2 Study Limitations and Overall Conclusions

The data presented here demonstrate that primary cardiac fibroblasts maintained under conditions which promote the resting fibroblast phenotype can be activated into synthetic myofibroblasts by the nuclear expression of TAZ. In addition, the activated myofibroblast phenotype can be reversed by SKI overexpression, which specifically targets TAZ for

proteasomal degradation, leaving its paralog, YAP, unaffected. Cardiac fibroblasts expressing

both active YAP and TAZ are myofibroblast-like in their phenotype; however, nuclear TAZ

expression exerts hyperactivation of fibrillar collagen expression *in vitro*. These data were

acquired and analyzed with the limitation that they were observed in isolated cells, which

normally co-exist in a strongly contractile environment with several other cell types. This

undoubtedly removed some of the paracrine action that is normally present in the myocardium,

and may not exactly reflect the response of cardiac myofibroblasts in their endogenous form.

Furthermore, we were limited in our ability to observe endogenous SKI behaviour, as there is

no validated antibody against the rat isoform; thus, we were required to detect ectopically

expressed protein to acquire better signal resolution for our molecular assays. However, to lend

some relevance of these observations to the whole heart in pathological setting, we made

certain to include studies of post-MI remodelling in a rat model.

When examining the advancing fibrotic scar in the post-MI heart, TAZ expression is

predominantly nuclear, while YAP expression is diffuse across the myofibroblast-rich infarct

border. These observations, combined with those mentioned above, suggest that TAZ plays an

important role in the persistence of the cardiac myofibroblast phenotype, and that the

mechanisms which govern its expression may be viable targets for future anti-fibrotic therapies

in the heart. Using BioID2 to isolate the human SKI and TAZ interactomes in primary cardiac

fibroblasts, we conclude that LIMD1 is a point of regulatory intersection between pro- and

anti-fibrotic signalling. This novel point of interaction between SKI, the actin cytoskeleton,

and TAZ, indicate that indeed, SKI is not only implicated in TGF-β inhibition. Rather, SKI

may function in a cell-specific manner to induce cytoskeletal changes which reduce focal

adhesion formation and cell proliferation—the same may be true for LIMD1. Further

investigation into the significance of LIMD1 in the context of cardiac fibroblast activation will also potentially identify other promising targets for therapeutic intervention.

5.3 Future Directions

The identification of biomarkers and protein targets for the treatment of cardiac fibrosis remains a primary goal for most researchers in the field, chiefly due to the absence of any effective treatments for the disease. Despite ongoing clinical trials testing promising anti-fibrotic candidates, there is still a dearth of information regarding the underlying molecular mechanisms which govern the progression and severity of cardiac fibrosis. Moreover, the lack of specificity of action in most drug candidates is the primary reason for the failure of fibrosis-targeting clinical trials. The likely reason behind the inability to find a viable drug candidate is due to the fact that fibrosis is a multi-stage disease whose prognosis is not predictable in most cases. The advent of personalized medicine may help to focus efforts on patient-specific therapy options, as much like other proliferative diseases (e.g. cancer), fibrosis does not affect the general patient population equally.

With respect to the precise targeting of SKI and/or TAZ, preclinical studies in transgenic animal models could be used to target them in the heart in a moderately specific manner. Using the *Tcf21* promoter, *Ski* could be conditionally knocked out in resting fibroblasts to determine whether it is required to stave off spontaneous age-related cardiac fibrosis. Similarly, under the control of the *Postn* promoter, conditional knockout of *Ski* after myofibroblast activation (i.e. post-MI, or in a pressure overload model) would allow for the examination of whether it is required for proper infarct scar formation and/or to prevent the spread of reactive fibrosis in the cardiac interstitium. Concurrent examination of *Taz* would determine whether its nuclear localization within the expanding infarct border is regulated in

part by the presence of or absence of *Ski*. We have already established the latter transgenic model, and are in the process of acquiring tissue from infarcted hearts in a small pilot study. Another avenue of enquiry could include the examination of miRNAs which regulate Hippo signalling and/or SKI in cardiac fibroblasts. For example, work by Li *et al*. in vascular smooth muscle cells demonstrated that overexpression of miR-21 creates conditions which worsen the severity of vascular injury by inhibiting SKI expression by binding its 3' untranslated region[470]. miR-21 has also been implicated in the pathogenesis of post-MI fibrosis; thus, its effects on SKI and potentially, TAZ, may be yet another regulatory element to better understand the pathophysiology of cardiac fibroblast activation[471, 472].

Another potential future avenue of exploration would include LIMD1, and whether its dysregulation is a contributing factor to cardiac fibrosis. Although this thesis demonstrates a specific requirement of LIMD1 to maintain TAZ expression in cardiac fibroblasts, there is very little information regarding its regulation beyond very specific types of cancer—at this time, only 58 publications on PubMed contain LIMD1 as a search term[356]. However, work by Zhou et al. has identified four possible phosphorylation sites in human LIMD1 (S272, S277, S421, and S424), and that A549 cells deficient in these specific sites showed significantly less proliferation and anchorage-dependent growth[355]. This would be an interesting point to consider with respect to the SKI-LIMD1 interaction, as it may induce hyperphosphorylation of LIMD1, rendering it unable to inhibit Hippo signalling. Furthermore, LIMD1 has also been shown to be mechanosensitive, as tension-dependent expression is intimately linked to Rho kinase activation[344]. This again would be a worthy notion to examine in the context of the post-MI heart, as biomechanics change over the course of the pathogenesis of fibrosis and heart failure. Of special interest would be to determine whether LIMD1 expression is dysregulated

with worsening fibrosis (i.e. stiffening of the matrix), and if a phosphor-deficient variant could reverse these effects. Evidently, the profound impact of biomechanical input, focal adhesions, and actin cytoskeleton dynamics are key components of cardiac fibroblast activation. To explore these factors in the context of LIMD1 expression would contribute further knowledge about scaffold proteins, and how their expression may contribute to the persistence of the pro-fibrotic myofibroblast phenotype.

The ultimate strategy to target cardiac fibrosis would be to develop a method which specifically inhibits both myofibroblast activation and the synthesis of ECM components in the weeks following infarct scar maturation. The future of the field is likely to depend on the availability of "big data" such as transcriptomes (i.e. RNAseq) and interactomes (i.e. Protein-Protein interactions), and whether we can mine those databases for relevant information. Because no two cases of cardiac fibrosis are the same, it is likely that the underlying molecular causes and response to therapy by individuals will also follow suit. Regardless of whether personalized therapy is even possible in the near future, significant exploration into specific etiologies of cardiac fibrosis will be necessary, as the current blanket approach to patient care is insufficient.

References

1. Santiago, J.J. *et al.* Cardiac fibroblast to myofibroblast differentiation in vivo and in vitro: expression of focal adhesion components in neonatal and adult rat ventricular myofibroblasts. *Developmental dynamics : an official publication of the American Association of Anatomists* **239**, 1573-1584 (2010).

2. Fowlkes, V. *et al.* Type II diabetes promotes a myofibroblast phenotype in cardiac fibroblasts. *Life sciences* **92**, 669-676 (2013).

3. Frangogiannis, N.G. Cardiac fibrosis: Cell biological mechanisms, molecular pathways and therapeutic opportunities. *Mol Aspects Med* **65**, 70-99 (2019).

4. Spinale, F.G. *et al.* Crossing Into the Next Frontier of Cardiac Extracellular Matrix Research. *Circ Res* **119**, 1040-1045 (2016).

5. Kong, P., Christia, P. & Frangogiannis, N.G. The pathogenesis of cardiac fibrosis. *Cell Mol Life Sci* **71**, 549-574 (2014).

6. Weber, K.T. Cardiac interstitium in health and disease: the fibrillar collagen network. *J Am Coll Cardiol* **13**, 1637-1652 (1989).

7. Talman, V. & Ruskoaho, H. Cardiac fibrosis in myocardial infarction-from repair and remodeling to regeneration. *Cell Tissue Res* **365**, 563-581 (2016).

8. Nielsen, S.H. *et al.* Understanding cardiac extracellular matrix remodeling to develop biomarkers of myocardial infarction outcomes. *Matrix Biol* **75-76**, 43-57 (2019).

9. Exposito, J.Y., Valcourt, U., Cluzel, C. & Lethias, C. The fibrillar collagen family. *Int J Mol Sci* **11**, 407-426 (2010).

10. Hagg, P. *et al.* Type XIII collagen: a novel cell adhesion component present in a range of cell-matrix adhesions and in the intercalated discs between cardiac muscle cells. *Matrix Biol* **19**, 727-742 (2001).

11. McCurdy, S., Baicu, C.F., Heymans, S. & Bradshaw, A.D. Cardiac extracellular matrix remodeling: fibrillar collagens and Secreted Protein Acidic and Rich in Cysteine (SPARC). *J Mol Cell Cardiol* **48**, 544-549 (2010).

12. Bella, J. & Hulmes, D.J. Fibrillar Collagens. *Subcell Biochem* **82**, 457-490 (2017).

13. Meng, X.M., Nikolic-Paterson, D.J. & Lan, H.Y. TGF-beta: the master regulator of fibrosis. *Nat Rev Nephrol* **12**, 325-338 (2016).

14. Ricard-Blum, S., Baffet, G. & Theret, N. Molecular and tissue alterations of collagens in fibrosis. *Matrix Biol* **68-69**, 122-149 (2018).

15.   Ricard-Blum, S. The collagen family. *Cold Spring Harb Perspect Biol* **3**, a004978 (2011).

16.   Horn, M.A. & Trafford, A.W. Aging and the cardiac collagen matrix: Novel mediators of fibrotic remodelling. *J Mol Cell Cardiol* **93**, 175-185 (2016).

17.   Ivey, M.J. & Tallquist, M.D. Defining the Cardiac Fibroblast. *Circ J* **80**, 2269-2276 (2016).

18.   Lindsey, M.L., Iyer, R.P., Jung, M., DeLeon-Pennell, K.Y. & Ma, Y. Matrix metalloproteinases as input and output signals for post-myocardial infarction remodeling. *J Mol Cell Cardiol* **91**, 134-140 (2016).

19.   DeLeon-Pennell, K.Y., Meschiari, C.A., Jung, M. & Lindsey, M.L. Matrix Metalloproteinases in Myocardial Infarction and Heart Failure. *Prog Mol Biol Transl Sci* **147**, 75-100 (2017).

20.   Wilson, E.M. *et al.* Plasma matrix metalloproteinase and inhibitor profiles in patients with heart failure. *J Card Fail* **8**, 390-398 (2002).

21.   Spinale, F.G. *et al.* Matrix metalloproteinase inhibition during the development of congestive heart failure : effects on left ventricular dimensions and function. *Circ Res* **85**, 364-376 (1999).

22.   Yang, H., Borg, T.K., Wang, Z., Ma, Z. & Gao, B.Z. Role of the basement membrane in regulation of cardiac electrical properties. *Ann Biomed Eng* **42**, 1148-1157 (2014).

23.   Pozzi, A., Yurchenco, P.D. & Iozzo, R.V. The nature and biology of basement membranes. *Matrix Biol* **57-58**, 1-11 (2017).

24.   Tzu, J. & Marinkovich, M.P. Bridging structure with function: structural, regulatory, and developmental role of laminins. *Int J Biochem Cell Biol* **40**, 199-214 (2008).

25.   Luther, D.J. *et al.* Absence of type VI collagen paradoxically improves cardiac function, structure, and remodeling after myocardial infarction. *Circ Res* **110**, 851-856 (2012).

26.   Cescon, M., Gattazzo, F., Chen, P. & Bonaldo, P. Collagen VI at a glance. *J Cell Sci* **128**, 3525-3531 (2015).

27.   McLeod, O. *et al.* Autoantibodies against basement membrane collagen type IV are associated with myocardial infarction. *Int J Cardiol Heart Vasc* **6**, 42-47 (2015).

28.   Xu, H. *et al.* Collagen binding specificity of the discoidin domain receptors: binding sites on collagens II and III and molecular determinants for collagen IV recognition by DDR1. *Matrix Biol* **30**, 16-26 (2011).

29. Tsilibary, E.C., Charonis, A.S., Reger, L.A., Wohlhueter, R.M. & Furcht, L.T. The effect of nonenzymatic glucosylation on the binding of the main noncollagenous NC1 domain to type IV collagen. *J Biol Chem* **263**, 4302-4308 (1988).

30. Haitoglou, C.S., Tsilibary, E.C., Brownlee, M. & Charonis, A.S. Altered cellular interactions between endothelial cells and nonenzymatically glucosylated laminin/type IV collagen. *J Biol Chem* **267**, 12404-12407 (1992).

31. Murakami, M. *et al.* Expression of the alpha 1 and alpha 2 chains of type IV collagen in the infarct zone of rat myocardial infarction. *J Mol Cell Cardiol* **30**, 1191-1202 (1998).

32. Tomasek, J.J., Gabbiani, G., Hinz, B., Chaponnier, C. & Brown, R.A. Myofibroblasts and mechano-regulation of connective tissue remodelling. *Nat Rev Mol Cell Biol* **3**, 349-363 (2002).

33. Johnson, C.M. & Helgeson, S.C. Fibronectin biosynthesis and cell-surface expression by cardiac and non-cardiac endothelial cells. *Am J Pathol* **142**, 1401-1408 (1993).

34. Zollinger, A.J. & Smith, M.L. Fibronectin, the extracellular glue. *Matrix Biol* **60-61**, 27-37 (2017).

35. Pankov, R. & Yamada, K.M. Fibronectin at a glance. *J Cell Sci* **115**, 3861-3863 (2002).

36. Sottile, J. *et al.* Fibronectin-dependent collagen I deposition modulates the cell response to fibronectin. *Am J Physiol Cell Physiol* **293**, C1934-1946 (2007).

37. Sottile, J. & Hocking, D.C. Fibronectin polymerization regulates the composition and stability of extracellular matrix fibrils and cell-matrix adhesions. *Mol Biol Cell* **13**, 3546-3559 (2002).

38. Valiente-Alandi, I. *et al.* Inhibiting Fibronectin Attenuates Fibrosis and Improves Cardiac Function in a Model of Heart Failure. *Circulation* **138**, 1236-1252 (2018).

39. Valiente-Alandi, I., Schafer, A.E. & Blaxall, B.C. Extracellular matrix-mediated cellular communication in the heart. *J Mol Cell Cardiol* **91**, 228-237 (2016).

40. Williams, C., Quinn, K.P., Georgakoudi, I. & Black, L.D., 3rd Young developmental age cardiac extracellular matrix promotes the expansion of neonatal cardiomyocytes in vitro. *Acta Biomater* **10**, 194-204 (2014).

41. Arslan, F. *et al.* Lack of fibronectin-EDA promotes survival and prevents adverse remodeling and heart function deterioration after myocardial infarction. *Circ Res* **108**, 582-592 (2011).

42. Kosmehl, H., Berndt, A. & Katenkamp, D. Molecular variants of fibronectin and laminin: structure, physiological occurrence and histopathological aspects. *Virchows Arch* **429**, 311-322 (1996).

43.   Serini, G. *et al.* The fibronectin domain ED-A is crucial for myofibroblastic phenotype induction by transforming growth factor-beta1. *J Cell Biol* **142**, 873-881 (1998).

44.   Romberger, D.J. Fibronectin. *Int J Biochem Cell Biol* **29**, 939-943 (1997).

45.   Ffrench-Constant, C., Van de Water, L., Dvorak, H.F. & Hynes, R.O. Reappearance of an embryonic pattern of fibronectin splicing during wound healing in the adult rat. *J Cell Biol* **109**, 903-914 (1989).

46.   Klingberg, F. *et al.* The fibronectin ED-A domain enhances recruitment of latent TGF-beta-binding protein-1 to the fibroblast matrix. *J Cell Sci* **131** (2018).

47.   Yu, Y., Yin, G., Bao, S. & Guo, Z. Kinetic alterations of collagen and elastic fibres and their association with cardiac function in acute myocardial infarction. *Mol Med Rep* **17**, 3519-3526 (2018).

48.   Ramos, I.T. *et al.* Simultaneous Assessment of Cardiac Inflammation and Extracellular Matrix Remodeling after Myocardial Infarction. *Circ Cardiovasc Imaging* **11** (2018).

49.   Protti, A. *et al.* Assessment of Myocardial Remodeling Using an Elastin/Tropoelastin Specific Agent with High Field Magnetic Resonance Imaging (MRI). *J Am Heart Assoc* **4**, e001851 (2015).

50.   Mizuno, T., Mickle, D.A., Kiani, C.G. & Li, R.K. Overexpression of elastin fragments in infarcted myocardium attenuates scar expansion and heart dysfunction. *Am J Physiol Heart Circ Physiol* **288**, H2819-2827 (2005).

51.   Kielty, C.M., Sherratt, M.J. & Shuttleworth, C.A. Elastic fibres. *J Cell Sci* **115**, 2817-2828 (2002).

52.   Faury, G. Function-structure relationship of elastic arteries in evolution: from microfibrils to elastin and elastic fibres. *Pathol Biol (Paris)* **49**, 310-325 (2001).

53.   Bornstein, P. & Sage, E.H. Matricellular proteins: extracellular modulators of cell function. *Curr Opin Cell Biol* **14**, 608-616 (2002).

54.   Frangogiannis, N.G. Matricellular proteins in cardiac adaptation and disease. *Physiol Rev* **92**, 635-688 (2012).

55.   Takeshita, S., Kikuno, R., Tezuka, K. & Amann, E. Osteoblast-specific factor 2: cloning of a putative bone adhesion protein with homology with the insect protein fasciclin I. *Biochem J* **294**, 271-278 (1993).

56.   Horiuchi, K. *et al.* Identification and characterization of a novel protein, periostin, with restricted expression to periosteum and periodontal ligament and increased expression by transforming growth factor beta. *J Bone Miner Res* **14**, 1239-1249 (1999).

57.   Walker, J.T., McLeod, K., Kim, S., Conway, S.J. & Hamilton, D.W. Periostin as a multifunctional modulator of the wound healing response. *Cell Tissue Res* **365**, 453-465 (2016).

58.   Kanisicak, O. *et al.* Genetic lineage tracing defines myofibroblast origin and function in the injured heart. *Nature communications* **7**, 12260 (2016).

59.   Crawford, J., Nygard, K., Gan, B.S. & O'Gorman, D.B. Periostin induces fibroblast proliferation and myofibroblast persistence in hypertrophic scarring. *Exp Dermatol* **24**, 120-126 (2015).

60.   Gillan, L. *et al.* Periostin Secreted by Epithelial Ovarian Carcinoma Is a Ligand for a_vb_3 and a_vb_5 Integrins and Promotes Cell Motility. *Cancer Res* **62**, 5358-5364 (2002).

61.   Taniyama, Y. *et al.* Selective Blockade of Periostin Exon 17 Preserves Cardiac Performance in Acute Myocardial Infarction. *Hypertension* **67**, 356-361 (2016).

62.   Morita, H. & Komuro, I. Periostin Isoforms and Cardiac Remodeling After Myocardial Infarction: Is the Dispute Settled? *Hypertension* **67**, 504-505 (2016).

63.   Bai, Y. *et al.* Novel isoforms of periostin expressed in the human thyroid. *Jpn Clin Med* **1**, 13-20 (2010).

64.   Norris, R.A. *et al.* Periostin regulates collagen fibrillogenesis and the biomechanical properties of connective tissues. *J Cell Biochem* **101**, 695-711 (2007).

65.   Snider, P. *et al.* Periostin is required for maturation and extracellular matrix stabilization of noncardiomyocyte lineages of the heart. *Circ Res* **102**, 752-760 (2008).

66.   Kudo, A. Periostin in fibrillogenesis for tissue regeneration: periostin actions inside and outside the cell. *Cell Mol Life Sci* **68**, 3201-3207 (2011).

67.   Ashley, S.L., Wilke, C.A., Kim, K.K. & Moore, B.B. Periostin regulates fibrocyte function to promote myofibroblast differentiation and lung fibrosis. *Mucosal immunology* **10**, 341-351 (2017).

68.   Li, G. *et al.* Phosphatidylinositol-3-kinase signaling mediates vascular smooth muscle cell expression of periostin in vivo and in vitro. *Atheroscler* **188**, 292-300 (2006).

69.   Ma, Y., Iyer, R.P., Jung, M., Czubryt, M.P. & Lindsey, M.L. Cardiac Fibroblast Activation Post-Myocardial Infarction: Current Knowledge Gaps. *Trends in pharmacological sciences* **38**, 448-458 (2017).

70.   Spinale, F.G. *et al.* Crossing Into the Next Frontier of Cardiac Extracellular Matrix Research. *Circ. Res.* **119**, 1040-1045 (2016).

71. Maruhashi, T., Kii, I., Saito, M. & Kudo, A. Interaction between periostin and BMP-1 promotes proteolytic activation of lysyl oxidase. *J Biol Chem* **285**, 13294-13303 (2010).

72. Garnero, P. The contribution of collagen crosslinks to bone strength. *Bonekey Rep* **1**, 182 (2012).

73. Kii, I. *et al.* Incorporation of tenascin-C into the extracellular matrix by periostin underlies an extracellular meshwork architecture. *J Biol Chem* **285**, 2028-2039 (2010).

74. Egbert, M. *et al.* The matricellular protein periostin contributes to proper collagen function and is downregulated during skin aging. *Journal of dermatological science* **73**, 40-48 (2014).

75. Takayama, G. *et al.* Periostin: a novel component of subepithelial fibrosis of bronchial asthma downstream of IL-4 and IL-13 signals. *The Journal of allergy and clinical immunology* **118**, 98-104 (2006).

76. Butcher, J.T., Norris, R.A., Hoffman, S., Mjaatvedt, C.H. & Markwald, R.R. Periostin promotes atrioventricular mesenchyme matrix invasion and remodeling mediated by integrin signaling through Rho/PI 3-kinase. *Dev Biol* **302**, 256-266 (2007).

77. Wu, C. *et al.* Genome-wide interrogation identifies YAP1 variants associated with survival of small-cell lung cancer patients. *Cancer Res* **70**, 9721-9729 (2010).

78. Ghatak, S. *et al.* Periostin induces intracellular cross-talk between kinases and hyaluronan in atrioventricular valvulogenesis. *J Biol Chem* **289**, 8545-8561 (2014).

79. Ali, O. *et al.* Cooperativity between integrin activation and mechanical stress leads to integrin clustering. *Biophysical journal* **100**, 2595-2604 (2011).

80. Katsumi, A., Naoe, T., Matsushita, T., Kaibuchi, K. & Schwartz, M.A. Integrin activation and matrix binding mediate cellular responses to mechanical stretch. *J Biol Chem* **280**, 16546-16549 (2005).

81. Henderson, N.C. *et al.* Targeting of alphav integrin identifies a core molecular pathway that regulates fibrosis in several organs. *Nature medicine* **19**, 1617-1624 (2013).

82. Wipff, P.J., Rifkin, D.B., Meister, J.J. & Hinz, B. Myofibroblast contraction activates latent TGF-beta1 from the extracellular matrix. *J Cell Biol* **179**, 1311-1323 (2007).

83. Shimazaki, M. *et al.* Periostin is essential for cardiac healing after acute myocardial infarction. *The Journal of experimental medicine* **205**, 295-303 (2008).

84. Chen, C.C. & Lau, L.F. Functions and mechanisms of action of CCN matricellular proteins. *Int J Biochem Cell Biol* **41**, 771-783 (2009).

85.   Leask, A. & Abraham, D.J. All in the CCN family: essential matricellular signaling modulators emerge from the bunker. *J Cell Sci* **119**, 4803-4810 (2006).

86.   Lau, L.F. & Lam, S.C. The CCN family of angiogenic regulators: the integrin connection. *Exp Cell Res* **248**, 44-57 (1999).

87.   Jeong, D. *et al.* Matricellular Protein CCN5 Reverses Established Cardiac Fibrosis. *J Am Coll Cardiol* **67**, 1556-1568 (2016).

88.   Zhao, B. *et al.* TEAD mediates YAP-dependent gene induction and growth control. *Genes Dev* **22**, 1962-1971 (2008).

89.   Hutchenreuther, J., Leask, A. & Thompson, K. Studying the CCN Proteins in Fibrosis. *Methods Mol Biol* **1489**, 423-429 (2017).

90.   Kireeva, M.L., Lam, S.C. & Lau, L.F. Adhesion of human umbilical vein endothelial cells to the immediate-early gene product Cyr61 is mediated through integrin alphavbeta3. *J Biol Chem* **273**, 3090-3096 (1998).

91.   Kireeva, M.L., Mo, F.E., Yang, G.P. & Lau, L.F. Cyr61, a product of a growth factor-inducible immediate-early gene, promotes cell proliferation, migration, and adhesion. *Mol Cell Biol* **16**, 1326-1334 (1996).

92.   Mo, F.E. & Lau, L.F. The matricellular protein CCN1 is essential for cardiac development. *Circ Res* **99**, 961-969 (2006).

93.   Hilfiker-Kleiner, D. *et al.* Regulation of proangiogenic factor CCN1 in cardiac muscle: impact of ischemia, pressure overload, and neurohumoral activation. *Circulation* **109**, 2227-2233 (2004).

94.   Rother, M. *et al.* Matricellular signaling molecule CCN1 attenuates experimental autoimmune myocarditis by acting as a novel immune cell migration modulator. *Circulation* **122**, 2688-2698 (2010).

95.   Igarashi, A., Okochi, H., Bradham, D.M. & Grotendorst, G.R. Regulation of connective tissue growth factor gene expression in human skin fibroblasts and during wound repair. *Mol Biol Cell* **4**, 637-645 (1993).

96.   Daniels, A., van Bilsen, M., Goldschmeding, R., van der Vusse, G.J. & van Nieuwenhoven, F.A. Connective tissue growth factor and cardiac fibrosis. *Acta Physiol (Oxf)* **195**, 321-338 (2009).

97.   Dorn, L.E., Petrosino, J.M., Wright, P. & Accornero, F. CTGF/CCN2 is an autocrine regulator of cardiac fibrosis. *J Mol Cell Cardiol* **121**, 205-211 (2018).

98.   Shi-wen, X. *et al.* CCN2 is necessary for adhesive responses to transforming growth factor-beta1 in embryonic fibroblasts. *J Biol Chem* **281**, 10715-10726 (2006).

99.   Jun, J.I. & Lau, L.F. Taking aim at the extracellular matrix: CCN proteins as emerging therapeutic targets. *Nat Rev Drug Discov* **10**, 945-963 (2011).

100.   Ivkovic, S. *et al.* Connective tissue growth factor coordinates chondrogenesis and angiogenesis during skeletal development. *Development* **130**, 2779-2791 (2003).

101.   Finckenberg, P. *et al.* Angiotensin II induces connective tissue growth factor gene expression via calcineurin-dependent pathways. *Am J Pathol* **163**, 355-366 (2003).

102.   Lang, C. *et al.* Connective tissue growth factor: a crucial cytokine-mediating cardiac fibrosis in ongoing enterovirus myocarditis. *J Mol Med (Berl)* **86**, 49-60 (2008).

103.   Iwamoto, M. *et al.* Connective tissue growth factor induction in a pressure-overloaded heart ameliorated by the angiotensin II type 1 receptor blocker olmesartan. *Hypertens Res* **33**, 1305-1311 (2010).

104.   Koitabashi, N. *et al.* Plasma connective tissue growth factor is a novel potential biomarker of cardiac dysfunction in patients with chronic heart failure. *Eur J Heart Fail* **10**, 373-379 (2008).

105.   Yoon, P.O. *et al.* The opposing effects of CCN2 and CCN5 on the development of cardiac hypertrophy and fibrosis. *J Mol Cell Cardiol* **49**, 294-303 (2010).

106.   Booth, A.J. *et al.* Connective tissue growth factor promotes fibrosis downstream of TGFbeta and IL-6 in chronic cardiac allograft rejection. *Am J Transplant* **10**, 220-230 (2010).

107.   Ahmed, M.S. *et al.* Mechanisms of novel cardioprotective functions of CCN2/CTGF in myocardial ischemia-reperfusion injury. *Am J Physiol Heart Circ Physiol* **300**, H1291-1302 (2011).

108.   Kim, J. *et al.* CCN5 knockout mice exhibit lipotoxic cardiomyopathy with mild obesity and diabetes. *PLoS One* **13**, e0207228 (2018).

109.   Gulati, K. & Poluri, K.M. Mechanistic and therapeutic overview of glycosaminoglycans: the unsung heroes of biomolecular signaling. *Glycoconj J* **33**, 1-17 (2016).

110.   Rienks, M., Papageorgiou, A.P., Frangogiannis, N.G. & Heymans, S. Myocardial extracellular matrix: an ever-changing and diverse entity. *Circ Res* **114**, 872-888 (2014).

111.   Takawale, A., Sakamuri, S.S. & Kassiri, Z. Extracellular matrix communication and turnover in cardiac physiology and pathology. *Compr Physiol* **5**, 687-719 (2015).

112.   Grande-Allen, K.J., Griffin, B.P., Ratliff, N.B., Cosgrove, D.M. & Vesely, I. Glycosaminoglycan profiles of myxomatous mitral leaflets and chordae parallel the severity of mechanical alterations. *J Am Coll Cardiol* **42**, 271-277 (2003).

113.   Bonafe, F. *et al.* Hyaluronan and cardiac regeneration. *J Biomed Sci* **21**, 100 (2014).

114.   Hao, J. *et al.* Elevation of expressio of Smads 2, 3, and 4, decorin and TGF-beta in the chronic phase of myocardial infarct scar healing. *J Mol Cell Cardiol* **31**, 667-678 (1999).

115.   Collins, A.R. *et al.* Osteopontin modulates angiotensin II-induced fibrosis in the intact murine heart. *J Am Coll Cardiol* **43**, 1698-1705 (2004).

116.   Nishioka, T. *et al.* Tenascin-C may aggravate left ventricular remodeling and function after myocardial infarction in mice. *Am J Physiol Heart Circ Physiol* **298**, H1072-1078 (2010).

117.   Frangogiannis, N.G. Syndecan-1: a critical mediator in cardiac fibrosis. *Hypertension* **55**, 233-235 (2010).

118.   Matsui, Y. *et al.* Syndecan-4 prevents cardiac rupture and dysfunction after myocardial infarction. *Circ Res* **108**, 1328-1339 (2011).

119.   Maquart, F.X., Pasco, S., Ramont, L., Hornebeck, W. & Monboisse, J.C. An introduction to matrikines: extracellular matrix-derived peptides which regulate cell activity. Implication in tumor invasion. *Crit Rev Oncol Hematol* **49**, 199-202 (2004).

120.   Ricard-Blum, S. & Salza, R. Matricryptins and matrikines: biologically active fragments of the extracellular matrix. *Exp Dermatol* **23**, 457-463 (2014).

121.   Lindsey, M.L., Hall, M.E., Harmancey, R. & Ma, Y. Adapting extracellular matrix proteomics for clinical studies on cardiac remodeling post-myocardial infarction. *Clin Proteomics* **13**, 19 (2016).

122.   Brassart, B., Randoux, A., Hornebeck, W. & Emonard, H. Regulation of matrix metalloproteinase-2 (gelatinase A, MMP-2), membrane-type matrix metalloproteinase-1 (MT1-MMP) and tissue inhibitor of metalloproteinases-2 (TIMP-2) expression by elastin-derived peptides in human HT-1080 fibrosarcoma cell line. *Clin Exp Metastasis* **16**, 489-500 (1998).

123.   Kamoun, A. *et al.* Growth stimulation of human skin fibroblasts by elastin-derived peptides. *Cell Adhes Commun* **3**, 273-281 (1995).

124.   Kawecki, C. *et al.* Elastin-derived peptides are new regulators of thrombosis. *Arterioscler Thromb Vasc Biol* **34**, 2570-2578 (2014).

125.   Monboisse, J.C., Bellon, G., Randoux, A., Dufer, J. & Borel, J.P. Activation of human neutrophils by type I collagen. Requirement of two different sequences. *Biochem J* **270**, 459-462 (1990).

126.   Floquet, N. *et al.* The antitumor properties of the alpha3(IV)-(185-203) peptide from the NC1 domain of type IV collagen (tumstatin) are conformation-dependent. *J Biol Chem* **279**, 2091-2100 (2004).

127.   Han, J. *et al.* A cell binding domain from the alpha3 chain of type IV collagen inhibits proliferation of melanoma cells. *J Biol Chem* **272**, 20395-20401 (1997).

128.   Davis, G.E. Matricryptic sites control tissue injury responses in the cardiovascular system: relationships to pattern recognition receptor regulated events. *J Mol Cell Cardiol* **48**, 454-460 (2010).

129.   Taubenberger, A.V., Woodruff, M.A., Bai, H., Muller, D.J. & Hutmacher, D.W. The effect of unlocking RGD-motifs in collagen I on pre-osteoblast adhesion and differentiation. *Biomaterials* **31**, 2827-2835 (2010).

130.   Ingham, K.C., Brew, S.A. & Migliorini, M. Type I collagen contains at least 14 cryptic fibronectin binding sites of similar affinity. *Arch Biochem Biophys* **407**, 217-223 (2002).

131.   Hersel, U., Dahmen, C. & Kessler, H. RGD modified polymers: biomaterials for stimulated cell adhesion and beyond. *Biomaterials* **24**, 4385-4415 (2003).

132.   Sarin, V., Gaffin, R.D., Meininger, G.A. & Muthuchamy, M. Arginine-glycine-aspartic acid (RGD)-containing peptides inhibit the force production of mouse papillary muscle bundles via alpha 5 beta 1 integrin. *J Physiol* **564**, 603-617 (2005).

133.   Mogford, J.E., Davis, G.E., Platts, S.H. & Meininger, G.A. Vascular smooth muscle alpha v beta 3 integrin mediates arteriolar vasodilation in response to RGD peptides. *Circ Res* **79**, 821-826 (1996).

134.   Shachar, M., Tsur-Gang, O., Dvir, T., Leor, J. & Cohen, S. The effect of immobilized RGD peptide in alginate scaffolds on cardiac tissue engineering. *Acta Biomater* **7**, 152-162 (2011).

135.   Davis, G.E., Bayless, K.J., Davis, M.J. & Meininger, G.A. Regulation of tissue injury responses by the exposure of matricryptic sites within extracellular matrix molecules. *Am J Pathol* **156**, 1489-1498 (2000).

136.   Lighthouse, J.K. & Small, E.M. Transcriptional control of cardiac fibroblast plasticity. *J Mol Cell Cardiol* **91**, 52-60 (2016).

137.   Tallquist, M.D. & Molkentin, J.D. Redefining the identity of cardiac fibroblasts. *Nat Rev Cardiol* **14**, 484-491 (2017).

138.   Fu, X. *et al.* Specialized fibroblast differentiated states underlie scar formation in the infarcted mouse heart. *J Clin Invest* **128**, 2127-2143 (2018).

139. Smith, C.L., Baek, S.T., Sung, C.Y. & Tallquist, M.D. Epicardial-derived cell epithelial-to-mesenchymal transition and fate specification require PDGF receptor signaling. *Circ Res* **108**, e15-26 (2011).

140. Acharya, A. *et al.* The bHLH transcription factor Tcf21 is required for lineage-specific EMT of cardiac fibroblast progenitors. *Development* **139**, 2139-2149 (2012).

141. Moore-Morris, T. *et al.* Resident fibroblast lineages mediate pressure overload-induced cardiac fibrosis. *J Clin Invest* **124**, 2921-2934 (2014).

142. Kramann, R. *et al.* Perivascular Gli1+ progenitors are key contributors to injury-induced organ fibrosis. *Cell Stem Cell* **16**, 51-66 (2015).

143. van Amerongen, M.J. *et al.* Bone marrow-derived myofibroblasts contribute functionally to scar formation after myocardial infarction. *J Pathol* **214**, 377-386 (2008).

144. Bucala, R., Spiegel, L.A., Chesney, J., Hogan, M. & Cerami, A. Circulating fibrocytes define a new leukocyte subpopulation that mediates tissue repair. *Mol Med* **1**, 71-81 (1994).

145. Ivey, M.J., Kuwabara, J.T., Riggsbee, K.L. & Tallquist, M.D. Platelet-derived growth factor receptor-alpha is essential for cardiac fibroblast survival. *Am J Physiol Heart Circ Physiol* **317**, H330-H344 (2019).

146. Moore-Morris, T., Guimaraes-Camboa, N., Yutzey, K.E., Puceat, M. & Evans, S.M. Cardiac fibroblasts: from development to heart failure. *J Mol Med (Berl)* **93**, 823-830 (2015).

147. Souders, C.A., Bowers, S.L. & Baudino, T.A. Cardiac fibroblast: the renaissance cell. *Circ Res* **105**, 1164-1176 (2009).

148. Swonger, J.M., Liu, J.S., Ivey, M.J. & Tallquist, M.D. Genetic tools for identifying and manipulating fibroblasts in the mouse. *Differentiation* **92**, 66-83 (2016).

149. Kong, P., Christia, P., Saxena, A., Su, Y. & Frangogiannis, N.G. Lack of specificity of fibroblast-specific protein 1 in cardiac remodeling and fibrosis. *Am J Physiol Heart Circ Physiol* **305**, H1363-1372 (2013).

150. Hudon-David, F., Bouzeghrane, F., Couture, P. & Thibault, G. Thy-1 expression by cardiac fibroblasts: lack of association with myofibroblast contractile markers. *J Mol Cell Cardiol* **42**, 991-1000 (2007).

151. Pinto, A.R. *et al.* Revisiting Cardiac Cellular Composition. *Circulation research* **118**, 400-409 (2016).

152. Hinz, B. Formation and function of the myofibroblast during tissue repair. *J Invest Dermatol* **127**, 526-537 (2007).

153. Darby, I., Skalli, O. & Gabbiani, G. Alpha-smooth muscle actin is transiently expressed by myofibroblasts during experimental wound healing. *Laboratory investigation; a journal of technical methods and pathology* **63**, 21-29 (1990).

154. Leslie, K.O., Taatjes, D.J., Schwarz, J., vonTurkovich, M. & Low, R.B. Cardiac myofibroblasts express alpha smooth muscle actin during right ventricular pressure overload in the rabbit. *The American journal of pathology* **139**, 207-216 (1991).

155. Eid, H., Chen, J.H. & de Bold, A.J. Regulation of alpha-smooth muscle actin expression in adult cardiomyocytes through a tyrosine kinase signal transduction pathway. *Annals of the New York Academy of Sciences* **752**, 192-201 (1995).

156. Jones, C. & Ehrlich, H.P. Fibroblast expression of alpha-smooth muscle actin, alpha2beta1 integrin and alphavbeta3 integrin: influence of surface rigidity. *Experimental and molecular pathology* **91**, 394-399 (2011).

157. Yu, J. *et al.* Topological Arrangement of Cardiac Fibroblasts Regulates Cellular Plasticity. *Circ Res* **123**, 73-85 (2018).

158. Shiojima, I., Aikawa, M., Suzuki, J., Yazaki, Y. & Nagai, R. Embryonic smooth muscle myosin heavy chain SMemb is expressed in pressure-overloaded cardiac fibroblasts. *Jpn Heart J* **40**, 803-818 (1999).

159. Turner, N.A. & Porter, K.E. Function and fate of myofibroblasts after myocardial infarction. *Fibrogenesis Tissue Repair* **6**, 5 (2013).

160. Travers, J.G., Kamal, F.A., Robbins, J., Yutzey, K.E. & Blaxall, B.C. Cardiac Fibrosis: The Fibroblast Awakens. *Circulation research* **118**, 1021-1040 (2016).

161. Van De Water, L., Varney, S. & Tomasek, J.J. Mechanoregulation of the Myofibroblast in Wound Contraction, Scarring, and Fibrosis: Opportunities for New Therapeutic Intervention. *Adv Wound Care (New Rochelle)* **2**, 122-141 (2013).

162. Goffin, J.M. *et al.* Focal adhesion size controls tension-dependent recruitment of alpha-smooth muscle actin to stress fibers. *The Journal of cell biology* **172**, 259-268 (2006).

163. Hinz, B. Masters and servants of the force: the role of matrix adhesions in myofibroblast force perception and transmission. *European journal of cell biology* **85**, 175-181 (2006).

164. Hinz, B., Dugina, V., Ballestrem, C., Wehrle-Haller, B. & Chaponnier, C. Alpha-smooth muscle actin is crucial for focal adhesion maturation in myofibroblasts. *Molecular biology of the cell* **14**, 2508-2519 (2003).

165. Landry, N.M., Rattan, S.G. & Dixon, I.M.C. An Improved Method of Maintaining Primary Murine Cardiac Fibroblasts in Two-Dimensional Cell Culture. *Sci Rep* **9**, 12889 (2019).

166.   Moore-Morris, T. *et al.* Infarct Fibroblasts Do Not Derive From Bone Marrow Lineages. *Circ Res* **122**, 583-590 (2018).

167.   Hinderer, S. & Schenke-Layland, K. Cardiac fibrosis - A short review of causes and therapeutic strategies. *Adv Drug Deliv Rev* **146**, 77-82 (2019).

168.   Anderson, K.R., Sutton, M.G. & Lie, J.T. Histopathological types of cardiac fibrosis in myocardial disease. *J Pathol* **128**, 79-85 (1979).

169.   Hinz, B. Tissue stiffness, latent TGF-beta1 activation, and mechanical signal transduction: implications for the pathogenesis and treatment of fibrosis. *Current rheumatology reports* **11**, 120-126 (2009).

170.   Buscemi, L. *et al.* The single-molecule mechanics of the latent TGF-beta1 complex. *Curr Biol* **21**, 2046-2054 (2011).

171.   Taipale, J., Saharinen, J. & Keski-Oja, J. Extracellular matrix-associated transforming growth factor-beta: role in cancer cell growth and invasion. *Adv Cancer Res* **75**, 87-134 (1998).

172.   Dobaczewski, M., Chen, W. & Frangogiannis, N.G. Transforming growth factor (TGF)-beta signaling in cardiac remodeling. *Journal of molecular and cellular cardiology* **51**, 600-606 (2011).

173.   Desmouliere, A., Geinoz, A., Gabbiani, F. & Gabbiani, G. Transforming growth factor-beta 1 induces alpha-smooth muscle actin expression in granulation tissue myofibroblasts and in quiescent and growing cultured fibroblasts. *J Cell Biol* **122**, 103-111 (1993).

174.   Caja, L. *et al.* TGF-beta and the Tissue Microenvironment: Relevance in Fibrosis and Cancer. *Int J Mol Sci* **19** (2018).

175.   Annes, J.P., Munger, J.S. & Rifkin, D.B. Making sense of latent TGFbeta activation. *J Cell Sci* **116**, 217-224 (2003).

176.   Annes, J.P., Chen, Y., Munger, J.S. & Rifkin, D.B. Integrin alphaVbeta6-mediated activation of latent TGF-beta requires the latent TGF-beta binding protein-1. *J Cell Biol* **165**, 723-734 (2004).

177.   Massague, J. TGF-beta signal transduction. *Annu Rev Biochem* **67**, 753-791 (1998).

178.   Derynck, R. & Zhang, Y.E. Smad-dependent and Smad-independent pathways in TGF-beta family signalling. *Nature* **425**, 577-584 (2003).

179.   Tecalco-Cruz, A.C., Rios-Lopez, D.G., Vazquez-Victorio, G., Rosales-Alvarez, R.E. & Macias-Silva, M. Transcriptional cofactors Ski and SnoN are major regulators of the TGF-beta/Smad signaling pathway in health and disease. *Signal Transduct Target Ther* **3**, 15 (2018).

180. Ramazani, Y. *et al.* Connective tissue growth factor (CTGF) from basics to clinics. *Matrix Biol* **68-69**, 44-66 (2018).

181. Rosin, N.L., Falkenham, A., Sopel, M.J., Lee, T.D. & Legare, J.F. Regulation and role of connective tissue growth factor in AngII-induced myocardial fibrosis. *Am J Pathol* **182**, 714-726 (2013).

182. Leask, A., Holmes, A., Black, C.M. & Abraham, D.J. Connective tissue growth factor gene regulation. Requirements for its induction by transforming growth factor-beta 2 in fibroblasts. *J Biol Chem* **278**, 13008-13015 (2003).

183. Lipson, K.E., Wong, C., Teng, Y. & Spong, S. CTGF is a central mediator of tissue remodeling and fibrosis and its inhibition can reverse the process of fibrosis. *Fibrogenesis Tissue Repair* **5**, S24 (2012).

184. Xiao, Y. *et al.* Hippo pathway deletion in adult resting cardiac fibroblasts initiates a cell state transition with spontaneous and self-sustaining fibrosis. *Genes Dev* **33**, 1491-1505 (2019).

185. Grotendorst, G.R., Rahmanie, H. & Duncan, M.R. Combinatorial signaling pathways determine fibroblast proliferation and myofibroblast differentiation. *FASEB J* **18**, 469-479 (2004).

186. Chuva de Sousa Lopes, S.M. *et al.* Connective tissue growth factor expression and Smad signaling during mouse heart development and myocardial infarction. *Dev Dyn* **231**, 542-550 (2004).

187. Szabo, Z. *et al.* Connective tissue growth factor inhibition attenuates left ventricular remodeling and dysfunction in pressure overload-induced heart failure. *Hypertension* **63**, 1235-1240 (2014).

188. Huang, Z.W., Tian, L.H., Yang, B. & Guo, R.M. Long Noncoding RNA H19 Acts as a Competing Endogenous RNA to Mediate CTGF Expression by Sponging miR-455 in Cardiac Fibrosis. *DNA Cell Biol* **36**, 759-766 (2017).

189. Angelini, A., Li, Z., Mericskay, M. & Decaux, J.F. Regulation of Connective Tissue Growth Factor and Cardiac Fibrosis by an SRF/MicroRNA-133a Axis. *PLoS One* **10**, e0139858 (2015).

190. Wu, C.K. *et al.* Connective tissue growth factor and cardiac diastolic dysfunction: human data from the Taiwan diastolic heart failure registry and molecular basis by cellular and animal models. *Eur J Heart Fail* **16**, 163-172 (2014).

191. Tallquist, M. & Kazlauskas, A. PDGF signaling in cells and mice. *Cytokine & growth factor reviews* **15**, 205-213 (2004).

192. Klinkhammer, B.M., Floege, J. & Boor, P. PDGF in organ fibrosis. *Mol Aspects Med* **62**, 44-62 (2018).

193. Xu, Y. *et al.* Connective tissue growth factor in regulation of RhoA mediated cytoskeletal tension associated osteogenesis of mouse adipose-derived stromal cells. *PLoS One* **5**, e11279 (2010).

194. Zymek, P. *et al.* The role of platelet-derived growth factor signaling in healing myocardial infarcts. *J Am Coll Cardiol* **48**, 2315-2323 (2006).

195. Liao, C.H. *et al.* Cardiac mast cells cause atrial fibrillation through PDGF-A-mediated fibrosis in pressure-overloaded mouse hearts. *J Clin Invest* **120**, 242-253 (2010).

196. Solon, J., Levental, I., Sengupta, K., Georges, P.C. & Janmey, P.A. Fibroblast adaptation and stiffness matching to soft elastic substrates. *Biophysical journal* **93**, 4453-4461 (2007).

197. Hiesinger, W. *et al.* Myocardial tissue elastic properties determined by atomic force microscopy after stromal cell-derived factor 1alpha angiogenic therapy for acute myocardial infarction in a murine model. *J Thorac Cardiovasc Surg* **143**, 962-966 (2012).

198. Zamir, E. & Geiger, B. Molecular complexity and dynamics of cell-matrix adhesions. *J Cell Sci* **114**, 3583-3590 (2001).

199. Herum, K.M., Lunde, I.G., McCulloch, A.D. & Christensen, G. The Soft- and Hard-Heartedness of Cardiac Fibroblasts: Mechanotransduction Signaling Pathways in Fibrosis of the Heart. *J Clin Med* **6** (2017).

200. Civitarese, R.A., Kapus, A., McCulloch, C.A. & Connelly, K.A. Role of integrins in mediating cardiac fibroblast-cardiomyocyte cross talk: a dynamic relationship in cardiac biology and pathophysiology. *Basic Res Cardiol* **112**, 6 (2017).

201. Chen, C., Li, R., Ross, R.S. & Manso, A.M. Integrins and integrin-related proteins in cardiac fibrosis. *J Mol Cell Cardiol* **93**, 162-174 (2016).

202. Schlaepfer, D.D. & Hunter, T. Integrin signalling and tyrosine phosphorylation: just the FAKs? *Trends Cell Biol* **8**, 151-157 (1998).

203. Shattil, S.J., Kim, C. & Ginsberg, M.H. The final steps of integrin activation: the end game. *Nat Rev Mol Cell Biol* **11**, 288-300 (2010).

204. Rodriguez, A. *et al.* Integrin alpha1beta1 is involved in the differentiation into myofibroblasts in adult reactive tissues in vivo. *J Cell Mol Med* **13**, 3449-3462 (2009).

205. Kim, K.K. *et al.* Epithelial cell alpha3beta1 integrin links beta-catenin and Smad signaling to promote myofibroblast formation and pulmonary fibrosis. *J Clin Invest* **119**, 213-224 (2009).

206. Wang, Z. *et al.* RGD-independent cell adhesion via a tissue transglutaminase-fibronectin matrix promotes fibronectin fibril deposition and requires syndecan-4/2 alpha5beta1 integrin co-signaling. *J Biol Chem* **285**, 40212-40229 (2010).

207. Sarrazy, V. *et al.* Integrins alphavbeta5 and alphavbeta3 promote latent TGF-beta1 activation by human cardiac fibroblast contraction. *Cardiovasc Res* **102**, 407-417 (2014).

208. Schroer, A.K. & Merryman, W.D. Mechanobiology of myofibroblast adhesion in fibrotic cardiac disease. *J Cell Sci* **128**, 1865-1875 (2015).

209. Hirota, T. *et al.* Zyxin, a regulator of actin filament assembly, targets the mitotic apparatus by interacting with h-warts/LATS1 tumor suppressor. *J Cell Biol* **149**, 1073-1086 (2000).

210. Wang, N. *et al.* Cell prestress. I. Stiffness and prestress are closely associated in adherent contractile cells. *Am J Physiol Cell Physiol* **282**, C606-616 (2002).

211. Dupont, S. *et al.* Role of YAP/TAZ in mechanotransduction. *Nature* **474**, 179-183 (2011).

212. Aragona, M. *et al.* A mechanical checkpoint controls multicellular growth through YAP/TAZ regulation by actin-processing factors. *Cell* **154**, 1047-1059 (2013).

213. Liu, F. *et al.* Mechanosignaling through YAP and TAZ drives fibroblast activation and fibrosis. *Am J Physiol Lung Cell Mol Physiol* **308**, L344-357 (2015).

214. Mannaerts, I. *et al.* The Hippo pathway effector YAP controls mouse hepatic stellate cell activation. *J Hepatol* **63**, 679-688 (2015).

215. Szeto, S.G. *et al.* YAP/TAZ Are Mechanoregulators of TGF-beta-Smad Signaling and Renal Fibrogenesis. *J Am Soc Nephrol* **27**, 3117-3128 (2016).

216. Porter, K.E. & Turner, N.A. Cardiac fibroblasts: at the heart of myocardial remodeling. *Pharmacol Ther* **123**, 255-278 (2009).

217. Vegter, E.L. *et al.* Rodent heart failure models do not reflect the human circulating microRNA signature in heart failure. *PLoS One* **12**, e0177242 (2017).

218. Camacho, P., Fan, H., Liu, Z. & He, J.Q. Small mammalian animal models of heart disease. *Am J Cardiovasc Dis* **6**, 70-80 (2016).

219. in *MI - Secondary Prevention: Secondary Prevention in Primary and Secondary Care for Patients Following a Myocardial Infarction: Partial Update of NICE CG48* (London; 2013).

220. Lewis, G.A. *et al.* Pirfenidone in Heart Failure with Preserved Ejection Fraction-Rationale and Design of the PIROUETTE Trial. *Cardiovasc Drugs Ther* **33**, 461-470 (2019).

221. Lin, X., Yu, M., Wu, K., Yuan, H. & Zhong, H. Effects of pirfenidone on proliferation, migration, and collagen contraction of human Tenon's fibroblasts in vitro. *Invest Ophthalmol Vis Sci* **50**, 3763-3770 (2009).

222. Lee, B.S., Margolin, S.B. & Nowak, R.A. Pirfenidone: a novel pharmacological agent that inhibits leiomyoma cell proliferation and collagen production. *J Clin Endocrinol Metab* **83**, 219-223 (1998).

223. Shubrook, J.H., Bokaie, B.B. & Adkins, S.E. Empagliflozin in the treatment of type 2 diabetes: evidence to date. *Drug Des Devel Ther* **9**, 5793-5803 (2015).

224. Lam, C.S.P., Chandramouli, C., Ahooja, V. & Verma, S. SGLT-2 Inhibitors in Heart Failure: Current Management, Unmet Needs, and Therapeutic Prospects. *J Am Heart Assoc* **8**, e013389 (2019).

225. Kang, S. *et al.* Direct Effects of Empagliflozin on Extracellular Matrix Remodelling in Human Cardiac Myofibroblasts: Novel Translational Clues to Explain EMPA-REG OUTCOME Results. *Can J Cardiol* (2019).

226. Traverse, J.H. *et al.* First-in-Man Study of a Cardiac Extracellular Matrix Hydrogel in Early and Late Myocardial Infarction Patients. *JACC Basic Transl Sci* **4**, 659-669 (2019).

227. Xu, T., Wang, W., Zhang, S., Stewart, R.A. & Yu, W. Identifying tumor suppressors in genetic mosaics: the Drosophila lats gene encodes a putative protein kinase. *Development* **121**, 1053-1063 (1995).

228. Justice, R.W., Zilian, O., Woods, D.F., Noll, M. & Bryant, P.J. The Drosophila tumor suppressor gene warts encodes a homolog of human myotonic dystrophy kinase and is required for the control of cell shape and proliferation. *Genes Dev* **9**, 534-546 (1995).

229. Tapon, N. *et al.* salvador Promotes both cell cycle exit and apoptosis in Drosophila and is mutated in human cancer cell lines. *Cell* **110**, 467-478 (2002).

230. Huang, J., Wu, S., Barrera, J., Matthews, K. & Pan, D. The Hippo signaling pathway coordinately regulates cell proliferation and apoptosis by inactivating Yorkie, the Drosophila Homolog of YAP. *Cell* **122**, 421-434 (2005).

231. Mueller, K.A. *et al.* Hippo Signaling Pathway Dysregulation in Human Huntington's Disease Brain and Neuronal Stem Cells. *Sci Rep* **8**, 11355 (2018).

232. Harvey, K.F., Zhang, X. & Thomas, D.M. The Hippo pathway and human cancer. *Nat Rev Cancer* **13**, 246-257 (2013).

233. Kim, C.L., Choi, S.H. & Mo, J.S. Role of the Hippo Pathway in Fibrosis and Cancer. *Cells* **8** (2019).

234. Bosl, W.J. & Li, R. Mitotic-exit control as an evolved complex system. *Cell* **121**, 325-333 (2005).

235. Pan, D. The hippo signaling pathway in development and cancer. *Dev Cell* **19**, 491-505 (2010).

236. Varelas, X. The Hippo pathway effectors TAZ and YAP in development, homeostasis and disease. *Development* **141**, 1614-1626 (2014).

237. Meng, Z., Moroishi, T. & Guan, K.L. Mechanisms of Hippo pathway regulation. *Genes Dev* **30**, 1-17 (2016).

238. Visser, S. & Yang, X. LATS tumor suppressor: a new governor of cellular homeostasis. *Cell Cycle* **9**, 3892-3903 (2010).

239. Furth, N. & Aylon, Y. The LATS1 and LATS2 tumor suppressors: beyond the Hippo pathway. *Cell Death Differ* **24**, 1488-1501 (2017).

240. Kwon, Y. *et al.* The Hippo signaling pathway interactome. *Science* **342**, 737-740 (2013).

241. Avruch, J. *et al.* Protein kinases of the Hippo pathway: regulation and substrates. *Semin Cell Dev Biol* **23**, 770-784 (2012).

242. Sudol, M. Newcomers to the WW Domain-Mediated Network of the Hippo Tumor Suppressor Pathway. *Genes Cancer* **1**, 1115-1118 (2010).

243. St John, M.A. *et al.* Mice deficient of Lats1 develop soft-tissue sarcomas, ovarian tumours and pituitary dysfunction. *Nat Genet* **21**, 182-186 (1999).

244. Yu, T., Bachman, J. & Lai, Z.C. Mutation analysis of large tumor suppressor genes LATS1 and LATS2 supports a tumor suppressor role in human cancer. *Protein Cell* **6**, 6-11 (2015).

245. Yabuta, N., Mukai, S., Okada, N., Aylon, Y. & Nojima, H. The tumor suppressor Lats2 is pivotal in Aurora A and Aurora B signaling during mitosis. *Cell Cycle* **10**, 2724-2736 (2011).

246. Uhlen, M. *et al.* Proteomics. Tissue-based map of the human proteome. *Science* **347**, 1260419 (2015).

247. Hong, W. & Guan, K.L. The YAP and TAZ transcription co-activators: key downstream effectors of the mammalian Hippo pathway. *Semin Cell Dev Biol* **23**, 785-793 (2012).

248.   Sudol, M. Yes-associated protein (YAP65) is a proline-rich phosphoprotein that binds to the SH3 domain of the Yes proto-oncogene product. *Oncogene* **9**, 2145-2152 (1994).

249.   Kanai, F. *et al.* TAZ: a novel transcriptional co-activator regulated by interactions with 14-3-3 and PDZ domain proteins. *EMBO J* **19**, 6778-6791 (2000).

250.   Noguchi, S., Saito, A. & Nagase, T. YAP/TAZ Signaling as a Molecular Link between Fibrosis and Cancer. *Int J Mol Sci* **19** (2018).

251.   Salah, Z., Alian, A. & Aqeilan, R.I. WW domain-containing proteins: retrospectives and the future. *Front Biosci (Landmark Ed)* **17**, 331-348 (2012).

252.   Sudol, M. YAP1 oncogene and its eight isoforms. *Oncogene* **32**, 3922 (2013).

253.   Manjunath, G.P., Ramanujam, P.L. & Galande, S. Structure function relations in PDZ-domain-containing proteins: Implications for protein networks in cellular signalling. *J Biosci* **43**, 155-171 (2018).

254.   Jang, E.J. *et al.* TAZ suppresses NFAT5 activity through tyrosine phosphorylation. *Mol Cell Biol* **32**, 4925-4932 (2012).

255.   Chen, L. *et al.* Structural basis of YAP recognition by TEAD4 in the hippo pathway. *Genes Dev* **24**, 290-300 (2010).

256.   Hau, J.C. *et al.* The TEAD4-YAP/TAZ protein-protein interaction: expected similarities and unexpected differences. *Chembiochem* **14**, 1218-1225 (2013).

257.   Lamar, J.M. *et al.* The Hippo pathway target, YAP, promotes metastasis through its TEAD-interaction domain. *Proc Natl Acad Sci U S A* **109**, E2441-2450 (2012).

258.   Zhang, H. *et al.* TEAD transcription factors mediate the function of TAZ in cell growth and epithelial-mesenchymal transition. *J Biol Chem* **284**, 13355-13362 (2009).

259.   Pocaterra, A., Romani, P. & Dupont, S. YAP/TAZ functions and their regulation at a glance. *J Cell Sci* **133** (2020).

260.   Ota, M. & Sasaki, H. Mammalian Tead proteins regulate cell proliferation and contact inhibition as transcriptional mediators of Hippo signaling. *Development* **135**, 4059-4069 (2008).

261.   Zhao, B. *et al.* Inactivation of YAP oncoprotein by the Hippo pathway is involved in cell contact inhibition and tissue growth control. *Genes Dev* **21**, 2747-2761 (2007).

262.   Callus, B.A., Finch-Edmondson, M.L., Fletcher, S. & Wilton, S.D. YAPping about and not forgetting TAZ. *FEBS Lett* **593**, 253-276 (2019).

263.   Sansores-Garcia, L. *et al.* Modulating F-actin organization induces organ growth by affecting the Hippo pathway. *EMBO J* **30**, 2325-2335 (2011).

264. Fernandez, B.G. *et al.* Actin-Capping Protein and the Hippo pathway regulate F-actin and tissue growth in Drosophila. *Development* **138**, 2337-2346 (2011).

265. Solon, J., Levental, I., Sengupta, K., Georges, P.C. & Janmey, P.A. Fibroblast adaptation and stiffness matching to soft elastic substrates. *Biophysical journal* **93**, 4453-4461 (2007).

266. Rottner, K., Faix, J., Bogdan, S., Linder, S. & Kerkhoff, E. Actin assembly mechanisms at a glance. *J Cell Sci* **130**, 3427-3435 (2017).

267. Wada, K., Itoga, K., Okano, T., Yonemura, S. & Sasaki, H. Hippo pathway regulation by cell morphology and stress fibers. *Development* **138**, 3907-3914 (2011).

268. Reddy, P., Deguchi, M., Cheng, Y. & Hsueh, A.J. Actin cytoskeleton regulates Hippo signaling. *PLoS One* **8**, e73763 (2013).

269. Zhao, B. *et al.* Cell detachment activates the Hippo pathway via cytoskeleton reorganization to induce anoikis. *Genes Dev* **26**, 54-68 (2012).

270. Sabra, H. *et al.* beta1 integrin-dependent Rac/group I PAK signaling mediates YAP activation of Yes-associated protein 1 (YAP1) via NF2/merlin. *J Biol Chem* **292**, 19179-19197 (2017).

271. Sero, J.E. & Bakal, C. Multiparametric Analysis of Cell Shape Demonstrates that beta-PIX Directly Couples YAP Activation to Extracellular Matrix Adhesion. *Cell Syst* **4**, 84-96 e86 (2017).

272. Plotnikov, S.V., Pasapera, A.M., Sabass, B. & Waterman, C.M. Force fluctuations within focal adhesions mediate ECM-rigidity sensing to guide directed cell migration. *Cell* **151**, 1513-1527 (2012).

273. Mana-Capelli, S., Paramasivam, M., Dutta, S. & McCollum, D. Angiomotins link F-actin architecture to Hippo pathway signaling. *Mol Biol Cell* **25**, 1676-1685 (2014).

274. Mana-Capelli, S. & McCollum, D. Angiomotins stimulate LATS kinase autophosphorylation and act as scaffolds that promote Hippo signaling. *J Biol Chem* **293**, 18230-18241 (2018).

275. Lamar, J.M. *et al.* SRC tyrosine kinase activates the YAP/TAZ axis and thereby drives tumor growth and metastasis. *J Biol Chem* **294**, 2302-2317 (2019).

276. Kim, N.G. & Gumbiner, B.M. Adhesion to fibronectin regulates Hippo signaling via the FAK-Src-PI3K pathway. *J Cell Biol* **210**, 503-515 (2015).

277. Oh, S. *et al.* Crucial role for Mst1 and Mst2 kinases in early embryonic development of the mouse. *Mol Cell Biol* **29**, 6309-6320 (2009).

278. Nishioka, N. *et al.* The Hippo signaling pathway components Lats and Yap pattern Tead4 activity to distinguish mouse trophectoderm from inner cell mass. *Dev Cell* **16**, 398-410 (2009).

279. Morin-Kensicki, E.M. *et al.* Defects in yolk sac vasculogenesis, chorioallantoic fusion, and embryonic axis elongation in mice with targeted disruption of Yap65. *Mol Cell Biol* **26**, 77-87 (2006).

280. Makita, R. *et al.* Multiple renal cysts, urinary concentration defects, and pulmonary emphysematous changes in mice lacking TAZ. *Am J Physiol Renal Physiol* **294**, F542-553 (2008).

281. Zhao, B., Li, L., Lei, Q. & Guan, K.L. The Hippo-YAP pathway in organ size control and tumorigenesis: an updated version. *Genes Dev* **24**, 862-874 (2010).

282. Zender, L. *et al.* Identification and validation of oncogenes in liver cancer using an integrative oncogenomic approach. *Cell* **125**, 1253-1267 (2006).

283. Antonescu, C.R. *et al.* Novel YAP1-TFE3 fusion defines a distinct subset of epithelioid hemangioendothelioma. *Genes Chromosomes Cancer* **52**, 775-784 (2013).

284. Tanas, M.R. *et al.* Identification of a disease-defining gene fusion in epithelioid hemangioendothelioma. *Sci Transl Med* **3**, 98ra82 (2011).

285. Wang, X. *et al.* Hepatocyte TAZ/WWTR1 Promotes Inflammation and Fibrosis in Nonalcoholic Steatohepatitis. *Cell Metab* **24**, 848-862 (2016).

286. Xin, M. *et al.* Hippo pathway effector Yap promotes cardiac regeneration. *Proc Natl Acad Sci U S A* **110**, 13839-13844 (2013).

287. Zhou, Q., Li, L., Zhao, B. & Guan, K.L. The hippo pathway in heart development, regeneration, and diseases. *Circ Res* **116**, 1431-1447 (2015).

288. von Gise, A. *et al.* YAP1, the nuclear target of Hippo signaling, stimulates heart growth through cardiomyocyte proliferation but not hypertrophy. *Proc Natl Acad Sci U S A* **109**, 2394-2399 (2012).

289. Colmenares, C., Teumer, J.K. & Stavnezer, E. Transformation-defective v-ski induces MyoD and myogenin expression but not myotube formation. *Mol Cell Biol* **11**, 1167-1170 (1991).

290. Colmenares, C., Sutrave, P., Hughes, S.H. & Stavnezer, E. Activation of the c-ski oncogene by overexpression. *J Virol* **65**, 4929-4935 (1991).

291. Xu, W. *et al.* Ski acts as a co-repressor with Smad2 and Smad3 to regulate the response to type beta transforming growth factor. *Proc Natl Acad Sci U S A* **97**, 5924-5929 (2000).

292. Nicol, R., Zheng, G., Sutrave, P., Foster, D.N. & Stavnezer, E. Association of specific DNA binding and transcriptional repression with the transforming and myogenic activities of c-Ski. *Cell Growth Differ* **10**, 243-254 (1999).

293. Nomura, N. *et al.* Isolation of human cDNA clones of ski and the ski-related gene, sno. *Nucleic Acids Res* **17**, 5489-5500 (1989).

294. Mardon, G., Solomon, N.M. & Rubin, G.M. dachshund encodes a nuclear protein required for normal eye and leg development in Drosophila. *Development* **120**, 3473-3486 (1994).

295. Wu, K. *et al.* DACH1 inhibits transforming growth factor-beta signaling through binding Smad4. *J Biol Chem* **278**, 51673-51684 (2003).

296. Sutrave, P., Copeland, T.D., Showalter, S.D. & Hughes, S.H. Characterization of chicken c-ski oncogene products expressed by retrovirus vectors. *Mol Cell Biol* **10**, 3137-3144 (1990).

297. Grimes, H.L., Ambrose, M.R. & Goodenow, M.M. C-ski transcripts with and without exon 2 are expressed in skeletal muscle and throughout chick embryogenesis. *Oncogene* **8**, 2863-2868 (1993).

298. Wilson, J.J., Malakhova, M., Zhang, R., Joachimiak, A. & Hegde, R.S. Crystal structure of the dachshund homology domain of human SKI. *Structure* **12**, 785-792 (2004).

299. Wu, J.W. *et al.* Structural mechanism of Smad4 recognition by the nuclear oncoprotein Ski: insights on Ski-mediated repression of TGF-beta signaling. *Cell* **111**, 357-367 (2002).

300. Bonnon, C. & Atanasoski, S. c-Ski in health and disease. *Cell Tissue Res* **347**, 51-64 (2012).

301. Heyman, H.C. & Stavnezer, E. A carboxyl-terminal region of the ski oncoprotein mediates homodimerization as well as heterodimerization with the related protein SnoN. *J Biol Chem* **269**, 26996-27003 (1994).

302. Akiyoshi, S. *et al.* c-Ski acts as a transcriptional co-repressor in transforming growth factor-beta signaling through interaction with smads. *J Biol Chem* **274**, 35269-35277 (1999).

303. Xie, M., Wu, X., Zhang, J., Zhang, J. & Li, X. Ski regulates Smads and TAZ signaling to suppress lung cancer progression. *Mol Carcinog* **56**, 2178-2189 (2017).

304. Melling, M.A., Friendship, C.R., Shepherd, T.G. & Drysdale, T.A. Expression of Ski can act as a negative feedback mechanism on retinoic acid signaling. *Dev Dyn* **242**, 604-613 (2013).

305. Zhang, S.X. *et al.* Identification of direct serum-response factor gene targets during Me2SO-induced P19 cardiac cell differentiation. *J Biol Chem* **280**, 19115-19126 (2005).

306. Imig, J. *et al.* microRNA profiling in Epstein-Barr virus-associated B-cell lymphoma. *Nucleic Acids Res* **39**, 1880-1893 (2011).

307. Levati, L. *et al.* MicroRNA-155 targets the SKI gene in human melanoma cell lines. *Pigment Cell Melanoma Res* **24**, 538-550 (2011).

308. Teichler, S. *et al.* MicroRNA29a regulates the expression of the nuclear oncogene Ski. *Blood* **118**, 1899-1902 (2011).

309. Jiang, H. *et al.* Next generation sequencing analysis of miRNAs: MiR-127-3p inhibits glioblastoma proliferation and activates TGF-beta signaling by targeting SKI. *OMICS* **18**, 196-206 (2014).

310. Mosquera, J. *et al.* Identification of Ski as a target for Aurora A kinase. *Biochem Biophys Res Commun* **409**, 539-543 (2011).

311. Band, A.M., Bjorklund, M. & Laiho, M. The phosphatidylinositol 3-kinase/Akt pathway regulates transforming growth factor-{beta} signaling by destabilizing ski and inducing Smad7. *J Biol Chem* **284**, 35441-35449 (2009).

312. Nagata, M. *et al.* Identification of a phosphorylation site in c-Ski as serine 515. *J Biochem* **148**, 423-427 (2010).

313. Nagano, Y. *et al.* Arkadia induces degradation of SnoN and c-Ski to enhance transforming growth factor-beta signaling. *J Biol Chem* **282**, 20492-20501 (2007).

314. Bonni, S. *et al.* TGF-beta induces assembly of a Smad2-Smurf2 ubiquitin ligase complex that targets SnoN for degradation. *Nat Cell Biol* **3**, 587-595 (2001).

315. Wrighton, K.H. *et al.* Transforming growth factor-beta-independent regulation of myogenesis by SnoN sumoylation. *J Biol Chem* **282**, 6517-6524 (2007).

316. Hsu, Y.H. *et al.* Sumoylated SnoN represses transcription in a promoter-specific manner. *J Biol Chem* **281**, 33008-33018 (2006).

317. Shinagawa, T. & Ishii, S. Generation of Ski-knockdown mice by expressing a long double-strand RNA from an RNA polymerase II promoter. *Genes Dev* **17**, 1340-1345 (2003).

318. Kaufman, C.D., Martinez-Rodriguez, G. & Hackett, P.B., Jr. Ectopic expression of c-ski disrupts gastrulation and neural patterning in zebrafish. *Mech Dev* **95**, 147-162 (2000).

319. Bruusgaard, J.C., Brack, A.S., Hughes, S.M. & Gundersen, K. Muscle hypertrophy induced by the Ski protein: cyto-architecture and ultrastructure. *Acta Physiol Scand* **185**, 141-149 (2005).

320. Sutrave, P., Kelly, A.M. & Hughes, S.H. ski can cause selective growth of skeletal muscle in transgenic mice. *Genes Dev* **4**, 1462-1472 (1990).

321. Engert, J.C., Servaes, S., Sutrave, P., Hughes, S.H. & Rosenthal, N. Activation of a muscle-specific enhancer by the Ski proto-oncogene. *Nucleic Acids Res* **23**, 2988-2994 (1995).

322. Kobayashi, N. *et al.* c-Ski activates MyoD in the nucleus of myoblastic cells through suppression of histone deacetylases. *Genes Cells* **12**, 375-385 (2007).

323. Zhu, X. *et al.* 576 kb deletion in 1p36.33-p36.32 containing SKI is associated with limb malformation, congenital heart disease and epilepsy. *Gene* **528**, 352-355 (2013).

324. Schepers, D. *et al.* The SMAD-binding domain of SKI: a hotspot for de novo mutations causing Shprintzen-Goldberg syndrome. *Eur J Hum Genet* **23**, 224-228 (2015).

325. Carmignac, V. *et al.* In-frame mutations in exon 1 of SKI cause dominant Shprintzen-Goldberg syndrome. *Am J Hum Genet* **91**, 950-957 (2012).

326. Robinson, P.N. *et al.* Shprintzen-Goldberg syndrome: fourteen new patients and a clinical analysis. *Am J Med Genet A* **135**, 251-262 (2005).

327. Doyle, A.J. *et al.* Mutations in the TGF-beta repressor SKI cause Shprintzen-Goldberg syndrome with aortic aneurysm. *Nat Genet* **44**, 1249-1254 (2012).

328. Wang, J. *et al.* The mechanism of TGF-beta/miR-155/c-Ski regulates endothelial-mesenchymal transition in human coronary artery endothelial cells. *Biosci Rep* **37** (2017).

329. Li, J. *et al.* c-Ski inhibits the proliferation of vascular smooth muscle cells via suppressing Smad3 signaling but stimulating p38 pathway. *Cell Signal* **25**, 159-167 (2013).

330. Cunnington, R.H. *et al.* Antifibrotic properties of c-Ski and its regulation of cardiac myofibroblast phenotype and contractility. *American journal of physiology. Cell physiology* **300**, C176-186 (2011).

331. Cunnington, R.H. *et al.* The Ski-Zeb2-Meox2 pathway provides a novel mechanism for regulation of the cardiac myofibroblast phenotype. *J Cell Sci* **127**, 40-49 (2014).

332. Zeglinski, M.R. *et al.* TGFbeta1 regulates Scleraxis expression in primary cardiac myofibroblasts by a Smad-independent mechanism. *Am J Physiol Heart Circ Physiol* **310**, H239-249 (2016).

333. Landry, N. *et al.* Ski drives an acute increase in MMP-9 gene expression and release in primary cardiac myofibroblasts. *Physiol Rep* **6**, e13897 (2018).

334. Gupta, S.S. *et al.* Inhibition of autophagy inhibits the conversion of cardiac fibroblasts to cardiac myofibroblasts. *Oncotarget* **7**, 78516-78531 (2016).

335. Zeglinski, M.R. *et al.* Chronic expression of Ski induces apoptosis and represses autophagy in cardiac myofibroblasts. *Biochim Biophys Acta* **1863**, 1261-1268 (2016).

336. Rashidian, J. *et al.* Ski regulates Hippo and TAZ signaling to suppress breast cancer progression. *Sci Signal* **8**, ra14 (2015).

337. Shinagawa, T. *et al.* Increased susceptibility to tumorigenesis of ski-deficient heterozygous mice. *Oncogene* **20**, 8100-8108 (2001).

338. Caligaris, C. *et al.* Actin-cytoskeleton polymerization differentially controls the stability of Ski and SnoN co-repressors in normal but not in transformed hepatocytes. *Biochim Biophys Acta* **1850**, 1832-1841 (2015).

339. Kiss, H. *et al.* A novel gene containing LIM domains (LIMD1) is located within the common eliminated region 1 (C3CER1) in 3p21.3. *Hum Genet* **105**, 552-559 (1999).

340. Jarvinen, P.M. & Laiho, M. LIM-domain proteins in transforming growth factor beta-induced epithelial-to-mesenchymal transition and myofibroblast differentiation. *Cell Signal* **24**, 819-825 (2012).

341. Kadrmas, J.L. & Beckerle, M.C. The LIM domain: from the cytoskeleton to the nucleus. *Nat Rev Mol Cell Biol* **5**, 920-931 (2004).

342. Bach, I. The LIM domain: regulation by association. *Mech Dev* **91**, 5-17 (2000).

343. Foxler, D.E. *et al.* The LIMD1 protein bridges an association between the prolyl hydroxylases and VHL to repress HIF-1 activity. *Nat Cell Biol* **14**, 201-208 (2012).

344. Ibar, C. *et al.* Tension-dependent regulation of mammalian Hippo signaling through LIMD1. *J Cell Sci* **131** (2018).

345. Khurana, T., Khurana, B. & Noegel, A.A. LIM proteins: association with the actin cytoskeleton. *Protoplasma* **219**, 1-12 (2002).

346. Weiskirchen, R., Pino, J.D., Macalma, T., Bister, K. & Beckerle, M.C. The cysteine-rich protein family of highly related LIM domain proteins. *J Biol Chem* **270**, 28946-28954 (1995).

347. Velyvis, A. & Qin, J. LIM Domain and Its Binding to Target Proteins, in *Zinc Finger Proteins*. (eds. S. Iuchi & N. Kuldell) (Springer Nature, Boston, MA; 2005).

348.	Zheng, Q. & Zhao, Y. The diverse biofunctions of LIM domain proteins: determined by subcellular localization and protein-protein interaction. *Biol Cell* **99**, 489-502 (2007).

349.	Schmeichel, K.L. & Beckerle, M.C. The LIM domain is a modular protein-binding interface. *Cell* **79**, 211-219 (1994).

350.	Feuerstein, R., Wang, X., Song, D., Cooke, N.E. & Liebhaber, S.A. The LIM/double zinc-finger motif functions as a protein dimerization domain. *Proc Natl Acad Sci U S A* **91**, 10655-10659 (1994).

351.	Gill, G.N. The enigma of LIM domains. *Structure* **3**, 1285-1289 (1995).

352.	Das Thakur, M. *et al.* Ajuba LIM proteins are negative regulators of the Hippo signaling pathway. *Curr Biol* **20**, 657-662 (2010).

353.	Sharp, T.V. *et al.* LIM domains-containing protein 1 (LIMD1), a tumor suppressor encoded at chromosome 3p21.3, binds pRB and represses E2F-driven transcription. *Proc Natl Acad Sci U S A* **101**, 16531-16536 (2004).

354.	Schimizzi, G.V. & Longmore, G.D. Ajuba proteins. *Curr Biol* **25**, R445-446 (2015).

355.	Zhou, J. *et al.* LIMD1 phosphorylation in mitosis is required for mitotic progression and its tumor-suppressing activity. *FEBS J* **286**, 963-974 (2019).

356.	Huggins, C.J. & Andrulis, I.L. Cell cycle regulated phosphorylation of LIMD1 in cell lines and expression in human breast cancers. *Cancer Lett* **267**, 55-66 (2008).

357.	Luderer, H.F., Bai, S. & Longmore, G.D. The LIM protein LIMD1 influences osteoblast differentiation and function. *Exp Cell Res* **314**, 2884-2894 (2008).

358.	Ezzell, R.M., Goldmann, W.H., Wang, N., Parashurama, N. & Ingber, D.E. Vinculin promotes cell spreading by mechanically coupling integrins to the cytoskeleton. *Exp Cell Res* **231**, 14-26 (1997).

359.	Jagannathan, R. *et al.* AJUBA LIM Proteins Limit Hippo Activity in Proliferating Cells by Sequestering the Hippo Core Kinase Complex in the Cytosol. *Mol Cell Biol* **36**, 2526-2542 (2016).

360.	Rauskolb, C., Sun, S., Sun, G., Pan, Y. & Irvine, K.D. Cytoskeletal tension inhibits Hippo signaling through an Ajuba-Warts complex. *Cell* **158**, 143-156 (2014).

361.	Feng, Y. *et al.* The LIM protein, Limd1, regulates AP-1 activation through an interaction with Traf6 to influence osteoclast development. *J Biol Chem* **282**, 39-48 (2007).

362.	Itonaga, I. *et al.* Transforming growth factor-beta induces osteoclast formation in the absence of RANKL. *Bone* **34**, 57-64 (2004).

363.   Windak, R. *et al.* The AP-1 transcription factor c-Jun prevents stress-imposed maladaptive remodeling of the heart. *PLoS One* **8**, e73294 (2013).

364.   Mayank, A.K., Sharma, S., Deshwal, R.K. & Lal, S.K. LIMD1 antagonizes E2F1 activity and cell cycle progression by enhancing Rb function in cancer cells. *Cell Biol Int* **38**, 809-817 (2014).

365.   Sharp, T.V. *et al.* The chromosome 3p21.3-encoded gene, LIMD1, is a critical tumor suppressor involved in human lung cancer development. *Proc Natl Acad Sci U S A* **105**, 19932-19937 (2008).

366.   Sarkar, S. *et al.* Reduction of proliferation and induction of apoptosis are associated with shrinkage of head and neck squamous cell carcinoma due to neoadjuvant chemotherapy. *Asian Pac J Cancer Prev* **14**, 6419-6425 (2013).

367.   Huggins, C.J., Gill, M. & Andrulis, I.L. Identification of rare variants in the hLIMD1 gene in breast cancer. *Cancer Genet Cytogenet* **178**, 36-41 (2007).

368.   Senchenko, V.N. *et al.* Discovery of frequent homozygous deletions in chromosome 3p21.3 LUCA and AP20 regions in renal, lung and breast carcinomas. *Oncogene* **23**, 5719-5728 (2004).

369.   Codelia, V.A., Sun, G. & Irvine, K.D. Regulation of YAP by mechanical strain through Jnk and Hippo signaling. *Curr Biol* **24**, 2012-2017 (2014).

370.   Sun, G. & Irvine, K.D. Ajuba family proteins link JNK to Hippo signaling. *Sci Signal* **6**, ra81 (2013).

371.   Prevention, C.f.D.C.a. (Centers for Disease Control and Prevention (CDC), 2019).

372.   Mozaffarian, D. *et al.* Heart disease and stroke statistics--2015 update: a report from the American Heart Association. *Circulation* **131**, e29-322 (2015).

373.   Ezekowtiz, J. *et al.* (Heart & Stroke Foundation of Canada, 2017).

374.   Goldsmith, E.C. *et al.* Organization of fibroblasts in the heart. *Developmental dynamics : an official publication of the American Association of Anatomists* **230**, 787-794 (2004).

375.   Molkentin, J.D. *et al.* Fibroblast-Specific Genetic Manipulation of p38 Mitogen-Activated Protein Kinase In Vivo Reveals Its Central Regulatory Role in Fibrosis. *Circulation* **136**, 549-561 (2017).

376.   Valiente-Alandi, I. *et al.* Inhibiting Fibronectin Attenuates Fibrosis and Improves Cardiac Function in a Model of Heart Failure. *Circulation* (2018).

377.   Cheng, F. *et al.* Vimentin coordinates fibroblast proliferation and keratinocyte differentiation in wound healing via TGF-beta-Slug signaling. *Proceedings of the*

National Academy of Sciences of the United States of America **113**, E4320-4327 (2016).

378. Souders, C.A., Bowers, S.L. & Baudino, T.A. Cardiac fibroblast: the renaissance cell. *Circulation research* **105**, 1164-1176 (2009).

379. Lane, E.B., Hogan, B.L., Kurkinen, M. & Garrels, J.I. Co-expression of vimentin and cytokeratins in parietal endoderm cells of early mouse embryo. *Nature* **303**, 701-704 (1983).

380. Hudon-David, F., Bouzeghrane, F., Couture, P. & Thibault, G. Thy-1 expression by cardiac fibroblasts: lack of association with myofibroblast contractile markers. *Journal of molecular and cellular cardiology* **42**, 991-1000 (2007).

381. Gago-Lopez, N. *et al.* THY-1 receptor expression differentiates cardiosphere-derived cells with divergent cardiogenic differentiation potential. *Stem cell reports* **2**, 576-591 (2014).

382. Chang, Y. *et al.* CD90(+) cardiac fibroblasts reduce fibrosis of acute myocardial injury in rats. *The international journal of biochemistry & cell biology* **96**, 20-28 (2018).

383. Black, F.M. *et al.* The vascular smooth muscle alpha-actin gene is reactivated during cardiac hypertrophy provoked by load. *The Journal of clinical investigation* **88**, 1581-1588 (1991).

384. Tomasek, J.J., Gabbiani, G., Hinz, B., Chaponnier, C. & Brown, R.A. Myofibroblasts and mechano-regulation of connective tissue remodelling. *Nature reviews. Molecular cell biology* **3**, 349-363 (2002).

385. Dugina, V., Fontao, L., Chaponnier, C., Vasiliev, J. & Gabbiani, G. Focal adhesion features during myofibroblastic differentiation are controlled by intracellular and extracellular factors. *Journal of cell science* **114**, 3285-3296 (2001).

386. Thannickal, V.J. *et al.* Myofibroblast differentiation by transforming growth factor-beta1 is dependent on cell adhesion and integrin signaling via focal adhesion kinase. *The Journal of biological chemistry* **278**, 12384-12389 (2003).

387. Zhao, S. *et al.* Periostin expression is upregulated and associated with myocardial fibrosis in human failing hearts. *Journal of cardiology* **63**, 373-378 (2014).

388. Snider, P. *et al.* Origin of cardiac fibroblasts and the role of periostin. *Circulation research* **105**, 934-947 (2009).

389. Zhang, K., Rekhter, M.D., Gordon, D. & Phan, S.H. Myofibroblasts and their role in lung collagen gene expression during pulmonary fibrosis. A combined immunohistochemical and in situ hybridization study. *The American journal of pathology* **145**, 114-125 (1994).

390. Klingberg, F., Hinz, B. & White, E.S. The myofibroblast matrix: implications for tissue repair and fibrosis. *The Journal of pathology* **229**, 298-309 (2013).

391. Serini, G. *et al.* The fibronectin domain ED-A is crucial for myofibroblastic phenotype induction by transforming growth factor-beta1. *The Journal of cell biology* **142**, 873-881 (1998).

392. Klingberg, F. *et al.* The fibronectin ED-A domain enhances recruitment of latent TGF-beta-binding protein-1 to the fibroblast matrix. *Journal of cell science* **131** (2018).

393. Schelbert, E.B. *et al.* Myocardial Fibrosis Quantified by Extracellular Volume Is Associated With Subsequent Hospitalization for Heart Failure, Death, or Both Across the Spectrum of Ejection Fraction and Heart Failure Stage. *J Am Heart Assoc* **4** (2015).

394. Ahmad, T. *et al.* Biomarkers of myocardial stress and fibrosis as predictors of mode of death in patients with chronic heart failure. *JACC. Heart failure* **2**, 260-268 (2014).

395. Letterio, J.J. & Roberts, A.B. Regulation of immune responses by TGF-beta. *Annual review of immunology* **16**, 137-161 (1998).

396. Bonner, J.C. Regulation of PDGF and its receptors in fibrotic diseases. *Cytokine & growth factor reviews* **15**, 255-273 (2004).

397. Ali, S.R. *et al.* Developmental heterogeneity of cardiac fibroblasts does not predict pathological proliferation and activation. *Circ Res* **115**, 625-635 (2014).

398. Lee, A.A., Dillmann, W.H., McCulloch, A.D. & Villarreal, F.J. Angiotensin II stimulates the autocrine production of transforming growth factor-beta 1 in adult rat cardiac fibroblasts. *Journal of molecular and cellular cardiology* **27**, 2347-2357 (1995).

399. Bai, J. *et al.* Metformin inhibits angiotensin II-induced differentiation of cardiac fibroblasts into myofibroblasts. *PloS One* **8**, e72120 (2013).

400. Hutchinson, K.R., Lord, C.K., West, T.A. & Stewart, J.A., Jr. Cardiac fibroblast-dependent extracellular matrix accumulation is associated with diastolic stiffness in type 2 diabetes. *PloS One* **8**, e72080 (2013).

401. Singh, V.P., Baker, K.M. & Kumar, R. Activation of the intracellular renin-angiotensin system in cardiac fibroblasts by high glucose: role in extracellular matrix production. *American journal of physiology. Heart and circulatory physiology* **294**, H1675-1684 (2008).

402. Xie, Z., Singh, M. & Singh, K. ERK1/2 and JNKs, but not p38 kinase, are involved in reactive oxygen species-mediated induction of osteopontin gene expression by angiotensin II and interleukin-1beta in adult rat cardiac fibroblasts. *Journal of cellular physiology* **198**, 399-407 (2004).

403. Sano, M. *et al.* ERK and p38 MAPK, but not NF-kappaB, are critically involved in reactive oxygen species-mediated induction of IL-6 by angiotensin II in cardiac fibroblasts. *Circulation research* **89**, 661-669 (2001).

404. Sarrazy, V. *et al.* Integrins alphavbeta5 and alphavbeta3 promote latent TGF-beta1 activation by human cardiac fibroblast contraction. *Cardiovascular research* **102**, 407-417 (2014).

405. Wipff, P.J., Rifkin, D.B., Meister, J.J. & Hinz, B. Myofibroblast contraction activates latent TGF-beta1 from the extracellular matrix. *The Journal of cell biology* **179**, 1311-1323 (2007).

406. Fu, X. *et al.* Specialized fibroblast differentiated states underlie scar formation in the infarcted mouse heart. *The Journal of clinical investigation* **128**, 2127-2143 (2018).

407. McKee, C.T., Last, J.A., Russell, P. & Murphy, C.J. Indentation versus tensile measurements of Young's modulus for soft biological tissues. *Tissue engineering. Part B, Reviews* **17**, 155-164 (2011).

408. Wells, R.G. Tissue mechanics and fibrosis. *Biochimica et biophysica acta* **1832**, 884-890 (2013).

409. van Putten, S., Shafieyan, Y. & Hinz, B. Mechanical control of cardiac myofibroblasts. *J Mol Cell Cardiol* **93**, 133-142 (2016).

410. Hinz, B. The myofibroblast: paradigm for a mechanically active cell. *Journal of biomechanics* **43**, 146-155 (2010).

411. Ackers-Johnson, M. *et al.* A Simplified, Langendorff-Free Method for Concomitant Isolation of Viable Cardiac Myocytes and Nonmyocytes From the Adult Mouse Heart. *Circ Res* **119**, 909-920 (2016).

412. Livak, K.J. & Schmittgen, T.D. Analysis of relative gene expression data using real-time quantitative PCR and the 2(-Delta Delta C(T)) Method. *Methods* **25**, 402-408 (2001).

413. Clement, S. *et al.* Expression and function of alpha-smooth muscle actin during embryonic-stem-cell-derived cardiomyocyte differentiation. *J Cell Sci* **120**, 229-238 (2007).

414. Li, Z. *et al.* Transforming growth factor-beta and substrate stiffness regulate portal fibroblast activation in culture. *Hepatology* **46**, 1246-1256 (2007).

415. Cunnington, R.H. *et al.* Antifibrotic properties of c-Ski and its regulation of cardiac myofibroblast phenotype and contractility. *American journal of physiology. Cell physiology* **300**, C176-186 (2011).

416.   Nagalingam, R.S. *et al.* Regulation of cardiac fibroblast MMP2 gene expression by scleraxis. *J Mol Cell Cardiol* **120**, 64-73 (2018).

417.   Chen, M.C. *et al.* Dedifferentiation of atrial cardiomyocytes in cardiac valve disease: unrelated to atrial fibrillation. *Cardiovascular pathology : the official journal of the Society for Cardiovascular Pathology* **17**, 156-165 (2008).

418.   Hinz, B., Celetta, G., Tomasek, J.J., Gabbiani, G. & Chaponnier, C. Alpha-Smooth Muscle Actin Expression Upregulates Fibroblast Contractile Activity. *Mol Biol Cell* **12**, 2730-2741 (2001).

419.   Talele, N.P., Fradette, J., Davies, J.E., Kapus, A. & Hinz, B. Expression of alpha-Smooth Muscle Actin Determines the Fate of Mesenchymal Stromal Cells. *Stem cell reports* **4**, 1016-1030 (2015).

420.   Ghosh, A.K., Quaggin, S.E. & Vaughan, D.E. Molecular basis of organ fibrosis: potential therapeutic approaches. *Exp Biol Med (Maywood)* **238**, 461-481 (2013).

421.   Karsdal, M.A. *et al.* The good and the bad collagens of fibrosis - Their role in signaling and organ function. *Adv Drug Deliv Rev* **121**, 43-56 (2017).

422.   Bhandary, B. *et al.* Cardiac Fibrosis in Proteotoxic Cardiac Disease is Dependent Upon Myofibroblast TGF -beta Signaling. *J Am Heart Assoc* **7**, e010013 (2018).

423.   Chaganti, R.S. *et al.* The cellular homologue of the transforming gene of SKV avian retrovirus maps to human chromosome region 1q22----q24. *Cytogenetics and cell genetics* **43**, 181-186 (1986).

424.   Ueki, N. & Hayman, M.J. Signal-dependent N-CoR requirement for repression by the Ski oncoprotein. *The Journal of biological chemistry* **278**, 24858-24864 (2003).

425.   Chen, W. *et al.* Competition between Ski and CREB-binding protein for binding to Smad proteins in transforming growth factor-beta signaling. *The Journal of biological chemistry* **282**, 11365-11376 (2007).

426.   Cunnington, R.H. *et al.* Antifibrotic properties of c-Ski and its regulation of cardiac myofibroblast phenotype and contractility. *American journal of physiology. Cell physiology* **300**, C176-186 (2011).

427.   Kaan, H.Y.K. *et al.* Crystal structure of TAZ-TEAD complex reveals a distinct interaction mode from that of YAP-TEAD complex. *Sci Rep* **7**, 2035 (2017).

428.   Bertero, T. *et al.* Matrix Remodeling Promotes Pulmonary Hypertension through Feedback Mechanoactivation of the YAP/TAZ-miR-130/301 Circuit. *Cell Rep* **13**, 1016-1032 (2015).

429.   Noguchi, S. *et al.* TAZ contributes to pulmonary fibrosis by activating profibrotic functions of lung fibroblasts. *Sci Rep* **7**, 42595 (2017).

430. Liu, F. *et al.* Feedback amplification of fibrosis through matrix stiffening and COX-2 suppression. *J Cell Biol* **190**, 693-706 (2010).

431. Dixon, I.M., Lee, S.L. & Dhalla, N.S. Nitrendipine binding in congestive heart failure due to myocardial infarction. *Circ Res* **66**, 782-788 (1990).

432. Zheng, L., Baumann, U. & Reymond, J.L. An efficient one-step site-directed and site-saturation mutagenesis protocol. *Nucleic Acids Res* **32**, e115 (2004).

433. Schneider, C.A., Rasband, W.S. & Eliceiri, K.W. NIH Image to ImageJ: 25 years of image analysis. *Nat Methods* **9**, 671-675 (2012).

434. Santiago, J.J. *et al.* High molecular weight fibroblast growth factor-2 in the human heart is a potential target for prevention of cardiac remodeling. *PLoS One* **9**, e97281 (2014).

435. Teo, G. *et al.* SAINTexpress: improvements and additional features in Significance Analysis of INTeractome software. *J Proteomics* **100**, 37-43 (2014).

436. Mellacheruvu, D. *et al.* The CRAPome: a contaminant repository for affinity purification-mass spectrometry data. *Nat Methods* **10**, 730-736 (2013).

437. Kelder, T. *et al.* Mining biological pathways using WikiPathways web services. *PLoS One* **4**, e6447 (2009).

438. Lei, Q.Y. *et al.* TAZ promotes cell proliferation and epithelial-mesenchymal transition and is inhibited by the hippo pathway. *Mol Cell Biol* **28**, 2426-2436 (2008).

439. Dieffenbach, P.B. *et al.* Arterial stiffness induces remodeling phenotypes in pulmonary artery smooth muscle cells via YAP/TAZ-mediated repression of cyclooxygenase-2. *Am J Physiol Lung Cell Mol Physiol* **313**, L628-L647 (2017).

440. Shimomura, T. *et al.* The PDZ-binding motif of Yes-associated protein is required for its co-activation of TEAD-mediated CTGF transcription and oncogenic cell transforming activity. *Biochem Biophys Res Commun* **443**, 917-923 (2014).

441. Lanier, M.H., McConnell, P. & Cooper, J.A. Cell Migration and Invadopodia Formation Require a Membrane-binding Domain of CARMIL2. *J Biol Chem* **291**, 1076-1091 (2016).

442. Zhang, X. *et al.* Palladin is a novel microtubule-associated protein responsible for spindle orientation. *Sci Rep* **7**, 11806 (2017).

443. Pizarro-Cerda, J., Chorev, D.S., Geiger, B. & Cossart, P. The Diverse Family of Arp2/3 Complexes. *Trends Cell Biol* **27**, 93-100 (2017).

444. Bu, H. *et al.* [Establishment and preliminary mechanism study of the zebrafish strain of KIAA0196: A candidate pathogenic gene for heart development]. *Zhong Nan Da Xue Xue Bao Yi Xue Ban* **44**, 968-975 (2019).

445. Lignitto, L. *et al.* Proteolysis of MOB1 by the ubiquitin ligase praja2 attenuates Hippo signalling and supports glioblastoma growth. *Nature communications* **4**, 1822 (2013).

446. Liang, X.H. *et al.* LIM protein JUB promotes epithelial-mesenchymal transition in colorectal cancer. *Cancer Sci* **105**, 660-666 (2014).

447. Zeglinski, M.R. *et al.* Chronic expression of Ski induces apoptosis and represses autophagy in cardiac myofibroblasts. *Biochim Biophys Acta* **1863**, 1261-1268 (2016).

448. Anorga, S. *et al.* Deregulation of Hippo-TAZ pathway during renal injury confers a fibrotic maladaptive phenotype. *FASEB J* **32**, 2644-2657 (2018).

449. Miranda, M.Z. *et al.* TGF-beta1 regulates the expression and transcriptional activity of TAZ protein via a Smad3-independent, myocardin-related transcription factor-mediated mechanism. *The Journal of biological chemistry* **292**, 14902-14920 (2017).

450. Elbediwy, A. *et al.* Enigma proteins regulate YAP mechanotransduction. *J Cell Sci* **131** (2018).

451. Bai, S.W. *et al.* Identification and characterization of a set of conserved and new regulators of cytoskeletal organization, cell morphology and migration. *BMC Biol* **9**, 54 (2011).

452. Jorgenson, A.J. *et al.* TAZ activation drives fibroblast spheroid growth, expression of profibrotic paracrine signals, and context-dependent ECM gene expression. *Am J Physiol Cell Physiol* **312**, C277-C285 (2017).

453. Bessler, N.M. & Vam Study Writing, C. Verteporfin therapy in age-related macular degeneration (VAM): an open-label multicenter photodynamic therapy study of 4,435 patients. *Retina* **24**, 512-520 (2004).

454. Liu-Chittenden, Y. *et al.* Genetic and pharmacological disruption of the TEAD-YAP complex suppresses the oncogenic activity of YAP. *Genes Dev* **26**, 1300-1305 (2012).

455. Granville, D.J. *et al.* Nuclear factor-kappaB activation by the photochemotherapeutic agent verteporfin. *Blood* **95**, 256-262 (2000).

456. Kramarenko, G.G., Wilke, W.W., Dayal, D., Buettner, G.R. & Schafer, F.Q. Ascorbate enhances the toxicity of the photodynamic action of Verteporfin in HL-60 cells. *Free Radic Biol Med* **40**, 1615-1627 (2006).

457. Scott, L.J. & Goa, K.L. Verteporfin. *Drugs Aging* **16**, 139-146; discussion 147-138 (2000).

458. Belzacq, A.S. *et al.* Apoptosis induction by the photosensitizer verteporfin: identification of mitochondrial adenine nucleotide translocator as a critical target. *Cancer Res* **61**, 1260-1264 (2001).

459. Wu, X., Edn. C07D 249/08. (ed. W.I.P. Organization) (United States of America; 2017).

460. Barth, M., Contal, S., Montalbetti, C. & Spitzer, L., Edn. C07D 417/12 (2006.01), A61K 31/428 (2006.01), C07D 275/06 (2006.01), A61P 35/00 (2006.01). (ed. W.I.P. Organization) (2017).

461. Gobbi, G. *et al.* The Hippo pathway modulates resistance to BET proteins inhibitors in lung cancer cells. *Oncogene* **38**, 6801-6817 (2019).

462. Kurimchak, A.M. *et al.* Resistance to BET Bromodomain Inhibitors Is Mediated by Kinome Reprogramming in Ovarian Cancer. *Cell Rep* **16**, 1273-1286 (2016).

463. Pervaiz, M., Mishra, P. & Gunther, S. Bromodomain Drug Discovery - the Past, the Present, and the Future. *Chem Rec* **18**, 1808-1817 (2018).

464. Vazquez-Victorio, G. *et al.* Novel regulation of Ski protein stability and endosomal sorting by actin cytoskeleton dynamics in hepatocytes. *J Biol Chem* **290**, 4487-4499 (2015).

465. Pollard, T.D. Regulation of actin filament assembly by Arp2/3 complex and formins. *Annu Rev Biophys Biomol Struct* **36**, 451-477 (2007).

466. Parast, M.M. & Otey, C.A. Characterization of palladin, a novel protein localized to stress fibers and cell adhesions. *J Cell Biol* **150**, 643-656 (2000).

467. Hirota, T. *et al.* Aurora-A and an interacting activator, the LIM protein Ajuba, are required for mitotic commitment in human cells. *Cell* **114**, 585-598 (2003).

468. Sabino, D., Brown, N.H. & Basto, R. Drosophila Ajuba is not an Aurora-A activator but is required to maintain Aurora-A at the centrosome. *J Cell Sci* **124**, 1156-1166 (2011).

469. Schmidt, T. *et al.* ProteomicsDB. *Nucleic Acids Res* **46**, D1271-D1281 (2018).

470. Li, J., Zhao, L., He, X., Yang, T. & Yang, K. MiR-21 inhibits c-Ski signaling to promote the proliferation of rat vascular smooth muscle cells. *Cell Signal* **26**, 724-729 (2014).

471. Yuan, J. *et al.* Mir-21 Promotes Cardiac Fibrosis After Myocardial Infarction Via Targeting Smad7. *Cell Physiol Biochem* **42**, 2207-2219 (2017).

472. Watanabe, K. *et al.* The association between microRNA-21 and hypertension-induced cardiac remodeling. *PLoS One* **15**, e0226053 (2020).

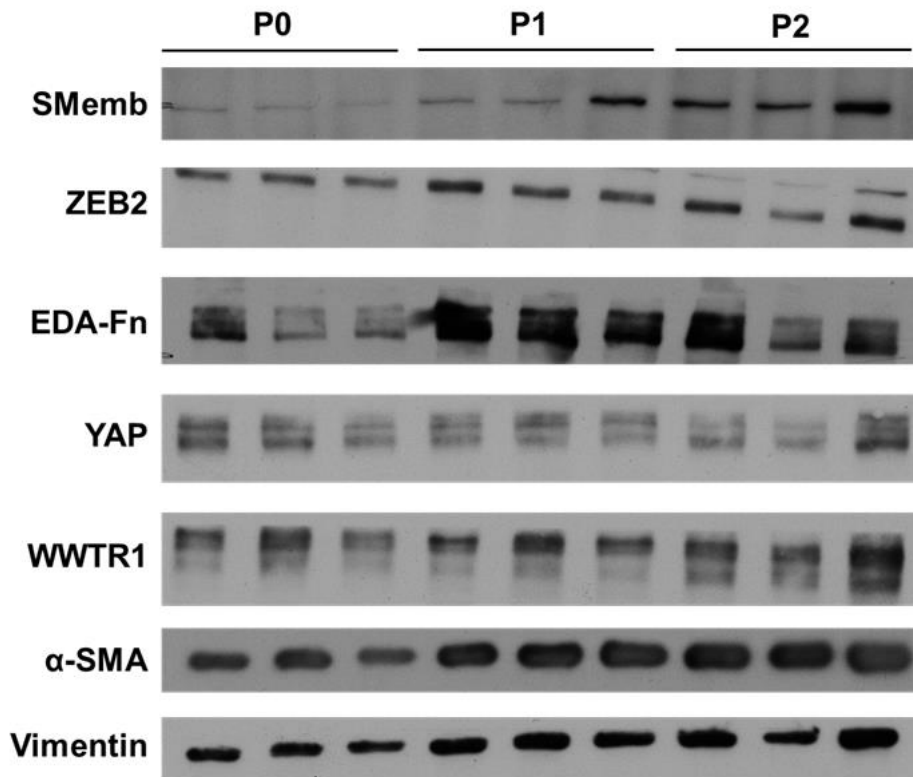## APPENDICES

Appendix A

Figure A.1: Protein expression pattern of unpassaged and passaged primary cardiac fibroblasts on 5 kPa compressible plates coated with fibronectin. P0 rat cardiac fibroblasts were seeded onto compressible plates coated with 2 ug/cm^2 human plasma fibronectin in F10 cell culture medium supplemented with 10% FBS. Cells were cultured for 48 hours prior to passaging (P1) onto new 5 kPa plates; this was repeated once to P2 and protein was harvested for immunoblotting. Vimentin was used as an endogenous phenotype control. Data shown is of n = 3 independent biological replicates. *ZEB2, Zinc Finger E-box Binding homeobox 2.*
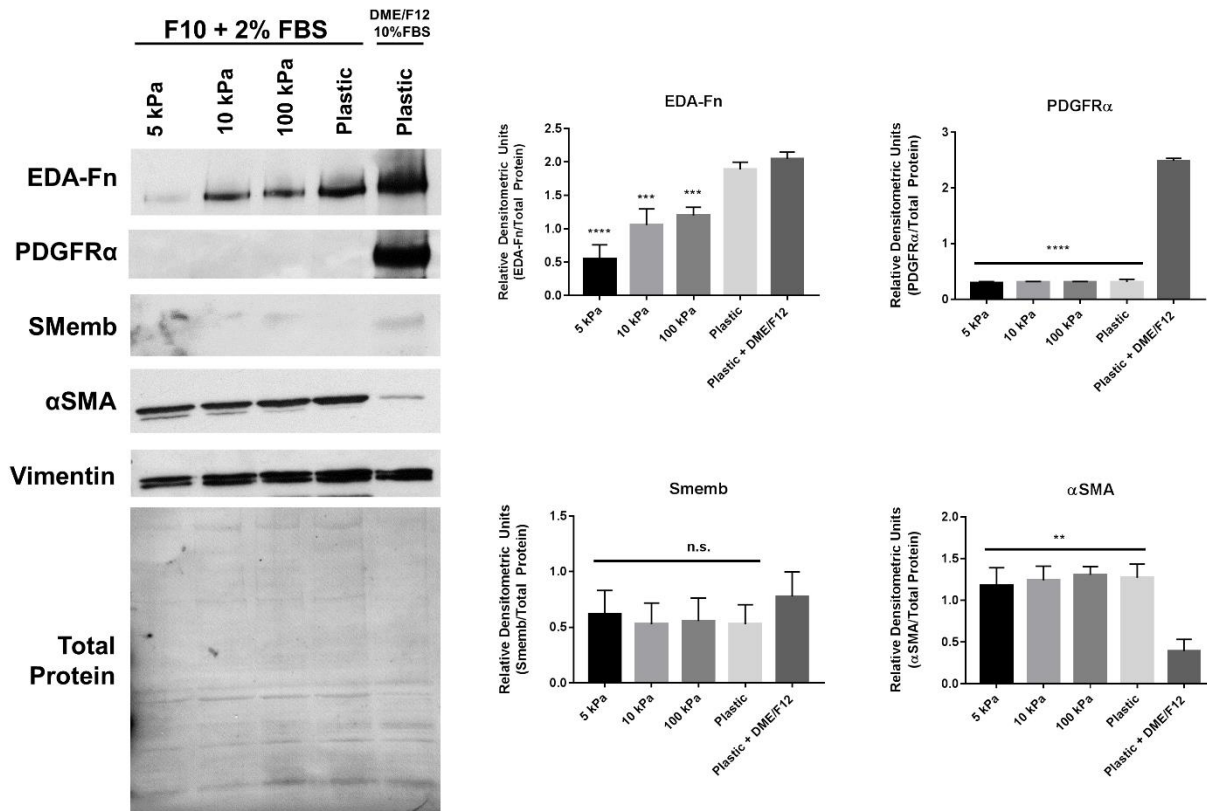
Figure A.2. Myofibroblast marker expression in mouse primary cardiac fibroblasts after 10 days in culture. Mouse primary cardiac fibroblasts were isolated from 8-12-week-old male C57BL/6 mice and plated on culture substrata of varying elastic moduli. One non-elastic plastic plate per replicate remained in DMEM/F12 + 10% FBS for the duration of the study as a comparative control, while the remaining plates were cultured in F10 + 2% FBS + ITS from 3 days post-isolation onward. Protein from unpassaged primary cardiac fibroblasts was harvested 10 days after plating, or once they reached 40-50% confluency. Vimentin expression was used as a pan-phenotypic control, and protein expression was normalized to total protein loading. n.s., not significant; **$P < 0.01$, ***$P < 0.005$, ****$P < 0.001$, when compared to cells cultured on stiff plastic in DMEM/F12 + 10% FBS.
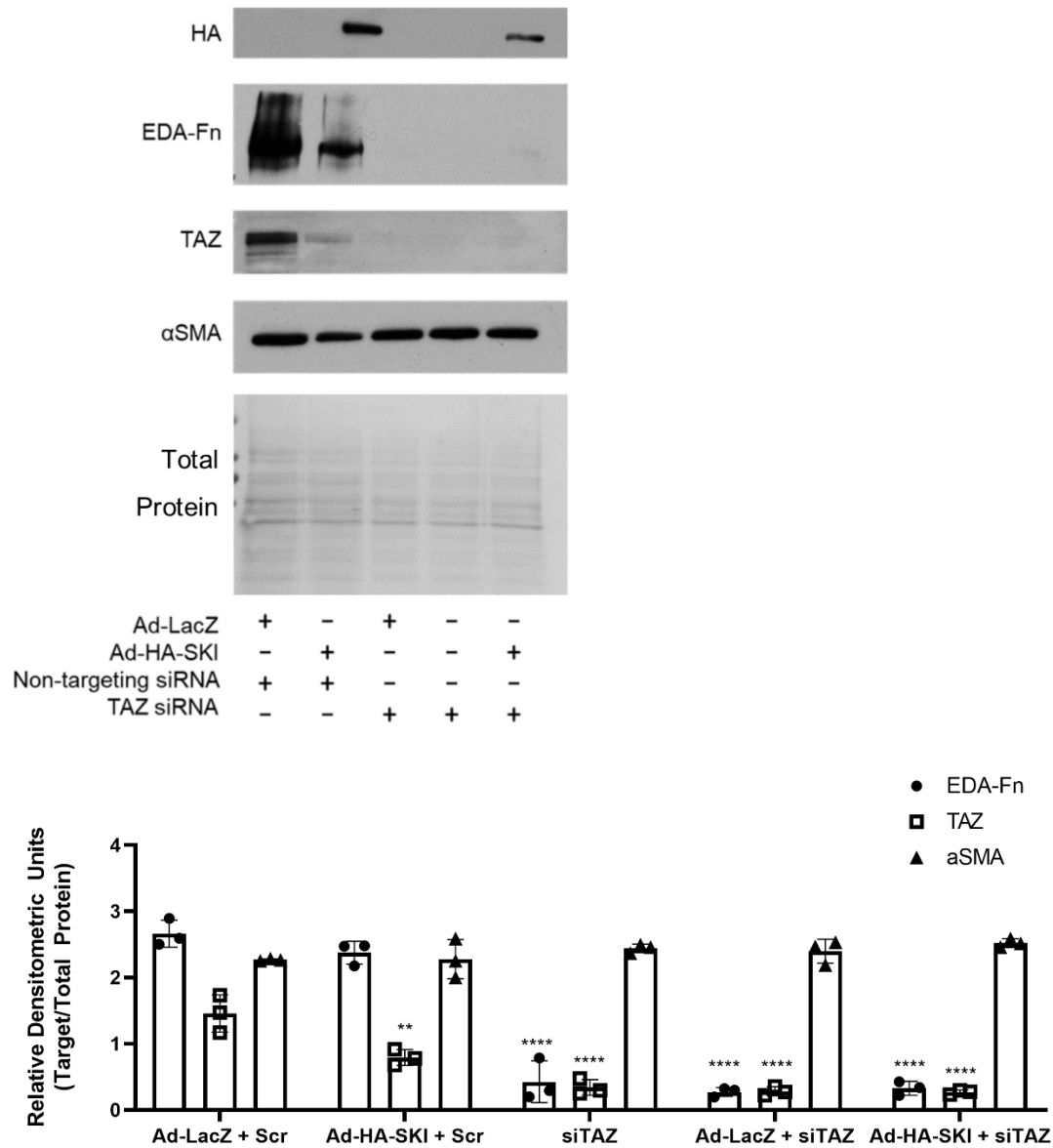
Appendix B

Figure B.1: *Taz* knockdown eliminates expression of EDA-Fn in primary cardiac myofibroblasts. Primary rat cardiac myofibroblasts (P1, cultured on plastic) were treated with 50 nM siRNA pools targeting *Taz* or non-targeting control for 24 hours, followed by infection with Ad-HA-SKI for another 36 hours. Whole cell lysates were probed for myofibroblast markers, EDA-Fn and αSMA by immunoblotting. Data displayed as the mean ± SD, and is representative of n=3 biological replicates. **P<0.01, ***P<0.001, when compared to Ad-LacZ + Scr controls.
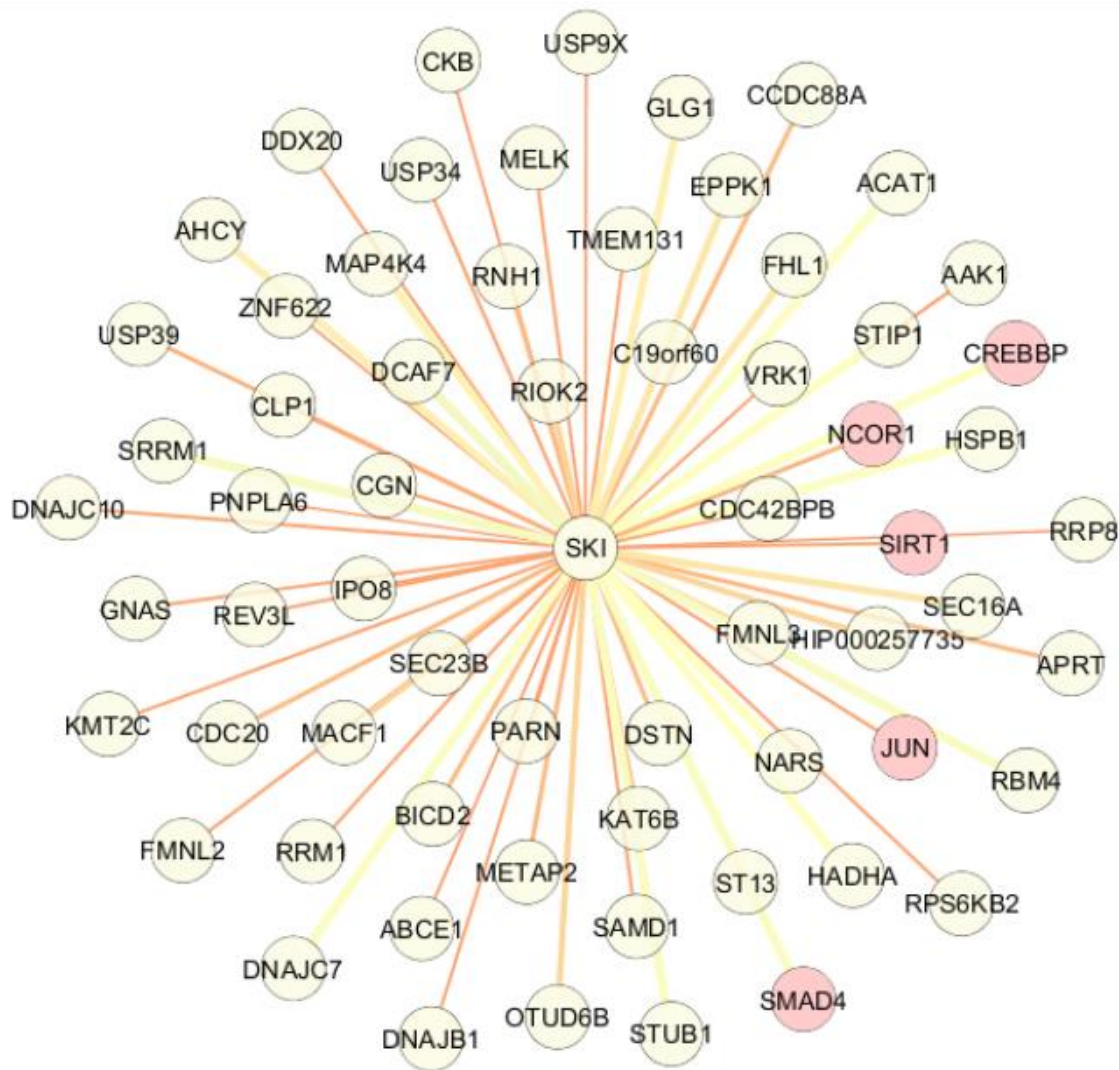
Appendix C

Figure C.1: The SKI interactome in HEK293A isolated from cells. Whole cells lysates from HEK 293A cells overexpressing BioID2-SKI were subject to streptavidin-mediated affinity capture of biotinylated proteins, which were then identified by Orbitrap™ mass spectrometry. Potential interactors were scored using the SAINT express algorithm, and visualized using Cytoscape. Nodes labelled in red indicate known (i.e. published) SKI interactors; edge thickness indicates fold-change enrichment compared to untreated controls. Graphic was generated using n = 2 biological replicates from two different cell passages.
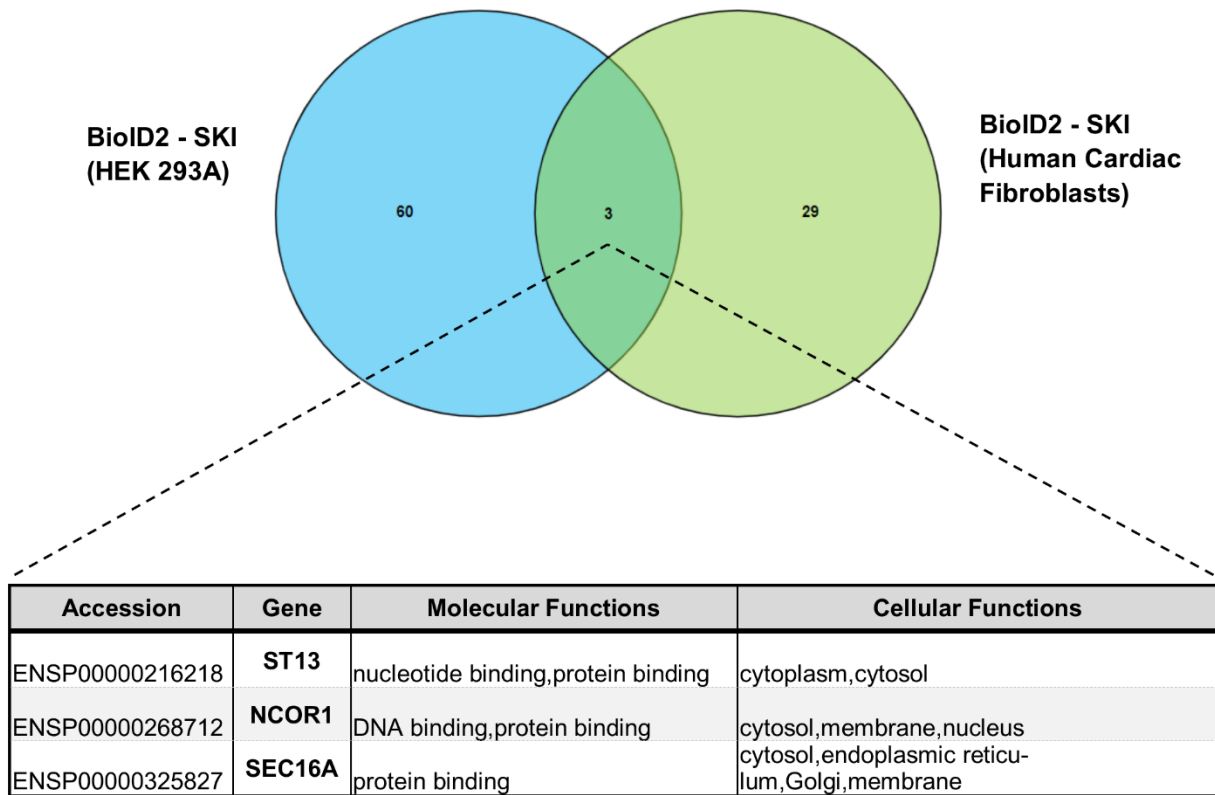
Appendix C

Accession	Gene	Molecular Functions	Cellular Functions
ENSP00000216218	**ST13**	nucleotide binding,protein binding	cytoplasm,cytosol
ENSP00000268712	**NCOR1**	DNA binding,protein binding	cytosol,membrane,nucleus
ENSP00000325827	**SEC16A**	protein binding	cytosol,endoplasmic reticulum,Golgi,membrane

Figure C.2: Overlap analysis of the SKI interactomes identified in HEK 293A cells *vs.* primary human cardiac fibroblasts. The SKI interactome in immortalized HEK 293A cells is two-fold greater than in primary human cardiac fibroblasts. Three candidates were similarly identified between the two interactomes: Suppression of Tumorigenicity 13 (ST13), Nuclear receptor Co-Repressor 1 (NCoR1), and Protein transport protein SEC16A.
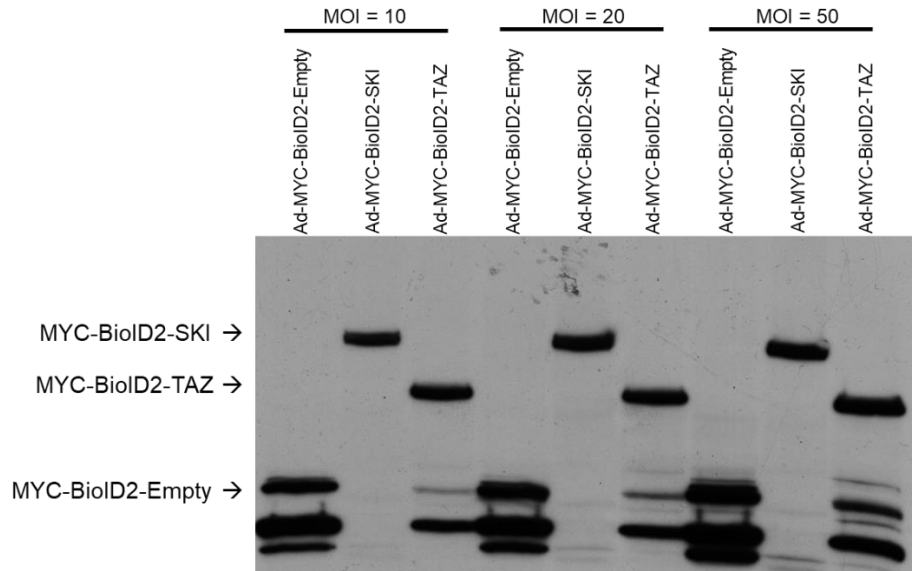
Appendix D

Figure D.1: Validation of BioID2 adenoviral constructs in Cos7 cells. Titration of adenoviral constructs containing the MYC-BioID2 domain alone, or fused to human SKI or TAZ, was performed by infecting Cos7 cells at various MOI. Whole cell lysates were probed for MYC to detect each fusion protein.
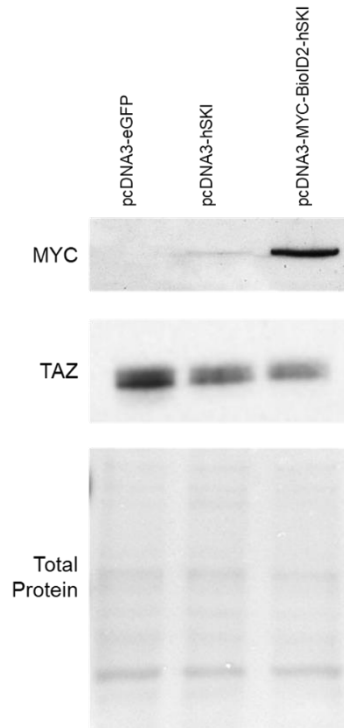

Figure D.2: Fusing the BirA* domain onto the N-terminus of human SKI does not affect its downstream effects on TAZ, *in vitro*. NIH-3T3 cells were transfected with pcDNA3 vectors containing eGFP, human SKI, or MYC-BioID2-SKI using Polyplus JetPRIME reagent and 1.0 µg DNA per well (6-well dish). Cell lysates were isolated after 48 hours of transfection, and probed for TAZ by Western blot.

Appendix E

Table E.1. Fold-Change Enrichment and SAINT scores for potential SKI interactors in primary human cardiac myofibroblasts

BAIT	PREY	PROTID	FOLD_CHANGE	SAINT_SCORE
SKI	DDX24	DDX24	21.84	0.99
SKI	PALLD	PALLD	16.94	1
SKI	PJA2	PJA2	8.61	1
SKI	TXNL1	TXNL1	7.69	1
SKI	SPRR1B	SPRR1B	3.69	0.5
SKI	TGM1	TGM1	3.43	0.5
SKI	WASHC5	WASHC5	5.68	0.96
SKI	SUMO2	SUMO2	2.86	0.48
SKI	BLMH	BLMH	2.86	0.5
SKI	NCOR1	NCOR1	4.56	0.32
SKI	CARMIL2	CARMIL2	4.56	0.97
SKI	HMGA1	HMGA1	4.46	0.96
SKI	S100A7	S100A7	4.36	0.96
SKI	LUC7L3	LUC7L3	3.72	0.9
SKI	NCCRP1	NCCRP1	2.53	0.5
SKI	SERPINB3	SERPINB3	2.53	0.5
SKI	POF1B	POF1B	2.53	0.5
SKI	UTP23	UTP23	3.57	0.49
SKI	VWCE	VWCE	3.57	0.49
SKI	ST13	ST13	3.57	0.49
SKI	STAC3	STAC3	3.56	0.49
SKI	SRSF2	SRSF2	2.51	0.47
SKI	PRMT3	PRMT3	2.51	0.5
SKI	LIMD1	LIMD1	3.45	0.52
SKI	MAGED1	MAGED1	3.34	0.75
SKI	DNAJB6	DNAJB6	3.31	0.91
SKI	RFWD3	RFWD3	3.3	0.96
SKI	ZCCHC17	ZCCHC17	3.28	0.9
SKI	PRPF38B	PRPF38B	2.83	0.61
SKI	SFSWAP	SFSWAP	3.18	0.58
SKI	SEC16A	SEC16A	3.02	0.56
SKI	LYAR	LYAR	3.08	0.9

Appendix E

Table E.2. Fold-Change Enrichment and SAINT scores for potential TAZ interactors in primary human cardiac myofibroblasts

BAIT	PREY	PROTID	FOLD_CHANGE	SAINT_SCORE
WWTR1	AMOTL2	AMOTL2	57	1
WWTR1	CGN	CGN	37.43	1
WWTR1	LATS2	LATS2	26.95	1
WWTR1	PTPN14	PTPN14	22.86	1
WWTR1	PALLD	PALLD	20.65	1
WWTR1	TP53BP2	TP53BP2	13.29	0.89
WWTR1	MPDZ	MPDZ	12.11	1
WWTR1	NCOA3	NCOA3	10.56	1
WWTR1	PDLIM7	PDLIM7	9.53	1
WWTR1	NCKAP5L	NCKAP5L	9.2	1
WWTR1	ZNF185	ZNF185	8.17	1
WWTR1	USP53	USP53	8.1	1
WWTR1	SNW1	SNW1	7.83	0.44
WWTR1	GTDC1	GTDC1	7.83	1
WWTR1	SYNPO2	SYNPO2	7.83	1
WWTR1	SORBS2	SORBS2	7.64	1
WWTR1	TNRC6A	TNRC6A	6.46	1
WWTR1	CC2D1A	CC2D1A	6.46	0.96
WWTR1	NAV3	NAV3	6.46	1
WWTR1	S100A7	S100A7	6.41	1
WWTR1	LMO7	LMO7	5.71	0.99
WWTR1	TXNL1	TXNL1	5.19	1
WWTR1	NUP98	NUP98	5.1	0.94
WWTR1	RUSC2	RUSC2	5.1	1
WWTR1	TEAD3	TEAD3	5.1	1
WWTR1	CSNK1A1	CSNK1A1	4.96	1
WWTR1	ADAMTS1	ADAMTS1	4.93	0.99
WWTR1	TJP1	TJP1	4.4	0.98
WWTR1	IGFBP7	IGFBP7	4.29	0.98
WWTR1	HMGA1	HMGA1	4.11	0.99
WWTR1	KIAA0196	KIAA0196	3.97	0.98
WWTR1	SNAPC4	SNAPC4	3.91	0.99
WWTR1	KBTBD3	KBTBD3	3.85	0.99
WWTR1	PARD3B	PARD3B	3.85	0.99
WWTR1	TJP2	TJP2	3.8	0.96
WWTR1	UTP23	UTP23	3.73	0.97
WWTR1	ABAT	ABAT	3.73	0.97

BAIT	PREY	PROTID	FOLD_CHANGE	SAINT_SCORE
WWTR1	NCOR2	NCOR2	3.73	0.97
WWTR1	TUFT1	TUFT1	3.73	0.97
WWTR1	RLTPR	RLTPR	3.73	0.97
WWTR1	ELAVL1	ELAVL1	3.73	0.51
WWTR1	DNAH9	DNAH9	3.73	0.97
WWTR1	PRRC2B	PRRC2B	3.73	0.62
WWTR1	CNOT2	CNOT2	3.73	0.43
WWTR1	MPP5	MPP5	3.73	0.97
WWTR1	RBM4	RBM4	3.53	0.94
WWTR1	PDLIM5	PDLIM5	3.44	0.96
WWTR1	DLGAP4	DLGAP4	3.35	0.97
WWTR1	ZCCHC17	ZCCHC17	3.35	0.97
WWTR1	SIPA1L1	SIPA1L1	3.17	0.94
WWTR1	NSFL1C	NSFL1C	3.16	0.81
WWTR1	CHD6	CHD6	3.13	0.86
WWTR1	TMCO5A	TMCO5A	3.13	0.97